Application of biomass char to tar conversion and producer gas upgrading to syngas

Ravenni, Giulia

Publication date:
2018

Document Version
Publisher's PDF, also known as Version of record

DTU Chemical Engineering
Department of Chemical and Biochemical Engineering

Application of biomass char to tar conversion and producer gas upgrading to syngas

Giulia Ravenni

Application of biomass char to tar conversion and producer gas upgrading to syngas

Giulia Ravenni

PhD Thesis

November 2018

Supervisors:

Ulrik B. Henriksen (DTU Chemical Engineering)

Jesper Ahrenfeldt (DTU Chemical Engineering)

Zsuzsa Sárossy (DTU Chemical Engineering)

Benny Gøbel (Ørsted A/S)

Technical University of Denmark

Department of Chemical and Biochemical Engineering

CHEC center

InnovationsFonden
FORSKNING, TEKNOLOGI & VÆKST I DANMARK

DTU Chemical Engineering
Department of Chemical and Biochemical Engineering

Preface

This dissertation collects the outcome of a PhD study, carried out between December 2015 and December 2018 at the Technical University of Denmark (DTU). The project was conducted in the Biomass Gasification Group, under the Combustion and Harmful Emission Control (CHEC) research center, at the Department of Chemical & Biochemical Engineering. The work was funded by DTU and by Innovation Fund Denmark, as part of the project 'Synfuel - Sustainable synthetic fuels from biomass gasification and electrolysis'. The PhD project was supervised by Senior Scientist Ulrik Birk Henriksen, Senior Scientist Jesper Ahrenfeldt, Scientist Zsuzsa Sárossy, and Benny Gøbel from Ørsted A/S. A part of the work was carried out in close collaboration with the research group "NWG-TCKON" under the Institute for Energy Technology at the Technical University of Berlin (TU Berlin), under the supervision of Dr.-Ing. York Neubauer.

Acknowledgements

I would like to especially thank all the people who contributed to this work and supported me through these years. Firstly, I would like to express sincere gratitude towards my supervisors, Ulrik B. Henriksen, Jesper Ahrenfeldt and Zsuzsa Sárossy, for guiding me, listening to my ideas and for the trust you have always put in me. Thank you to Benny Gøbel for participating in this project. I would also like to thank the colleagues who were always ready to provide help, in particular Maria Puig Arnavat, Tobias P. Thomsen and the rest of the CHEC-Risø group. A special thanks goes to the technical staff, Hanne Wojtaszewski, Freddy Christiansen, Peter T. Christensen, Erik E. Hansen and especially to Kristian Estrup. Most of the experimental work would not have been possible without your contribution and patient support. I am truly thankful to Dr.-Ing. York Neubauer for having welcomed me with enthusiasm in his research group at TU Berlin, and for the many interesting discussions we have had. A sincere thank you goes also to Omid H. Elhami, for being a brilliant colleague and collaborator. Your contribution has been decisive for this work. Also, thanks to Mrs. Susanne Hoffmann for the precious and very patient help in the analytical lab. Moreover, thanks to all the people who dedicated time and effort to help me out in the midst of various laboratory misadventures: Trine M. Hartmann Dabros, Soheila Ghafarnejad Parto, Alexander Fateev and Philipp Schröder. Special thanks to Helge Egsgaard for the help with analytical chemistry, to Janet J. Bentzen (DTU Energy) for teaching me how to use an electron microscope and to Simone Sanna (DTU Energy) for the assistance with X-Ray diffraction.

I would also like to express my gratitude to Innovation Fund Denmark, for the financial support given to this work. Thank you also to Peter Vang Hendriksen (DTU Energy) for the excellent coordination of the Synfuel project. My gratitude goes also to Otto Mønsteds Fund, for granting my work financial support in several occasions, and especially for the external research stay at TU Berlin.

My deepest gratitude goes to Giovanni Cafaggi, for your relentless trust and unconditioned support, but also for offering technical and scientific advice with competence and intelligence that I will always admire. Thanks to my family, and to the friends who supported me during these years, especially to those who did it despite the geographical distance that separates our everyday lives.

Finally, my gratitude goes to all those who contributed to the construction of a united Europe, allowing me to live and work beyond the constrictions of national borders. This work would not have been possible otherwise.

Table of Contents

Preface ..... **I**

Acknowledgements II

English summary V

Dansk sammenfatning VII

List of publications IX

Conferences and workshops contributions X

Introduction ..... **XI**

Project objectives XII

Thesis structure XIII

Chapter 1: Literature study **1**

Paper I - "Activity of chars and activated carbons for removal and decomposition of tar model compounds – A review" 2

1.1 Activity of chars and activated carbons for removal and decomposition of tar generated by pyrolysis and gasification 38

Chapter 2: Laboratory tests with tar model compounds **67**

2.1 Preliminary tests with gasification residual char and tar model compounds 68

Paper II - "Adsorption and decomposition of tar model compounds over the surface of gasification char and active carbon within the temperature range 250-800°C" 78

2.2 Scanning Electron Microscopy of fresh and spent char samples 104

Chapter 3: Producer gas upgrading **113**

3.1 Design and construction of the gas upgrading unit 114

Paper III - "Application of residual char from biomass gasification in a producer gas upgrading system" 120

3.2 Details of mass and energy balances for the operation of the gas upgrading unit 147

Chapter 4: Char Characterization 161
4.1 Samples description and analytical methods 162
4.2 Characterization of Viking residual char 166
4.3 Comparison of composition results obtained from spruce wood chips and Viking char 170
4.4 Structural evolution of char within the TwoStage process 172
4.5 Additional analyses of Viking char samples used for gas upgrading tests 176
4.6 Conclusions 180
Conclusion 185
Appendix I: Gas analysis methods: sampling, quantification and analysis ..... A.I
A.1 Solid Phase Adsorption ..... A.I
A.2 Petersen column ..... A.IV
A.3 Total tar and water content measurement with total tar condenser ..... A.VIII
Appendix II: Collection of conference proceedings ..... A.XIII
EUBCE 2017 ..... A.XV
EUBCE 2018 ..... A.XXI
WasteEng 2018 ..... A.XXV

English summary

Application of biomass char to tar conversion and producer gas upgrading to syngas

Improving the quality of producer gas is one of the major steps to be taken for integrating biomass gasification in the energy system and to allow the use of synthesis gas in the production of fossil–free biofuels and bio-chemicals. For this reason, it is important to develop effective and low-cost gas upgrading solutions, in particular to reduce the tar content of producer gas. Tar is mostly made up of aromatic substances and it is a problematic contaminant, as it forms deposits that may damage or compromise components. The use of residual gasification char for the removal of tar and upgrading of producer gas represents a convenient solution. Char is generated as a solid residue by gasifiers and it is an inexpensive waste material. In some cases, it features suitable properties to be used for adsorption and conversion of tar species.

This study has focused on the residual char generated by TwoStage "Viking" gasifier at DTU, Risø Campus. The Viking char is known for being highly porous and thermally stable, therefore it is well suited to the task, even for high temperature applications.

This work was aimed at understanding and optimizing the use of char for the upgrading of producer gas. The main objective was to investigate the interaction between the surface of char and tar species, in order to design and operate a char-based gas cleaning unit for the upgrading of producer gas with a high tar load. As a first step, laboratory experiments were conducted with the purpose to compare the performance of residual gasification char with other chars and commercial active carbon. Experiments were designed to estimate the ability of small char beds at different temperature to remove aromatic compounds by adsorption or cracking.

Following positive experimental results, a char-based gas upgrading unit was designed and constructed. The unit combined a zone for partial oxidation, via sub-stoichiometric air injection, with a fixed bed of char. Residual char from the Viking gasifier was used. Producer gas with a high tar load was generated by the 100 kW_{th} Low Temperature – Circulating Fluidized bed (LT-CFB) gasifier operated at DTU, Risø

Campus. Gas and tar analysis up- and downstream of the unit revealed that, in presence of a char bed, tar conversion could be as high as 98%. At the same time, the product gas was enriched with H_2 generated by reforming reactions. Char itself participated in steam reforming reactions, but was consumed at a slow rate. The durability of the effect on the gas quality was demonstrated with a 5 hours long experiment, after which the gas upgrading unit was still working and delivering a clean producer gas. Detailed chemical and structural characterization of char samples revealed the interesting properties of the Viking residual char before and after being used as a substrate for gas cleaning and suggested possible end-life application such as biochar. The experimental activity produced valuable knowledge about the interaction between char and tar species and demonstrated the feasibility of a char-based solution for the upgrading of producer gas.

Dansk sammenfatning

Anvendelse af biomassekoks til tjæreomdannelse og produktgasopgradering til syngas

Forbedring af kvaliteten af produktgasen er et af de vigtigste skridt, der skal tages for at integrere biomasseforgasning i energisystemet og at muliggøre anvendelsen af gassen til produktion af fossil-fri biobrændstoffer og biokemikalier. Derfor er det vigtigt at udvikle effektive og billige gasopgraderingsløsninger, især til at reducere tjæreindholdet i produktgasen. Tjære består hovedsageligt af aromatiske stoffer, og tjæreindholdet er problematisk, da det danner aflejringer, der kan beskadige komponenter i efterfølgende processer. Anvendelsen af restkoks fra forgasning til fjernelse af tjære og opgradering af produktgas udgør en attraktiv løsning. Koks fremkommer som et billigt restprodukt fra termisk forgasning, og i nogle tilfælde har koksen egenskaber, der gør at den er egnede til adsorption og omdannelse af tjærestoffer.

Dette studie har fokuseret på anvendelsen af restkoks fra TwoStage "Viking" forgaseren på DTU, Risø Campus. Viking koksen er kendetegnet ved at være yderst porøs og termisk stabil, derfor er den velegnet til formålet, selv ved høj temperatur.

Dette arbejde har haft til formål at undersøge og optimere brugen af koks til opgradering af produktgas. Hovedformålet har været at undersøge reaktioner mellem koksoverfladen og tjærestoffer med henblik på at designe og teste en koks-baseret gasrensningsenhed til opgradering af produkt gas med et højt tjæreindhold. Som et første trin blev laboratorieforsøg udført med det formål at sammenligne performance af restkoks fra forgasning med andre typer koks og kommercielt aktivt kul. Eksperimenter blev designet til at undersøge effektiviteten af koks-beds, i forhold til at fjerne aromatiske forbindelser ved adsorption eller krakning eller reforming ved forskellige temperaturer.

Baseret på positive eksperimentelle resultater blev en koks-baseret gasopgraderingsreaktor designet og bygget. Enheden kombinerede en zone til partiel oxidering via under-støkiometrisk luftinjektion, med en fixed bed af koks. Restkoks fra Viking forgaseren blev anvendt og produktgas med en høj tjæreindhold blev genereret med en 100 kW_{th} Low Temperature- Circulating Fluidized Bed (LT-CFB)

forgasser, på DTU, Risø Campus. Gas og tjæreanalysen op- og nedstrøms af reaktor viste, en tjæreomdannelse på 98% ved krakning over koks beden. På samme tid blev produktgasen beriget med H_2, dannet ved reformering af tjæren. Forgasningsreaktioner mellem koks og damp var aktive, men forgik ved lav hastighed. Langtids effekten på gaskvaliteten blev demonstreret ved et 5 timers forsøg. Ved afslutningen af forsøget var gasopgraderingreaktore stadig fuldt funktionsdygtig og leverede en ren produktgas.

Detaljeret kemisk og strukturel karakterisering af koksprøver afslørede interessante egenskaber af Viking restkoks, med mulighed for udnyttelse af koksen til biochar både før og efter anveldensen som gasrensningsmedie. Den eksperimentelle aktivitet gav værdifuld viden om samspillet mellem koks og tjærekomponenter og demonstrerede muligheden for en koks-baseret løsning til opgradering af produktgas.

List of publications

The following list includes the publications which are part of this thesis. The manuscripts are included as sections of the first three chapters of this work, and they will be referred to with roman numerals.

Chapter 1 - Paper I: Ravenni G, Sárossy Z, Ahrenfeldt J, Henriksen U.B. "*Activity of chars and activated carbons for removal and decomposition of tar model compounds – A review*". Published in "Renewable and Sustainable Energy Reviews" 2018;94:1044–56, Elsevier https://doi.org/10.1016/j.rser.2018.07.001

Chapter 2 - Paper II: Ravenni G., Elhami H.O., Ahrenfeldt J., Henriksen U.B., Neubauer Y. "*Adsorption and decomposition of tar model compounds over the surface of gasification char and active carbon within the temperature range 250-800 °C*". Research paper, under review for Elsevier journal "Applied Energy"(*)

Chapter 3 - Paper III: Ravenni G, Sárossy Z, Ahrenfeldt J, Henriksen UB. "*Application of residual char from biomass gasification in a producer gas upgrading system*". Research paper submitted to Elsevier journal "Fuel"

(*) Manuscript published in "Applied Energy" 241 (2019) 139 – 151, Elsevier
https://doi.org/10.1016/j.apenergy.2019.03.032

Conferences and workshops contributions

The following list includes conferences and workshops contributions. The conference proceedings are collected in Appendix II

- Ravenni G. Henriksen U.B., Ahrenfeldt J., Sárossy Z. "*Tar Removal from Biomass Producer Gas by Using Biochar*". Oral presentation. Proceedings 25th European Biomass Conference (EUBCE) 2017, Stockholm, Sweden
- Ravenni G., "*Tar measurement with Petersen column and SPA*". Oral presentation. International Gas Analysis Workshop, Berlin, September 2017
- Ravenni G., Sárossy Z., Ahrenfeldt J., Henriksen, U.B. "*Residual char from gasification integrated in a tar removal system*". Oral presentation. Proceedings of 26th European Biomass Conference (EUBCE) 2018, Copenhagen, Denmark
- Ravenni G., Elhami H.O., Neubauer Y., Ahrenfeldt J., Henriksen U.B. "*Comparison of wood chars from gasification and pyrolysis for adsorption and conversion of tar model compounds*". Oral presentation. Proceedings of the International conference in Engineering for Waste and Biomass valorization (WasteEng) 2018, Prague, Czech Republic
- Ravenni G., T.P. Thomsen, J. Ahrenfeldt, U.B. Henriksen. "*Characterization and assessment of PAH content in spent char to be used for soil amendment and carbon sequestration*". Poster presentation. International Conference on Negative CO_2 Emissions 2018, Gothenburg, Sweden

Introduction

This work was part of the project Synfuel - Sustainable synthetic fuels from biomass gasification and electrolysis. The project was aimed at integrating high temperature steam electrolysis with gasification of biomass to produce methane or methanol as a biofuel (Figure 1).

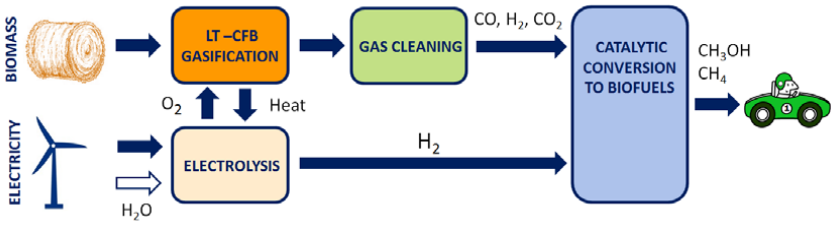

Figure 1: Synfuel integration concept

In this process, the gas cleaning step is critical, as contaminants in the syngas may undermine the catalytic synthesis to biofuels. The need to improve the quality of the producer gas is especially important for the Low-Temperature Circulating Fluidized Bed (LT-CFB) gasifier. This gasification technology operates at moderate temperature (650-750˚C), therefore it is suitable for the conversion of ash-rich fuels such as wheat straw and other agricultural residues. The use of marginal and residual biomass contributes to improving the sustainability of the system, avoiding the utilization of high quality resources such as wood. However, the LT-CFB producer gas has only moderate heating value and has a high tar load. Tar is a mixture of organic compounds including phenol, heterocyclic aromatics and polycyclic aromatic hydrocarbon (PAH) species; it is difficult to handle and can forms deposits causing operational problems. The tar issue is considered as one of the major obstacles currently hindering the commercialization of gasification technologies [1–3].

Commercial solutions are available for the elimination of tar. Among those are physical methods such as filters and scrubbers, and thermochemical methods that use high temperatures or catalysts to convert tar into syngas. However, if the tar load is high, the physical removal of tar deprives producer gas of a

significant fraction of its energy content. For this reason, thermal and catalytic methods are considered as the most convenient, as they convert tar into useful gas species such as H_2 and CO.

The thermal conversion of aromatic hydrocarbons in producer gas is very energy intensive, as it requires temperatures around 1200-1400°C [4]. The use of catalytic materials can lower the temperature needed for the cracking of tar, while supporting reforming reactions. In particular, catalytic steam reforming is considered a promising pathway to convert tar into stable and combustible gases without harming the overall efficiency of the process [5]. Several catalysts have been commercially developed for this application, but the progress in this field is still under way. The optimal catalyst to support the reforming of tar should effectively sustain the desired reactions while being resistant to deactivation. In addition, to make the process economically and environmentally sustainable, the catalyst should be inexpensive and free from polluting, toxic substances.

The use of carbonization products such as char and active carbon is raising interest in the scientific community, as it represents a potentially effective and inexpensive solution to the problem of tar in biomass producer gas. In particular, char is produced as a solid residue by gasification plants. It is often burned or disposed, causing additional costs for the plant owners, especially for small scale gasifiers [6]. The re-use and valorization of this material would be beneficial to the overall economy of any gasification plant.

The TwoStage process developed in the last two decades at DTU, is a good example of how the properties of char can be used to eliminate tar and upgrade the gaseous products. Indeed, this gasifier is able to deliver an almost tar-free producer gas. The high quality of producer gas is a result of the process design, where pyrolysis and gasification are controlled separately. In the reduction stage, the temperature is above 1100°C, due to air injection for partial oxidation. Solids are then gasified with the char bed, which has an average temperature of 800°C. The demonstration plant that is operated at DTU, the 75 kW_{th} Viking gasifier, also generates char as a solid residue. Due to the operating conditions of the process, residual char has properties comparable with commercial active carbon. It is rich in carbon (90 wt%), it has a specific surface area above 1000 m^2/g and is highly porous; in addition it contains inorganic species derived from the parent material (softwood). All of these features make this material particularly interesting for adsorption and catalytic applications.

Project objectives

The aim of the study was to develop a producer gas upgrading system using residual gasification char, and demonstrate its feasibility. To achieve this, a deeper understanding of the tar conversion mechanism taking place in the char bed of the Viking gasifier was needed. For this reason, experimental tests were designed and performed at different scales. At the same time, a thorough characterization of the solid residue generated by the Viking gasifier was conducted. The main objectives of the work can be summarized as follows:

- Understand the interaction between tar and carbonaceous surfaces, under different conditions, by researching the available literature and performing relevant laboratory tests.
- Investigate the properties of residual gasification char generated in the TwoStage Viking gasifier, in order to evaluate its potential applications, in particular for adsorption, cracking and reforming of tar.
- Design a gas upgrading unit, adopting a bed of residual char combined with partial oxidation of tar, for the treatment of producer gas generated in the LT-CFB gasifier.
- Optimize the operating conditions and demonstrate the feasibility of the gas upgrading system.

Thesis structure

The thesis is structured in four chapters.

The initial chapter is dedicated to the review of the relevant studies available in literature. The chapter includes a published review paper – Paper I. This review is focused on experimental studies investigating the adsorption and decomposition of tar model compounds on the surface of carbonaceous materials. The additional section of the chapter reports a series of experimental studies evaluating the effects of hot char beds on actual tar mixtures generated by pyrolysis or gasification.

Chapter 2 describes the experimental activity and the results obtained in the first stage of the project, through laboratory-scale experiments with tar model species. Most of the results were obtained during a collaborative experimental campaign at the Technical University of Berlin - Institute for Energy Technology and are reported in Paper II.

The third chapter reports on the demonstrative char-based gas cleaning unit operated on the LT-CFB gasifier. The design and construction of the setup are presented. The operation and the tests results are described in Paper III. The final section of this chapter presents in detail the mass and energy balance calculations that were performed on the gas upgrading unit.

The final chapter collects the results from various characterization analyses that have been conducted on char samples. The aim was to investigate in detail the properties of Viking char. Furthermore, char samples extracted at different locations inside the gasifier were analyzed to study the progress of carbonization. Finally, additional analyses have been performed on spent char samples used for hot gas treatment, to evaluate the structural modifications occurring during the operation of the gas upgrading unit. These samples were also evaluated in terms of suitability for soil application, as biochar.

Finally, a closing section summarizes the main conclusions of this work. A comprehensive description of the gas analysis methods applied on the LT-CFB producer gas is given in Appendix A1, while Appendix A2 collects the proceedings relative to oral presentations given at conferences over the years 2017-2018.

Note that for ease of the reader, reference lists are given separately, at the end of each section. The three manuscripts included in the chapters follow their own numeration for Figures, Tables and Equations.

References

[1] Asadullah M. Biomass gasification gas cleaning for downstream applications: A comparative critical review. Renew Sustain Energy Rev 2014;40:118–32. doi:10.1016/j.rser.2014.07.132.

[2] Sansaniwal SK, Rosen MA, Tyagi SK. Global challenges in the sustainable development of biomass gasification: An overview. Renew Sustain Energy Rev 2017;80:23–43. doi:10.1016/j.rser.2017.05.215.

[3] Ruiz JA, Juárez MC, Morales MP, Muñoz P, Mendívil MA. Biomass gasification for electricity generation: Review of current technology barriers. Renew Sustain Energy Rev 2013;18:174–83. doi:10.1016/j.rser.2012.10.021.

[4] Jess A. Mechanisms and kinetics of thermal reactions of aromatic hydrocarbons from pyrolysis of solid fuels. Fuel 1996;75:1441–8. doi:10.1016/0016-2361(96)00136-6.

[5] Guan G, Kaewpanha M, Hao X, Abudula A. Catalytic steam reforming of biomass tar: Prospects and challenges. Renew Sustain Energy Rev 2016;58:450–61. doi:10.1016/j.rser.2015.12.316.

[6] Patuzzi F, Prando D, Vakalis S, Rizzo AM, Chiaramonti D, Tirler W, et al. Small-scale biomass gasification CHP systems: Comparative performance assessment and monitoring experiences in South Tyrol (Italy). Energy 2016;112:285–93. doi:10.1016/j.energy.2016.06.077.

Chapter 1

Literature study

This chapter is dedicated to the review of literature relevant to the scope of this thesis. Due to the number of available publications, the review was divided into two main sections. The first part is dedicated to the studies that investigated the performance of chars and active carbon for the adsorption and conversion of tar model compounds, including alkanes and aromatic species. This section is published in Elsevier journal "Sustainable and Renewable Energy Reviews" (doi:10.16/j.rser.2018.07.001). The second section of this chapter gathers and describes the studies where the performance of carbonaceous materials has been evaluated using actual tar mixtures generated via thermal processes. These studies focused on cracking and reforming of tar at high temperature (above 600°C). The final part reports a few examples of gasification plants where the use of char or active carbon has been integrated into the process.

Activity of chars and activated carbons for removal and decomposition of tar model compounds – A review

*Giulia Ravenni, Zsuzsa Sárossy, Jesper Ahrenfeldt, Ulrik Birk Henriksen
Technical University of Denmark (DTU), Department of Chemical and Biochemical Engineering
Frederiksborgvej 399, 4000 Roskilde, Denmark
*Corresponding author: Giulia Ravenni Phone: +45 93 51 15 92 E-mail: grav@kt.dtu.dk

Manuscript published in Elsevier journal "Renewable and Sustainable Energy reviews"
(https://doi.org/10.1016/j.rser.2018.07.001)

Abstract

Chars, or carbonized products produced by pyrolysis or gasification, have a porous structure, a high specific surface area and they can be rich in micropores. Such characteristics make them suitable to be used in the cleaning of gasification producer gas. Several authors have been investigating the mechanism of the interaction between tar compounds and char, in order to understand the potential of this application. This review is aimed at summarizing results from reported experimental campaigns, carried out to study the effect of char beds on tar compounds: several research groups have been investigating the subject over the years, using different experimental methods and different chars or activated carbon (AC).

After a first section dedicated to the definition of char and tars, this work reviews a series of studies where model compounds were used to predict the behavior of real tars upon contact with char surface. The review includes research works focused on alkanes decomposition (methane, propane) and more traditional aromatic model tars. The overview of the results shows that the use of biomass char is effective in converting up to 100% of model tars in a gaseous stream, with coke, H_2, and CO and CO_2 as major products of cracking and reforming reactions. In particular, multi-ring aromatics such as naphthalene showed higher conversion rates. Tar conversion at 700-900°C is favored by the presence of reforming agents (H_2O, CO_2), which also contribute in preserving the activity of char over time. Residual char properties that enhance the activity toward tar decomposition include a large surface area and a well-developed microporosity. Both the char properties and the process parameters need to be carefully optimized for the successful application of residual gasification char to producer gas cleaning, and further experiments on real producer gas are needed to implement char-based gas cleaning systems.

Keywords: gasification, biomass, char, active carbon, model tar, gas cleaning

1. Introduction

In recent years, the increased CO_2 emissions and the related global climatic issues have encouraged research about alternative energy sources to replace fossil fuels. Biomass does not contain fossil carbon, and therefore it has the potential to be a source of renewable energy. Particularly, one of the most promising technologies for biomass-to-energy conversion is gasification. The producer gas can be used for several applications: it can fuel gas turbines or reciprocating engines, or it can be used to produce methane, methanol or Fischer-Tropsch fuels. Gasification has the major drawback of requiring extensive gas cleaning, and the most problematic substance in producer gas is considered to be tar. Tar compounds are generally high molecular weight hydrocarbons that can easily condense, causing several operational problems in downstream processes and components. They are formed during pyrolysis and evolve during gasification in a series of complex reactions: their nature is strongly dependent on the process conditions.

Many methods for removing tars from producer gas have been investigated, and they can be divided into two main groups: primary and secondary methods [1]. Primary methods act inside the gasifier (*in-situ*) to prevent tar formation or convert nascent tars, e.g. modification of the gasifier design or optimization of operating conditions, and addition of bed additives or catalysts. Common bed additives are Ni-based catalysts, dolomites and magnesites, zeolites, olivine and iron catalysts: they are effective in reducing the amount of tars, by converting them into stable gases (H_2, CO and CO_2), but they encounter deactivation and cause problems related with the carryover of fines [1]. Secondary methods include various downstream treatments such as hot gas cleaning (thermal or catalytic cracking, oxidative and steam conversion), and mechanical methods such as cyclones and filters. In general, thermal and catalytic methods are considered the most attractive because of their high effectivity. However, they require careful optimization in order to minimize the energy consumption and preserve the overall efficiency of the process. At present, none of these methods has been found to be a breakthrough, in terms of effectivity and economic viability.

A potential solution for downstream tar removal is the use of char. Ideally, after gasification the feedstock is reduced to pure ash, but usually the more stable fraction of carbon is preserved in the residues of the process, especially in gasifiers operating at low temperature (750-800°C) [2]. Being a by-product of gasification, char is continuously produced and available. If used for gas cleaning it could avoid the problem of deactivation, which is usually limiting for other catalysts: spent char can be continuously recycled in the system and gasified along with fresh feedstock. In addition, residual char is

currently considered a waste for disposal, therefore its repurposing would represent an economic benefit for any gasification plant [3].

Understanding and optimizing the interaction between char and tars is not an easy task and it requires bringing together carbon science and tar chemistry. Depending on the composition of the tar mixture, char properties and reaction conditions, different physical and chemical processes can take place on char surface when contacting with tars. The complexity of the problem is given by the heterogeneity of the tar mixture and by the nature of char, which can have manifold characteristics depending on the conditions of carbonization. In order to simplify the matter, model compounds are often used in laboratory-scale experiments to predict the behavior of the real tar mixture. Several research groups have used single tar compounds for investigating reaction paths and quantify the conversion of certain aromatics or alkanes. Adsorption capacity and catalytic activity for model tars conversion were measured for different carbon materials, and often commercial activated carbon was chosen as reference. In some cases, char was impregnated with metal oxides or alkali, or acid washed to remove all inorganics with the aim of investigating separately the effect of different char characteristics.

This work collects results from a series of studies dedicated to tar model compounds interacting with a solid carbon surface. The need for organizing such results is given by the lack of a method for establishing the efficiency of char for tar conversion, and the lack of a systematic evaluation of the main parameters influencing the efficiency of char for tar conversion (char properties and reaction conditions). Researchers have been using a variety of different setups, reaction conditions and char types in the experiments. The aim of this review is to identify the main reaction pathways and to list the most important parameters affecting tar decomposition on the char surface. Such overview provides basis for a more rigorous definition of the interaction mechanisms between tar compounds and solid carbon, paving the way to the design of tar removal systems based on char.

The first section of this review is dedicated to clarifying the terminology to define char and similar carbonaceous materials. Next, the most commonly used model tar compounds are shortly presented. The following section is dedicated to the effect of char on alkanes, while the last focuses on mono-ring aromatics and Polycyclic Aromatic Hydrocarbons (PAHs).

2. Defining carbon materials for gas cleaning applications

Carbon can be found in nature with different shapes and structures: diamond, graphite, graphene, or less ordered forms such as char or activated carbon. To avoid disarray, it is useful to clarify the terminology used for the different carbon materials treated in this review, referring to the definitions given by the International Committee for Characterization and terminology of Carbon [4,5].

2.1 Carbonization

The carbonaceous materials treated in this work are the solid products of carbonization, a process which is defined as "*the formation of material with increasing carbon content from organic material, usually by pyrolysis*" [4]. Carbonization can take place under different conditions (pressure, temperature, oxygen level), thus producing different carbonaceous structures. The process leads to a progressive increase in the crystalline order: during pyrolysis, volatiles are removed from the organic material, and the carbon atoms are arranged in stacks of flat aromatic sheets randomly cross-linked [6]. The sequence of structural changes occurring during biomass carbonization is well described by Keiluweit et al.[7]. At temperatures higher than 700°C, turbostratic carbon (Figure 1a) is formed: it is still less packed and less ordered in comparison with graphite-like carbon (Figure 1b), therefore it results in higher porosity and high surface area [8]. High carbonization temperatures (1000°C) decrease the total porosity because of the formation of graphite with a more closely packed structure [9].

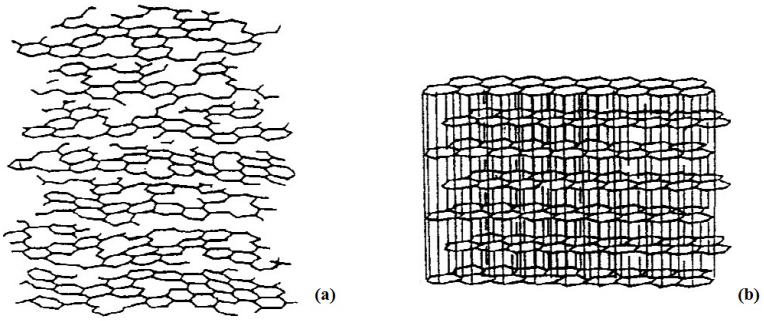

Figure 1*: Schematic difference between turbostratic (a) and graphite (b) structure. (Adapted from* [10] *with permission from Taylor & Francis Ltd.)*

In presence of a limited amount of oxidizing agent (sub-stoichiometric), partial combustion leads to an increase in temperature and char is exposed to the endothermic gasification reactions: some of the

carbon will react leaving the residual char structure with a more stable carbon fraction, fewer functional groups and a larger ash fraction.

2.2 Char and activated carbon

Two types of carbonization products are of particular interest in this context: char and activated carbon (AC). As defined by the International Committee, char is "*a carbonization product of a natural or synthetic organic material, which has not passed through a fluid stage during carbonization*" [5]. The parent material for char can be coal or biomass.

Biochar is a particular type of char which is mainly intended for soil application, and should meet specific criteria as described in the European Biochar Certificate (EBC) [11] or the International Biochar Initiative (IBI) Standard [12]. Both are voluntary standards and describe biochar as a material produced through oxygen-limited thermal conversion of biomass, thus including pyrolysis and gasification processes. On the other hand, AC is "*a char, which has been subjected to reaction with gases, sometimes adding chemicals, e.g. $ZnCl_2$, during or after carbonization in order to increase its porosity*" [5]. During activation, the irregular structure of char reacts with gases, enhancing the porosity of the material. This gives the ACs a large surface area (up to 2500 m^2/g), a microporous structure and a high surface reactivity [13]. The structure of activated carbons has been described by Stoeckli [14] as constituted by bent aromatic sheets and strips with gaps of various dimension between them, forming slit-shaped micropores (Figure 2).

Figure 2*: Schematic structure of AC. (Reprinted from* [14]*, pag.2. Copyright 1990 Elsevier)*

ACs are widely used in adsorption processes. They may assist the capture of organic volatile compounds and adsorb hydrocarbons and PAHs [15–22]. ACs are also commonly used for gas cleaning in combustion plants, to remove metals and dioxins at 150-200°C [23].

The structural characteristics of carbon materials are defined by the distribution of micropores (cavities with mouths smaller than 2 nm), mesopores and macropores (>50 nm), while the chemical properties are defined by the inorganics dispersed on the surface and by the presence of oxygen-containing functional groups at the edges of the graphite sheets: acidic groups such as lactones, carboxylic acid or phenol and basic groups such as carbonylic, quinonic and pyrone structures. Oxygen sites enhance the adsorption of polar molecules and in general they are known to influence the adsorption capacity and catalytic activity of char [6,18,24].

Biomass-derived char generally has a lower surface area and adsorption capacity in comparison with ACs, but nonetheless shares many of their features. This is particularly true if char undergoes a certain degree of gasification, which is analogue to an activation process. Even if it does not undergo activation, char usually has a porous structure, a high surface area and it is rich in micropores.

The parent material naturally contains minor elements such as Alkali and Alkaline Earth Metals (AAEM), Fe, Al, Si and P that can increase the catalytic properties [25]. Moreover, depending on the carbonization conditions, the surface of char can have oxygen functional groups.

Because of its AC-like characteristics, char has a good potential to be used as adsorbent, catalyst support, and even as a catalyst on its own [6,25–28]. Specifically, it offers a number of favorable features for adsorption and catalytic conversion of aromatics and alkanes. In recent years, the application of non-activated carbonization products to gas treatment has been suggested and studied by several authors. A study by Benedetti et al.[3], considers gasification-derived biochar as a substitute for AC, pointing out that double-stage gasifiers are particularly suitable for producing residual char with characteristics comparable with AC. As a matter of fact, in staged processes the pyrolysis and the gasification steps are carried out separately, thus resembling an AC manufacturing process. Residual char has therefore the potential to be used as AC without any further activation treatment: operating conditions of gasification can be tuned to deliver a residual char with suitable properties to be directly used for adsorption or gas treatment.

3. Tar model compounds

A general classification of the compounds in the tar mixture is based on their order of appearance within the gasification process [29]:

- **Primary tars** are produced during pyrolysis, in the temperature range 400-700°C. They are completely converted if the temperature surpasses 800°C. This class includes oxygenated compounds such as levoglucosan, hydroxyacetaldehyde and furfurals originating from cellulose and hemicellulose, together with methoxyphenols which are derived from lignin.
- **Secondary tars** are formed by gas-phase reactions of primary tars at 700-850°C and they include phenolic compounds and alkenes (Table 1). The abundance of this class of tars has a peak around 750°C
- **Tertiary tars** include methyl-derivatives of aromatics, such as methyl-acenaphthylene, methylnaphthalene, toluene and indene. They are formed in the temperature range 650 to 1000°C. Polycyclic Aromatic Hydrocarbons (PAH) are also formed such as naphthalene, acenaphthylene, anthracene/phenanthrene and pyrene (Table 1). Above 1000°C naphthalene is dominant over other species.

To investigate and predict the behavior of tars, model compounds have been widely used as representatives of different tar classes. Some of the most common model tar molecules are reported in Table 1. Toluene, phenol and naphthalene are frequently used, as these compounds generally make up the most part of total tar. PAHs are also often used as model tars because they are problematic pollutants in the producer gas, and they are highly refractory. In some cases, alkanes such as methane and propane have been used as model tars, even if they lack the aromatic structure or not defined as members of the above tar classes.

Indeed, there may be differences in the behavior of model tars in comparison with real tar mixtures, and results should always be treated considering the differences with actual process conditions. It is here appropriate to consider the works published by Mastral and colleagues, where the adsorption of pure model PAHs on ACs was compared with the behavior of PAHs mixtures [30], PAHs with steam [31], and PAHs-containing flue gases from real combustion [9]. The differences in the adsorption dynamics showed that the process is affected by the presence of molecules different from the pure model compounds. Specifically, a mixture of naphthalene and phenanthrene was adsorbed on AC, and it was observed that the presence of a second PAH in the gas stream reduced the adsorption efficiency, as both

molecules compete for adsorption sites [30]. Similarly, adsorption tests of various PAHs in presence of combustion flue gas revealed that other molecules (H_2O, smaller volatile organic compounds) can compete with PAHs, blocking the narrowest adsorption sites and affecting the overall adsorption capacity [9]. Indeed, the presence of steam in the gas phase (10%) decreased the adsorption capacity of phenanthrene for 13 out of 16 tested ACs [31].

This suggests that results obtained by using model compounds alone should be verified in conditions as similar as possible to reality. Nonetheless, studying the behavior of model compounds can be useful in understanding the adsorption or decomposition dynamic of real tars.

Table 1: *Common tar model compounds*

Model tar	Tar class	Formula	Structure
Methane	-	CH_4	
Toluene	II	C_6H_5-CH_3	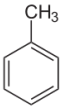
Phenol	II	C_6H_6O	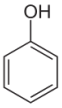
Naphthalene	III	$C_{10}H_8$	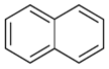
Phenanthrene	III	$C_{14}H_{10}$	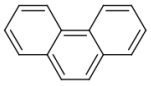
Anthracene	III	$C_{14}H_{10}$	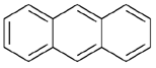
Pyrene	III	$C_{16}H_{10}$	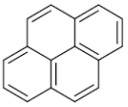

4. High temperature chemistry of alkanes as tar model compounds over char

Studies on heterogeneous reactions of light hydrocarbons have been investigated in order to understand the catalytic properties of a carbonaceous surface within the temperature range 850-1000°C. An overview of the experimental conditions in the reviewed papers can be found in Table 2. It is worthwhile to include this section in the present review, as many of the processes observed at the surface of char or AC are similar to those encountered for aromatic model tars. Particularly, the decomposition of methane through carbon deposition, often referred to as thermocatalytic decomposition (Reaction (1)), has been object of study because carbon materials offer advantages to be used as catalyst for H_2 production [32].

$CH_4 \rightarrow C_{(s)} + 2H_2 \quad \Delta H^\circ = 75.6$ KJ/mol (1)

Muradov [32] tested different types of commercial AC as catalysts for this application: ACs exhibited high initial catalytic activity, but showed deactivation over 1-hour period. A proportional relationship was observed between the catalytic activity and the BET specific surface area of AC. The same author [33] worked also with various carbon materials (AC, carbon black, graphite, glassy carbon, acetylene black), with the aim to determine the structural or chemical factors influencing CH_4 decomposition. The "degree of order" in the carbon structure was found to affect heterogeneous reactions: amorphous or microcrystalline carbons such as ACs appear to be richer in energetic discontinuities (e.g. reactive edges of carbon crystallites), forming active sites for CH_4 decomposition. Furthermore, these results showed that transition metals impurities on the carbon surface play a minor role in catalysis. Oxygen-containing functional groups appeared to have an effect solely in the first stages of the process.

Likewise, Moliner et al.[34] compared the activity of various ACs for CH_4 decomposition. They focused on the effect of surface chemistry and porosity and concluded that the most effective chars were the ones with a BET surface area around 1000 m^2/g. The concentration of oxygen functional groups on the surface only influenced the initial activity, but did not correlate with longer-term activity of chars, in agreement with [33]. Deactivation was observed and ascribed to micropores blocking by carbon deposition. Prolonged activity (240 min) was ensured by large surface area, together with an appropriate pore size distribution including mesopores and wide microporosity to facilitate diffusion. Suelves et al.[35] further evaluated the effect of different textural characteristics of AC on CH_4 conversion by using thermogravimetric analysis (TGA) to quantify the deposition of solid carbon. The results showed that the higher the total pore volume of fresh char, the higher the amount of deposited carbon, meaning that

a larger pore volume implies an increased activity. They also confirmed the relation between the concentration of oxygenated functional groups and the initial reaction rate.

Dufour et al.[36] evaluated the catalytic activity of wood char (non-activated) for CH_4 decomposition investigating the role of inorganics (K, Ca and Mg), pore texture and surface chemistry. Since demineralized samples exerted the same methane conversion as untreated ones, the authors surmise that the effect of inorganics is negligible. Similar remarks were made for the role of oxygen surface groups. As a consequence, active sites for carbon deposition are rather likely to be constituted by unsaturated carbon atoms, forming high energy sites as described also in [33]. CH_4 reacting in a N_2 atmosphere rapidly deactivated the carbon catalyst, probably because of the pores closure due to carbon deposition. In agreement with results from other studies ([37–39]), the presence of CO_2 or H_2O was found to prevent the pores blocking and to maintain the char catalytic activity. In a latter work, Dufour et al.[40] examined more closely the mechanism of deactivation and regeneration of wood char, confirming the role of steam gasification for the long-term sustainability of H_2 production. During CH_4 conversion, a thin coating of reactive pyrolytic carbon was formed on the surface. The authors suggest that wood char might represent a cheap and effective catalyst for converting both CH_4 and tars into an H_2–rich syngas.

The catalytic properties of gasification-derived char for the decomposition of CH_4 and C_3H_8 were investigated by Klinghoffer et al.[41]. The properties of wood char produced in a fluid bed gasifier under different conditions (steam, CO_2, 550, 750 and 920°C) were investigated alongside with the char activity toward alkanes decomposition. Results showed that char surface area and the micropore structure strongly depends on the gasification conditions: longer residence time and higher temperature favored the development of a large surface area. The use of CO_2 as a gasifying agent, in comparison with steam, enhanced the formation of micropores.

Char catalytic activity on the decomposition of CH_4 and C_3H_8, was measured by TGA. The mass gain of char was used to quantify the deposition on the surface from hydrocarbon decomposition. Exposure to CH_4 induced an increase of the char mass starting at 700°C. At the same temperature, C_3H_8 induced a higher mass gain. According to the author, these results demonstrate the ability of char to catalyze hydrocarbon decomposition via cleavage of C-C and C-H bonds, suggesting that char may be a good catalyst for tar decomposition. Post-test characterization of char surface in Environmental Scanning Microscopy and Energy Dispersive X-ray (ESEM/EDX) showed a high carbon concentration on the pores, especially at the iron sites, suggesting that the metal acts as an active site for catalytic reactions.

Table 2*: Overview of experimental conditions for tests on alkanes decomposition*

Author	Tested model compounds	Tested char (carbonization temperature)	Char bed temperature	Char particle size [µm]	Reaction atmosphere composition
[33] Muradov et al.	Methane	Carbon black Commercial AC Various carbon materials (graphite, glassy carbon, acetylene black)	850°C	n.r.	CH_4
[34] Moliner et al.	Methane	Commercial ACs Coal char (800°C)	850°C-950°C	<100	CH_4
[35] Suelves et al.	Methane	Carbon black Commercial AC	900°C	n.r.	CH_4
[36] Dufour et al.	Methane	Pine wood char (750°C)	1000 °C	200-400	N_2, CH_4, mix of $H_2/CO/CO_2$ (artificial syngas)
[40] Dufour et al.	Methane	Pine wood char (750°C) Demineralised pine wood char (750°C)	1000 °C	200-400	N_2, H_2O
[41] Klinghoffer et al.	Methane Propane	Poplar char (CO_2 and H_2O gasified at 550, 750 and 920°C)	20°C- 900°C	(Parent) 1000-4000	N_2
[25] Klinghoffer et al.	Methane	Poplar char (CO_2 and H_2O gasified at 550, 750 and 920°C)	700°C - 750°C 850°C	(Parent) 1000-4000	N_2

The same research group [25] further studied the role of inorganics at the char surface and oxygen functional groups as well. The effect of acidic oxygen groups was tested on CH_4 decomposition at 850°C and was found not to play an important role: this is ascribed to the fact that acidic oxygen groups are desorbed from the char surface at temperatures lower than 850°C.

Inorganics such as Ca, Na, K, Mg, P, Si, Fe, Al and Mn were present in the char and in general higher concentrations lead to a higher catalytic activity. Furthermore, the activity of char was higher than that of pure ashes, indicating that carbon works as support on which inorganics are dispersed. Indeed, the author refers to gasification char as a "supported metal catalyst" [41] where the carbonaceous structure with a high surface area provides support for the ash elements.

These studies highlight the most important characteristics of a carbon material such as char for its activity in acyclic hydrocarbons decomposition. Textural characteristics such as large surface area and pore volume are considered essential to the activity of char, especially for the longevity of its catalytic effect. The role of inorganic impurities is not yet defined: to some extent, transition metals such as Ni

and Fe and AAEMs were found to play a role in CH_4 decomposition. Certainly the presence of heteroatoms in the carbon structure, together with a low degree of crystalline order promoted the abundance of active sites. In general, results obtained on the decomposition of alkanes showed some promising characteristics of AC, as well as non-activated biomass char for the decomposition of hydrocarbons.

5. Adsorption and high temperature chemistry of aromatics as tar model compounds over char

Aromatics are usually the main components of the tar mixture, and they are highly refractory as a consequence of their molecular structure. Their stability is given by the delocalization of electrons in the π-bonds between carbon atoms in the cyclic structure. This effect increases with the number of conjugated rings, making larger PAHs more difficult to remove by thermal treatment. Such process leaves the aromatic structure unchanged. The range of temperatures where physical adsorption is applied is in generally below 250°C because, as temperature is increased, the adsorption capacity is reduced as a result of the exothermic nature of adsorption processes [42]. On the other hand, at higher temperatures chemical bonding with the surface (chemisorption) can take place. Chemisorption is characterized by large interaction potentials: it is often found to occur at temperatures higher than the critical temperature of the adsorbate [43] (e.g. 748.4°C for naphthalene, 869°C for phenanthrene [44]). If aromatics are chemisorbed, their molecular structure is modified, and this can be the first stage of a catalytic process leading to cracking and reforming of heavy aromatics. In the following, a series of papers are reviewed were physisorption or chemisorption were studied. An overview of all the experimental conditions is given in Table 3 and Table 4.

The conversion of model tars is commonly expressed as X (Equation (2))

$$X = \frac{C_{in} - C_{out}}{C_{in}} * 100\ [\%] \quad (2)$$

Being C_{in} and C_{out} the model tar concentrations at the inlet and outlet, respectively.

5.1 Physical adsorption

Physical adsorption plays an important role in the interaction between hydrocarbons and the surface of chars, therefore it is useful to understand what parameters control this process. ACs are popular for adsorption of PAHs from aqueous solutions [45]. Such a process has been object of several studies, and

some of them also investigated the use of biochars for this application [46,47]. In particular, Li et al.[46] found the adsorption capacity of biochars for phenanthrene, fluorene and pyrene to increase with the carbonization temperature (600 to 800°C): Biomass char produced at 800°C performed comparably with ACs. The adsorption of PAHs in gaseous phase on ACs and chars was investigated in the works gathered in Table 3. Mastral et al. investigated the matter testing many varieties of carbon materials for adsorption of PAHs with 2-4 rings [9,16,17,31,48,49] and found that the adsorption capacity of ACs was mostly dependent on their porous-textural characteristics, especially microporosity (or the ratio between the micropore volume to the total pore volume). Specifically, a large micropore volume enhanced the adsorption of pure multi ring compounds [17,48] and their binary mixtures [49]. The adsorption of larger molecules such as phenanthrene and pyrene was favored by large micropores diameters (>0.7nm) and by mesoporosity. Mesopores helped accessing the micropores and promoted multilayer interactions [49]. Each compound appeared to have specific needs in terms of pore size distribution, for being optimally adsorbed: for example, larger PAHs were found to be adsorbed more easily on the surface of tested ACs [48]. The role of surface chemistry of chars was investigated by García et al.[50], by measuring the adsorption of phenanthrene on AC with different degrees of surface oxidation: results showed that adsorption capacity is lower for AC with a higher content of surface oxygen groups, which means that the increased polarity of the surface hinders adsorption [50]. These results were later confirmed by Lillo Ródenas et al.[51]. They studied the adsorption of benzene and toluene on ACs with different porosities and with a reduced content of surface oxygen groups. Adsorption capacities for the two molecules varied on the same char. Narrow microporosity (<0.7nm) was found to govern the adsorption of benzene, while all micropores (<2nm) participated in the adsorption of toluene. Oxygen functional groups were removed from the char surface by heating to 900°C: thermally treated AC always showed an increased adsorption capacity. The negative effect of oxygen surface groups was explained with the interaction between aromatic rings of the adsorbate and electron-rich regions of the graphene layers: the oxygen groups withdraw electrons from such layers, hindering the interaction with the adsorbate.

Hu et al.[15] also compared the adsorption on ACs, focusing on their interaction with phenol, naphthalene, o-cresol and 1-methylnaphthalene. Interestingly, tars containing methyl groups were found to be adsorbed more efficiently in comparison with phenol and naphthalene. The authors suggest that this may be due to interaction between the methyl groups and the hydrophobic functional groups on the surface of the ACs. In agreement with Mastral et al., naphthalene was adsorbed better on

microporous AC. The average pore diameter was found to influence the adsorption capacity, depending on the molecular shape and dimensions of the adsorbate: the two most favorable ACs for model tars adsorption had a specific surface area of about 1100 m^2/g and an average pore size of 1.2 and 1.9 nm.

In conclusion, to achieve high adsorption of aromatics, chars should have:

(i) Large specific surface area (BET with N_2 around 1000 m^2/g)

(ii) Low content of oxygen-containing surface groups

(iii) Large micropore volume (N_2 measured >0.3 cm^3/g)

(iv) Appropriate pore size distribution

The last parameter varies according to the molecules to be adsorbed: narrow microporosity can induce diffusional problems for large molecules (pyrene), whereas it promotes the adsorption of smaller molecules such as benzene.

Table 3: *Overview of experimental conditions for adsorption of aromatics on char*

Author	Tested model compounds	Tested char (carbonization temperature)	Char bed temperature	Char particle size [µm]	Reaction atmosphere composition
[17] Mastral et al.	Phenanthrene (1.5 ppm)	10 carbonaceous materials (various parent materials)	125, 150, 175˚C (15-50mg)	100-200	Helium
[48] Mastral et al.	Naphthalene Phenanthrene Pyrene (1.5 ppm)	16 carbonaceous materials (various parent materials)	n.r. (15-50mg)	100-200	Helium
[31] Mastral et al.	Phenanthrene (1.5 ppm)	16 carbonaceous materials (various parent materials)	150˚C (25mg)	100-200	Helium Steam (0-20%)
[16] Mastral et al.	Naphthalene Acenaphthene, Fluorene, Phenanthrene, Anthracene, Fluoranthene, Pyrene	Coke from German Rhenish lignite	150˚C (25mg)	100-200	Helium
[49] Mastral et al	Naphthalene Fluorene, Phenanthrene, Fluoranthene, Pyrene	Coke from German Rhenish lignite	150˚C (25mg)	100-200	Helium
[50] García et al.	Phenanthrene (1.5 ppm)	Commercial AC (with various degrees of surface oxidation)	150˚C (25mg)	100-200	Helium
[15] Hu et al.	Phenol o-cresol Naphthalene 1-methylnaphthalene	Commercial activated carbons	150˚C - 250˚C	1000 2000 4000	N_2
[51] Lillo-Ródenas et al.	Benzene Toluene	Commercial activated carbons Steam activated char Chemical activated chars (NaOH, KOH)	25 ˚C	Powder Granular (1300-1500) Pellets (2200)	Helium

5.2 Chemical adsorption and catalysis

When reaction temperature is above 500-600˚C, chemisorption of aromatics can take place possibly followed by catalyzed reactions resulting in carbon deposition with release of products as H_2, CO or CO_2 (depending on the reaction atmosphere). An overview of the conditions of experiments at high temperatures is given in Table 4.

Table 4: *Experimental conditions overview of tar model compounds tests*

Author	Tested model compounds	Tested Char (carbonization temperature)	Char bed temperature	Char particle size [µm]	Reaction atmosphere composition
[52] Egsgaard et al.	Benzene Phenol Naphthalene Phenanthrene	Pine char (800 ℃)	600˚C- 800˚C	100-500	N_2 H_2O
[53] Abu El-Rub et al.	Phenol Naphthalene	Calcinated dolomite, Olivine Fluid catalytic cracking Nickel catalyst Commercial biomass char Pinewood char (500℃) Pinewood ash (600℃)	700˚C - 900˚C	1400-1700	N_2, CO_2 H_2O
[37] Hosokai et al.	Benzene Phenol Naphthalene Phenanthrene Pyrene	Commercial char (800 ℃)	700˚C - 900˚C	1300-2400	N_2 H_2O/ N_2 $H_2O/H_2/N_2$
[38] Fuentes-Cano et al.	Toluene Naphthalene	Coconut char (commercial) Coal char (commercial) Dry sewage sludge char (900℃)	750˚C, 850˚C, 950˚C	1000-2800	N_2 H_2/ H_2O
[54] Nitsch et al.	Phenol	Beech wood char (750 ℃)	850˚C	700-1000	N_2 H_2/ H_2O
[55]Huang et al.	Toluene	Sewage Sludge char (900˚C) Bottom ashes Dolomite NiO/γ-Al_2O_3	750˚C, 850˚C, 950˚C	1000-1700	N_2
[56]Lu et al.	Toluene	Sewage Sludge char (900˚C)	750˚C, 850˚C, 950˚C	1000-1700	N_2 CO_2/H_2O $CO/H_2/HCl$
[57] Bhandari et al.	Toluene	Switchgrass char (downdraft gasifier) Activated switchgrass char Acidic surface activated char	700˚C; 800˚C	150-600	N_2 Artificial syngas (CH_4/ $H_2/CO/CO_2$)
[58]Mani et al.	Toluene	Pine bark char (950˚C)	600˚C - 900˚C	212-420	N_2/ H_2O
[59] Korus et al.	Toluene	Coal-derived activated carbon	650˚C - 850˚C	400-850	N_2
[39] Y. Zhang et al.	Naphthalene	Rice straw char (500 ℃) $Ni(NO_3)_2$ loaded char Water-washed char	700˚C - 900˚C	(Parent) 100-150	Argon Artificial syngas (CH_4/ $H_2/CO/CO_2$)
[23] Di Gregorio et al.	Naphthalene	Commercial ACs (three types)	750˚C- 900˚C	3000 (pellets)	N_2
[60] Nestler at al.	Naphthalene	Spruce char (500˚C, 800 ˚C) CO_2-activated spruce char Commercial AC	850˚C, 1050˚C	500-2000	N_2
[61] Feng et al.	Toluene, Phenol, Naphthalene	Rice husk char (RHC) Acid washed RHC (H-form) K-loaded RHC (K-form) Ca-loaded RHC (800˚C)	800˚C	900-1500 (parent)	H_2O/CO_2
[62] Hervy et al	Ethylbenzene	Wood pallets/Food waste/ Sludge char (700˚C)	400, 650˚C	500 -1600	N_2, CO

The effect of temperature on the reaction pathways taking place at the char surface were investigated by Egsgaard et al.[52]. They evaluated the irreversible binding of aromatic compounds on wood char up to 800°C, by using a small char bed (6 g). The breakthrough of the model compounds was observed by stable isotope dilution analysis: binding within the bed was measured by the ^{13}C content of the char using $^{13}C_6$-benzene as a tracer. Starting already at 600-650°C char was able to bind tars, with increasing efficiency at higher temperature (up to 800°C). It was observed that, at 700-800°C, aromatics were covalently bound to the char surface by radical reactions, becoming part of the char. Naphthalene and phenanthrene were bound more efficiently than lighter compounds whereas phenol showed a different behavior. None of the introduced phenol could be collected after the char bed, partly because of decarbonylation and conversion to naphthalene. Such results suggest that in presence of a gasifying agent, aromatics could form covalent bonds with the char bed, while carbon could simultaneously be removed by gasification reactions in what the authors call a "living char bed".

Several studies have focused on the evaluation of the achievable conversion values for tar model compounds over char, depending on the properties of char and on the reaction conditions.

The catalytic effect of wood char in cracking and reforming of phenol and naphthalene was investigated by El-Rub et al.[53]. The activities of pine wood char, commercial biochar and pine wood ashes were compared with common catalysts for tar removal, by measuring the change in concentration between inlet and outlet of a heated reactor. At 700°C, over commercial biochar, 82 wt% of phenol and 99.6 wt% of naphthalene were converted. For naphthalene, biomass char showed the second highest activity among the tested catalysts, after the nickel catalyst. Pure biomass ash produced at 600°C showed a lower activity for naphthalene conversion in comparison with biomass char. This suggests that the carbon structure has a role itself in the enhancement of the catalytic activity, acting as a support for the inorganics contained in the parent feedstock (in this case MgO, CaO, K_2O).

These results validate the hypothesis that char has a catalytic effect on decomposition of tars, but the mechanism of the process is not clarified. Hosokai et al.[37] provided a more detailed description of the decomposition process**.** They monitored the decomposition rate of model tars over char and the concurrent formation rate of CO, CO_2 and CH_4 under different atmospheres: N_2, N_2/steam, and N_2/H_2/steam. Under all conditions, aromatics were found to decompose mainly by deposition on the char surface by coking (Reaction (3)), and not by steam reforming (Reaction (4)).

$$C_mH_n \text{ (aromatics)} = C_mH_x \text{ (coke)} + (n-x)/2H_2 \quad \text{(Coking/Cracking)} \tag{3}$$

$$C_mH_n \text{ (aromatics)} + H_2O = (m+ n/2)H_2 + mCO \quad \text{(Steam Reforming)} \tag{4}$$

Micropores constituted active sites for deposition. Deactivation of char was observed under N_2 atmosphere, whereas catalytic activity of char was maintained in presence of steam: gasification reactions enhanced the formation of micropores, preventing the blockage of active sites by coking. For this reason, it is suggested that the gasification rate should be equivalent or greater than the carbon deposition rate, in order to preserve the catalytic activity of char. On the other hand, the addition of H_2 resulted in a slower, but still extensive, decomposition of aromatics. For benzene and naphthalene, lower inlet concentrations led to increased conversion: the initial concentration appeared to be a factor influencing the decomposition.

It is concluded that, if char has a sufficiently large micropore surface area, naphthalene can decompose completely at 750°C, with a residence time of 0.2 s. Naphthalene, phenol and phenanthrene can reach almost total conversion at 800-900°C with a steam concentration of 15.5% v/v. Aromatics with more rings per molecule, hence phenanthrene and pyrene, were found to decompose more rapidly than lighter compounds.

Some of these results were verified by Fuentes Cano et al.[38]. Using a laboratory fixed bed reactor, they investigated the influence of temperature, steam concentration in the gas on the decomposition rate of toluene and naphthalene, and proposed kinetic expressions to describe the process. Tests were run on three chars originating from various materials and with different surface structure, but the parent material of char did not significantly affect the tar conversion. At 750°C the conversion rate reached 0.8% for toluene and nearly 100% for naphthalene. Above 850°C, the decomposition of both compounds was fast and almost complete. However, continuous deactivation of the char activity was observed in both cases. In contrast, at 950°C, and with a steam concentration of 15% v/v in the gas, the activity of char was maintained. In general, higher temperatures led to a higher conversion and a lower degree of char deactivation with time. The authors propose a two-step conversion mechanism:

(i) tar deposition on active sites and polymerization, with H_2 and carbon deposition;

(ii) gasification of deposited carbon.

Such steps retrace the mechanism proposed by Hosokai et al.[37], a mechanism which is also corroborated by Nitsch et al.[54], who further investigated the role of steam in the interaction between tars and the char surface. Phenol degradation was measured over a fixed bed of char in N_2 atmosphere, and with injection of steam and H_2. In inert atmosphere, a large amount of phenol was observed in the outlet stream, and coking on micropores was evident. Addition of H_2 did not show any major effect on

tar reforming. In contrast, in the presence of steam, char showed a strong catalytic activity for phenol removal.

Huang et al.[55] measured the decomposition of toluene over the surface of sewage sludge char (SSC), in N_2 atmosphere. They compared the activity of SSC with bottom ashes from a waste incinerator, dolomite and catalyst $NiO/\gamma\text{-}Al_2O_3$. The latter one produced the highest toluene conversion ratio, followed by dolomite, SSC and bottom ashes. SSC gave a conversion rate as high as 94.5% at 950°C. The conversion increased significantly when the temperature was raised from 750°C to 950°C, and since the H_2 yield followed the same trend in presence of a catalyst, the authors infer that all tested materials promoted cracking of toluene. In all cases coke deposition occurred, followed by a decrease in BET area. The same phenomenon was also observed in further experiments by the same research group [56], where the effect of the addition of H_2, CO, CO_2, steam and HCl was studied on tar cracking and conversion, char pore structure and stability have been examined. The addition of CO_2 and H_2O favored the further reaction of deposited coke thus limiting the loss of surface area. At 950°C and in presence of CO_2, and H_2O mixed with N_2, the toluene conversion reached 97.1%. The authors surmise that H_2O plays a crucial role in the tar cracking process as it takes part in steam reforming as well as in water gas and water-gas shift (Reactions (5) and (6)).

$C+H_2O \rightarrow H_2 + CO$ (Water gas) (5)

$CO+H_2O \rightarrow H_2 + CO_2$ (Water-gas shift) (6)

The addition of HCl (which is a common compound produced from municipal solid waste gasification) had a negative effect on the activity of SSC, because it induced the nucleation of chlorides that participated in blocking the pores. In agreement with Fuentes Cano et al.[38], they observed that presence of CO_2 and H_2O and higher temperatures prevent deactivation of char.

The decomposition of toluene over char was also investigated by Bhandari et al.[57] at 700 and 800°C in a fixed bed reactor. The activity of gasification-derived biochar was compared with the activity of the same material after activation and after being coated with citric acid to obtain an acidic carbon surface. The toluene conversion was measured in N_2 atmosphere: the three materials were effective in reducing the toluene concentration with conversion in the range 79-92%. The average conversion was higher for activated carbons than for raw biochar: 86% against 9% at 700°C. The acidification of the surface improved the conversion of toluene only at 800°C. In contrast with other studies, the addition of artificial syngas was not beneficial but slightly decreased the conversion rate in the range 69-88%. According to the authors, this effect was due to the adsorption of the gases on the carbon surface.

However, the composition of the artificial syngas could have affected the results, particularly because of the abundance of CO. For comparison, the compositions of artificial syngases used in the studies of Bhandari et al.[57] and Lu et al.[56] are reported in Table 5.

Table 5: *Artificial syngas compositions from Bhandari et al.*[57] *and Lu et al.*[56]

	H_2 [%]	CH_4	CO_2	CO	H_2O	others
[57]**Bhandari et al.**	5.2	7.5	16.8	19.3	-	N_2 balance
[56]**Lu et al.**	-	-	12.5	-	15	N_2 72.5%
	6	-	-	5	15	N_2 74%

Activated carbon with acidic surface was less efficient in toluene removal in comparison with the other tested chars; however, the authors suggest that the increased acidity could be useful for removing NH_3 in the producer gas. The significant difference in the performance of raw biochar and activated biochar is ascribed to the low surface area (64 m^2/g) and pore volume (0.09 cm^3/g) of the raw material, whereas the tested AC had a pore volume five times higher and a BET surface of 944 m^2/g.

The effectivity of biochar in enhancing the conversion of toluene was also reported by Mani et al.[58], who measured a conversion ratio of 94% at 900°C in N_2/H_2O atmosphere, with benzene as intermediate product of the cracking reactions. Formation of benzene as a product of toluene decomposition was also observed by Korus et al.[59]. During tests in the temperature range 650-950 °C under inert atmosphere, coke deposition on the surface of AC was measured simultaneously with the benzene production: these two effects resulted to be products of competing pathways of toluene decomposition. The measured conversion of toluene was over 90% when the temperature was 800°C and higher. Conversion was very efficient only as long as the AC surface was active (20 minutes). As soon as the coke deposition became hindered by coking on the AC surface, benzene formation was enhanced. An overview of the toluene conversion ratios obtained over different chars can be found in Table 6.

Table 6: *Overview of conversion efficiencies for toluene (n.r. = not reported)*

Toluene	Char	BET	Initial concentration C_{in}	Atmosphere	Reaction T	Residence time	Conversion ratio $\frac{C_{in}-C_{out}}{C_{in}} * 100$
		[m^2/g]	[g/Nm^3]		[°C]	[s]	[%]
[38] Fuentes Cano et al.	Coconut char	597	12	N_2 ,H_2O, H_2	750	0.3	80 - 40
[55]Huang et al.	Sewage sludge char	38	12.9	N_2	750	0.3	68.8
[56] Lu et al.	Sewage sludge char	74	12.9	N_2, H_2O,CO_2	750	0.3	69.2
				N_2, H_2O, H_2, CO	750	0.3	69.0
[57] Bhandari et al.	Switchgrass char	64	2 ml/h	N_2	700	0.035 [Kg*h/m^3]	78.7
	Activated switchgrass char	944					86.3
[58] Mani et al.	Pine bark char	310-331	9.6 (2500 ppmv)	N_2 ,H_2O	700	1.3	~25
[38] Fuentes Cano et al.	Coconut char	597	12	N_2 ,H_2O, H_2	850	0.3	100 - 50
[55] Huang et al.	Sewage sludge char	38	12.9	N_2	850	0.3	81.5
[56] Lu et al.	Sewage sludge char	74	12.9	N_2, H_2O,CO_2	850	0.3	86.5
				N_2, H_2O, H_2, CO			86.0
[57] Bhandari et al.	Switchgrass char	64	2 ml/h	N_2	800	0.035 [Kg*h/m^3]	81
	Activated switchgrass char	944					91.7
[58] Mani et al.	Pine bark char	310-331	9.6 (2500 ppmv)	N_2 ,H_2O	800	1.3	~ 45
					900		94
[61] Feng et al.	K-loaded rice husk char	n.r.	0.1 ml/min	CO_2, H_2O	800	n.r.	100

Naphthalene is a widely used model tar, as it represents one of the most abundant and recalcitrant components of the tar mixture in producer gas. Results on naphthalene conversion efficiencies are gathered in Table 7. Zhang et al.[39] compared the heterogeneous cracking of naphthalene over char with homogeneous decomposition in inert atmosphere. Three different chars were tested: rice straw char, rice straw char loaded with $Ni(NO_3)_2$ and water-washed char. Heterogeneous conversion was generally higher than homogeneous conversion, but char showed decreased catalytic activity with time, accompanied by a lower BET surface area. In agreement with previous works, this effect was attributed

to the carbon deposition on the active sites of the surface, which is identified as the main decomposition pathway. Nickel-loaded char showed a higher initial activity but a more rapid deactivation, whereas water-washed char induced a generally lower naphthalene conversion in comparison with original rice straw char. Addition of artificial syngas (a mixture of H_2, CO, CO_2 and CH_4) resulted in a delayed deactivation of the original rice straw char. Zhang et al.[39] formulated the heterogeneous catalysis for naphthalene decomposition over char in 3 steps:

(i) adsorption on active sites;
(ii) dissociation into radicals (naphthyl and hydrogen);
(iii) desorption of radicals.

In an inert atmosphere, radicals react with each other in polymerization and soot formation. If oxidative species are present, they generate mono-ring aromatics, hydrocarbons and gases.

Di Gregorio et al.[23] focused on naphthalene as well and tested the effectivity of three commercial ACs for adsorption and cracking. The characterization of ACs showed that they had different surface areas and pore size distributions and contained varying amount of inorganics on the surface. The comparison between the performances of the ACs showed that Fe, Mg and Al enhance the cracking of tars. The highest and most stable naphthalene conversion in a 4 hours test was obtained on AC with larger specific surface area accompanied by a high micropore volume and appropriate pore size distribution (as described by [17] and [15]). Complete removal of naphthalene from the gas stream was achieved by all ACs at low naphthalene concentration (< 50 g/Nm^3), and for one of the tested ACs, also at higher concentrations (up to 176.7 g/Nm^3). The cracking efficiency decreased with higher concentrations, in agreement with the findings from Hosokai et al.[37].

Likewise Nestler et al.[60] investigated the catalytic activity of biochar towards naphthalene decomposition in inert atmosphere. Spruce wood was carbonized at 500°C and 800°C, and part of it was CO_2–activated. The activities of these chars were compared with that of commercial AC at 850 °C and 1050°C. CO_2 activation treatment increased the BET surface area (Table 7) and the microporosity (surface and volume) of char, resulting in an improved naphthalene conversion. All chars showed deactivation with time, due to coking and blocking of the active sites. Particularly, non-activated wood chars showed a low conversion rate and a fast deactivation, probably due to low pore volume (~0.15 cm^3/g). In contrast, activated wood chars with a higher surface area and a larger pore volume (~0.25 cm^3/g) performed similarly to the commercial AC.

Feng et al.[61] used K-loaded and Ca-loaded rice straw char to investigate the influence of AAEM on the char catalytic activity towards tar reforming, under H_2O or CO_2 atmosphere. Toluene, naphthalene and phenol were converted more efficiently in presence of steam, on the surface of K-loaded char. The authors suggest that carbon deposition is promoted by C-O-K clusters on the char surface, which constitute active sites. In contrast, Ca provides fewer active sites, as it bonds to the char with strong double bonds.

Overall, these results indicate that the char activity for tar model compounds decomposition is affected by the volume and size distribution of the pores (especially micropores), but also the inorganics on the surface affect the catalytic activity for tar cracking. Indeed, the effect of the mineral composition of char on tar cracking was also investigated by Hervy et al.[62]. Ethylbenzene was used as a model compound for aromatic hydrocarbons, and its conversion was measured on three different chars produced from waste materials: wood pallets (WP), food waste (FW), sludge (S). The chars were produced with pure WP, and mixing FW/S and WP/FW/S. Chars were thoroughly characterized with various analytical techniques in order to establish their structural and chemical characteristics: significant differences were observed in the composition of the inorganic fraction and in the carbon structure. In comparison with WP char, char produced from a mixture of FW and S was more effective in removing ethylbenzene from the gas stream, enhancing the cracking onto styrene, benzene, ethylene and toluene. The stronger catalytic activity was partly ascribed to a more disordered carbonaceous structure, but mostly to the higher ash content including Ca, P, Al and K oxides which were well dispersed on the surface.

Table 7: *Overview of conversion efficiencies for naphthalene (n.r. = not reported)*

Naphthalene	Char	BET	Initial concentration C_{in}	Atmosphere	Reaction T	Residence time	Conversion ratio $\frac{C_{in}-C_{out}}{C_{in}} * 100$
		[m^2/g]	[g/Nm^3]		[°C]	[s]	[%]
[37] Hosokai et al.	Commercial char	740	1.5	N_2 ,H_2O, H_2	700	0.2	73
[38] Fuentes Cano et al.	Coconut char	597	8	N_2 ,H_2O, H_2	750	0.3	90 – 30 (60 min)
[39] Zhang et al.	Rice straw char	262	25.2	Ar	700	20-30 mm bed height; 12mL/min gas flow	58
[23] Di Gregorio et al.	Activated coal char	740	50-176.7	N_2	750	50 mm bed height; 20mL/min gas flow	42
[53] El-Rub et al.	Commercial biomass char	n.r.	90	N_2, CO_2 ,H_2O	900	0.3	99.6
[37] Hosokai et al.	Commercial char	740	3	N_2 ,H_2O	850	0.2	> 99.9
				N_2 ,H_2O, H_2	850	0.2	94
[38] Fuentes Cano et al.	Coconut char	597	8	N_2 ,H_2O, H_2	850	0.3	100-60 (60 min)
[39] Zhang et al.	Rice straw char	262	25.2	Ar	800	20-30 mm bed height; 12mL/min gas flow	77
[23] Di Gregorio et al.	Activated coal char	740	14.2-176.7	N_2	850	50 mm bed height; 20mL/min gas flow	100
[60] Nestler et al.	Activated wood char	600	0.57	N_2	850	0.19	93-15 (120 min)
	Commercial AC	950	0.57	N_2			85-65 (120 min)
[61] Feng et al.	K-loaded rice husk char	n.r.	0.1 ml/min	CO_2, H_2O	800	n.r.	93.9

The overview of these works shows that the effectiveness of biochar in removing tar compounds in gas phase is comparable to that of commercial catalysts: conversion of model compounds can reach 100% under favorable conditions. However, the interaction between tars and char surface implies a complicated synergy of gas-phase and solid-gas reactions, and they can vary significantly depending on the char characteristics and on the reaction conditions: the achievable conversion is difficult to predict. It is evident that temperature plays an important role, and in order to reach a conversion rate over 90%, a minimum temperature of 800°C is needed.

The presence of reforming agents (H_2O, CO_2) appears to induce higher conversions, whereas addition of H_2 results slightly detrimental for both toluene [56] and naphthalene [37] conversions. This effect, even if not strong, could be due to the inhibitory effect of H_2 on gasification reactions also observed by Barrio et al.[63].

In general, naphthalene shows higher conversions in comparison to toluene, revealing a preferential interaction of char with heavier aromatics. This is in agreement with the findings of Hosokai et al.[37], who stated that molecules with more fused rings were decomposed faster, and with the preferential adsorption for PAH observed on AC by Mastral et al.[17]. Selectivity towards multi-ring aromatics has also been observed by researchers working with thermal decomposition of pyrolysis-derived tars [64,65]. Such evidence suggests a beneficial effect of partial oxidation of tars before contacting the char: oxidation modifies the tar composition, converting oxygenated compounds into simple PAHs, especially naphthalene [66].

5.2.1 Determination of kinetic parameters for Toluene and Naphthalene decomposition

Only a few papers have investigated kinetic parameters for decomposition of model tars, focusing on the kinetics of toluene and naphthalene [38,53,58,67]. For both compounds, the rate equations were found to follow first order kinetics, showing a linear increase in the reaction rate when increasing the inlet concentration.

$$-r_{tar} = k * [C_{tar}] \quad (7)$$

where r_{tar} is the tar decomposition rate, k is the rate constant and C_{tar} is the model compound concentration in the gas flow. The rate constant was estimated according to Arrhenius′ law

$$K = A * e^{\frac{-E_a}{RT}} \quad (8)$$

El-Rub et al.[53] evaluated the kinetic parameters of naphthalene when reacting on commercial biomass char, whereas Mani et al.[58] studied the reaction rate of toluene steam reforming over pine bark biochar. The same research group further investigated the change in the kinetics of toluene steam reforming when the same biochar was impregnated and calcined with iron. Results were published by Kastner et al.[68]. The effect of Fe was to increase the reaction rate and to lower the activation energy. Table 8 reports the kinetics values estimated from experiments on model tar decomposition.

Table 8: *Kinetics parameters for naphthalene and toluene decomposition over different chars*

Model tar	Catalyst	A [$m^3 Kg^{-1}h^{-1}$]	Ea [KJ/mol]
Naphthalene [53]	Commercial biomass char	$7.6 * 10^4$	61
Naphthalene [38]	Coconut biochar	$4 * 10^5$	72
Toluene [38]	Coconut biochar	$3.1 * 10^5$	75
Toluene [58]	Pine bark biochar	$2.6 * 10^5$	90.6
Toluene [68]	18.7% Fe-loaded biochar	$5.4 * 10^3$	48.4

These kinetic expressions only consider the initial activity of char for tar decomposition and they do not take into account any deactivation effect.

Fuentes Cano et al.[38] proposed an extended kinetic expression describing the effect of deactivation, introducing the activity factor a: the reaction rate is therefore expressed as in Equation (9).

$$-r_{tar} = k * [C_{tar}] * a \quad (9)$$

Where a=1 for fresh char; a<1 for partially deactivated char. Activity of char is defined as in Equation (10)

$$a = \frac{-r_{tar,t}}{-r_{tar,0}} \quad (10)$$

Where $r_{tar,t}$ is the reaction rate at time t and $r_{tar,o}$ is the initial reaction rate. The activity of char as a function of time was fitted to the empirical expression in Equation (11).

$$a = \frac{1}{1 + k_d t^p} \quad \text{with} \quad p = p_1 + p_2 \left(\frac{T}{1023}\right) \quad (11)$$

Where k_d, p_1 and p_2 are empirical parameters, and T is the char bed temperature, expressed in Kelvin. Comparison of the experimental results with this kinetic model showed a good agreement, being most data within ±20% of error, as showed in Figure 3. Based on these results, the kinetics of tar decomposition on char surfaces should be further investigated with the aim to develop accurate kinetic models and describe the reaction mechanism for different compounds.

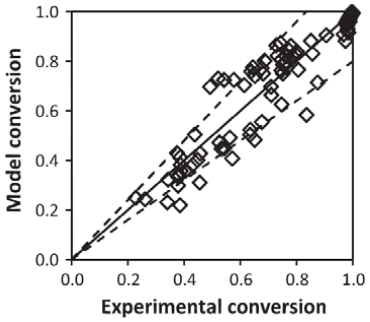

Figure 3: *Comparison of kinetic model (heavy line) with experimental results (squares). Dotted lines show ±20% deviation. (Reprinted from*[38]*, pag. 1233. Copyright 2013 Elsevier)*

5.2.2 Carbon deposition and char deactivation

The main reaction pathway for model tars decomposition over char appears to be carbon deposition by polymerization (or coking) on the active sites of the surface. This was observed for both alkanes and aromatics: Figure 4 shows spent char samples after propane and methane exposure, Figure 5 and 6 show coke formation after toluene decomposition, whereas the effect of naphthalene exposure on the char structure are captured in Figure 7 . Coking was often found to cause deactivation of the carbon surface, especially under inert atmosphere. SEM analysis has been widely applied for visualization of deposited carbon [41,57,58,60]: Carbon deposits take up different shapes depending on the reaction conditions. The polymerization is enhanced by specific active sites, as visible in Figure 4(b) for methane deposition.

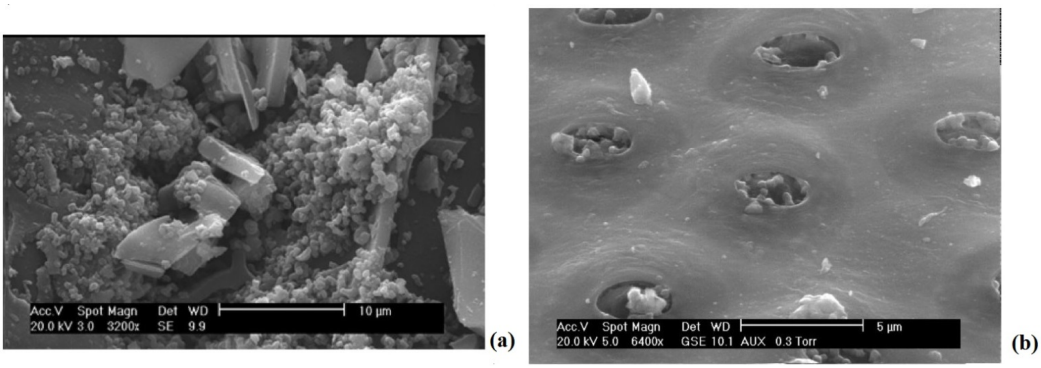

Figure 4: *Carbon deposits on char after propane (a) and methane (b) catalytic decomposition. (Adapted with permission from [41] Copyright 2012 American Chemical Society).*

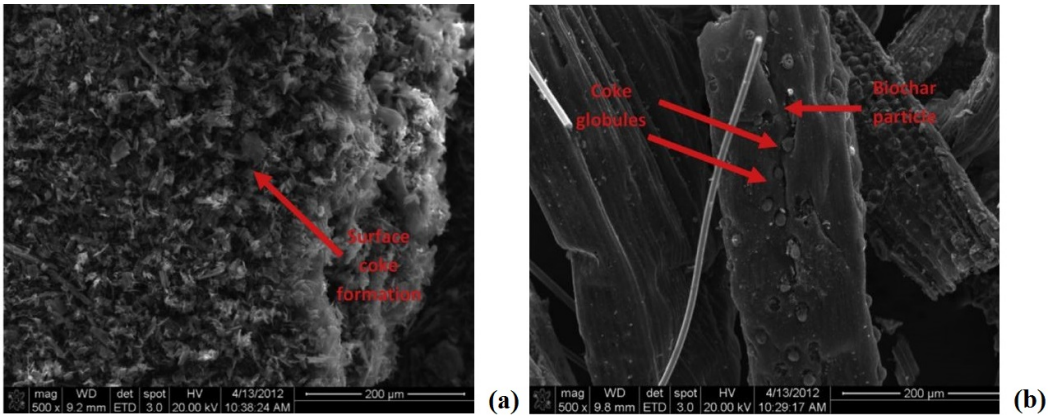

Figure 5: *Carbon deposits on AC (a) and biochar (b) from toluene decomposition in producer gas atmosphere at 700 °C. (Adapted from* [45] *pag 351. Copyright 2014 Elsevier)*

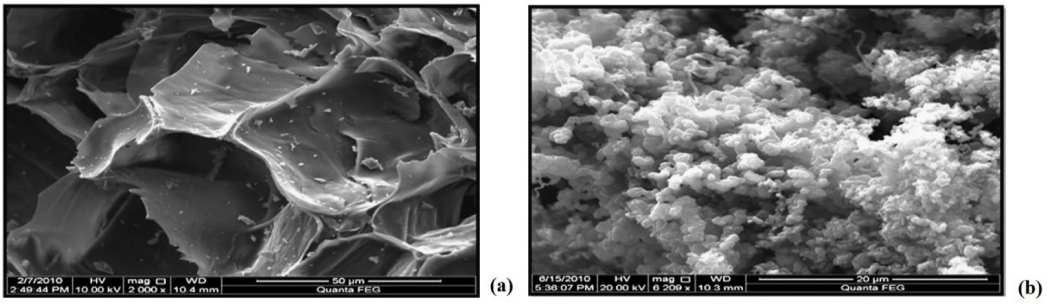

Figure 6: *Fresh pine bark char (a) and spent char (b) after 6 days of toluene exposure at 800°C. (Reprinted from* [46], *pag 124. Copyright 2013 Elsevier)*

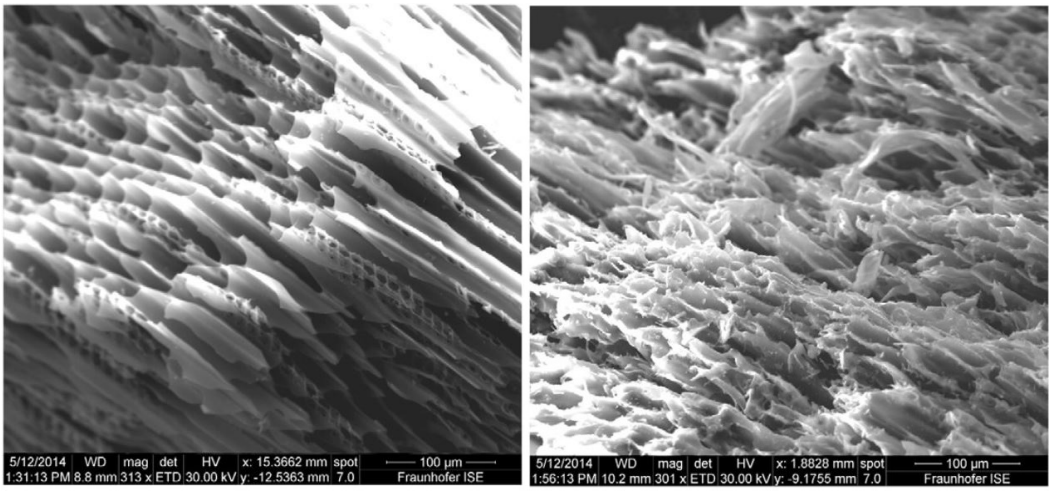

Figure 7: *Structural changes in activated biochar after 5 hours of naphthalene exposure at 850°C. The tracheids fracturing is due to cracking reactions, including carbon deposition. (Adapted from* [60]*, pag 38. Copyright 2016 Elsevier)*

Both Hosokai et al.[37] and Nestler et al.[60] observed that on deactivated char, micropore volume was reduced, whereas mesopore volume remained unaltered. This result clearly indicates that micropores are active sites for carbon deposition. This also explains the fact that deactivation is faster on microporous carbons under inert atmosphere, when the deposited carbon quickly blocks the micropore mouths [60]. In contrast, in presence of H_2O and CO_2, the activity of char is maintained in time and the yield of stable gases is improved, particularly H_2, CO, CO_2 and, to a lesser extent, CH_4.

6. Conclusion

The overview of the above summarized studies outlines the state-of-the -art in the understanding of interactions between tar compounds and carbonaceous surface. All in all, it is evident that char has a beneficial effect on the removal or conversion of tar model compounds from a gaseous flow, and could be used as adsorbent or catalyst for gas cleaning. Chars produced with gasification and pyrolysis can be comparable to activated carbons in terms of effectivity for decomposition of model tars. The processes taking place at the surface strongly depend on the reaction conditions: adsorption is predominant at lower temperatures, whereas reforming reactions require higher temperatures and presence of CO_2 or H_2O in the gas phase. Biomass char can catalyze the decomposition of CH_4 and C_3H_8 producing H_2. The

induced conversion of toluene and phenol can be higher than 80% at 800°, whereas naphthalene can reach 100% conversion upon contact with the char surface.

Biomass char can be suitable to be used as a catalyst in producer gas treatment for removing tars, especially multi-ring aromatics: indeed, biochar appears to catalyze tars cracking and reforming due to a synergy of surface chemistry and morphology. However, the properties of the char surface and the reaction conditions must be optimized in order to achieve complete conversion

In general, the abundance of active sites is favored by defects in the carbon structure (microcrystallinity, turbostratic carbon), and in presence of inorganic impurities. In particular, AAEM and metals (e.g. Fe, Al) appear to be effective in forming active sites, when they are well dispersed at accessible sites (micropores) on the surface. As a matter of fact, pure biomass ash always showed a lower activity in comparison with biomass char [25,53,55], indicating that the presence of carbon improves the catalytic activity acting as support.

It is difficult to quantify the effect of oxygen-containing functional groups, because at high temperature they are disrupted and simultaneously created by carbon deposition. For CH_4 decomposition they were found to have an effect only in the initial activity of char [34] or no effect at all [25], and to have a negative effect on PAHs adsorption [51] and toluene decomposition [57]. In general, their effect on the decomposition of both alkanes and aromatics appears as secondary.

In contrast, the surface area (generally quantified with BET values) emerges as an important factor, together with the pore volume and the pore size distribution: the ratio between the micropore volume and the total pore volume should be high, as active sites appear to be housed in the micropores. A good pore structure enhances the long term activity of biochar as a catalyst, especially in presence of a reforming agent. In inert atmosphere, coking on the char surface leads to blocking of the active sites. Therefore, to prevent deactivation, the following points should be considered:

(i) The char should have a high micropore volume, but the pore size distribution should include mesopores, so that diffusion is not hindered.

(ii) H_2O or CO_2 should be present, together with a temperature high enough to allow the gasification of deposited carbon.

Steam or dry reforming can be useful to create a dynamic equilibrium of coke deposition and gasification in the catalytic bed: the rate of gasification should be equal or higher to the rate of coke deposition, but not so high to quickly consume the solid bed.

An optimal solution for gas cleaning in biomass gasification would be the use of residual char as catalyst, possibly without further treatments. For the practical implementation of such solution, it would be useful to define correlations between the rate of tar decomposition, or the tar reactivity, and the char characteristics and reaction conditions, for representative model tars.

The reaction conditions to be considered should be:

- Temperature and pressure
- Gas phase composition (N_2, H_2O, H_2, O_2, CO)
- Tar species concentration
- Residence time

Determinant char properties that should be regarded are:

- Specific surface area (BET)
- Total pore volume
- Pore size distribution: micropores volume to total volume ratio, or average pore diameter
- Concentration of inorganic elements on the char surface

All of these parameters are interdependent, and together they influence the effectivity of model tar conversion. With this in mind, it would be beneficial to dedicate future research activities to testing of char beds for the cleaning of real producer gas, with the aim to optimize and balance tar conversion and char gasification for an effective and stable gas cleaning.

Acknowledgements

The authors thank Innovationsfonden for the financial support received as part of the project "SYNFUEL - Sustainable synthetic fuels from biomass gasification and electrolysis" (4106-00006B).

References

[1] Devi L, Ptasinski KJ, Janssen FJJG. A review of the primary measures for tar elimination in biomass gasification processes. Biomass and Bioenergy 2003;24:125–40.

[2] Brewer CE, Schmidt-Rohr K, Satrio JA, Brown RC. Characterization of Biochar from Fast Pyrolysis and Gasification Systems. Environ Prog Sustain Energy 2009;28:386–96. doi:DOI 10.1002/ep.

[3] Benedetti V, Patuzzi F, Baratieri M. Characterization of char from biomass gasification and its similarities with activated carbon in adsorption applications. Appl Energy 2018;227:92–9. doi:10.1016/j.apenergy.2017.08.076.

[4] Köchling K, McEnaney B, Rozploch F, Fitzer E. International Committee for Characterization Terminology of Carbon " First Publication of 30 Tentative Definitions ." Carbon N Y 1982;20:445–9.

[5] Köchling K, McEnaney B, Müller S, Fitzer E. International Committee for Characterization and Terminology of Carbon "First Publication of Further 24 Tentative Definitions". Carbon N Y 1985;23:601–3. doi:10.1016/0008-6223(83)90145-8.

[6] Rodríguez-Reinoso F. The role of carbon materials in heterogeneous catalysis. Carbon N Y 1998;36:159–75. doi:10.1016/S0008-6223(97)00173-5.

[7] Keiluweit M, Nico PS, Johnson M, Kleber M. Dynamic molecular structure of plant biomass-derived black carbon (biochar). Environ Sci Technol 2010;44:1247–53. doi:10.1021/es9031419.

[8] Schimmelpfennig S, Glaser B. One Step Forward toward Characterization: Some Important Material Properties to Distinguish Biochars. J Environ Qual 2012;32. doi:10.2134/jeq2011.0146.

[9] Mastral AM, García T, Murillo R, Callen MS, Lopez JM, Navarro M V. Development of efficient adsorbent materials for PAH cleaning from AFBC hot gas. Energy and Fuels 2004;18:202–8. doi:10.1021/ef030058+.

[10] Dasgupta K, Sathiyamoorthy D. Disordered carbon–its preparation, structure, and characterisation. Mater Sci Technol 2003;19:995–1002. doi:10.1179/026708303225004693.

[11] European Biochar Foundation (EBC). Guidelines for a Sustainable Production of Biochar. Arbaz, Switzerland, 2016. doi:10.13140/RG.2.1.4658.7043.

[12] International Biochar Initiative. Standardized Product Definition and Product Testing Guidelines for Biochar That Is Used in Soil 2015:1–61.

[13] Bansal RC, Donnet J-B, Stoeckli F. Active Carbon. New York and Basel: Marcel Dekker, Inc.; 1988.

[14] Stoeckli HF. Microporous carbons and their characterization: The present state of the art. Carbon N Y 1990;28:1–6. doi:10.1016/0008-6223(90)90086-E.

[15] Hu X, Hanaoka T, Sakanishi K, Shinagawa T, Matsui S, Tada M, et al. Removal of Tar Model Compounds Produced from Biomass Gasification Using Activated Carbons. J Japan Inst Energy

2007;86:707–7011. doi:10.1093/bioinformatics/btu635.

[16] Mastral AM, García T, Murillo R, Callén MS, López JM, Navarro M V. Measurements of Polycyclic Aromatic Hydrocarbon Adsorption on Activated Carbons at Very Low Concentrations. Ind Eng Chem Res 2003:155–61.

[17] Mastral A, García T, Callén M, Navarro M, Galbán J. Assessement of Phenanthrene Removal from Hot Gas by Porous Carbons. Energy & Fuels 2001;15:1–7. doi:10.1021/ef000116g.

[18] Franz M, Arafat HA, Pinto NG. Effect of chemical surface heterogeneity on the adsorption mechanism of dissolved aromatics on activated carbon. Carbon N Y 2000;38:1807–19. doi:Doi 10.1016/S0008-6223(00)00012-9.

[19] Vidic RD, Suidan MT. Role of dissolved oxygen on the adsorptive capacity of activated carbon for synthetic and natural organic matter. Environ Sci Technol 1991;25:1612–8. doi:10.1021/es00021a013.

[20] Leng C-C, Pinto NG. Effects of surface properties of activated carbons on adsorption behavior of selected aromatics. Carbon N Y 1997;35:1375–85. doi:10.1016/S0008-6223(97)00091-2.

[21] Arafat HA, Franz M, Pinto NG. Effect of Salt on the Mechanism of Adsorption of Aromatics on Activated Carbon. Langmuir 1999:5997–6003.

[22] Cudahy JJ, Helsel RW. Removal of products of incomplete combustion with carbon. Waste Manag 2000;20:339–45. doi:10.1016/S0956-053X(99)00335-9.

[23] Di Gregorio F, Parrillo F, Salzano E, Cammarota F, Arena U. Removal of naphthalene by activated carbons from hot gas. Chem Eng J 2016;291:244–53. doi:10.1016/j.cej.2016.01.081.

[24] Liu W-J, Zeng F-X, Jiang H, Zhang X-S. Preparation of high adsorption capacity bio-chars from waste biomass. Bioresour Technol 2011;102:8247–52. doi:10.1016/j.biortech.2011.06.014.

[25] Klinghoffer NB, Castaldi MJ, Nzihou A. Influence of char composition and inorganics on catalytic activity of char from biomass gasification. Fuel 2015;157:37–47. doi:10.1016/j.fuel.2015.04.036.

[26] Min Z, Yimsiri P, Asadullah M, Zhang S, Li C-Z. Catalytic reforming of tar during gasification. Part II. Char as a catalyst or as a catalyst support for tar reforming. Fuel 2011;90:2545–52. doi:10.1016/j.fuel.2011.03.027.

[27] Benedetti V, Patuzzi F, Baratieri M. Gasification char as a potential substitute of activated carbon in adsorption applications. Energy Procedia 2016;00.

[28] Qian K, Kumar A. Catalytic reforming of toluene and naphthalene (model tar) by char supported nickel catalyst. Fuel 2017;187:128–36. doi:10.1016/j.fuel.2016.09.043.

[29] Font Palma C. Modelling of tar formation and evolution for biomass gasification: A review. Appl Energy 2013;111:129–41. doi:10.1016/j.apenergy.2013.04.082.

[30] Mastral AM, García T, Murillo R, Callén MS, López JM, Navarro M V. PAH Mixture Removal from Hot Gas by Porous Carbons . From Model Compounds to Real Conditions 2003:5280–6.

[31] Mastral AM, García T, Murillo R, Callen MS, Lopez JM, Navarro M V. Moisture effects on the phenanthrene adsorption capacity by carbonaceous materials. Energy and Fuels 2002;16:205–10. doi:10.1021/ef010214h.

[32] Muradov N. Hydrogen via methane decomposition : an application for decarbonization of fossil fuels. Int J Hydrogen Energy 2001;26:1165–75.

[33] Muradov N, Smith F, T-Raissi A. Catalytic activity of carbons for methane decomposition reaction. Catal Today 2005;102–103:225–33. doi:10.1016/j.cattod.2005.02.018.

[34] Moliner R, Suelves I, Lázaro MJ, Moreno O. Thermocatalytic decomposition of methane over activated carbons: Influence of textural properties and surface chemistry. Int J Hydrogen Energy 2005;30:293–300. doi:10.1016/j.ijhydene.2004.03.035.

[35] Suelves I, Pinilla JL, Lázaro MJ, Moliner R. Carbonaceous materials as catalysts for decomposition of methane. Chem Eng J 2008;140:432–8. doi:10.1016/j.cej.2007.11.014.

[36] Dufour A, Celzard A, Fierro V, Martin E, Broust F, Zoulalian A. Catalytic decomposition of methane over a wood char concurrently activated by a pyrolysis gas. Appl Catal A Gen 2008;346:164–73. doi:10.1016/j.apcata.2008.05.023.

[37] Hosokai S, Kumabe K, Ohshita M, Norinaga K, Li C, Hayashi J-I. Mechanism of decomposition of aromatics over charcoal and necessary condition for maintaining its activity. Fuel 2008;87:2914–22. doi:10.1016/j.fuel.2008.04.019.

[38] Fuentes-Cano D, Gómez-Barea A, Nilsson S, Ollero P. Decomposition kinetics of model tar compounds over chars with different internal structure to model hot tar removal in biomass gasification. Chem Eng J 2013;228:1223–33. doi:10.1016/j.cej.2013.03.130.

[39] Zhang Y, Luo Y, Wu W, Zhao S, Long Y. Heterogeneous Cracking Reaction of Tar over Biomass Char, Using Naphthalene as Model Biomass Tar. Energy & Fuels 2014;28:3129–37. doi:10.1021/ef4024349.

[40] Dufour A, Celzard A, Fierro V, Broust F, Courson C, Zoulalian A, et al. Catalytic conversion of methane over a biomass char for hydrogen production: deactivation and regeneration by steam gasification. Appl Catal A Gen 2015;490:170–80. doi:10.1016/j.apcata.2014.10.038.

[41] Klinghoffer N, Castaldi MJ, Nzihou A. Catalyst Properties and Catalytic Performance of Char from Biomass Gasification. I&Ec 2012:13113–22. doi:10.1021/ie3014082.

[42] Karatza D, Musmarra D. Fly Ash Capture of Mercuric Chloride Vapors from Exhaust Combustion Gas. Environ Sci Technol 1998;32:3999–4004.

[43] Lowell, S. ; Shields, Joan E.; Thomas, Martin A.; Thommes M. Characterization of porous solids and powders: surface area, pore size and density. Kluwer Academic; 2004.

[44] Tsonopoulos C, Ambrose D. Vapor-Liquid Critical Properties of Elements and Compounds . 3 . Aromatic Hydrocarbons. J Chem Eng Data 1995:547–58. doi:10.1021/je00019a002.

[45] Lamichhane S, Krishna KCB, Sarukkalige R. Polycyclic aromatic hydrocarbons (PAHs) removal by sorption : A review. Chemosphere 2016;148:336–53. doi:10.1016/j.chemosphere.2016.01.036.

[46] Li H, Qu R, Li C, Guo W, Han X, He F, et al. Selective removal of polycyclic aromatic hydrocarbons (PAHs) from soil washing effluents using biochars produced at different pyrolytic temperatures. Bioresour Technol 2014;163:193–8. doi:10.1016/j.biortech.2014.04.042.

[47] Chen B, Zhou D. Transitional Adsorption and Partition of Nonpolar and Polar Aromatic Contaminants by Biochars of Pine Needles with Different Pyrolytic Temperatures. Environ Sci Technol 2008;42:5137–43.

[48] Mastral AM, García T, Callén MS, Navarro M V., Galbán J. Removal of naphthalene, phenanthrene, and pyrene by sorbents from hot gas. Environ Sci Technol 2001;35:2395–400. doi:10.1021/es000152u.

[49] Mastral A, García T, Murrillo R, Callén MS, Lopez JM, Navarro M V, et al. Study of the Adsorption of Polyaromatic Hydrocarbon Binary Mixtures on Carbon Materials by Gas-Phase Fluorescence Detection. Energy & Fuels 2003:669–76.

[50] García T, Murillo R, Cazorla-Amorós D, Mastral AM, Linares-Solano A. Role of the activated carbon surface chemistry in the adsorption of phenanthrene. Carbon N Y 2004;42:1683–9. doi:10.1016/j.carbon.2004.02.029.

[51] Lillo-Ródenas M, Cazorla-Amorós D, Linares-Solano A. Behaviour of activated carbons with different pore size distributions and surface oxygen groups for benzene and toluene adsorption at low concentrations. Carbon N Y 2005;43:1758–67. doi:10.1016/j.carbon.2005.02.023.

[52] Egsgaard H, Ahrenfeldt J, Ambus P, Schaumburg K, Henriksen UB. Gas cleaning with hot char beds studied by stable isotopes. J Anal Appl Pyrolysis 2014;107:174–82. doi:10.1016/j.jaap.2014.02.019.

[53] Abu El-Rub Z, Bramer EA, Brem G. Experimental comparison of biomass chars with other catalysts for tar reduction. Fuel 2008;87:2243–52. doi:10.1016/j.fuel.2008.01.004.

[54] Nitsch X, Commandré J-M, Valette J, Volle G, Martin E. Conversion of Phenol-Based Tars over Biomass Char under H2 and H2O Atmospheres. Energy & Fuels 2014:28 (2014) 6936-6940. doi:10.1021/ef500980g.

[55] Huang Q, Lu P, Hu B, Chi Y, Yan J. Cracking of model tar species from the gasification of municipal solid waste using commercial and waste derived catalysts. Energy & Fuels 2016:acs.energyfuels.6b00711. doi:10.1021/acs.energyfuels.6b00711.

[56] Lu P, Qian X, Huang Q, Chi Y, Yan J. Catalytic cracking of toluene as a tar model compound using sewage sludge derived char. Energy & Fuels 2016:acs.energyfuels.6b01832. doi:10.1021/acs.energyfuels.6b01832.

[57] Bhandari PN, Kumar A, Bellmer DD, Huhnke RL. Synthesis and evaluation of biochar-derived catalysts for removal of toluene (model tar) from biomass-generated producer gas. Renew Energy 2014;66:346–53. doi:10.1016/j.renene.2013.12.017.

[58] Mani S, Kastner JR, Juneja A. Catalytic decomposition of toluene using a biomass derived catalyst. Fuel Process Technol 2013;114:118–25. doi:10.1016/j.fuproc.2013.03.015.

[59] Korus A, Samson A, Szle A, Katelbach-woz A. Pyrolytic toluene conversion to benzene and coke over activated carbon in a fixed-bed reactor. Fuel 2017;207:283–92. doi:10.1016/j.fuel.2017.06.088.

[60] Nestler F, Burhenne L, Amtenbrink MJ, Aicher T. Catalytic decomposition of biomass tars: The impact of wood char surface characteristics on the catalytic performance for naphthalene removal. Fuel Process Technol 2016;145:31–41. doi:10.1016/j.fuproc.2016.01.020.

[61] Feng D, Zhao Y, Zhang Y, Sun S, Meng S, Guo Y, et al. Effects of K and Ca on reforming of model tar compounds with pyrolysis biochars under H2O or CO2. Chem Eng J 2016;306:422–32. doi:10.1016/j.cej.2016.07.065.

[62] Hervy M, Berhanu S, Weiss-Hortala E, Chesnaud A, Gérente C, Villot A, et al. Multi-scale characterisation of chars mineral species for tar cracking. Fuel 2017;189:88–97. doi:10.1016/j.fuel.2016.10.089.

[63] Barrio M, Gøbel B, Rimes H, Henriksen U, Hustad JE, Sørensen LH. Steam Gasification of Wood Char and the Effect of Hydrogen Inhibition on the Chemical Kinetics. Prog Thermochem Biomass Convers 2008:32–46. doi:10.1002/9780470694954.ch2.

[64] Boroson ML, Howard JB, Longwell JP, Peters W a. Heterogeneous cracking of wood pyrolysis tars over fresh wood char surfaces. Energy & Fuels 1989;3:735–40. doi:10.1021/ef00018a014.

[65] Krerkkaiwan S, Tsutsumi A, Kuchonthara P. Biomass derived tar decomposition over coal char bed. ScienceAsia 2013;39:511. doi:10.2306/scienceasia1513-1874.2013.39.511.

[66] Ahrenfeldt J, Egsgaard H, Stelte W, Thomsen T, Henriksen UB. The influence of partial oxidation mechanisms on tar destruction in TwoStage biomass gasification. Fuel 2013;112:662–80. doi:10.1016/j.fuel.2012.09.048.

[67] Juneja, Ankita; Mani, Sudhagar; Kastner J. Catalytic Cracking of Tar using BioChar as a Catalyst. ASABE Annu. Int. Meet., 2010.

[68] Kastner JR, Mani S, Juneja A. Catalytic decomposition of tar using iron supported biochar. Fuel Process Technol 2015;130:31–7. doi:10.1016/j.fuproc.2014.09.038.

Activity of chars and activated carbons for removal and decomposition of tar generated by pyrolysis and gasification

1.1 Introduction

The previous section of this review was dedicated to those studies where model compounds such as phenol, toluene and naphthalene were used to investigate the interaction between tar and the surface of carbonaceous materials. The results of these works can be useful to predict the behavior of real tar mixtures upon contact with char. However, several authors have been working with actual tar generated by pyrolysis or gasification. Real tar mixtures are constituted by a wide variety of compounds, mostly aromatics. These include mono-ring molecules such as phenolic compounds or toluene, heterocyclic aromatics, polycyclic aromatic hydrocarbons (PAH). Various authors [1–3] focused their work on the complexity of tar formation and evolution. In general, tar species are classified as primary, secondary or tertiary tar depending on the temperature at which they are formed within thermochemical conversion processes. This review summarizes results from experimental campaigns where various types of char were tested for the upgrading of real tar mixtures at different temperatures and under different atmospheres.

The carbonaceous materials that have been tested for this application are mainly produced from biomass or coal by carbonization process. At times, high temperature treatments with steam or CO_2 are used for char activation, to increase its surface area and porosity. A few studies have also considered the use of commercial activated carbon (AC).

The conditions of char production and activation are critical for the surface characteristics of the final product, defining the surface area and the porosity. The content of inorganic species such as metals (Fe, Al) and Alkali and Alkali Earth Metals (AAEM) depends on the type of feedstock that is used, while their distribution at the surface can change with the pyrolysis and activation conditions. For example, higher temperatures are thought to induce a migration of inorganics towards the surface.

For an easier overview of the results, the papers have been sorted according to the tar conversion conditions: the first section describes tar conversion over chars under inert atmosphere. The second section groups the experimental campaigns where steam has been added to support the reforming of tar. The third part of the review includes studies investigating the effects of introducing reforming or oxidizing agents (H_2, CO_2, O_2 or air) in tar decomposition upon contact with char. The potential of char and active carbon as a gas upgrading substrate has driven the design of novel gasification

plants. The final section of this review reports a few examples of char-based gas cleaning solutions integrated into gasification systems.

1.2 Pyrolysis derived tar – Inert atmosphere

This section is dedicated to the behavior of pyrolysis-derived tar over char beds in inert atmosphere, without the addition of any reforming agent. The presence of steam is only due to moisture content of the feedstock or to the formation of pyrolytic steam (steam formed during pyrolysis). The investigation of tar interaction with char started already in the 60´s, when Griffiths et al. [4] published results from experiments performed by passing volatiles from low-temperature pyrolysis through a bed of AC, varying the temperature from 350 to 900°C, with N_2 as carrier gas. AC appeared to retain a considerable part of tar as deposit, and to increase the yields of H_2 and CO_2. At 500°C and higher temperatures, the extent of tar decomposition increased with the molecular weight: some PAHs and phenol formed marked deposits, and an increased yield of benzene and alkyl benzene was detected. Char was found to act as cracking catalyst for lower boiling point constituents of tar and as a polymerization promoter for heavier compounds. Oxygenated compounds appeared to contribute markedly to the deposits on the carbon surface. The reactivity of char was found to decrease with continued use.

Later on, Chembukulam et al. [5] performed experiments with wood sawdust pyrolysis, followed by the cracking of the gaseous products over firebricks, charcoal and semicoke. When vapors were passed through carbonaceous beds at 950°C, tar and pyroligneous liquor were completely decomposed. At the same time, gaseous products had higher yield and higher heating value, in comparison with tests where an inert bed of firebricks was used. Some carbon in the bed was consumed in the decomposition process.

In 1989, Boroson and colleagues [6] measured the conversion of wood tars induced by heterogeneous reaction with char, obtained by pyrolysis of the same wood (sweet gum hardwood). Tar vapors were swept through char with helium. In order to isolate the effect of char-induced tar conversion, the effect of homogeneous reactions was quantified and it resulted to be 14wt% in the range 400-600°C. Heterogeneous reactions increased the CO and CO_2 yields and induced a loss of the char surface area, probably because of coke deposits. The authors suggested that only a fraction of tar is susceptible to char-induced conversion. Such fraction is stable towards homogeneous conversion up to 600°C, and it forms coke polymerizing on the char surface, thus it is probably the more aromatic tar fraction. Also, because CO_2 and CO were the products of its conversion, they claim it must have

contained oxygen. This work is the first to suggest that char from biomass pyrolysis could react selectively on tar compounds with higher aromaticity.

Table 1.1: *Overview of experimental tests with pyrolysis volatiles over char beds*

Author	Pyrolysis feedstock	Pyrolysis temperature [°C]	Char (pyrolysis temperature, [°C])	Char bed temperature [°C]	Carrier gas
Griffiths & Mainhood [4]	Coal	500	Activated carbon	350 - 900	N_2
Chembukulam et al. [5]	Wood sawdust	600	Semicoke/charcoal	600 - 950	-
Boroson et al. [6]	Sweet gum hardwood	450	Sweet gum hardwood char (800)	400 - 600	He
Monteiro Nunes et al. [7]	Silver birch wood	500	Spruce wood char (1000)	80 -1000	He
Dabai et al.[8]	Silver birch Pine sawdust Beech wood	500	Oak and Spruce char (commercially available)	700-1000	He
Gilbert et al.[9]	Pinewood	500	Pinewood char (500)	500 -800	N_2
Matsuhara et al.[10]	Loy Yang brown coal	600	Brown coal char (800)	750 - 900	N_2
Chaiwat et al., [11]	Japanese Cedar wood	340	Japanese cedar wood char (900)	600 ,800, 900	N_2
Sun et al. [12]	Pine sawdust	750	Pine wood char Anthracite char Bituminous coal char Lignite char (750)	500 -700	Ar
Z. Z. Zhang et al. [13]	Pine sawdust	850	Pine sawdust biochar (850)	650, 750, 850	N_2
Y. Zhang et al. [14]	Rice straw	500	Rice straw char (500) Water washed char, char added with K_2CO_3	700 -1000	N_2
Al-Rahbi et al. [15]	Wood pellets (waste wood)	500	Tyre char RDF char Date stones char (800)	600 , 700, 800	N_2
Park et al. [16]	Fir wood	500	Wood char Paddy straw char Palm kernel shells char (800)	600 , 700, 800	N_2
Jin et al. [17]	Shenmu coal	650	Shenmu coal char (850) Coconut shell commercial AC	450-750	N_2
Song et al. [18]	Mallee wood	400-700	Rice straw (800)	400-700	Ar

Both Monteiro-Nunes et al. [7,19] and Dabai et al. [8] investigated the tar production and evolution. They used a two-stage laboratory apparatus developed at the Imperial College in London to simulate a downdraft gasifier. The system was shaped as a vertical rod, divided in two separated stages: the

upper stage is for pyrolysis to take place; the lower one contains the char reduction zone. The bottom stage could be heated up separately and pre-charged with char to study the effect of tar-char interaction. In between the two stages, a gas inlet was arranged for introduction of inert gas or air/O_2. The same apparatus has been used by different researchers to investigate the effect of reactive gases addition, but in the papers reviewed in this section, the gas inlet has only been used for inert gas flow. Other studies are treated in paragraph 1.4 of this section. Monteiro Nunes and colleagues [7] were the first to use this set-up to investigate the role of the second stage on the tar yield. They observed that both the temperature and the presence of the char bed influenced the tar content in the product gas. The presence of the char bed at 1000°C decreased the tar yield from 47% to less than 0.1%. Moreover, the char bed caused a significant increase in CO and CH_4 yields. The two-stage system was then modified by Dabai et al. [8] with the aim of collecting C_2-C_5 alkanes and alkenes and CO_2 which were not retained in the tar trap. The new design allowed for a more precise analysis of the reactions taking place in the second stage of the system. Tar reduction was evaluated under thermal cracking conditions, and when packing the stage with char of different particle size. The results showed that the presence of the char bed improved the tar reduction significantly, especially when a small particle size (212-850 μm) was used. Beside a high tar reduction, a change in the product gas composition (higher CO, CO_2, H_2O yields) was also observed in the presence of char, especially at 900-1000°C where CO_2 and steam gasification were expected to take place. Further investigations by the same authors with addition of air over the char bed are reported in paragraph 4 [19,20].

The study by Gilbert and colleagues [9], further investigated the influence of a char bed on the cracking of pyrolysis tar. They used a laboratory-scale reactor with a pyrolysis section at 500°C and a heated cracking section (500 to 800°C). Tar and product gas sampling at the outlet of such system showed that thermal cracking was the main mechanism of tar decomposition, and the effect of the char bed was not significant. The presence of char however induced a higher production of H_2 and CO_2. According to the authors, the effectiveness of char on tars destruction could have been limited by two main factors: (i) the char used in the bed had a large particle size (10 mm cubes), and (ii) char was not activated by injection of steam or CO_2 as in other studies [21]. In addition, the char used as a tar cracking substrate was prepared at the relatively low temperature of 500°C, therefore it is likely that the specific surface area available was low.

Matsuhara and colleagues [10] worked with brown coal char and volatiles from coal pyrolysis. Within the temperature range 750-900°C, tar reforming was found to be rapid and extensive. The authors suggest that tar was converted in a sequence of coking and steam gasification (in agreement with the

tar decomposition mechanism proposed by Hosokai et al.[22]). At 750°C, 96% of heavy tars were found to be converted into non-condensable gases and solid deposits over the char surface. At 900 °C, the yield of coke decreased due to the progress of steam gasification, which was faster than coke deposition. The authors suggest that aromatics with more fused rings are more reactive with the char surface in agreement with the suggestion made by Boroson [6].

Chaiwat et al. [11] worked on tar decomposition in a two stage reactor. Cedar wood was pyrolyzed in a lower reactor under N_2 atmosphere, and the volatiles were passed through the upper reactor, packed with char produced from the same feedstock. The effect of char on the volatile products composition was substantial at 600°C, when the presence of char resulted in lower tar and higher CO and hydrocarbon gases: biochar was found to behave as a catalyst to produce gaseous products. At 800-900°C, the thermal effect contributed heavily to tar destruction, nonetheless char induced some visible effect. At 800°C, it led to complete tar decomposition, and at 900°C the presence of biochar increased the CO yield significantly. The author concludes that CO could be selectively obtained by taking advantage of the catalytic effect of char at 900°C.

The catalytic effect of char on tars has been further investigated by Sun and coworkers [12]. They observed the conversion of tars produced from pine wood pyrolysis in a temperature range 500-700°C, by passing the volatiles in a coal char-packed tubular reactor. Argon was used as carrier gas. Results suggested that up to 600°C, the catalytic effect of char on tar cracking increased the gas yield; at higher temperatures the effect of char was concealed by thermal cracking and gasification via auto-generated steam, both responsible for the high gas yield. The authors suggest that the char catalytic effect depends on the tar composition: oxygenated tars (saccharides, furans, guaiacols) are affected at temperatures lower than 600°C, while phenol and naphthalene, which are thermally more stable, are catalytically and/or thermally decomposed only at higher temperatures.

More recently, Zhang et al. [13] investigated the cracking of tar from pyrolysis of pine sawdust over biochar produced with the same feedstock, investigating the effect of vapor residence time and temperature. N_2 was used as a carrier gas. They found that the abundance of tar compounds decreased with increasing vapor residence time at all three cracking temperatures (650, 750 and 850°C) but was more marked at higher temperatures. This trend was accompanied by an increase in H_2 yield, and a decrease in CH_4 and other light hydrocarbons. Y. Zhang et al.[14] investigated heterogeneous conversion of pyrolysis tars over rice straw char, focusing on the role of temperature and alkali content in the char. N_2 was used as carrier gas. In a temperature range 700-1000°C, tar removal efficiency resulted higher in presence of a char bed in comparison with pure thermal degradation at the same temperature. Also, the char bed was found to promote the catalytic

conversion of primary tars (mainly methoxyphenols) to alkyl monoaromatics and, at the same time, to inhibit the conversion of primary tars to PAHs. Evolution of the char porosity and surface area during pyrolysis was also evaluated in this work. Increasing the pyrolysis temperature up to 700°C was found to produce the largest surface area and pore volume and the minimum pore size. Treatment at higher temperatures was found to deteriorate the pore structure, resulting in a diminished catalytic activity of char. To investigate the effect of salts on tar conversion, they also tested water-washed char and char with added K_2CO_3: the results showed that alkali metal elements might be responsible for the catalytic active sites for tar removal.

Recently, Al-Rahbi and colleagues [15] also investigated the effect of char on tar reduction. They used a hot bed of waste-derived char (600 to 800°C) flushed with wood pyrolysis gas. They tested three kinds of char: produced from waste tyres, RDF and date stones. Tyre and RDF chars were found to be more effective in tar reduction in comparison with date stones and the authors suggested three possible reasons: (i) a higher number of acidic functional groups on the surface, especially for tyre derived char, (ii) higher ash content in both tyre char and RDF, and the presence of potential catalysts such as Zn (iii) higher BET surface area and pore volume for both tyre char and RDF.

Park and co-workers [16] conducted a similar study by studying the conversion of pyrolysis tar over hot char beds at 600, 700 and 800°C. Different chars were tested (obtained from wood, paddy straw and palm kernel shells) with different bed volumes and residence times. The presence of char resulted in an improved tar reduction in comparison with thermal cracking conditions. The largest tar reduction, together with the highest yield of gaseous products (H_2, CO, CO_2 and hydrocarbons), was observed at 800°C and with the largest reactor volume. Tar decomposition was not significantly influenced by the char type.

Jin et al. [17] focused on the optimization of coal pyrolysis through reforming of volatiles. For this purpose, they tested the catalytic effect of a bed of coal char in comparison with a bed of commercial activated carbon. Tar was produced by pyrolyzing coal at 650°C. Reforming of volatiles was enhanced by the presence of the catalyst in the reforming stage, especially when active carbon was used. The marked difference between the performance of char and active carbon can be ascribed to the large discrepancy in the surface area: 2.2 m^2/g for char and 803 m^2/g for active carbon. Both materials were found to have a decreased surface area and pore volume after the experiments, as a consequence of pore collapse and carbon deposition.

Song et al. [18] used a fixed bed of rice straw char to decompose pyrolysis tar generated by fluidized bed pyrolysis of mallee wood. They reported an increasing efficiency of tar conversion at higher temperatures, with the lowest tar yield obtained at 700°C. In particular, the non-aromatic structures

were converted more easily at temperatures as low as 400-500°C. On the other hand, a temperature of 600°C or higher is required for the conversion of aromatic structures via coking at the surface of char. Interestingly, by analysing the surface of spent char with Raman Spectroscopy, they observed an increased amount of oxygen-containing groups on the char surface. The authors concluded that under the tested conditions, oxygen is removed from oxygenated tar molecules (such as phenols or guaiacols) and transferred to the char matrix.

The results from the studies included in this section seem to verify some of the findings derived from experiments with tar model compounds. The mechanism proposed by Hosokai et al.[22] appears to be verified by other researchers. Cracking of tar with coke deposition on the char surface is indicated as the mechanism responsible for tar decomposition. This seems also to be the cause of char deactivation with time, particularly in inert atmosphere. Indeed, under such conditions, coke deposits are not gasified, but endure on the surface blocking the pores (especially micropores) and the active sites. Several authors have observed a reduced specific surface area of chars after contacting with tars at high temperatures, and attributed this to polymerization and coking of tar compounds.

The majority of these studies testified an increase in yield of permanent gases when pyrolysis tar was passed over char, particularly CO, CO_2, H_2 and CH_4.

Boroson et al.[6] and Matsuhara et al. [10] suggested a possible selectivity of char towards the oxygen-containing and more aromatic fraction of tar. In general, the experimental campaigns carried out in inert atmosphere confirmed the effectiveness of char towards tar decomposition. All the various discrepancies in the observations could be ascribed to the different conditions adopted by the authors. Specifically, the effectiveness of char in reforming tar might depend mainly on two factors: (i) the tar composition (which changes with the feedstock and the pyrolysis conditions) and (ii) the char characteristics (specific surface area, pore size distribution, mineral content). Indeed, it appears as the origin of char, and therefore its content in inorganics, is not as important as its surface structure. A large surface area and pore volume are crucial for the enhancement of tar cracking.

1.3 Pyrolysis derived tar- steam atmosphere

The following reviewed works were carried out considering the effect of steam as a reforming agent in the process of tar decomposition over the surface of char. The presence of steam at high temperature is expected to enhance the production of CO and H_2, as in steam reforming reaction (1).

$$C + H_2O \rightarrow CO + H_2 \quad (+118.5\ kJ/mol) \qquad (1)$$

An overview of the experimental conditions applied in the reviewed studies is given in Table 1.2.

Table 1.2: *Overview of experimental tests with pyrolysis volatiles over char beds, with steam addition*

Author	Pyrolysis feedstock	Pyrolysis temperature [°C]	Char (pyrolysis temperature, [°C])	Char bed temperature [°C]
Krerkkaiwan et al. [23]	Rice straw	600, 700, 800	Sub-bituminuos coal char (600, 800)	800
Krerkkaiwan et al. [24]	Giant *Leucaena* wood	800	Sub-bituminuos coal char *Leucaena* char (600)	800
Hayashi et al. [25]	Brown coal	850	Brown coal (800-900)	800 -900
Widayatno et al. [26]	*Fallopia Japonica*	650,700	*Fallopia Japonica* char (500, 600,700,800)	650,700
Wang et al. [27]	Shengli brown coal	700-900	Brown coal char Brown coal char- steam activated (900)	700-900
Min et al. [28]	Mallee Wood	500 -850	Acid washed brown coal Iron loaded brown coal Nickel loaded brown coal (800)	500 -850
Sueyasu et al. [29]	K-loaded cedar wood	550	K-loaded cedar wood (550)	600 -700

Krerkkaiwan et al. [23] worked with pyrolysis of rice straw, and focused on the effect of preparation conditions for coal char on its activity towards conversion of pyrolysis tar. Coal char prepared at 800°C resulted to be much more effective than the one prepared at 600°C: this was ascribed to the higher surface area, pore volume and higher concentration of AAEM species on the surface. Elsewhere [30], higher pyrolysis temperature has been found to induce the migration of AAEM species toward the surface. The catalytic activity of the char pointed towards the decomposition of heavier aromatic hydrocarbons generated by pyrolysis at 800°C. Later on, the same authors [24] investigated the effect of chars from co-pyrolysis of coal and biomass on biomass-derived tar. The catalytic effect of biomass char, coal char and a blend of the two was studied under N_2 and steam/N_2 mixture. Blended char was found to provide a better catalytic performance, because it provided higher CO_2 and H_2 yields, especially when steam was used as reforming agent. Higher surface area and AAEM content of the char surface were considered as key parameters for increasing the extent of tar conversion.

Hayashi et al. [25] worked with pyrolysis of brown coal in a drop-tube reactor. Brown coal char, containing inherent inorganics (Na, Ca, Mg, Fe), was co-fed in the pyrolysis unit, with the aim to evaluate the role of metallic species in the secondary reactions of nascent tar. Brown coal char was produced at 850°C, and part of it was treated with acid washing to remove any metallic species. The

effect of steam addition in the carrier gas was also evaluated. During pyrolysis at 900°C with co-feeding of brown coal char (not washed) the presence of steam increased the H_2 yield significantly and decreased the tar and soot yields. This effect was not observed with co-feeding of acid-washed char. Metallic species exerted a catalytic effect on secondary reactions, reforming tar up to 99%. According to this study, elements such as K, Ca, Na, Mg and Fe were essential for the rapid steam reforming of nascent tar, as well as for preventing the formation of soot.

In 2014, Widayatno et al. [26] focused on char produced from *Fallopia Japonica* (FJ). This is a fast-growing, perennial herbaceous biomass rich in lignin and AAEM species. Chars were produced and used as catalyst for the reforming of FJ-derived tar in a fixed bed reactor, with steam (0.1 g/min) as a gasifying agent. The study compared the performance of FJ char prepared with different pyrolysis conditions (temperature 500-800°C, 1-4 hours treatment). As expected, the different pyrolysis conditions affected the chemical and physical properties of chars. In general, when used in the fixed bed reactor, the FJ char increased the yield of H_2, CO and CO_2 significantly and to a lesser extent, CH_4. This effect was ascribed to the induced steam reforming of tar. The authors determined the presence of an optimal pyrolysis temperature and duration, which improved the catalytic activity of chars. Specifically, the char prepared with pyrolysis at 800°C with 1 hour retention time had a surface area of 105 m^2/g and provided the best performance. On the other hand, char prepared at 700°C with 4 h retention time had a larger surface area (189 m^2/g) but gave a lower gas yield, probably as a result of a lower AAEM concentration at the surface.

Wang et al. [27] used the same experimental setup as Jin et al. [17] to study the optimization of the reforming of volatiles produced during the pyrolysis and gasification of brown coal.

For this purpose they passed the pyrolysis products over a bed of brown coal char prepared at 900°C, and a bed of the same char after it was steam-activated. Both materials decreased the yield of tar. The lowest tar concentration at the outlet of the system was measured when active carbon was used at the highest tested temperature (900°C). Again, as in Jin et al. [17], the improved performance of the activated char was a result of the increase in the surface area from 9.3 m^2/g to 422.7 m^2/g after activation.

In general, carbon is considered as a possible catalyst support in various applications [31]. Min et al. [28] and Sueyasu et al.[29] investigated the effectiveness of catalyst-loaded char for tar reforming.

Min et al.[28] investigated the property of char as catalyst support for steam reforming of biomass tar. Their focus was on reforming of aromatic ring systems in tar. Brown coal char was acid-washed, then catalyst were prepared by loading it with Fe and Ni. The catalytic effect of acid-washed char, Ni and Fe catalysts were compared with ilmenite (titanium/iron oxide mineral) for the steam reforming

of tar derived from mallee wood pyrolysis. Loaded chars showed a much higher activity in comparison with the acid-washed char. Nevertheless, the acid washed char was found not to be inert, but to have a role in the catalysis of steam reforming. Comparing the Fe-loaded char with Fe-loaded ilmenite showed that the catalyst support plays an important role in the reaction pathway of steam reforming. The role of the carbon structure is critical: it would not only disperse the catalytic species but also become involved in the reaction itself. The authors stated that an important mechanism of support-catalyst interactions is the migration of radicals between the active sites on char and the Fe clusters.

Sueyasu et al. [29] proposed a two stage conversion of K-loaded biomass, where K acted as catalyst for simultaneous steam reforming of tar and char. Japanese cedar wood was first loaded with K_2CO_3, then pyrolyzed at 550°C to be used in a fixed-bed reformer. The char bed was at a temperature in the range 600-700°C and was flushed by pyrolysis volatiles generated with the same feedstock. Heavy tars (pyrene and larger molecules) and light tars (benzene to phenanthrene) were both found to be reformed in the char bed, but light tars were not so extensively reduced because of their higher thermochemical stability. The authors suggest that light tars should be eliminated otherwise: for example by partial oxidation, feeding oxygen or air to the headspace of the reformer. The effect of K-loading of char was almost complete steam reforming of heavy tar. The rapid steam gasification of char itself prevented catalytic deactivation.

All in all, results from these studies confirmed that char is particularly effective in catalyzing steam reforming. Coal char appears to be particularly active in this sense, and several authors agree that this is mainly due to its high content of metallic species. However, this is also true for certain herbaceous biomass types, such as *Fallopia Japonica*. The selectivity of char towards certain tar fractions proposed in some of the works reviewed in paragraph 2 is mentioned also by Krerkkaiwan et al.[24], who observed a stronger effect of char on heavy compounds, and Sueyasu et al. [29], who pointed out that heavy tar species are preferentially decomposed on the char surface and suggested the use of partial oxidation to completely remove light aromatic compounds.

Several researchers verified that the presence of a reforming agent is necessary to maintain the char catalytic activity: steam gasification of newly formed coke prevents the blocking of pores, which contain active sites.

1.4 Pyrolysis derived tar – Oxidizing atmosphere

This section reviews a series of studies where the effect of air or O_2 addition has been evaluated during tar reforming over char. The addition of O_2 is expected to assist the endothermic reforming

reaction by locally increasing the temperature through partial combustion of the available carbon. Indeed, in many cases, steam or CO_2 were also added to support reactions of steam reforming (1) or dry reforming (2).

$C + CO_2 \rightarrow 2CO$ (+159.9 kJ/mol) (2)

An overview of the experimental conditions is given in Table 1.3.

Table 1.3: *Overview of experimental tests with pyrolysis volatiles over char beds, with addition of oxidizing and reforming agents*

Author	Feedstock	Tar generation temperature [°C]	Char (preparation temperature [°C])	Char bed temperature [°C]	Carrier gas /oxidating agent
Hosokai et al. [32]	Cedar wood chips	550	Cedar wood (commercially available)	750 - 850	N_2 N_2/O_2 N_2/Steam
Monteiro Nunes et al. [19]	Eucalyptus wood Industrial sludge Silver Birch wood	500	Oak char Pine bark char Spruce char	700 -1000	He He/O_2
Chen et al. [33]	Rice straw Corn straw Fir sawdust	250 - 400	Rice straw char Corn straw char Fir sawdust char (1000)	700 - 1000	N_2 N_2/Air
Wu et al. [34]	Rice straw	200 - 700	Rice straw char (500)	815 , 900	N_2 N_2/CO_2 N_2/O_2 N_2/H_2O
Dabai et al. [20]	Silver birch Pine sawdust Beech wood Palm fiber Olive bagasse Sewage sludge	500	Oak char Pine bark char Spruce char	700 -1000	He He/O_2
Zhao et al. [35]	Rice straw	500	Rice straw char (500)	700 - 900	He He/O_2
Phuphuakrat et al. [36]	Cedar wood	600	Activated char Wood chips Synthetic porous cordierite	800	N_2 Steam Air
Feng et al. [37]	Rice husks (acid-washed)	500	Rice husks char (700)	800	Ar H_2O CO_2

Hosokai and colleagues [32] compared the effect of different atmospheres on the char and its effect towards tar. Pyrolysis-derived tars were passed over a biochar bed at 750-850°C. The extent of tar decomposition was compared when using N_2 (thermal cracking conditions), O_2/N_2 mixture (partial oxidation) and in the presence of steam (steam reforming conditions). Reduction in the micropore

volume was observed in inert atmosphere and in presence of O_2, whereas the pore structure was maintained and improved in presence of steam, as a consequence of gasification. Steam was found to enhance the merging of micropores into larger pores, thereby favoring the diffusion of tar into the char particle: steam addition is confirmed to be useful for preserving the activity of char. O_2 addition was important because it caused an increase in bed temperature, thereby a faster progress in steam gasification. Naphthalene, phenol and phenanthrene were decomposed with a conversion close to 100% at 800-900°C, from an initial concentration of 1.5-3 g/Nm^3_{dry} .The authors conclude that the combination of steam gasification and partial oxidation could potentially attain a tar concentration lower than 100 mg/Nm^3 in the producer gas.

Monteiro Nunes and colleagues [19] further investigated the effect of the operating conditions on tar yield in the second stage of the two-stage apparatus already described in section 1.3. They focused on the effect of temperature (700 to 1000°C), wood char type and particle size, residence time and addition of air. Tar derived from pyrolysis at 500°C was destroyed very efficiently when the char bed was present, especially at high temperatures. Increased residence time caused a further tar destruction. The amount of tar entering the second stage was 47%wt of the feedstock. The thermal treatment at 1000°C reduced it to 0.7%wt, while the presence of the char bed further decreased it to 0.1%wt. The kind of char used in the second stage did not significantly affect the tar yield, whereas smaller particle size enhanced tar decomposition only in the lower range of temperature. The addition of helium-diluted air over the char bed achieved a total elimination of tar in some experiments. The authors suggest that the increased temperature produced by oxidation reactions favors the cracking and polymerization of tar.

Chen and co-workers [33] investigated the release and destruction of tar using the same two-stage laboratory setup developed at the Imperial College in London. At first, the authors investigated how the process operating conditions affected the tar yield from different feedstocks (rice straw, corn straw, fir sawdust). The results indicated that nascent pyrolysis tar contains a large amount of oxygenated constituents, but the abundance of individual compounds can vary depending on the feedstock. Subsequently, they focused on the lower (cracking) stage and evaluated the effects on tar destruction of temperature, residence time, char particle size, char type, fuel type and diluted air feeding. The parent material of char did not appear to influence the behavior towards tar. The highest tar reduction (96% to 98% conversion, depending on the feedstock) was achieved when the introduction of diluted air through the nozzle was combined with the presence of a char bed in the lower part of the system. Such condition showed a higher tar destruction in comparison with pure thermal cracking (empty lower stage) and partial oxidation (diluted air addition on empty lower

stage). Complete removal of pyrolysis tar could not be achieved, but the presence of the char bed caused the tar species to polymerize forming larger PAH molecules.

The same two-stage system was also used by Wu et al. [34] to further investigate the mechanisms of tar formation and decomposition. They characterized the surface of rice straw char produced at different pyrolysis temperature (200-700°C) using Fourier Transform Infrared (FTIR) spectroscopy. They found that the quantity of aliphatic hydrocarbons and oxygen functional groups decreased with increasing temperature. Higher pyrolysis temperature also caused an increased concentration of AAEM (Ca, K, Na, Mg) and Al, Fe and Si, indicating a migration of such species towards the char surface, also observed for Fe by Klinghoffer et al. [30]. The yield of tar was measured at reforming temperatures 815-900°C, using different reforming agents (CO_2, H_2O, O_2) at different concentrations. The tar conversion efficiency varied from 88% in thermal cracking conditions (900°C) to 96.5% with steam reforming over a char bed at 900°C. A high concentration of CO_2 (100 ml/min) at 815°C achieved the highest tar conversion, 97.2%. Char was found to selectively reduce PAH species and increase toluene yields. Toluene might therefore be a byproduct of tar reforming over char. The authors suggest that the effectiveness of rice straw char in tar decomposition might be due to the high AAEM content and to the pore structure, high in micropores and mesopores. The proposed tar destruction-mechanism in the two stage gasifier is a sequence of primary tars reforming into PAHs, mono-ring aromatics and non-condensable gases induced by partial oxidation, followed by almost total decomposition within the char bed.

Dabai and colleagues [20] carried out an investigation about tar destruction in the two-stage laboratory reactor already described in section 2 and also used by Monteiro Nunes [19], Chen [33] and Wu [34]. They pyrolyzed different kind of biomass in the first stage, and investigated the effect of the lower stage (cracking stage) on the gas composition (tars, CH_4, CO, CO_2) in a temperature range 800 to 1000°C. Particularly, they investigated the effect of packing the tar reduction stage with char and changing the residence time, char particle size and type, addition of O_2. Adding different amount of char to the second stage showed that even a little amount of char (0.3 g of char for 1g of fresh biomass) is effective in enhancing tar destruction. The char particle size (from 212 to 3000μm) and the kind of char used in the bed did not appear to influence significantly the tar removal effect, in agreement with the results of Monteiro Nunes et al. [19] and Fuentes Cano et al. [38]. Thanks to the char bed, tar was decreased by 98%, regardless of the feedstock used for pyrolysis. The addition of O_2 in general contributed to tar reduction with combustion. However, with this configuration, in presence of char bed at 1000°C, O_2 reacted preferentially with char and was not available to burn tars.

Using the same two-stage apparatus, Zhao et al. [35] focused on the investigation of the synergy between partial oxidation and biochar on tar reduction. Tar conversion rates were measured at different temperatures (700 to 900°C), at different O_2 concentrations (1%, 5%), with and without a char bed downstream. Temperature was found to be a dominant factor in tar conversion: in general higher temperature decreased the number of tar compounds. Because of the high temperature produced by combustion, partial oxidation is more effective in tar decomposition than a char bed under inert atmosphere. However, the highest tar conversion was observed when both O_2 and char were involved. At 900°C, the synergy of oxidation and char catalysis was found to reach the best efficiency, attaining a tar reduction efficiency of 95.8%. The selectivity of char towards multi-ring molecules was indicated as the cause for such a high reduction. O_2 was found to promote the development of biochar porosity under different concentrations. However, an excessive O_2 concentration (5%) would lead instead to carbon deposition on the pores. The authors conclude that the coupling of partial oxidation and char catalysis is a feasible method for tar reduction in biomass gasification.

Phuphuakrat et al.[36] investigated the mechanism of tar removal by the two step function of decomposition and char adsorption, where decomposition was carried out by thermal cracking, and reforming with steam or air: both were added in different concentrations. Additionally, three adsorbents were tested: activated carbon, wood chips, and synthetic porous cordierite. The addition of reforming agents improved tar decomposition in comparison with pure thermal cracking. All reforming agents enhanced tar reduction and increased the yields of benzene and light PAH. In the adsorption step, activated carbon showed the highest efficiency for tar adsorption, acting also on both light hydrocarbons and light PAH. Cordierite showed very low tar adsorbency, because of a quick deactivation; it is considered to be inadequate for tar adsorption. Wood chips showed a good efficiency in adsorption, with an evident selectivity towards condensable tars.

Feng et al. [37] compared the homogeneous and heterogeneous conversion of pyrolysis tar in presence of H_2O and CO_2. They pyrolyzed rice husk to produce tar, and used the same feedstock to generate char to be used as a support for heterogeneous reforming at 800°C. Results showed that the presence of char in the reforming stage was beneficial for tar conversion. Addition of H_2O induced lower tar yield and higher char consumption in comparison with CO_2. Both the reforming agents reacted with tar and also with the char surface, modifying its structure. The char surface was enriched in oxygen-containing functional groups and large aromatic ring systems. Similar conclusion are also confirmed later by the same authors [39], by using different char surface characterization techniques.

In general, the review of the works in this section suggests that the addition of an oxidizing agent improves the tar removal efficiency, especially when using biomass char as a catalyst for cracking of tar. Temperature is a key parameter to control tar decomposition, and oxidation reactions provide the heat necessary to enhance tar destruction. The presence of a reforming agent supports the gasification reaction of solid carbon generated during tar cracking. In particular, steam reforming is useful to preserve the activity of the char surface and its pore structure. Using CO_2 is not as efficient as H_2O because of the slower rate of dry reforming in comparison with steam reforming. Indeed, dry reforming needs higher activation energy. To attain a similar reforming affect as with steam, high concentrations of CO_2 are required which can decrease the heating value of the product gas.
The synergy between oxidation and reforming reactions can be optimized to achieve an almost complete tar reduction while preserving the heating value of the gas phase.

1.5 Examples of process integration of char-based gas cleaning systems

The performance of carbonaceous materials for the cracking and reforming of tar encouraged the design of gasification systems where producer gas is brought in contact with char or active carbon before leaving the system. Different design solutions are presented in this section. In 2000, Brandt and colleagues [40] observed a very high tar reduction in a two stage gasifier, the Viking gasifier. Tar was sampled at three different ports: after the pyrolysis unit, over the char bed and just beneath it. Air was added for partial oxidation of tar right after the pyrolysis stage. Volatiles were then passed through a fixed bed of char before leaving as producer gas. Figure 1.1 shows a diagram of the Viking gasifier and the positions of tar sampling ports. Tar content and composition were determined after partial oxidation above the bed and below the bed. After partial oxidation, low levels of phenols were detected while stable.aromatic hydrocarbons were predominant. These compounds, including PAH species, were produced by oxidation of primary tar. Following the passage through the char bed, a significant reduction in the tar content was observed. Most of the residual tar detected in the exit gas was made up of naphthalene. The authors concluded that the combination of partial oxidation followed by a passage through a hot char bed can result in a producer gas with a tar content less than 15 mg/Nm^3, none of which was heavy tar.

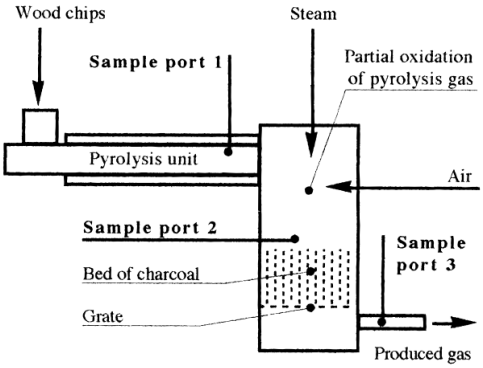

Figure 1.1: *Block diagram of the 100 kWth two stage gasifier (Viking)*
(Reprinted with permission from [40], American Chemical Society)

The described mechanism of tar reaction was also observed, years later, by Wu et al. [34].

Zhang et al. [41] followed the work of Matsuhara et al. [10], implementing the use of char in a pyrolysis system as a primary method to enhance the *in situ* reforming of nascent tar. For this purpose, they developed a triple-bed combined circulating fluidized bed reactor including a downer (pyrolyzer), a bubbling fluidized bed (BFB gasifier) and a riser (combustor). The system is schematized in Figure 1.2.

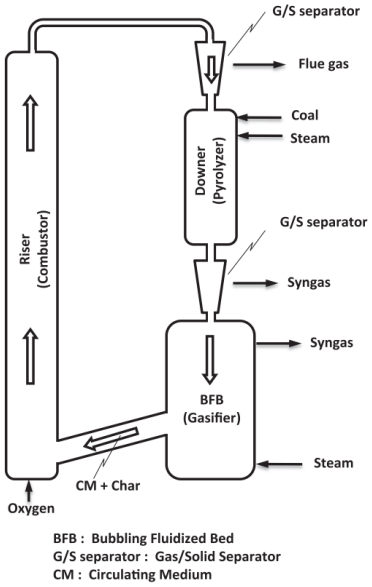

Figure 1.2: *Diagram of the triple-bed combined circulating fluidized bed reactor system*
(Reprinted with permission from [41], Elsevier)

To simulate the conditions in the downer reactor, a drop tube reactor was used. Brown coal and char (produced from the same kind of coal) were co-fed to the reactor in presence of 50% steam in order to test *in situ* tar reforming at 900 and 950°C. Two kinds of char have been tested: the first was prepared by brown coal pyrolysis in a fluid bed at 800°C, the other was first pyrolyzed and then gasified with steam at 900°C.

The amount of tar obtained by pyrolysis at 600 and 900°C was compared with the one obtained with char co-feeding. Even at 900°C, the effect of pyrolysis char addition was significant to tar reduction. The tar yield was further reduced when more char was added in the bed. When gasification char was used, the effect on tar reduction was even higher, for both light and heavy tars. The authors suggest that the improved effectiveness of gasification char was given by the higher surface area and a higher concentration of Na and Ca. They suggest the mechanism of coke deposition on active sites and gasification for tar reduction, in agreement with others [10,22].

In 2010, Mun and coworkers [42] tested a two stage gasifier integrating a fluidized bed reactor with a fixed bed of activated carbon with the function to reform tar and increase the heating value of the producer gas. A diagram of the two stage gasification system is shown in Figure 1.3.

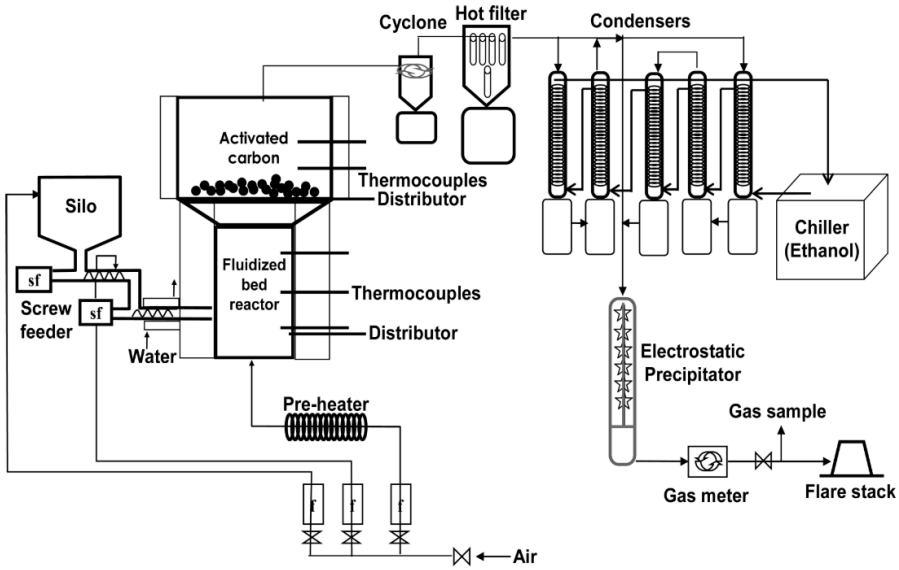

Figure 1.3: *Scheme of the two-stage gasification system integrating a fixed bed reformer with activated carbon (Reprinted with permission from [42], American Chemical Society).*

The system was used to gasify dried sewage sludge in the bottom reactor, and upgrade the producer gas in the top reactor. Tested conditions included varying the bottom reactor temperature, the top reactor temperature and the air equivalence ratio (ER). The effect of the activated carbon bed was evaluated by running experiments with an empty top reactor. The presence of the bed enhanced the production of H_2 greatly, as a result of tar cracking reactions. Increasing the temperature of the top reactor from 698 to 793˚C was beneficial for tar conversion. On the other hand, increasing the ER resulted in a higher CO_2 production and lowered the yields of H_2, CH_4 and hydrocarbons, lowering the heating value of the producer gas.

The same gasification concept was tested again by Mun et al. [43], this time by using wood waste as a feedstock. Tar yield and gas composition have been measured at different temperatures of the upper stage (675-794˚C), at different O_2 equivalent ratio (ER), and when the second stage was empty, filled with activated carbon, or spent activated carbon. The temperature increase in the upper stage led to higher H_2 production, especially when active carbon was present. The increase in ER from 0.20 to 0.68 exerted a similar effect as the one described in the previous study. Light and heavy tars were best removed by using AC and spent AC in the upper stage, instead of leaving it empty. Tar yield was decreased six-fold by fresh char and three-fold by spent AC, in comparison with runs with empty upper stage. The diminished effect on tar removal exerted by the spent AC is a result of surface deactivation. Indeed, imaging with Field Emission Scanning Microscopy (FE-SEM) showed deposits on the surface of spent char, which could have blocked the pores and decreased the activity of char.

Choi et al.[44] further developed the two-stage system by adding an auger reactor for devolatilisation of dried sewage sludge prior to the fluidized bed reactor. Again, the fixed bed reactor at the top was filled with activated carbon to remove tar generated during gasification. The addition of the auger reactor induced a more gradual devolatilisation of the feedstock and longer residence time in the lower stages of the system, with the effect of increasing the producer gas yield and decreasing the tar yield. The top reactor packed with active carbon had a further beneficial effect on the gas quality. The temperature of the fixed bed was varied in the range 657-832˚C. At the highest temperature, tar concentration was reduced to a minimum of 22 mg/Nm^3.

Gómez-Barea et al. [45] conceived a three-stage gasification process with the aim to optimize the char and tar conversion in fluidized bed gasification of biomass and waste. The proposed design includes a fluidized bed reactor for the devolatilisation of the feedstock, followed by a high temperature intermediate reactor where the volatile products are partially oxidized. The solid products from the first stage are transferred to the final stage, where a fixed bed of char is meant to

act as a catalytic filter to reform tar in the gas phase. A diagram of the three-stage gasification concept is shown in Figure 1.4.

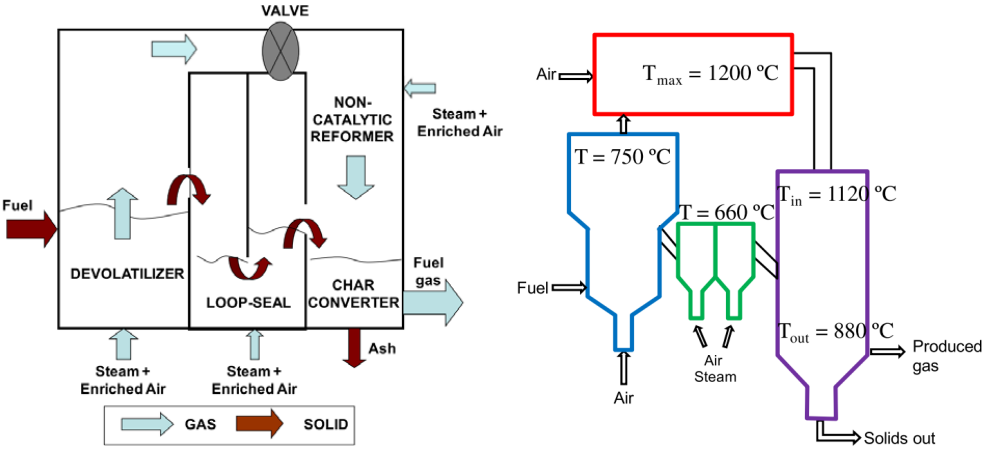

Figure 1.4: *Diagram with gas and solid fluxes in the three-stage gasification concept (left). Scheme of the reactors arrangement (right). (Reprinted with permission from [45], Elsevier)*

Zeng et al. [46] proposed another two-stage system for the gasification of coal. The system is schematized in Figure 1.5 and includes a fluidized bed pyrolyzer combined with a down-draft fixed bed gasifier with air injection. A similar concept is applied here as in the Viking gasifier, as the solid products of pyrolysis are used to form a fixed bed for simultaneous gasification and reforming of tar.

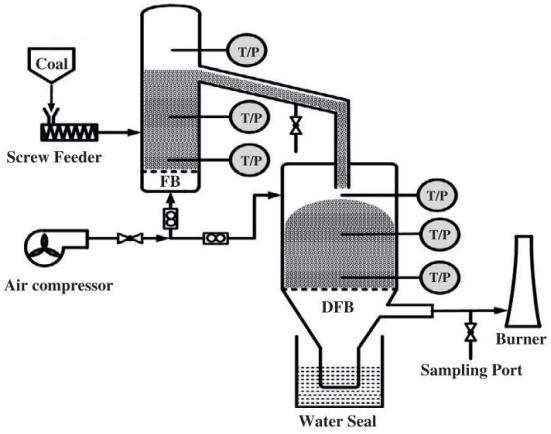

Figure 1.5: *Diagram of the two stage low-tar coal gasification system. (FB = Fluidized bed, DFB = Downdraft fixed bed) (Reproduced with permission from [46], Elsevier)*

The gasification unit was operated with a feeding rate of 50 Kg/h in mode 1 and 2. In mode 1 the pyrolyzer and gasifier were maintained at 860 and 1100°C, respectively; in mode 2 the temperatures were lowered to 800 and 1000°C. Analysis of gas composition and tar concentration after the first reactor and after the second stage showed that most of the tar generated in the first reactor was reformed in the hot char bed. Reforming of tar was more extensive in mode 1, with higher reactor temperatures. The lowest concentration of tar achieved in the producer gas was 84 mg/Nm^3.

Zhang et al. [47] implemented and tested a hot gas cleaning system based on biomass char in a gasification system fed with mallee wood. The gasification system is described in detail in [48]. A scheme and a process diagram of the system are reported in Figure 1.6. The system was operated with two biomass feeding rates (2 and 4 Kg/h) and was externally heated with electricity. A cylindrical catalytic reactor (0.5 m tall, with an internal diameter of 0.16 m) was installed at the outlet of the gasifier. The gasifier was operated at 880°C, while the temperature in the catalytic reactor was 800°C.

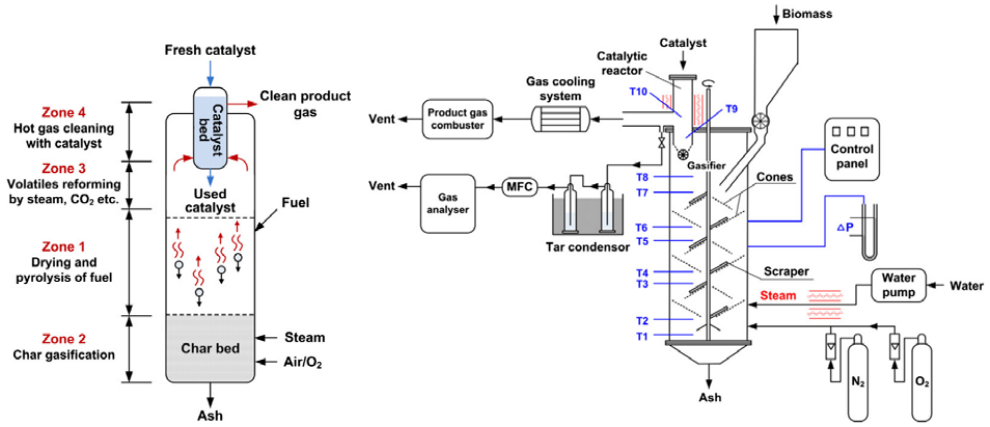

Figure 1.6: *Concept diagram (left) and process scheme (right) of the proposed gasification system with integrated fixed bed catalytic reactor. (Reproduced with permission from [48], Elsevier)*

The catalytic stage for tar reforming was packed with mallee wood char, mallee wood char loaded with Fe and brown coal char loaded with Fe. Biomass char had the effect to increase the CO and H_2 content in the exit gas, by supporting reforming reactions. The effect was enhanced by the addition of dispersed Fe. Interestingly, the coal char based catalyst exhibited an inferior performance. The Fe loaded biochar used in the catalyst reactor was able to deliver a tar concentration as low as 30 mg/Nm^3 in the exit gas. The authors further investigated the role of inorganic species present at the surface of char during heterogeneous conversion of tar [49]. They compared the catalytic

performance of raw char and acid washed char prepared from mallee wood. Results showed that both materials were able to efficiently reform tar, confirming the important role of the carbon structure in the catalysis of tar conversion. The char bed in the catalyst reactor was also found to be effective as a filter for volatilized inorganics and possibly fine ashes present in the producer gas.

Palla Assima et al. [50] used pellets of residual char and ash from a commercial gasification plant (Enerkem Alberta Biofuels) for reforming of pure tar. The inorganic fraction of char (which formed the char-derived ash) included Ca, Mg, Na, iron silicates, aluminates and oxides. Tar was extracted from the producer gas within the gasification process via acqueous scrubbing. Before feeding to the reformer, water was eliminated via Soxhlet extraction and pure tar was concentrated in a rotary evaporator. Pure tar was then injected in the evaporator to generate a concentration of 65 g/Nm^3. Steam was also injected alongside tar, and the mixed vapors were sent to the reformer reactor, which was empty in the thermal reforming test, and packed with char in a fixed bed of char or char-derived ashes. Tar sampling and online gas analysis at the outlet of the system was used to monitor the reforming of tar. The system is schematized in Figure 1.7.

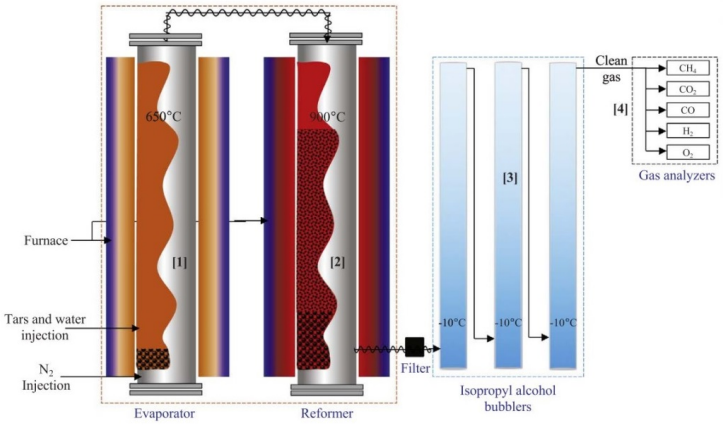

Figure 1.7: *Experimental system for the evaporation and reforming of pure tar (Adapted with permission from [50], Elsevier)*

When the reformer was packed with the residual materials, most of the tar was cracked and reformed into permanent gases. However, when char was used, the reforming reactions were enhanced and the equilibrium was reached in a shorter time: this effect was ascribed to the presence of fixed carbon which increased the available surface area and available porosity. The use of char also induced a more extensive tar reduction which was as low as 90.2 mg/Nm^3. The production of CO and

H_2 was increased when a larger amount of steam was introduced together with tar, thanks to reforming, water gas-shift and Boudouard reactions.

1.6 Conclusion

A selection of papers concerning the use of carbonaceous material for the cracking and reforming of tar derived from pyrolysis or gasification has been presented. Tar decomposition was studied under different conditions, by changing the reaction temperature and atmosphere and by using different carbonaceous materials as substrates for heterogeneous reactions.

An overview of these works indicates that the application of char enhances the reduction of tar species by supporting cracking and reforming reactions. Various studies report a tar conversion close to 100%. However, complete tar elimination is difficult to achieve, and two and three-rings aromatics are often found to survive the passage through char beds even under harsh reaction conditions. In particular, naphthalene appears as the most refractory species. In general, the application of char needs to be adapted and optimized in order to achieve an extensive effect.

The intrinsic properties of chars have an influence on the interaction with tar species. It is often reported that the parent material from which char is produced does not have a significant influence on the conversion of tar. For this reason, the chemical composition of char does not appear as a fundamental factor. Indeed, biomass and coal naturally contain AAEM and other metallic species (Fe, Al), which are often found to favor the decomposition of tar. However, their effect can only be fully realized if they are well dispersed and accessible at the surface of char. Therefore the surface structure of char plays a critical role.

The most important characteristics to look at are the specific surface area, the pore volume and the pore size distribution. Chars with extremely low surface area (below 100 m^2/g) have a limited effectivity. Overall, it is preferable to adopt chars with surface area above 500 m^2/g so that a broad contact area is available for heterogeneous reactions. A large pore volume distributed in both micro- and mesopores facilitates diffusion and accessibility of the active sites. Considering that the range of required surface properties is quite broad, it can be concluded that it is not necessary to adopt a specifically tailored activated carbon. An adequate surface structure can be achieved by tuning the operating conditions at which char is produced. For example, higher pyrolysis temperature increases the char burn–off and is beneficial for the surface texture. However, excessive pyrolysis temperatures (above 900°C) can also damage the pore structure by causing the collapse of small pores. Addition of a reforming agent and gasification reactions during carbonization can further improve the surface area and porosity of the solids.

All in all, both biomass and coal chars with an adequate surface structure are able to deliver extensive tar conversion, without addition of supplementary catalytic species. Naturally occurring inorganics, in synergy with the carbon scaffold, are able to provide an adequate catalytic effect.

The dynamics of tar-char interaction which is described for tar model compounds seems to be confirmed when actual tar is used. Aromatic species undergo heterogeneous cracking reactions over char, with coke deposition over active sites. The presence of a reforming agent (steam or CO_2) is important to react with the deposited carbon, preserving the accessibility of the active sites.

H_2O appears as a more effective reforming agent for this application. This is due to the fact that, during the heterogeneous conversion of tar over char, steam reforming reactions are more likely to happen and have a faster rate in comparison with dry reforming reaction. Therefore addition of steam is more effective in reducing the tar content and preventing char deactivation. The addition of sub-stoichiometric air or O_2 for partial oxidation is useful to provide the heat necessary to sustain the endothermic reforming reactions. Such reactions are useful to prolong the activity of char: the experiments carried out in inert atmosphere very often show char deactivation due to coke formation and blocking of micropores.

Different authors observed a preferential activity of char towards heavy PAH species. As a consequence, mild oxidative reaction conditions can also be useful to convert mono-aromatic tar such as phenols, toluene and heterocyclic aromatics into multi-aromatic molecules.

The overview of the results from all the campaigns conducted on the topic show that, under appropriate conditions, the use of char produced from pyrolysis or gasification can achieve a high tar reduction also at relatively low temperatures (700-800°C). Nevertheless, the application of char for tar reforming requires not only an extensive tar reduction, but also an efficient reforming into combustible gases such as CO and H_2. In this way, the chemical energy of tar is transferred in permanent gas species which can be used for clean combustion or even for chemical synthesis. This process has to be as efficient as possible, so to limit the depletion of energy to actualize the reforming of tar. The use of char as a substrate for reforming reactions can assist in this task, but for the purpose of implementing of char-based gas upgrading systems, it is important to quantify the energy flows and take into account how much of the energy contained in the volatiles is depleted in the process.

The high number of research groups who have been working on this topic show that the idea of applying char to attain a low tar producer gas is widespread and potentially ready to be implemented in demonstration plants. A few authors have actually proposed gasification process designs integrating the use of char to improve the quality of producer gas. In general, the separation of the

process into stages seems to be the most efficient solution to take advantage of the catalytic properties of char. The few demonstration plants presented in literature gave encouraging results, concluding that char is a promising material to support the reforming of tar into stable gases. However, the examples of carbon-based gas upgrading integrated into gasification systems are still limited and further research and optimization is needed for full-scale application.

References

[1] Milne T, Evans R. Biomass Gasifier "Tars": Their Nature , Formation , and Conversion. NREL 1998.

[2] Li C, Suzuki K. Tar property , analysis , reforming mechanism and model for biomass gasification — An overview 2010;13:594–604. doi:10.1016/j.rser.2008.01.009.

[3] Font Palma C. Modelling of tar formation and evolution for biomass gasification: A review. Appl Energy 2013;111:129–41. doi:10.1016/j.apenergy.2013.04.082.

[4] Griffiths DML, Mainhood JSR. The cracking of tar vapour and aromatic compounds on activated carbon. Fuel 1967:167–76.

[5] Chembukulam SK, Dandge AS, Kovllur NL, Seshaglri RK. Smokeless Fuel from Carbonized Sawdust. Ind Eng Chem Prod Res Dev 1981;719:714–9.

[6] Boroson ML, Howard JB, Longwell JP, Peters W a. Heterogeneous cracking of wood pyrolysis tars over fresh wood char surfaces. Energy & Fuels 1989;3:735–40. doi:10.1021/ef00018a014.

[7] Monteiro Nunes S, Paterson N, Dugwell DR, Kandiyoti R. Tar formation and destruction in a simulated downdraft, fixed-bed gasifier: Reactor design and initial results. Energy & Fuels 2007;21:3028–35. doi:10.1021/ef070137b.

[8] Dabai F, Paterson N, Millan M, Fennell P, Kandiyoti R. Tar formation and destruction in a fixed-bed reactor simulating downdraft gasification: Equipment development and characterization of tar-cracking products. Energy & Fuels 2010;24:4560–70. doi:10.1021/ef100681u.

[9] Gilbert P, Ryu C, Sharifi V, Swithenbank J. Tar reduction in pyrolysis vapours from biomass over a hot char bed. Bioresour Technol 2009;100:6045–51. doi:10.1016/j.biortech.2009.06.041.

[10] Matsuhara T, Hosokai S, Norinaga K, Matsuoka K, Li CZ, Hayashi JI. In-situ reforming of tar from the rapid pyrolysis of a brown coal over char. Energy & Fuels 2010;24:76–83. doi:10.1021/ef9005109.

[11] Chaiwat W, Hasegawa I, Mae K. Alternative reforming methods of primary tar released from gas treatment of biomass at low temperature for development of pyrolysis/gasification process. Ind Eng Chem Res 2010;49:3577–84. doi:10.1021/ie901695r.

[12] Sun Q, Yu S, Wang F, Wang J. Decomposition and gasification of pyrolysis volatiles from pine wood through a bed of hot char. Fuel 2011;90:1041–8. doi:10.1016/j.fuel.2010.12.015.

[13] Zhang ZZ, Zhu MM, Liu PF, Wan WC, Zhou WX, Chan YL, et al. Effect of Biochar on the Cracking of Tar from the Pyrolysis of a Pine Sawdust in a Fixed Bed Reactor. Energy Procedia 2015;75:196–201. doi:10.1016/j.egypro.2015.07.299.

[14] Zhang Y, Wu W, Zhao S, Long Y, Luo Y. Experimental study on pyrolysis tar removal over rice straw char and inner pore structure evolution of char. Fuel Process Technol 2015;134:333–44. doi:10.1016/j.fuproc.2015.01.047.

[15] Al-Rahbi AS, Onwudili JA, Williams PT. Thermal decomposition and gasification of biomass pyrolysis gases using a hot bed of waste derived pyrolysis char. Bioresour Technol 2016;204:71–9. doi:10.1016/j.biortech.2015.12.016.

[16] Park J, Lee Y, Ryu C. Reduction of primary tar vapor from biomass by hot char particles in fixed bed gasification. Biomass and Bioenergy 2016;90:114–21. doi:10.1016/j.biombioe.2016.04.001.

[17] Jin L, Bai X, Li Y, Dong C, Hu H, Li X. In-situ catalytic upgrading of coal pyrolysis tar on carbon-based catalyst in a fixed-bed reactor. Fuel Process Technol 2016;147:41–6. doi:10.1016/j.fuproc.2015.12.028.

[18] Song Y, Zhao Y, Hu X, Zhang L, Sun S, Li CZ. Destruction of tar during volatile-char interactions at low temperature. Fuel Process Technol 2018;171:215–22. doi:10.1016/j.fuproc.2017.11.023.

[19] Monteiro Nunes S, Paterson N, Herod AA, Dugwell DR, Kandiyoti R. Tar formation and destruction in a fixed bed reactor simulating downdraft gasification: optimization of conditions. Energy & Fuels 2008;22:1955–64. doi:10.1021/ef402293m.

[20] Dabai F, Paterson N, Millan M, Fennell P, Kandiyoti R. Tar formation and destruction in a fixed bed reactor simulating downdraft gasification: Effect of reaction conditions on tar cracking products. Energy & Fuels 2014;28:1970–82. doi:10.1021/ef402293m.

[21] Abu El-Rub Z, Bramer EA, Brem G. Experimental comparison of biomass chars with other catalysts for tar reduction. Fuel 2008;87:2243–52. doi:10.1016/j.fuel.2008.01.004.

[22] Hosokai S, Kumabe K, Ohshita M, Norinaga K, Li C, Hayashi J-I. Mechanism of decomposition of aromatics over charcoal and necessary condition for maintaining its activity. Fuel 2008;87:2914–22. doi:10.1016/j.fuel.2008.04.019.

[23] Krerkkaiwan S, Tsutsumi A, Kuchonthara P. Biomass derived tar decomposition over coal char bed. ScienceAsia 2013;39:511. doi:10.2306/scienceasia1513-1874.2013.39.511.

[24] Krerkkaiwan S, Mueangta S, Thammarat P, Jaisat L, Kuchonthara P. Catalytic Biomass-Derived Tar Decomposition Using Char from the Co-pyrolysis of Coal and Giant Leucaena Wood Biomass. Energy & Fuels 2015;29:3119–26. doi:10.1021/ef502792x.

[25] Hayashi JI, Iwatsuki M, Morishita K, Tsutsumi A, Li CZ, Chiba T. Roles of inherent metallic species in secondary reactions of tar and char during rapid pyrolysis of brown coals in a drop-tube reactor. Fuel 2002;81:1977–87. doi:10.1016/S0016-2361(02)00128-X.

[26] Widayatno WB, Guan G, Rizkiana J, Hao X, Wang Z, Samart C, et al. Steam reforming of tar derived from Fallopia Japonica stem over its own chars prepared at different conditions. Fuel 2014;132:204–10. doi:10.1016/j.fuel.2014.04.089.

[27] Wang FJ, Zhang S, Chen ZD, Liu C, Wang YG. Tar reforming using char as catalyst during pyrolysis and gasification of Shengli brown coal. J Anal Appl Pyrolysis 2014;105:269–75. doi:10.1016/j.jaap.2013.11.013.

[28] Min Z, Yimsiri P, Asadullah M, Zhang S, Li C-Z. Catalytic reforming of tar during gasification. Part II. Char as a catalyst or as a catalyst support for tar reforming. Fuel 2011;90:2545–52. doi:10.1016/j.fuel.2011.03.027.

[29] Sueyasu T, Oike T, Mori A, Kudo S, Norinaga K, Hayashi JI. Simultaneous steam reforming of tar and steam gasification of char from the pyrolysis of potassium-loaded woody biomass. Energy & Fuels 2012;26:199–208. doi:10.1021/ef201166a.

[30] Klinghoffer N, Castaldi MJ, Nzihou A. Catalyst Properties and Catalytic Performance of Char from Biomass Gasification. I&Ec 2012:13113–22. doi:10.1021/ie3014082.

[31] Rodríguez-Reinoso F. The role of carbon materials in heterogeneous catalysis. Carbon N Y 1998;36:159–75. doi:10.1016/S0008-6223(97)00173-5.

[32] Hosokai S, Norinaga K, Kimura T, Nakano M, Li C-Z, Hayashi J. Reforming of Volatiles from the Biomass Pyrolysis over Charcoal in a Sequence of Coke Deposition and Steam Gasification of Coke. Energy & Fuels 2011;25:5387–93. doi:10.1021/ef2003766.

[33] Chen Y, Luo YH, Wu WG, Su Y. Experimental investigation on tar formation and destruction in a lab-scale two-stage reactor. Energy & Fuels 2009;23:4659–67. doi:10.1021/ef900623n.

[34] Wu W, Luo Y, Su Y, Zhang Y, Zhao S, Wang Y. Nascent Biomass Tar Evolution Properties under Homogeneous/Heterogeneous Decomposition Conditions in a Two-Stage Reactor. Energy & Fuels 2011;25:5394–406. doi:10.1021/ef2007276.

[35] Zhao S, Luo Y, Zhang Y, Long Y. Experimental investigation of the synergy effect of partial oxidation and bio-char on biomass tar reduction. J Anal Appl Pyrolysis 2015;112:262–9. doi:10.1016/j.jaap.2015.01.016.

[36] Phuphuakrat T, Namioka T, Yoshikawa K. Tar removal from biomass pyrolysis gas in two-step function of decomposition and adsorption. Appl Energy 2010;87:2203–11. doi:10.1016/j.apenergy.2009.12.002.

[37] Feng D, Zhao Y, Zhang Y, Sun S. Effects of H2O and CO2 on the homogeneous conversion and heterogeneous reforming of biomass tar over biochar. Int J Hydrogen Energy 2017;42:13070–84. doi:10.1016/j.ijhydene.2017.04.018.

[38] Fuentes-Cano D, Gómez-Barea A, Nilsson S, Ollero P. Decomposition kinetics of model tar compounds over chars with different internal structure to model hot tar removal in biomass gasification. Chem Eng J 2013;228:1223–33. doi:10.1016/j.cej.2013.03.130.

[39] Feng D, Zhao Y, Zhang Y, Gao J, Sun S. Changes of biochar physiochemical structures during tar H2O and CO2heterogeneous reforming with biochar. Fuel Process Technol 2017;165:72–9. doi:10.1016/j.fuproc.2017.05.011.

[40] Brandt P, Larsen E, Henriksen U. High tar reduction in a two-stage gasifier. Energy & Fuels 2000;14:816–9. doi:10.1021/ef990182m.

[41] Zhang LX, Matsuhara T, Kudo S, Hayashi JI, Norinaga K. Rapid pyrolysis of brown coal in a drop-tube reactor with co-feeding of char as a promoter of in situ tar reforming. Fuel 2013;112:681–6. doi:10.1016/j.fuel.2011.12.030.

[42] Mun TY, Kang BS, Kim JS. Production of a producer gas with high heating values and less tar from dried sewage sludge through air gasification using a two-stage gasifier and activated carbon. Energy & Fuels 2009;23:3268–76. doi:10.1021/ef900028n.

[43] Mun TY, Seon PG, Kim JS. Production of a producer gas from woody waste via air gasification using activated carbon and a two-stage gasifier and characterization of tar. Fuel 2010;89:3226–34. doi:10.1016/j.fuel.2010.05.042.

[44] Choi YK, Mun TY, Cho MH, Kim JS. Gasification of dried sewage sludge in a newly developed three-stage gasifier: Effect of each reactor temperature on the producer gas composition and impurity removal. Energy 2016;114:121–8. doi:10.1016/j.energy.2016.07.166.

[45] Gómez-Barea A, Leckner B, Villanueva Perales A, Nilsson S, Fuentes Cano D. Improving the performance of fluidized bed biomass/waste gasifiers for distributed electricity: A new three-stage gasification system. Appl Therm Eng 2013;50:1453–62. doi:10.1016/j.applthermaleng.2011.12.025.

[46] Zeng X, Wang F, Li H, Wang Y, Dong L, Yu J, et al. Pilot verification of a low-tar two-stage coal gasification process with a fluidized bed pyrolyzer and fixed bed gasifier. Appl Energy 2014;115:9–16. doi:10.1016/j.apenergy.2013.10.052.

[47] Zhang S, Asadullah M, Dong L, Tay HL, Li CZ. An advanced biomass gasification technology with integrated catalytic hot gas cleaning. Part II: Tar reforming using char as a catalyst or as a catalyst support. Fuel 2013;112:645–53. doi:10.1016/j.fuel.2013.03.015.

[48] Dong L, Asadullah M, Zhang S, Wang XS, Wu H, Li CZ. An advanced biomass gasification technology with integrated catalytic hot gas cleaning Part I. Technology and initial experimental results in a lab-scale facility. Fuel 2013;108:409–16. doi:10.1016/j.fuel.2012.11.043.

[49] Zhang S, Song Y, Song YC, Yi Q, Dong L, Li TT, et al. An advanced biomass gasification technology with integrated catalytic hot gas cleaning. Part III: Effects of inorganic species in char on the reforming of tars from wood and agricultural wastes. Fuel 2016;183:177–84. doi:10.1016/j.fuel.2016.06.078.

[50] Palla Assima G, Marie-Rose S, Lavoie JM. Role of fixed carbon and metal oxides in char during the catalytic conversion of tar from RDF gasification. Fuel 2018;218:406–16. doi:10.1016/j.fuel.2017.12.039.

Chapter 2

Laboratory tests with tar model compounds

The literature review reported in Chapter 1 showed that the use of char beds for the removal of tar can be highly effective. However, the contact between char and tar has to take place under optimized condition to achieve a good and stable gas quality.

Residual char from TwoStage gasification, generated at the "Viking" demonstration plant is particularly interesting for this application, for different reasons. First of all, it is a process residue, and therefore an inexpensive waste material. Secondly, this material is known to have a large specific surface area and pore volume [23]. The porous surface structure of Viking char suggests that it could be particularly effective if re-used as bed material for producer gas treatment.

The experimental work performed at laboratory scale aimed at observing the interaction between the surface of char and tar model compounds, and in particular to test the ability of Viking char to remove or convert tar species under different conditions. From the literature study conducted, it was clear that the temperature was determinant in the interaction between char and tar. Therefore, experiments were designed primarily to assess the effect of the char bed temperature on tar species.

A tentative laboratory setup was assembled at DTU, Risø Campus. The setup and the obtained results are presented in the first section of this chapter. Most of the laboratory-scale experimental work was conducted during the external research stay at Institute for Energy Technology at TU Berlin. During the research stay, it was also possible to characterize the Viking char and other tested materials with various analytical techniques. The results are comprehensively presented in Paper II. The final section of this chapter shows SEM analysis that was conducted at DTU Energy, on the samples produced at TU Berlin.

2.1 Preliminary tests with gasification residual char and tar model compounds

The first steps in investigating the potential of this material for tar removal and decomposition were taken by assembling an experimental setup for laboratory tests with tar model compounds. The preliminary objective of the experimental activity was to verify the ability of a small char bed to decrease the concentration of aromatic compounds in a gaseous flow. With this in mind, a setup was assembled at DTU, Risø.

2.1.1 Experimental setup

The purpose of the system was to flush a hot char bed with a nitrogen flow enriched with aromatic compounds, and monitor the concentration of aromatics before and after the passage through the char bed. Naphthalene and phenol were chosen as models representatives of different tar classes. The setup consisted of a system to entrain aromatic compounds into the gaseous flow, an electrically heated reactor containing the char bed and a gas sampling system. The experimental setup is schematically presented in Figure 2.1.

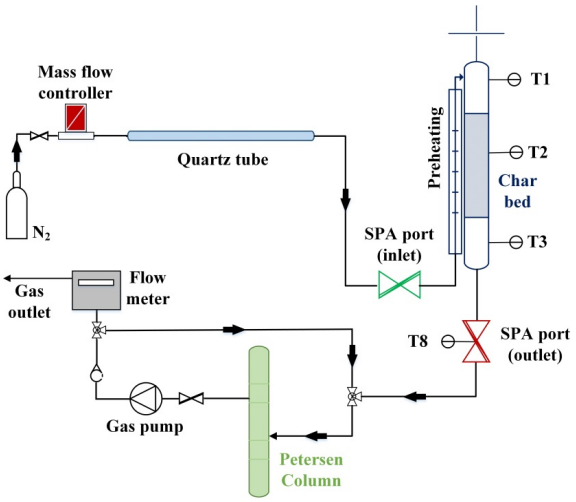

Figure 2.1: *Laboratory setup with sampling system*

Both phenol and naphthalene are in solid phase at ambient temperature and pressure. In order to entrain vapors in the gaseous flow, about 2 g of the substance were melted inside a quartz glass tube by means of a heat gun, to cover the inner surface of the tube with crystals. Two different tubes were prepared, one with phenol and the other with naphthalene, so that they could be used alternatively in the setup. The N_2 flow (1 l/min) through the system was regulated by a mass flow controller (Bronkhorst, Holland). The quartz tube covered with crystals was maintained at room temperature, and was submerged with liquid water to buffer the ambient temperature fluctuations.

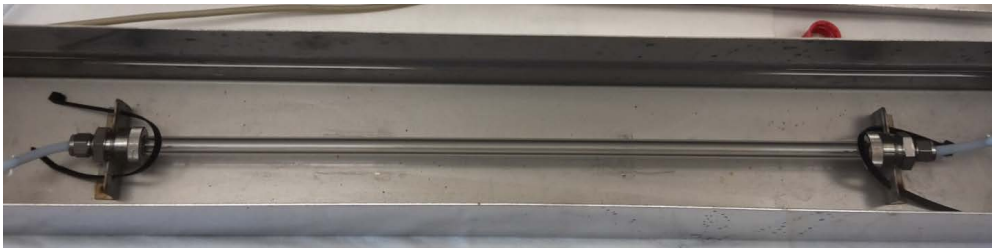

Figure 2.2: *The quartz tube connected in the system, submerged in water.*

Because of the relatively high vapor pressure of both phenol and naphthalene under these conditions, a significant amount of phenol or naphthalene could be added to the flow. The quartz tube in the water bath is showed in Figure 2.2. The reactor containing the char bed was enclosed in an electric furnace. The gas flow enriched with vapors of aromatics was led to the oven where it was first preheated, then passed through the bed of char. The reactor was built of stainless steel 316L, it had an internal diameter of 55 mm and total height of 300 mm. The char bed was supported by a grate. The preheating pipe (2.2 m long, with 2.5 mm internal diameter,) was coiled around the reactor body. Prior to the start of each test, the reactor was loaded with char from the top and it was sealed with a graphite gasket and bolts. Three thermocouples were mounted (T1-T2-T3 in Figure 2.1) to monitor the temperature along the reactor. The reactor is showed, disassembled, in Figure 2.3.

Figure 2.3: *The reactor used in the laboratory setup at DTU, Risø Campus*

In order to guarantee a uniform temperature along the height of the reactor, the temperature control of the electric furnace was divided into two equal parts, one at the top and one at the bottom. In this way, it was possible to adopt different set-points and maintain a uniform temperature in different zones of the reactor. The different components of the setup were connected by a 6 mm Teflon tube. Leak-free connections were arranged using appropriate fittings (Swagelok, USA). The metal tubing section right downstream of the reactor was covered with glass wool, to avoid condensation of aromatic compounds upstream of the SPA sampling port.

2.1.2 Gas sampling and analysis

The concentration of the model compounds in the gas flow was measured before and after the passage through the bed by sampling with Solid Phase Adsorption (SPA) technique. SPA samples were collected manually by means of a needle and a syringe: for this purpose, two sampling ports were arranged before and after the char reactor. SPA tubes were LC-NH_2 SPE tubes (Supelco/Merck, Germany). In addition, the outlet gas flow was washed with acetone through a Petersen Column, to verify the results obtained from the SPA measurements. The column was jacket-refrigerated and was filled with about 250 ml of acetone. A gas pump was connected at the outlet of the system to induce the gas flow through the column. The flow was controlled using a rotameter placed downstream of the pump, which was not as accurate as the mass flow controller at the inlet of the setup. For this reason, the bypass loop showed in Figure 2. 1 was arranged to prevent the pump to accidentally cause excessive depressurization in the lines upstream.

The concentration of the model compounds in the gas flow was quantified by Gas Chromatography-Mass Spectrometry (GC-MS) analysis, using deuterium labelled compounds (phenol d5, naphthalene d8) as internal standards. The sampling, processing and analysis methods are described in detail in Appendix 1. All the samples were analyzed using a Hewlett Packard HP 6890 gas chromatograph interfaced to a HP5973 Mass Selective Detector (Agilent, Denmark). Samples (1µl) were injected in the split mode (1:20) using an HP 7683 autosampler (Agilent, Denmark). The source and rod temperatures were 230 ˚C and 150 ˚C, respectively. The products were separated using a 30 m WCOT-fused silica column (VF-23ms) with 0.32 mm of internal diameter (Agilent, Denmark). The carrier gas was Helium with a flow rate of 1.2 ml/min. Separation of products was achieved using a temperature program from 70 to 250˚C at 10˚C / min.

2.1.3 Setup operation and experimental conditions

The char used for all tests was recovered from the ash container of the TwoStage “Viking” gasifier at DTU, Risø Campus, which had been fed with spruce wood chips. The material was used without any pre-treatment. In preparation of the tests, the reactor was loaded and heated up until the temperatures measured by T2 and T3 were constant. T2 was placed about 1 cm below the surface of the char bed, while T3 measured the temperature beneath the grate. When the reactor was filled with char, the same bed was tested in 3 consecutive experiments, without changing the temperature set-points of the oven. The

gas flow was kept constant in all the tests (1 l/min), and the temperature of sublimation was maintained as constant as possible with the water bath. However, the concentration of phenol and naphthalene in the flow upstream of the reactor was found to have significant fluctuations. When phenol was used, the average inlet concentration was 569 ± 92 mg/Nm^3. The baseline concentration of naphthalene was more stable, 240 ± 37 mg/Nm^3. The removal of the model compounds was evaluated with the empty reactor at 250°C, 500°C and 600°C. Subsequently, the same temperature set-points were applied with the char-loaded reactor. An overview of experimental conditions is given in Table 2.1.

Table 2.1: *Experimental conditions tested with the char bed setup*

Model compound	Temperature [°C]	Char bed [g]	Residence time [s]
Phenol	250	-	
	250	30	10.4
	500	-	
	500	30	7
	600	-	
	600	30	6.2
Naphthalene	250	-	
	250	30	10.4
	600	-	
	600	30	6.2
	600	17	2.7

Each test was run for 60 minutes: during this time, 6 samples were collected with SPA, 3 at inlet and 3 at outlet. Samples were extracted after 20, 40 and 50 minutes from the start of the experiment. In the experiments with char, the same bed was used for 3 consecutive experiments in the same conditions. Sampling with Petersen column was run continuously during each test. The removal efficiency of aromatics (X) was calculated based on the inlet and outlet concentrations of aromatics (C_{in} and C_{out}) as defined in equation 1.

$$X\,[\%] = \frac{C_{in} - C_{out}}{C_{in}} * 100 \qquad (1)$$

The values used in the calculation of X were obtained by averaging the results from SPA samples. The Petersen column measurements were used to validate the results obtained by SPA.

2.1.4 Results and Discussion

The data collected during experiments with phenol are presented in Table 2.2.

Table 2.2: *Overview of results obtained from experiments with phenol. σ indicates the standard deviation*

Reactor temperature [°C]	Bed	Duration [min]	SPA inlet [mg/m³]	σ ±	SPA outlet [mg/m³]	σ ±	X [%]	Petersen [mg/m³]	σ ±	X [%]
250	empty	33	699	53	755	49	**-8.0**	882	26	**-26**
250	char (30 g)	60	508	35	3.04	2.2	99.4	0.66	0.02	99.9
250	//	60	605	7.0	5.74	4.2	99.1	0.25	0.3	100
250	//	60	500	6.7	1.63	1.5	99.7	1.12	0.1	99.8
500	empty	60	399	31	273	3.9	**31.6**	346	11.3	**13.4**
500	char (30 g)	60	453	2.4	5.25	1.7	98.8	73.2	0.8	83.8
500	//	60	568	14	5.41	0.9	99.0	6.4	0.0	98.9
500	//	60	534	34	7.11	4.1	98.7	35.5	0.0	93.3
600	empty	60	679	16	13.2	6.7	**98.1**	1.76	0.6	**99.7**
600	char (30 g)	60	613	100	15.8	6.2	97.4	2.02	0.3	99.7
600	//	60	746	105	22.5	4.2	97.0	0.20	0.2	100
600	//	60	679	71	11.5	2.5	98.3	0.00	0.0	100

The effect of the char bed was especially evident at 250°C. At this temperature, phenol was virtually unaffected by the passage through the empty reactor. The average phenol concentration measured at the outlet was slightly higher than the one at the inlet, but the difference was within the measurement uncertainty. In contrast, in presence of the char bed, virtually no phenol was detected at the outlet. The concentration of phenol, following the passage through the empty reactor at 500°C and 600°C, decreased by 32% and 99.7%, respectively. Therefore it was not possible to reliably quantify the effect of the char bed at these temperatures. Nevertheless, in presence of the char bed at 500°C, the removal level was close to 98% during three consecutive experiments.

The almost complete removal of phenol in the empty reactor at 600°C was probably due to a catalytic effect of the reactor material (Stainless steel 316L). This material indeed contains a certain amount of Ni

and Cr that might have had an effect on the decomposition of phenol. Obviously, removal efficiency was virtually complete also in presence of the char bed, during the three consecutive experiments.

The agreement between the concentration values measured with Petersen column and the average of the values measured with SPA at the outlet was not always very good. For the highest concentrations, the error was as high as 20%, with the column giving a higher result in comparison with SPA. When measuring low concentrations of phenol, the relative error was even higher. Figure 2.4 shows a comparison of the results obtained with SPA and with the Petersen column.

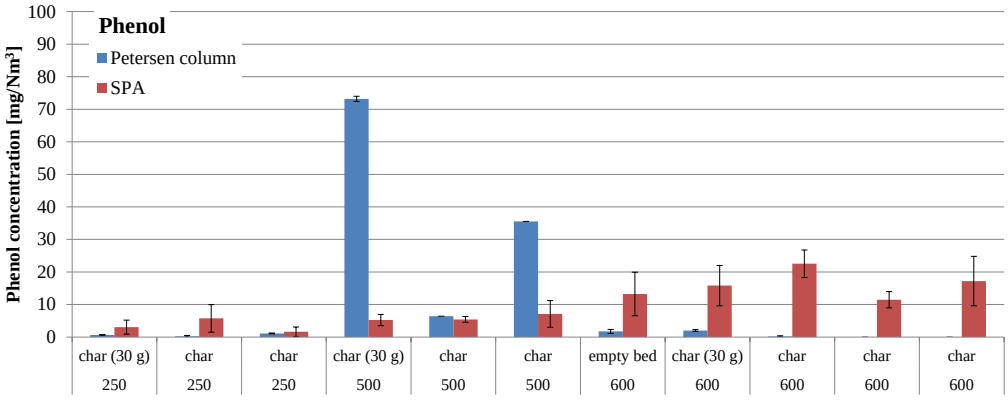

Figure 2.4: *Comparison of SPA and Petersen column results on the phenol concentration measured at the outlet of the system.*

Results from the experiments carried out with naphthalene are summarized in Table 2.3. No significant effect on the concentration of naphthalene was observed after the passage through the empty reactor at 250 and 600°C. This was due to the fact that naphthalene has a very stable and refractory structure in comparison with phenol. In presence of the char bed at 250°C the removal of naphthalene was particularly efficient: no naphthalene was detected in the outlet gas during three consecutive tests. In contrast, at 600°C naphthalene was not completely eliminated.

Table 2.3: *Overview of results obtained from experiments with naphthalene. (*the outlet SPA sample was lost, and removal efficiency was calculated based on the Petersen column result)*

Reactor temperature [°C]	Bed	Duration [min]	SPA inlet [mg/m³]	σ ±	SPA outlet [mg/m³]	σ ±	X [%]	Petersen [mg/m³]	σ ±	X [%]
250	empty	70	231	33.9	226	9.3	**1.8**	229	1.27	0.8
250	char (30 g)	60	239	17.6	0.0	0.0	100	0.0	0.0	100
250	//	60	193	20.6	0.0	0.0	100	0.0	0.0	100
250	//	60	201	28	0.0	0.0	100	0.0	0.0	100
600	empty	60	212	13	202	0.9	**4.6**	203.3	0.96	4.0
600	char (30 g)	60	230	21.9	(no sample)*		95.4	10.6	0.18	95.4
600	//	60	255	14	16.0	22.6	93.8	22.4	1.6	91.2
600	//	60	247	8.2	33.1	23.4	86.6	35.8	0.60	85.5
600	char (17 g)	60	291	6.7	20.9	29.5	92.8	29.8	3.01	89.7
600	//	60	265	15.4	45.2	0.0	82.9	46.3	1.72	82.6
600	//	60	318	11.2	58.7	0.9	81.6	46.3	1.72	85.5

The highest naphthalene conversion (95.4%) was measured during the first hour of experiment with a char bed of 30 g. During the two following hours, conversion decreased to 93.8% and 86.6%. When the reactor was loaded with a smaller amount char (17 g), the same trend was observed. In this case, the conversion of naphthalene decreased from 92.8% to 81.6% over 3 hours. It has to be noticed that in some cases (especially for the tests at 600°C) the average concentrations obtained with SPA samples had a very large deviation. However, the average values were in much better agreement with the results obtained with the Petersen column, in comparison with the case of phenol. Figure 2.5 shows a comparison between the values of naphthalene concentration measured at the outlet with SPA and Petersen column.

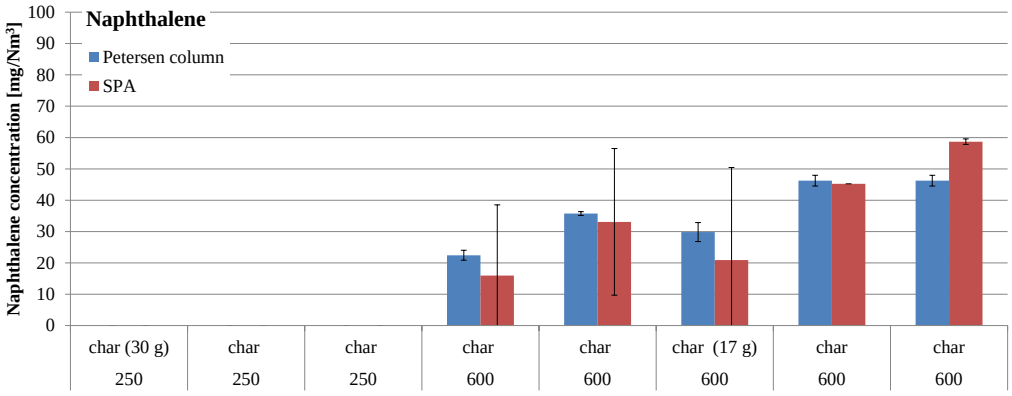

Figure 2.5: *Comparison of SPA and Petersen column results on naphthalene concentration measured at the outlet of the system.*

2.1.5 Conclusion

The aim of this work was to preliminarily investigate the capacity of a char bed to decrease the concentration of tar model compounds entrained in a nitrogen flow, at different temperatures. An experimental setup was prepared for testing a bed of residual gasification char generated by the TwoStage "Viking" gasifier. Tests were carried out using phenol and naphthalene as model tar compounds. SPA sampling and GC-MS analysis were used to quantify the change in the concentration of aromatics induced by the passage through the reactor.

The effect of the char bed on the concentration of phenol was evident at 250°C, when the conversion was virtually complete. Lower removal efficiency was observed with a char bed at 500°C. The removal of phenol from the gas flow under these conditions was due to simple adsorption on the char surface, as the temperature was too low for decomposition reactions to take place. The interaction of phenol with the char bed at 600°C was shadowed by an extensive decomposition of phenol caused by the blank test in an empty reactor, probably caused by a catalytic effect of steel 316L.

When using naphthalene, this problem did not arise. Naphthalene was completely eliminated from the N_2 flow when using a char bed at 250°C, but the removal efficiency decreased significantly at 600°C. The decreasing efficiency observed with increasing temperature suggests that naphthalene was adsorbed on

the surface of char. High temperatures are known to hinder adsorption and diminish the adsorption capacity of solids [35].

Overall, results obtained with this laboratory setup suggest that a bed of Viking char is able to efficiently remove phenol and naphthalene from a N_2 flow, and that removal shows a maximum at the lowest tested temperature (250°C). The interaction between char and model tar species is probably limited to physical adsorption at this temperature.

These general conclusions are the only ones that can be drawn from these results. The experimental setup had many practical limitations that influenced the quality and the repeatability of the results. Because of the adopted gas sampling methods, the concentration of aromatics in the gas phase could only be measured discontinuously. Each sample required a complex, multi-step processing which probably contributed to the uncertainty of the final results. Another limitation of the setup was that the gas generation system was not able to deliver a very accurate baseline concentration of phenol or naphthalene. In addition, no instrument was available for the evaluation of the composition of the gas phase. Therefore it was not possible to detect decomposition products of the aromatic compounds, i.e. CO or H_2. The following recommendations should be followed in order to improve this setup:

1) Modify the gas generation system, so that the baseline concentration of aromatics can be set with accuracy (eg. by heating the quartz tube or by using a syringe pump instead)
2) Making use of an online system to measure the concentration of aromatics in the flow with a higher resolution. The optimal solution would be to have a GC directly connected to the outlet of the system.

An improved experimental system was available to be used at the Institute for Energy Technology at the Technical University of Berlin, for the evaluation of the char bed performance in the adsorption and decomposition of model tar compounds. Therefore, further laboratory tests conducted with tar model compounds were performed using the setup at TU Berlin.

Adsorption and decomposition of tar model compounds over the surface of gasification char and active carbon within the temperature range 250-800°C

G. Ravenni[1*], O.H. Elhami[2], J. Ahrenfeldt[1], U.B. Henriksen[1], Y. Neubauer[2]
[1]Technical University of Denmark (DTU), Department of Chemical and Biochemical Engineering, Frederiksborgvej 399, 4000 Roskilde, Denmark
[2]Technische Universität Berlin, Institute of Energy Technology Fasanenstrasse 89, 10623 Berlin, Germany
*Corresponding author: Giulia Ravenni Phone: +45 93 51 15 92 E-mail: grav@kt.dtu.dk

Manuscript under review for Elsevier journal "Applied Energy" (*)

Abstract

The carbonaceous products of gasification or pyrolysis (chars) and active carbon (AC) have been found effective as adsorbents for tar species and active as catalysts for tar conversion. However, a deeper understanding of the interaction between aromatic compounds and carbonaceous surfaces is needed for the practical implementation and optimization of carbon–based gas cleaning systems. The aim of this work is to investigate the performance of various wood-derived chars and AC within a wide temperature range (250-800°C). Residual char from gasification, pyrolysis char and two types of AC were tested for their capability to remove tar model compounds (toluene and naphthalene) from a gaseous flow. A dedicated setup was used for this purpose, while post-experimental characterization revealed the modifications occurring at the surface of chars. Adsorption was observed in the lower temperature range, whereas cracking reactions were found to initiate at 600°C and to become significant at 800°C. Results suggested that AC represents a better option for tar adsorption applications (e.g. carbon filters) operating at temperatures of 250°C and possibly below, whereas gasification residual char resulted as the most promising substrate for tar cracking at temperatures of 800°C and above.

(*) Published version in "Applied Energy" 241 (2019) 139 – 151, Elsevier

1. Introduction

The quality of producer gas generated by gasification of biomass is one of the main issues hindering the commercialization of this thermochemical conversion process. In general, biomass producer gas contains tar, a mixture of condensable substances including light 1-ring aromatics, polycyclic aromatic hydrocarbons and heterocyclic aromatics [1]. Tar contamination prevents the widespread use of biomass producer gas as an alternative to fossil resources. If the gas quality issue is overcome, it could be used to fuel engines and turbines or for synthesis of biofuels and bio-chemicals.

Several options for producer gas treatment have been proposed and implemented including cold gas cleaning, hot gas filtration, thermal cracking, catalytic cracking by using metal-based catalysts (e.g. nickel, iron, noble metals) or mineral catalysts (e.g. dolomite, olivine) [2].

The use of char and active carbon (AC) to reduce the content of tar in producer gas has been suggested by a number of authors who worked with tar model compounds [3–6] and with tar derived from pyrolysis or gasification [7–12]. Overall, these carbonaceous materials appear as a viable alternative to metal and mineral catalysts, with manifold advantages. Firstly, they can be inexpensive, especially if residual char is used (for example from gasification plants). Secondly, they can be less harmful for the environment and for human health in comparison with synthetic catalysts [13], especially if not impregnated with metals, but directly used as a gas cleaning substrate. In addition, chars and AC can find several end-life applications such as being recycled as a solid fuel or as a precursor for carbon materials. Potentially they could even be used as biochar for soil amendment and carbon sequestration, if the relevant thresholds for noxious contaminants (e.g. heavy metals, polycyclic aromatic hydrocarbons, dioxins) are verified.

The solid residue of gasification is a specific kind of char which is usually considered as a waste material or a by-product of gasification plants. The properties of this char vary significantly depending on the feedstock and on the operating conditions of the gasifier. In general, it contains inorganics such as alkali and alkaline earth metals, which are naturally contained in the feedstock, and is rich in carbon. Indeed, only the carbon atoms arranged in the most stable structures endure gasification reactions. Such reactions are also responsible for the physical activation of char, which can produce a microporous material with a significant specific surface area. Oftentimes this material presents surface properties which are comparable to commercial AC [14]. For this reason, gasification char has been considered for various applications as a cheaper alternative to manufactured AC [15–19], as well as for tar removal and

conversion applications [20,21]. The latter solution would be economically and environmentally beneficial for gasification plants: indeed the valorization of the solid by–product, which often does not meet the requirements for soil application as biochar, would improve the economic feasibility especially for small-scale systems [22].

The TwoStage gasification platform developed at DTU, Risø Campus (also known as "Viking gasifier") is able to produce a virtually tar-free gas as described in [9]. The solid residue of the TwoStage gasification process (hereby called "Viking char") presents a high carbon content and a very large specific surface area in comparison with chars generated from other gasification processes [14,23]. For these reasons it could be especially effective for gas treatment applications.

The practical implementation of carbon-based gas cleaning systems is still at the initial stage, as it is not yet clear which are the char characteristic and the reaction conditions required to optimize the removal of tar. In particular, some authors considered char as an adsorbent for tar [24–26], whereas others used it as a substrate for tar cracking [8,10,12,27,28] and reforming [11,29–32].

Adsorption on carbon surfaces has been extensively studied and used for removal of organic contaminants from gaseous streams [33,34]. Being an exothermic process, adsorption is hindered at high temperatures [35], as a consequence of the increased vapor pressure of the adsorbate [33]. Nevertheless, for adsorption of tar compounds on chars, it is advisable to work at a minimum temperature of 250°C, as lower temperatures could lead to condensation of tar from the producer gas.

On the other hand, cracking of aromatic molecules making up the tar mixture requires much higher temperatures: around 1200°C in homogeneous conditions [36]. Char is able to act as a catalyst for cracking and reforming of aromatics. Indeed, an enhancement in the conversion of aromatic structures at temperatures as low as 600°C has been observed in presence of char [27,37–39].

Under inert atmosphere, the decomposition of aromatics on the surface of chars and activated carbons is considered to take place through carbon deposition by coking according to reaction (1) [4]:

$$C_mH_n(aromatic) = C_mH_x(coke) + \frac{n-x}{2} H_2 \quad (1)$$

Such reaction is catalyzed by active sites. In absence of a reforming agent that can gasify the newly formed deposits, the carbon build-up gradually deactivates the carbonaceous surface. As a consequence, in practical applications it is advisable to consider the addition of air, steam or CO_2 to prolong the activity of carbonaceous surfaces. The process has been documented by several authors in the

temperature range 700-1000°C for different chars: commercial charcoal [4], activated carbons [40–42], char from pyrolysis of wood [31,43], rice straw [44], coal [29,45] or waste [10].
On these grounds, temperature appears as the determinant factor defining the nature of the interaction between char and aromatic compounds. With this in mind, the purpose of this work was to observe the course of interaction between aromatics and the surface of char within the temperature range 250 – 800°C, differentiating between adsorption and cracking phenomena. A dedicated setup developed at TU Berlin has been used to examine the effects of char beds on selected tar model compounds, namely toluene and naphthalene. Both these substances are commonly used as tar model compounds, as representatives of light 1-ring aromatics and light polycyclic aromatic hydrocarbons, respectively. Naphthalene is also one of the most refractory and stable substances found in biomass tar [46].
Moreover, to gain useful information for the design of an actual carbon-based tar removal system, residual gasification char was compared with similar carbonaceous materials with different surface structures: a commercial microporous AC and two pyrolysis-derived chars: one of them CO_2-activated and the other one heat-treated under N_2-atmosphere.
Tar removal and conversion efficiencies were evaluated and surface characterization was performed before and after the experiments to investigate the mechanism of interaction between aromatics and the surface of chars in the mentioned temperature range.

2. Materials and methods

2.1 Chars and activated carbons

Four carbonaceous materials were tested in the setup. Residual gasification char was collected at the TwoStage demonstration plant at DTU (the Viking gasifier), where the solid residue is stockpiled inside a dedicated container. Before being used as a bed material in the experiments, the Viking char was crushed and sieved to obtain a particle size similar the other chars (1.4 to 2 mm). The commercial AC has been kindly provided by Silcarbon Aktivkohle GmbH (Kirchhundem, Germany). According to the manufacturer this was a wood-derived AC which had been activated with steam for about 120 minutes at 800°C. In the following it will be referred to as AC-H_2O. The remaining two materials were produced in a screw pyrolysis unit at TU Berlin. Here, beech wood chips (Räuchergold ®, intended for food smoking) were pyrolyzed at 400°C. After pyrolysis, char was subject to CO_2 activation for 180 minutes at 750°C: the final product is referred to as AC-CO_2. Some of the material pyrolyzed at 400°C did not undergo

activation, but heat treatment at 900°C under N_2 atmosphere, to guarantee its thermal stability during high temperature experiments. Such pyrolysis-derived char will be referred to as PC-N_2. Figure 1 shows the different production and activation pathways. All chars were dried at 105°C for 3 hours and stored in a desiccator prior to be used in the experiments.

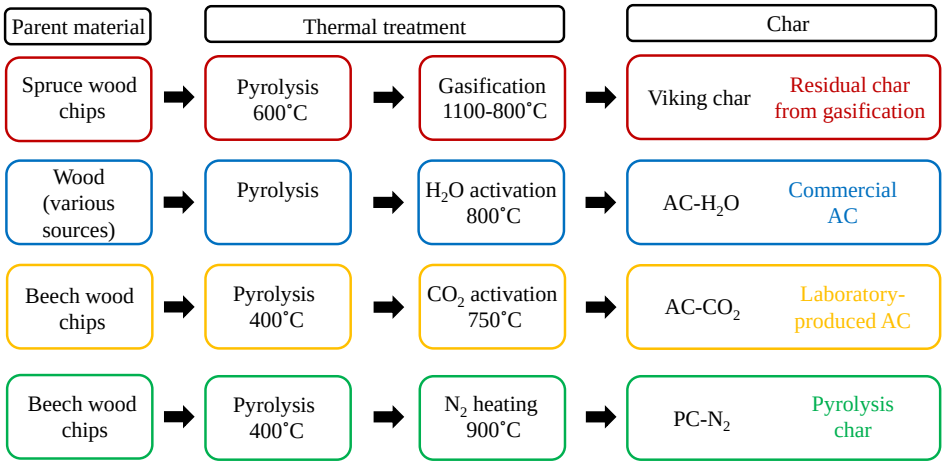

Figure 1*: Production and activation of the tested chars.*

2.2 Characterization of chars

All the selected chars were characterized in terms of composition and surface properties. Prior to any analysis, chars were reduced to powder in a ball mill. The volatile and ash content of chars were evaluated by using a muffle furnace, following CEN/TS 15148 and DIN 51719 (815°C) respectively. The fixed carbon content was calculated by difference. The elemental composition (CHNS) was measured with a VarioEL III (Elementar Analysensystem GmbH, Germany). The trace elements present in the chars were detected by Inductively Coupled Plasma- Optical Emission Spectrometry (ICP-OES) (Varian 720 ES).

The specific surface area was quantified by Brunauer-Emmett-Teller (BET) analysis through N_2 adsorption at 77 K (Nova 2200, Quantachrome Instruments, USA). Before each measurement, char samples were degassed at 150°C for 6 hours. The pore volume distribution was evaluated through Quenched Solid Density Functional Theory (QSDFT) using the calculation model for slit and cylindrical pores on the adsorption branch: this method is recommended for chemically and physically activated

carbons [47]. The densities of char powders, used as inputs for the BET and DFT calculations, were measured with a helium pycnometer (Quantachrome Instruments, USA).

The bulk density of the chars used as bed materials (not grinded) was evaluated by using a scale and a graduated cylinder. The elemental composition (CHNS) and BET surface area were measured also on chars recovered after the tests, to evaluate the differences with fresh materials.

2.3 Experimental setup

The experimental setup for testing the performance of char beds (Figure 2) was designed and built at TU Berlin. The setup consisted of a stainless steel tube reactor 500 mm in length, with an internal diameter of 36 mm to contain the char bed. The reactor was placed inside an electric furnace (Lenton, UK) and connected at the top with a gas generation system, whereas the outlet at the bottom was connected to the gas analysis train.

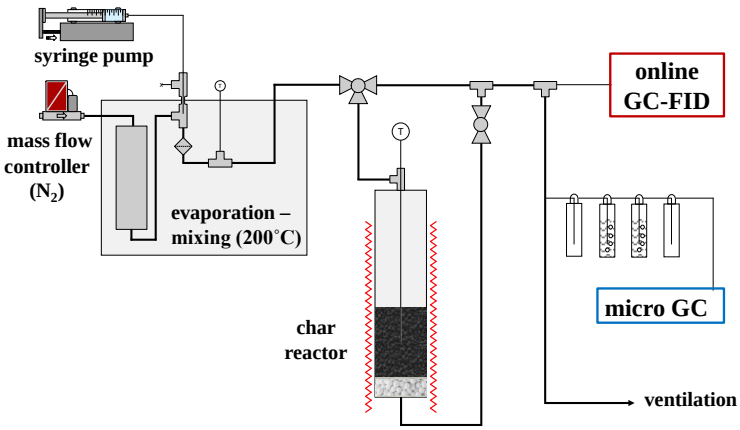

Figure 2*: Diagram of the experimental setup*

A N_2 flow (4.7 l/min) was mixed with vapors of a toluene–naphthalene solution dosed with a syringe pump (Nemesys, Cetoni, Germany). The feed solution was prepared by mixing analytical grade toluene (purity>=99.5%, Carl Roth, Germany) with naphthalene crystals (purity >=99%, Carl Roth, Germany). The solution was prepared with a concentration of 0.63 mol/L. The dosing of the syringe was set between 107-109 µl/min, according to the exact concentration of naphthalene in the solution, so to maintain a stable feed in all tests. The concentrations of toluene and naphthalene in the N_2 were calculated to be 18345 ± 0.5% and 1852 ± 0.1% mg/Nm^3, respectively. Evaporation of the solution took

place inside a capillary which was kept at a temperature of 200°C by a dedicated oven. Vapors were mixed with a pre-heated flow of N_2 in the tubing contained in the oven. The aromatics-enriched gas was delivered to the char reactor through heated lines (180°C) to avoid condensation. The system was equipped with a 3-way switching valve allowing the aromatics-enriched N_2 flow to be conveyed directly to the analytical instruments for background measurements (reactor bypass mode), or to be passed through the heated reactor during experiments.

2.4 Online gas analysis

The online analysis consisted of a compact GC–FID (SRI Instruments, USA) for detection of toluene and naphthalene in the flow: the samples were eluted through a 30 m FS Supreme-5ms (5% Phenylpolysilphenylenphase) column, heated to a constant temperature of 180°C. A system of valves was used for automatic sampling of the gas: injections were made in series of ten, every 2 minutes. For the duration of the experiment, each series was set to start automatically after 1 minute. Downstream, the flow was washed through cooled bottles filled with 2-propanol before being fed to a double channel micro-GC (Inficon, Switzerland) with TCD detectors. Channel A was equipped with a Molar Sieve 5Å column (10m x 320μm) for detection of N_2, O_2, H_2, CO and CH_4. Samples were injected at 70°C and eluted at 80°C and 1.72 bar with Argon as carrier gas. Channel B mounted a PoraPlotQ column (8 m x 320 μm) for detection of CO_2 and light hydrocarbons. Samples were injected at 70°C and eluted at 100°C and 1.38 bar with Helium as carrier gas. The micro-GC was programmed to inject a gas sample in both channels every 4.5 minutes.

2.5 Adsorption and cracking tests

Prior to each test, the reactor was carefully cleaned with compressed air. At the bottom of the reactor, 30 g of Al_2O_3 cylindrical beads 5x5 mm (Sasol, Germany) were placed between two plugs of quartz wool to create a 5 cm tall support for the char. The support was necessary so that the char bed would be positioned in the central part of the furnace, where the temperature was the closest to the oven set point. The bed material was then added in the reactor. The height of the char bed was kept constant in all experiments (10 cm) and the weight of the fresh bed varied from 8 g to 22 g depending on the bulk density of each char. In this way, the gas residence time in the char bed was maintained constant in the tests at the same temperature, varying from 0.72 s at 250°C to 0.35 s at 800°C. The reactor was then

sealed and placed inside the furnace. A thermocouple with the tip placed in the middle of the char bed was used to monitor the temperature inside the reactor.

Before the start of each experiment, the system was flushed with N_2 to remove any oxygen present in the reactor or in the lines. As soon as no oxygen was detected by the micro-GC, the furnace and the lines were heated up to the desired set point. When the temperature set points in the system were reached and stable, the char bed was flushed with N_2 for 60 minutes. Afterwards the syringe pump started dosing with the system in bypass mode, to verify the stability of the baseline concentrations. Each experiment was started by turning the 3-way valve so that the aromatics-enriched flow would pass through the reactor before encountering the gas analysis train. Long tests had to be interrupted for a refill of the syringe pump with fresh toluene-naphthalene solution. During refilling (1-2 minutes) the system was switched to bypass mode. Viking char and the two types of active carbon were tested at 250, 400, 600 and 800°C. PC–N_2 char was tested only at the lowest and the highest temperature. An additional test was run with Viking char at the intermediate temperature of 500°C. An overview of the experimental conditions is given in Table 1.

Table 1*: Overview of experimental conditions. The gas residence time was calculated dividing the char bed height to the gas superficial velocity.*

Temperature [°C]	250	400	500	600	800
Residence time [s]	0.72	0.56	0.49	0.43	0.35
Char bed (100 mm)	Viking	Viking	Viking	Viking	Viking
	AC-H_2O	AC-H_2O		AC-H_2O	AC-H_2O
	AC-CO_2	AC-CO_2		AC-CO_2	AC-CO_2
	PC-N_2				PC-N_2

The baseline concentrations (C_0) of both toluene and naphthalene were measured with dedicated bypass runs for each experiment. During the whole campaign, the uncertainty on the baseline measurements was 7% for both compounds. This relatively large deviation was caused by the limited volume available in the lines between the syringe pump injection port and the measuring instrument. Whenever the flow was deviated through the reactor, therefore covering a longer path before reaching the instrument, the measured concentrations appeared more stable. Despite the oscillations recorded in the bypass mode, the average baseline values were stable from test to test. On these premises, the steadiness of the concentrations delivered by the mixing system was deemed satisfactory.

3. Results and discussion

3.1 Preliminary char characterization

Table 2 and 3 show the results of char compositional analysis, while Table 4 shows the results obtained by BET and DFT analysis, together with the bulk density of the bed materials.

Table 2*: Proximate and elemental composition (dry basis) of the tested chars*

	Proximate composition (dry basis)			Elemental composition			
	Volatiles	**Fixed C**	**Ash**	**C**	**H**	**N**	**S**
Viking [wt%]	6.8	83.7	9.4	87.6	0.6	0.1	< 0.1
AC-H_2O [wt%]	4.4	90.8	4.9	88.9	0.2	0.3	< 0.1
AC-CO_2 [wt%]	4.1	93.1	2.6	90.9	0.7	0.3	< 0.1
PC-N_2 [wt%]	2.4	94.9	2.7	91.4	0.5	0.8	< 0.1

Table 3*: Overview of results of ICP-OES analysis*

	Na	**Mg**	**P**	**K**	**Ca**	**Al**	**S**	**Cr**	**Mn**	**Fe**	**Ni**
Viking [wt%]	0.101	0.205	0.124	2.070	2.092	0.024	0.081	0.002	0.047	0.089	0.001
AC-H_2O [wt%]	0.027	0.258	0.109	2.358	0.141	0.151	0.075	0.005	0.043	0.138	0.001
AC-CO_2 [wt%]	0.026	0.204	0.061	0.720	1.065	0.034	0.061	0.004	0.036	0.048	0

The compositional analysis showed that the Viking char, in comparison with the other materials, had a smaller fraction of fixed carbon and higher ash content. This was expected considering that the Viking char had been exposed to harsh gasification reactions, as the TwoStage gasifier is known to achieve a carbon conversion efficiency close to 99% [48]. The most abundant elements in the ashes were Ca and K, followed by Mg, Fe and P. The largest difference among the tested materials was found in the abundance of Ca in the Viking char, and of K in both Viking char and AC-H_2O.

Table 4*: Surface properties obtained with N_2 adsorption at 77K*

	BET specific surface area	DFT pore volume	DFT micropore volume	Bulk density
	[m^2/g]	[cm^3/g]	[cm^3/g]	[Kg/m^3]
Viking char	1253	0.79	0.37	84
AC-H_2O	553	0.24	0.18	221
AC-CO_2	564	0.24	0.19	138
PC-N_2	35	0.02	0.01	198

The BET analysis showed that Viking char had the largest specific surface area, whereas PC-N_2 char had by far the lowest. The other two chars, that had undergone similar activation treatments, had a comparable BET area and pore volume. In order to understand the difference in the surface morphology of the tested materials, it is useful to consider the isotherms obtained with N_2 adsorption at 77 K (Figure 3). Following the IUPAC classification [49], the isotherms obtained from both AC-H_2O and AC-CO_2 resemble a reversible type I, suggesting that these materials are microporous. Particularly the latter shows the narrowest pore size distribution. PC-N_2 char also generated an isotherm resembling type I, but with much lower N_2-uptake. In contrast, the isotherm obtained from Viking char is a composite of type I and II, with a marked hysteresis (type H4). This kind of isotherm indicates a micro – mesoporous materials, and is often associated with slit-shaped pores [49,50]. The adsorbed volume increasing at higher relative pressures indicates the presence of mesopores (> 2 nm) and macropores (> 50 nm).

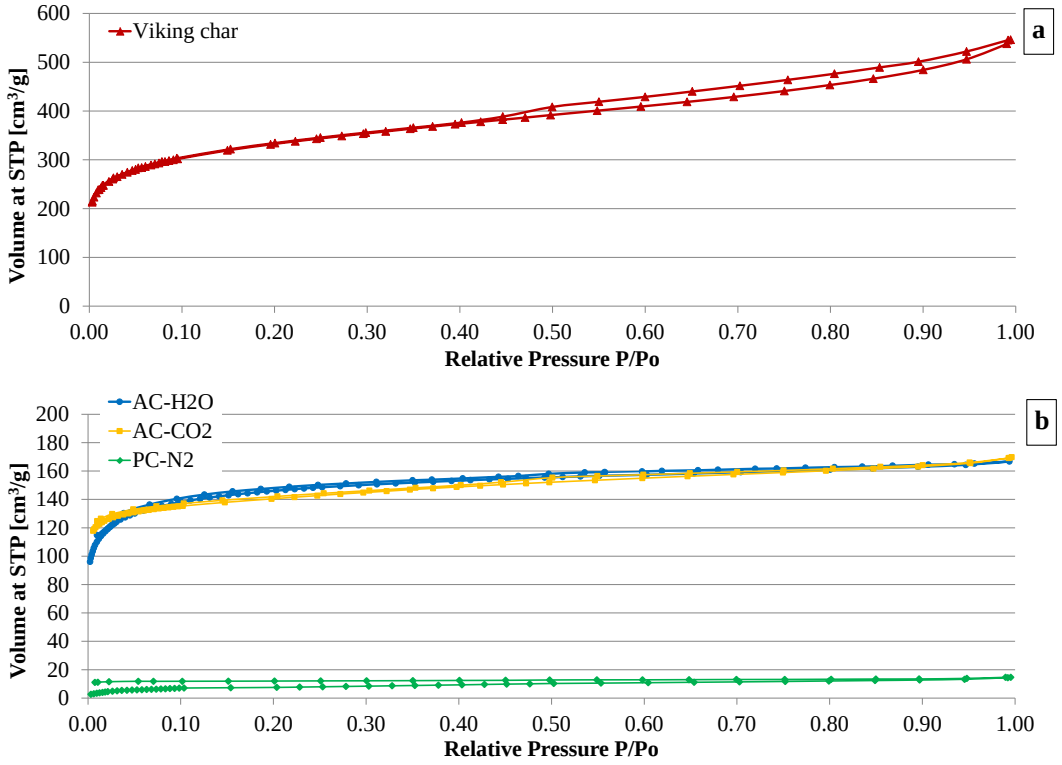

Figure 3: *Comparison of isotherms obtained with N_2 adsorption at 77 K on Viking char (a), AC-H_2O, AC-CO_2 and PC-N_2 (b). Isotherms are plotted separately as they have a different scale on the y-axis*

Even though N_2 adsorption at 77 K is not the optimal method to determine the micropore size distribution, in this instance it has been used to estimate the total micropore volumes for the sake of comparing the chars. The total pore volumes and micropore volumes obtained through DFT analysis are reported in Table 4. As for the BET surface area, the highest and lowest values were observed for the Viking char and the PC-N_2 char, respectively. The differences in the textural characteristics of the chars were confirmed by the distribution of the surface area over the pore sizes: significant deviations were observed in the pore size range between 2 and 15 nm, showed in Figure 4.

Viking char appears to have the largest surface associated with mesopores, with pore width spanning from 2 to 12 nm. AC-H_2O exhibits a narrower distribution, confined between 2 and 5 nm. In this size range, PC-N_2 and AC-CO_2 show similar distributions. This is not unexpected, as they are derived from

the same parent material; however the effect of CO_2 activation is evident not only in the increased surface area associated with micropores but also with mesopores between 2.5 and 6 nm.

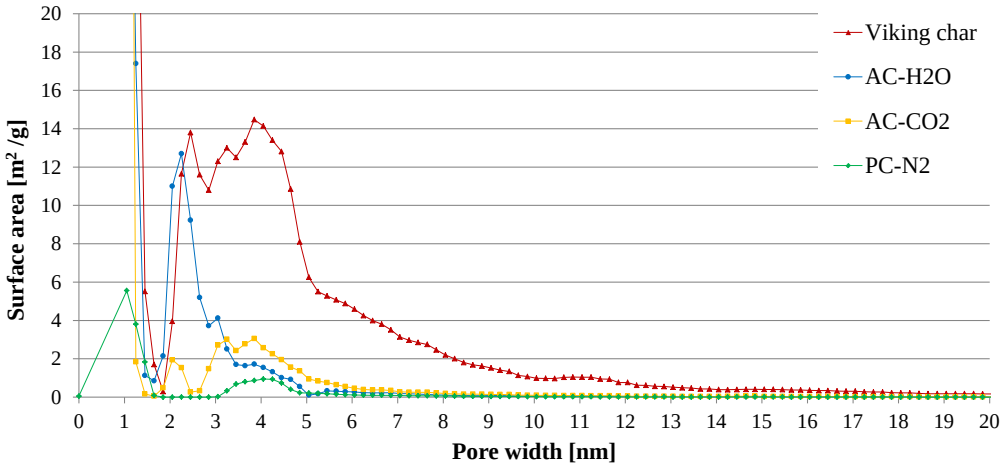

Figure 4: *Comparison of surface area distributions in the small mesopores range, obtained with QSDFT analysis for the different chars*

The characterization analysis on the tested materials showed the marked differences among them, especially in regard to surface structure and pore distribution. The different surface properties affected significantly the interaction with the tested aromatic compounds.

The surface oxygen groups present on the surface of chars (lactones, carboxylic acid or phenol and basic groups such as carbonylic, quinonic and pyrone structures) are known to have an influence on the adsorption capacity at low adsorbate concentrations [51]. They might also affect the catalytic properties of chars [52]. However, the oxygen content of active carbon is known to decrease with increasing activation temperatures, reaching a minimum at temperatures above 1000°C [53]. Moreover, oxygen groups were found to desorb from the surface of chars at temperatures lower than 800°C [54]. In light of this, because the chars that have been tested in this work were treated at temperatures of 750°C or higher before being used as bed materials, oxygen functional groups were not considered to significantly affect the performances of chars.

3.2 Results from experiments in the temperature range 250 - 400˚C

During the experiments performed with reactor temperatures of 250 and 400˚C, toluene permeated very quickly through the char beds. It regained the baseline concentration level after 10 minutes when the reactor contained Viking char, and in about 20 minutes with the two types of AC. When PC-N_2 char was used in the reactor, the toluene concentration was hardly affected. The abrupt breakthroughs did not allow a reliable calculation of the adsorption capacity of toluene for the tested materials.

In contrast, chars and AC had a more pronounced effect on the concentration of naphthalene, which took a longer time to breakthrough in all tests. This effect can be ascribed to the high concentration of toluene that prompted a sudden breakthrough, but also to the predilection of the char surfaces for purely aromatic compounds. This is due to the specific interactions between π-electron rich regions of solid carbon and the aromatic rings and has been described for low adsorbate concentrations [25,55].

The breakthrough curves traced by the relative concentration of naphthalene C/C_0 are shown in Figure 5. C and C_0 indicate the instantaneous concentration and the baseline concentration, respectively.

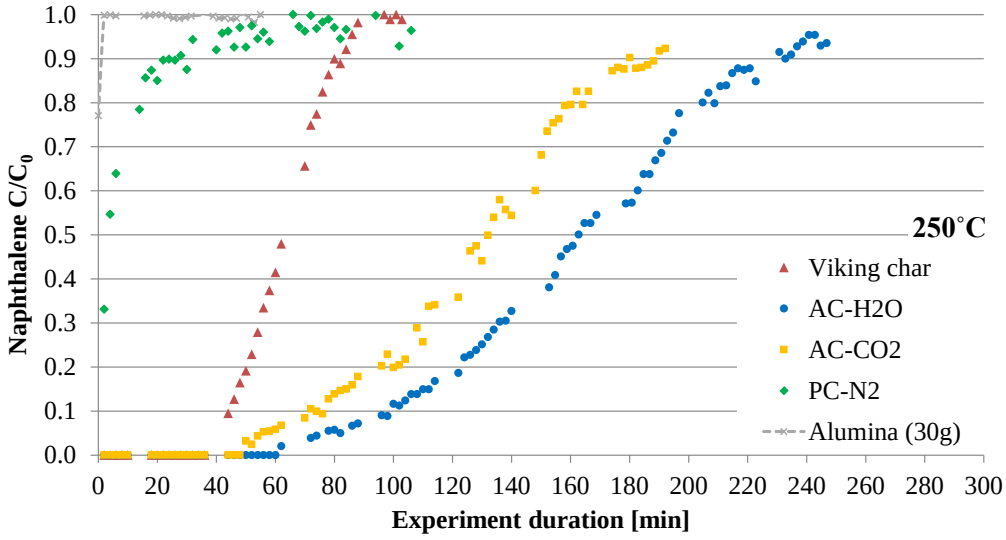

Figure 5: *Naphthalene breakthrough curves obtained with different chars, bed temperature 250˚C*

The tested chars showed different effects on the naphthalene concentration. AC-H_2O attained the longest breakthrough time, followed by AC-CO_2. Both chars produced a similar, gradual breakthrough

curve. The long time to breakthrough was partly due to their well-developed microporosity, but also to the higher bulk density of these chars (see Table 4). Indeed, even if the bed volume was constant, the Viking char bed weighed 8 g, while the beds of AC-H_2O and AC-CO_2 weighed 22.5 and 15 g, respectively. Despite the shorter breakthrough time, the specific adsorption capacity of Viking char was comparable with the two activated materials. The bed of PC-N_2 char had a minor effect on the naphthalene concentration, and the very short breakthrough time reflected a very low adsorption capacity.

The breakthrough curves obtained from the GC-FID measurements were used to calculate adsorption capacity q (mg/g_{char}) of the chars following (2)

$$q = \frac{Q}{W}\left[C_0 t_f - \frac{1}{2}\sum_0^{t_f}[C(t_n) + C(t_{n-1})] * \Delta t\right] \quad (2)$$

Where Q is the nitrogen flow (Nm^3/min), W is the weight of the bed material in the reactor (g), C_o is the inlet concentration (mg/Nm^3), t_n is the n_{th} data point, t_f is the time (min) when complete breakthrough is reached and $\Delta t = t_n - t_{n-1}$.

Viking char, AC-H_2O and AC-CO_2 were also tested for adsorption at 400°C. At this temperature, breakthroughs were significantly faster: for Viking char, less than 30 minutes were sufficient for the relative concentration of naphthalene to reach 1. Table 5 collects the calculated adsorption capacities for the tested materials.

Table 5*: Naphthalene adsorption capacities at 250°C and 400°C*

	Adsorption capacity for naphthalene	
Char bed temperature	250°C	400°C
	mg/g_{char}	mg/g_{char}
Viking	66.7	9.5
AC-H_2O	60.5	9.7
AC-CO_2	75.4	21.1
PC-N_2	4.1	Not measured

The increase in bed temperature caused a sharp decline in the adsorption capacity for the tested chars. The negative correlation between adsorption capacity and temperature is due to the exothermic nature of the adsorption process and has been observed in previous works [26,35,56].

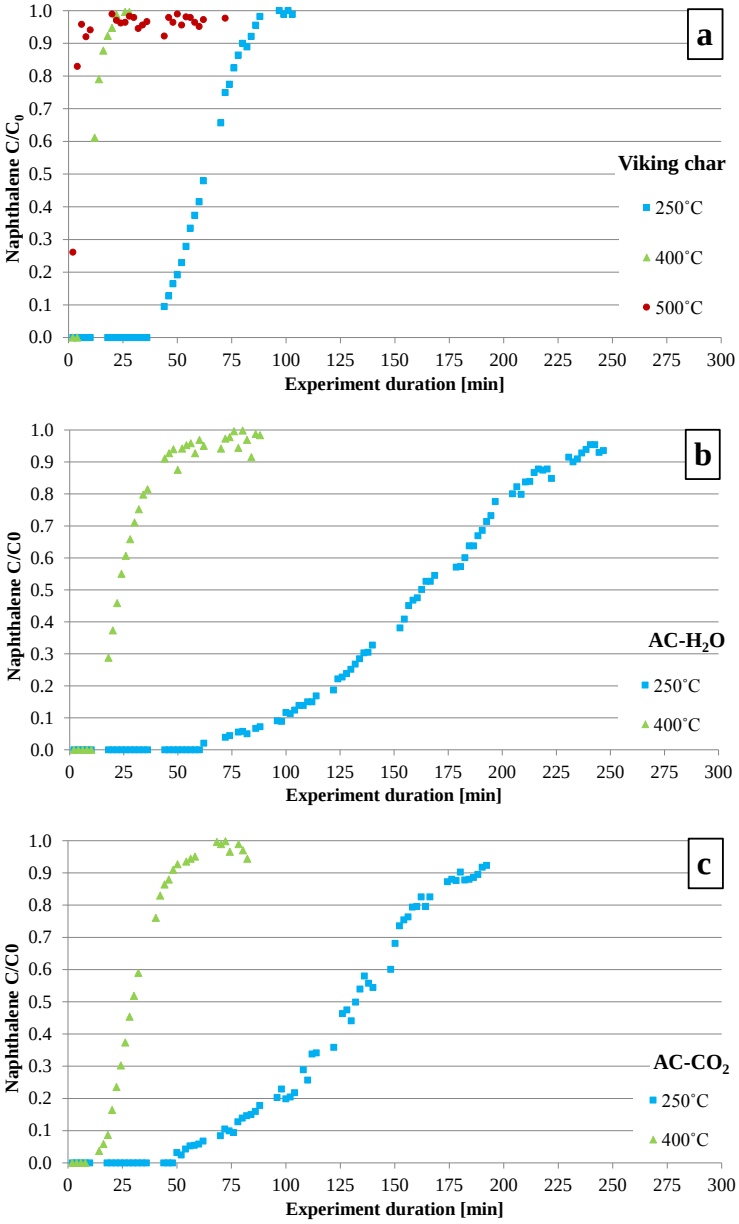

Figure 6: *Naphthalene breakthrough obtained with Viking char (a), AC-H_2O (b) and AC-CO_2 (c) at different temperature levels*

This trend was confirmed with an experiment performed with Viking char at 500˚C: the breakthroughs of both toluene and naphthalene were almost instantaneous and the naphthalene adsorption capacity was found to drop further to 1.3 mg/g_{char} . Figure 6 (a-c) shows the breakthrough curves obtained at different temperatures using Viking char, AC-H_2O and AC-CO_2 as bed materials.

These results suggested that adsorption performance of chars and activated carbons (e.g. if used in carbon filters) can be hindered by medium-high temperatures.

At 250 and 400˚C, AC-CO_2 showed the highest adsorption capacity for naphthalene: this can be ascribed to the surface texture of this char, which is the richest in micropores as a consequence of CO_2 activation [57]. Viking char and AC-H_2O exhibited somehow comparable adsorption capacities, even though the highest density of char AC-H_2O led to a longer time to breakthrough. PC-N_2 showed a dramatically lower adsorption capacity in comparison with the other materials. According to Mastral et al. [58], total microporosity is the main factor influencing adsorption of aromatics on the surface of AC: the lack of micropores explains the poor performance of non-activated char.

Overall, microporous AC with high bulk density appeared as a promising material for tar adsorption applications at temperatures of 250˚C and below. The performance of AC could be improved if the activation process during manufacturing would be optimized for this specific application. In real conditions, the tar mixture also contains aromatics larger than naphthalene (4- or 5- rings) which would also require pores in the mesoporous range for optimal adsorption [24]. In this instance, AC could be particularly useful in the fine cleaning of biomass producer gas, with low levels of tar contamination.

It is worth to point out that in the temperature range 250 to 400˚C no gases other than N_2 were detected with micro-GC in the exit gas. The typical shape of breakthrough curves associated with adsorption phenomena and the absence of other gas species at the outlet of the system confirmed that no decomposition reactions took place in these conditions. Only in the experiment at 500˚C with Viking char, traces of hydrogen were detected (< 0.01 Vol%), suggesting that cracking reactions were incipient at this temperature.

3.3 Cracking of aromatics at 600 and 800˚C

During experiments carried out at higher temperatures, the concentration of both toluene and naphthalene at the outlet of the system evolved somehow differently, and at the highest temperature complete breakthrough was not achieved. The evolution of relative concentrations (C/C_0) of

naphthalene and toluene at 600°C are depicted in Figure 7. The relative conversion of aromatics was calculated by using the average bypass concentration values measured for each experiment.

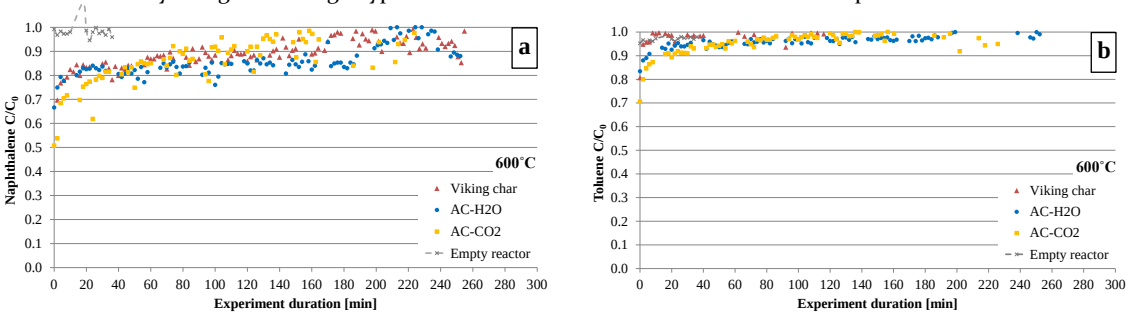

Figure 7: *Evolution of the relative concentrations of naphthalene (a) and toluene (b) at the outlet of the reactor during experiments at 600°C.*

The change of C/C_0 over time shows that at 600°C the char beds had a limited effect on the concentration of aromatics in the gaseous flow, particularly in the case of toluene. Viking char, AC-H_2O and AC-CO_2 were tested in these conditions, but the type of char used in the reactor did not appear to significantly influence the conversion values. For all tested chars, small amounts of H_2 were detected at the outlet of the system. H_2 concentration in the exit gas exhibited similar trends over time with the three chars, peaking around 0.07 Vol% during the first hour of experiment, to decrease gradually afterwards and stabilizing around 0.03-0.04 Vol%.

On the other hand, at 800°C both toluene and naphthalene were converted more efficiently by Viking char and activated carbons and clear differences emerged in the conversion performances of the different materials. The evolution of the relative concentrations of toluene and naphthalene are showed in Figure 8. Because of the long duration of these tests, the measurements had to be interrupted once in every test to refill the syringe pump. Refilling required 1-2 minutes, but the instruments required a longer time to stabilize the measures, therefore the gaps in the plots in Figure 8 and 9.

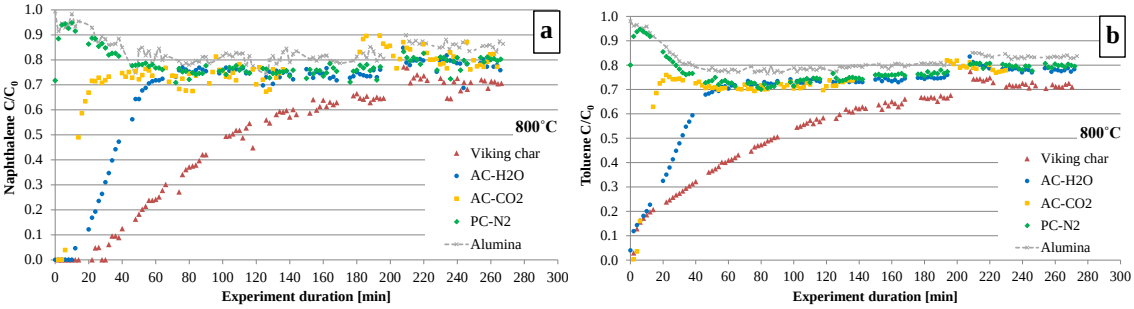

Figure 8: *Evolution of the relative concentrations of naphthalene (a) and toluene (b) at the outlet of the reactor during experiments at 800 °C.*

In these conditions the char PC-N_2 was also tested and it produced conversion values very similar to the blank test. However, in presence of this char, C/C_0 values remained slightly lower than the blank test, indicating a mild activity of the char surface. It is also interesting to notice the trend showed by both blank test and pyrolysis char test at the beginning of the experiment, with C/Co peaking close to 1, then decreasing and stabilizing at C/C_0 between 0.7 and 0.8. These trends indicate that in these two cases the deposition of carbon could actually support the decomposition of aromatics. The same effect was observed by Korus et al. [42], who found that coke-covered AC was still able to interact and decompose toluene, even if with a low level of conversion.

For the other chars, the very high conversion values were measured at the beginning of the tests: Viking char was the one performing better for naphthalene removal, attaining a complete conversion for about 30 minutes. Both AC-H_2O and AC-CO_2 achieved complete conversion for a shorter time (about 12 and 6 minutes, respectively). For toluene, complete conversion was observed for these chars only at the very beginning of the test. It appears as naphthalene was converted more efficiently than toluene. This observation agrees with the increased reactivity of chars towards compounds with increased aromaticity that has been observed in previous works [4,8,9,29,45]. However, it is worth to keep in mind that the concentrations of toluene and naphthalene differ by an order of magnitude (18345 ± 0.5% and 1852 ± 0.1% mg/Nm^3, respectively). This might have influenced their conversion efficiency.

Viking char, AC-H_2O and AC-CO_2 provided decreasing conversions over time as a consequence of surface deactivation. AC-H_2O and AC-CO_2 exhibited a fast deactivation, as they both converged with the C/C_0 values of PC-N_2 char in about 20 and 60 minutes, respectively. In contrast, Viking char produced a less abrupt increase of C/C_0, reaching a plateau after about 220 minutes from the start of the experiment. Also, the plateau value was still below the other chars.

The exact same trends can also be observed in the composition of the exit gas measured by micro-GC at the outlet of the system, as depicted in Figure 9. Again, the data gaps starting at 200 minutes originate from the measurement interruption to allow the syringe pump refilling. The gas conditioning system before the micro-GC required about 40 minutes for the instrument to show stable measurements. In the exit gas, H_2 and CH_4 were the only gases other than N_2 that were detected by micro-GC. The absence of CO and CO_2 was expected due to the lack of O_2 and of any other reforming agent inside the reactor.

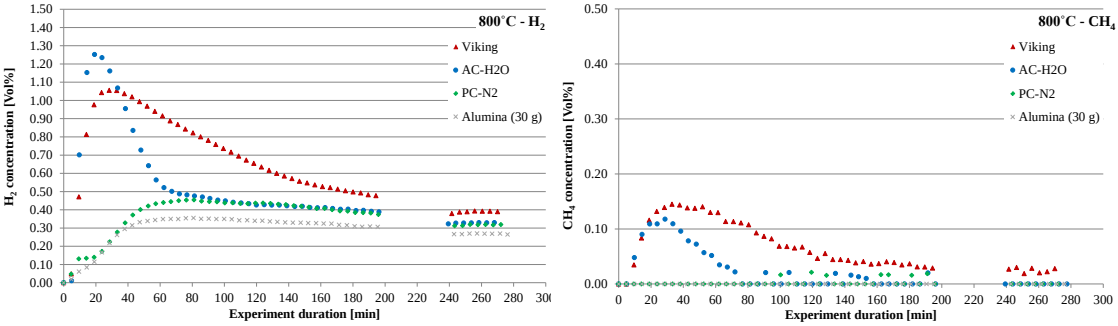

Figure 9: *H_2 and CH_4 concentrations measured during of tests with Viking char, AC-H_2O,* PC-N_2 *and blank test (Al_2O_3). Note that different scales are used on the y-axes.*

At 800°C, the H_2 production increased significantly if compared with the results at 600°C, reaching peaks above 1 Vol% for both Viking char and AC-H_2O. In addition, small amounts of CH_4 could be detected in the exit gas. H_2 formation was expected as a product of reaction (1). The presence of CH_4 as a reaction product most probably originated from the hydrogenation of methyl radicals, which form upon the initiation of toluene pyrolysis [42,59]. It is possible that benzene was also a product of decomposition, but this molecule was not detected by the applied GC-FID method.

The declining trends in the production of both H_2 and CH_4 confirm the deactivation of the char surfaces, with the same patterns observed on the GC-FID results. AC-H_2O showed a steeper decline in comparison with Viking char, and the production of both gases reached the levels of PC-N_2 char between 60 and 80 minutes from the start. It was not possible to quantitavely compare the H_2 and CH_4 production generated by AC-CO_2 with the other results, because of a slight variation in the quantification baseline for the micro-GC. However, it was qualitatively similar to AC-H_2O, with even steeper decreases in the concentration of both gases.

The same deactivation tendencies for the different chars are suggested by the evolution of the relative concentrations over time and by the composition of the exit gas. Viking char showed the slowest deactivation, even though considering the differences in the density of chars, the total surface area within the char beds was comparable (around 10.000 m^2). The prolonged activity of the residual gasification char can be ascribed to the wide pore size distribution including micro- and mesopores that could have facilitated the diffusion of the aromatic molecules. Indeed, mesoporous chars with large surface area are in general considered to have better long-term activity than microporous chars [41,60].
On the other hand, the pore size distribution of both types of AC was narrow and shifted towards small pores, therefore parts of their surface area could have been inaccessible; or easily made so by carbon deposition. Because of the pore structures their activity declined quickly, once most of the micropores were clogged. The slower deactivation tendency of Viking char is therefore ascribed in part to the larger specific surface area and to the wider pore size distribution, but also to the higher content in minerals (especially Ca and K), which might have migrated to the surface a consequence of the high temperatures encountered within the TwoStage gasification process. Indeed, the features that favored the activity of Viking char originated from the high degree of burn-off of this char.
The detection of H_2 as the main reaction product and the lack of light hydrocarbons in the exit gas confirm the mechanism of decomposition of aromatics over char described elsewhere [4,39,44], with dehydrogenation and coke formation through condensation/polymerization reactions. This reaction pathway was also confirmed by the characterization tests performed on the spent chars.

3.4 Analysis on spent chars

The results from tests at 600 and especially at 800°C gave evidence that the aromatic compounds were decomposed. In order to study the effect of such reactions on the surface of chars, the spent materials were carefully collected and analyzed.
The tests performed at 600°C had duration between 2 and 5 hours with the different char, depending on how fast deactivation was proceeding. As a result, it is difficult to compare the spent chars. However, the char beds (Viking char, AC-H_2O and AC-CO_2) all showed a slight weight gain around 2% of the original value.
On the other hand, all the experiments performed at 800°C had similar duration, therefore the results from post-analysis characterization can be compared. Significant differences between fresh and spent

chars were found in the bed weight, specific surface area and carbon content on the samples obtained with experiments at 800°C. Table 6 collects some of the values measured on the fresh and spent chars.

Table 6: *Overview of the characterization results relative to fresh and spent chars (after tests at 800°C). The duration of all the tests was 270 min, with the exception of AC-CO_2 which was tested for 230 minutes.*

	Bed weight		**Carbon content**		**Surface area**		**DFT pore volume**		**DFT micropore volume**	
	[g]		**[g]**		**[m^2/g]**		**[cm^3/g]**		**[cm^3/g]**	
	Fresh	Spent	Fresh	Spent	Fresh	Spent	Fresh	Spent	Fresh	Spent
Viking	9.0	14.7	7.9	13.8	1235	55.3	0.79	0.04	0.37	0.02
AC-H_2O	22.4	24.2	19.9	22.8	553	389	0.24	0.17	0.19	0.13
AC-CO_2	14.1	14.6	12.8	13.7	564	366	0.24	0.16	0.19	0.12
PC-N_2	20.5	19.8	19.0	18.7	35	267	0.02	0.13	0.01	0.08

Viking char, AC-H_2O and AC-CO_2 after the tests exhibited a weight gain together with increased carbon content and decreased surface area. These results indicate that deactivation of the chars was a consequence of solid carbon deposition (via polymerization/coking) on the active sites as a result of cracking reactions. This effect was expected due to the fact that no reforming or oxidizing agent was made available to react with deposited carbon during the tests.

The characterization of PC-N_2 delivered opposite results: the bed weight loss, accompanied by reductions in C, H, N and S is ascribed to further pyrolysis reaction that took place inside the reactor prior to the start of the experiment. Indeed, CO was detected in the exit gas during the preliminary flushing of the reactor with pure N_2 before the start of the test.

Experiments at 800°C were repeated for Viking char and AC-H_2O, where chars were exposed to the flow of N_2 and aromatics for a different duration. The repetitions confirmed the conversion values and deactivation patterns previously discussed and provided additional materials for the post-experiment characterization. It is important to keep in mind that the volume of the char beds was maintained constant in all experiments, but the weight of the materials varied as a consequence of the different density values (Table 4). Therefore, the change relative to the initial value (measured on the fresh char bed) is displayed in Figure 10 (a-c) for the bed weight, specific surface area and carbon content respectively.

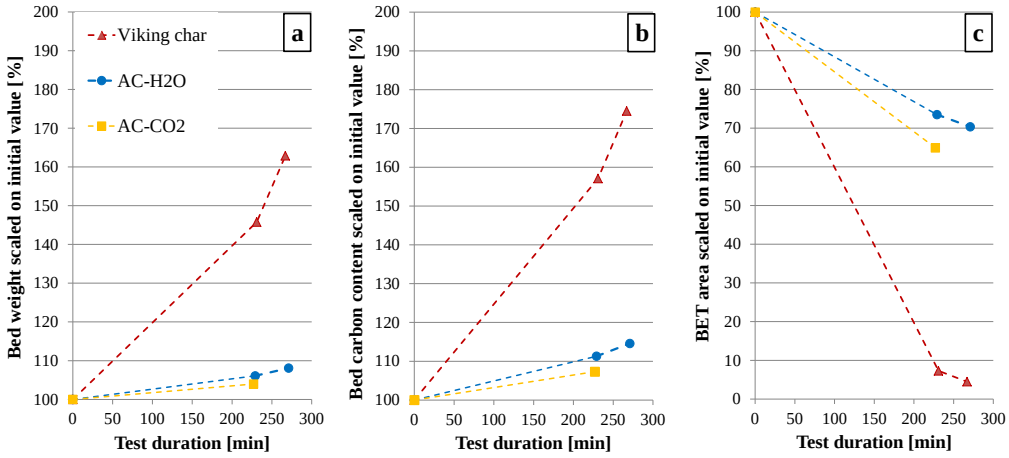

Figure 10: *Change relative to the values of fresh char beds of bed weight (a), carbon content (b), surface area (c) for Viking char, AC-H_2O and AC-CO_2 spent at 800°C.*

The increase in bed weight reflects the increased carbon content in the char beds, showing that the weight gain is given by deposition of elemental carbon. The decrease of specific surface area mirrors similar trends. The change in the DFT pore volume is not shown as it was virtually identical to the one for the BET surface area. Comparing the three materials, it is evident that Viking char was the one most affected by the experiments. Not only it gained the most weight (5.6 g in 270 minutes), but also its surface area decreased dramatically (from 1235 to 55 m^2/g in 270 minutes). The strong decrease in surface area was accompanied by a sharp reduction of pore volume. In this regard, it can be interesting to consider how the pore size distribution changed for the different materials after the tests at 800°C (Figure 11).

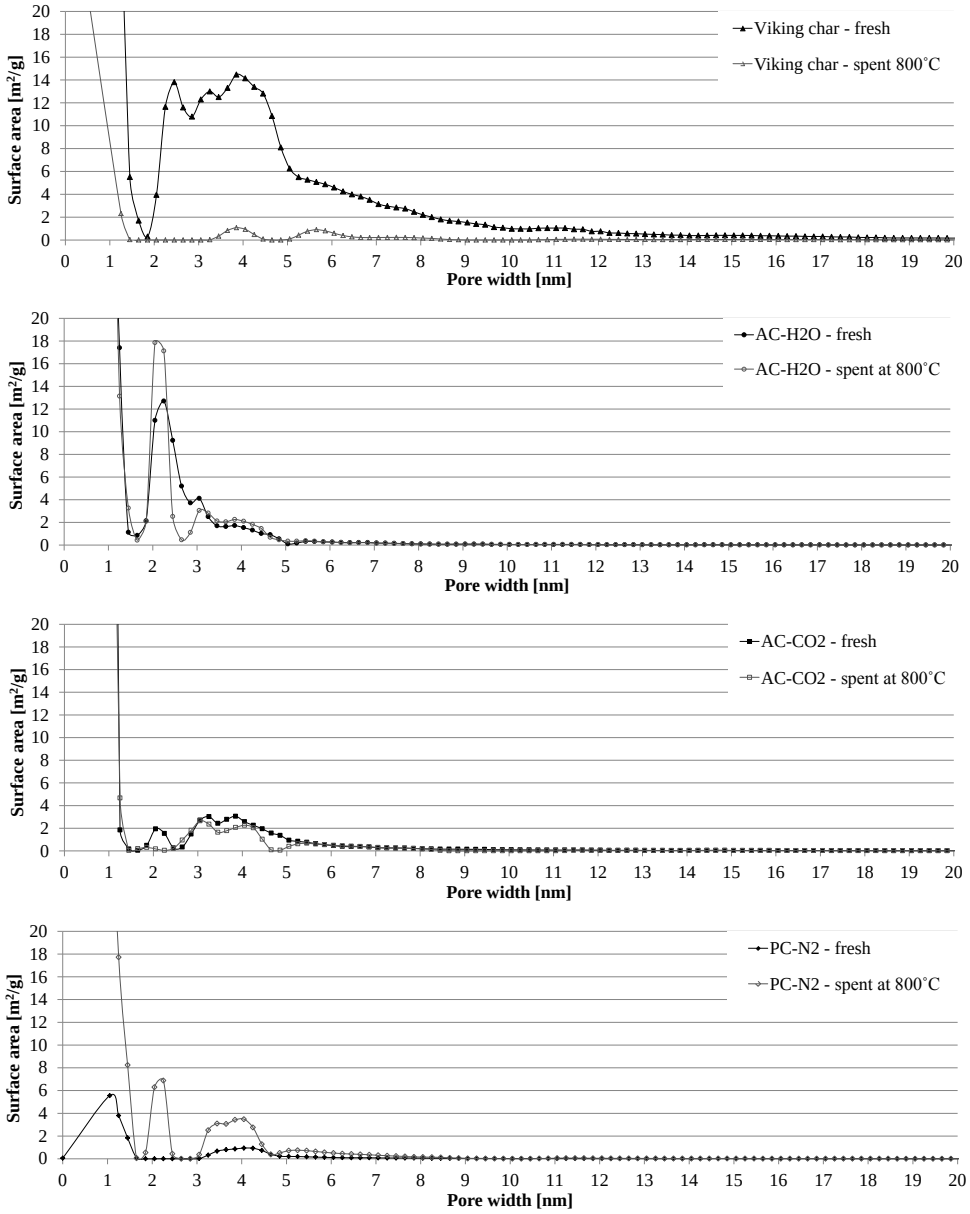

Figure 11: *Surface area distribution over the pore size range <20 nm for the tested chars. The plots represent fresh samples and spent ones after tests at 800˚C.*

It appears as, in the case of Viking char, the surface area reduction affected not only the micropores, but also the mesopores in the range 2-14 nm. Interestingly, some of the mesopores on the surfaces of AC-H_2O and AC-CO_2 remained accessible for N_2 even after the tests at 800°C. Moreover, the spent AC maintained a larger micropore volume in comparison with Viking char (Table 6).

These results indicate that a larger fraction of the Viking char surface was active for tar decomposition, including surface area associated with micropores and small mesopores (< 13 nm). Moreover, despite the remarkable drop in surface area and pore volume, Viking char showed a higher activity at the end of the tests in comparison with the two types of AC.

The greater activity of the Viking char surface can be explained by the higher content of inorganics, especially Ca. It is possible that the inorganics contained in the Viking char were also more accessible thanks to the migration of mineral species towards the surface during gasification. This phenomenon has been observed on chars gasified at high temperature [6,61], such as Viking char was.

As in the previous results, also the change in the pore size distribution was completely different for the PC-N_2 char that gained surface area both in the micropore and mesopore region. These results corroborate the hypothesis that this char underwent mild pyrolysis during the test: even though this char had been heat treated at 900°C for 2 hours prior to the test, this was not sufficient to guarantee its complete stability at 800°C.

4. Conclusions

The performances of four wood-derived chars and AC in the adsorption and decomposition of toluene and naphthalene were evaluated and compared. Chars and AC were produced with different processes and featured various degrees of activation. Surface characterization revealed different surface areas and pore textures, while the compositional analysis showed discrepancies in the content of minerals and metals. The surface and compositional characteristics varied as a consequence of the different heat treatments that each material had undergone: gasification, pyrolysis, H_2O- or CO_2-activation.

During experiments in the lower range of temperatures (250-400°C), char beds exerted a minimal effect on the concentration of toluene, but adsorbed naphthalene more efficiently. The absence of gaseous species other than N_2 in the exit gas confirmed that the interaction between aromatic molecules and the surface of chars was limited to adsorption, as no decomposition reactions took place under these conditions. The highest naphthalene adsorption capacity was given by AC-CO_2. Viking char provided an

adsorption capacity of naphthalene which was comparable with the two types of AC. On the contrary, PC-N_2 char (non-activated) showed a poor adsorption capacity quantified as one order of magnitude below the other materials.

Increasing the char beds temperature to 400°C significantly diminished the adsorption capacities of the Viking char, AC-H_2O and AC-CO_2 without triggering cracking reactions.

On the other hand, when the temperature of the char bed was set to 600°C, the aromatic compounds were subject to decomposition reactions yielding H_2. At 800°C the H_2 production increased significantly and was associated with CH_4 generation; moreover, the difference in the performances of the different chars became appreciable. The performance of char PC-N_2 was very similar to the blank test, with very low levels of conversion. In contrast, the other chars achieved complete conversion of naphthalene and toluene for a limited time at the beginning of the tests. Overall, naphthalene appeared to be cracked more extensively than toluene. Viking char AC-H_2O and AC-CO_2 surface deactivation following different trends. Viking char remained active for a longer time in comparison with the two types of AC. The same deactivation trends were observed in the production of H_2 and CH_4. The slower deactivation showed by Viking char was mainly ascribed to a better surface accessibility given by its pore texture, but also to a higher number of active sites as a results of a larger content of inorganics.

The characterization of the chars spent at 800°C clarified that deactivation was a consequence of solid carbon deposition on the surface of chars.

Results from tests in the temperature range 600-800°C indicated that gasification char performed better than AC, providing a higher and protracted removal of both aromatic compounds. Chars with high burn-off, as the ones produced as solid residues of gasification process, might be particularly suitable for tar conversion applications in hot producer gas treatment at temperatures of 800°C and above. Nevertheless, the solid residues of gasification, or gasification chars, can have very different properties and surface structure depending on the operating conditions of the process and on the feedstock used. In order to be suitable and effective for hot gas treatment, the gasifier should have high carbon conversion efficiency, and should produce a solid residue with a large specific surface area and well-developed porosity.

Acknowledgements

The authors thank Innovationsfonden (Denmark) for the financial support received as part of the project "SYNFUEL - Sustainable synthetic fuels from biomass gasification and electrolysis" (4106-00006B), as well as the German Federal Ministry of Education and Research for the funding to the junior research group "NWG-TCKON" (FKZ: 03SF0442).

The authors would also like to thank Mrs. Susanne Hoffmann (Technische Universität Berlin, Institut für Energietechnik) for the assistance with char analysis.

2.2 Scanning Electron Microscopy (SEM) of fresh and spent char samples

The characterization results on the fresh and spent char samples have been described and discussed in Paper II. In addition to the compositional and textural modifications that were detected with the described analytical methods, char samples recovered after the experiments were also visibly different from the fresh materials with a naked eye. The color of the surface had shifted from black to grey, and the surface appeared to reflect light differently. The effect was evident only for the samples that had been used for high temperature tests (600 and 800°C), and in particular for those used at the highest temperature. Because of this, SEM microscopy was used on these samples, with the aim to visualize morphological changes in the surface of chars after experiments at 800°C. However, actual modifications of the char surfaces were not so obvious, and it was difficult to define and quantify them. In the following, some examples of SEM images of fresh and spent samples are shown (Figures 2.6 to 2.8). The instrument was a table-top SEM, TM 3000 (Hitachi, Japan). Samples were prepared by placing char particles on sample holders, covered with double-faced carbon adhesive tape. Because of the high carbon content of the char samples, they were considered as conductive enough not to require metal coating prior to observations. The accelerating voltage applied during the observations was 15 kV.

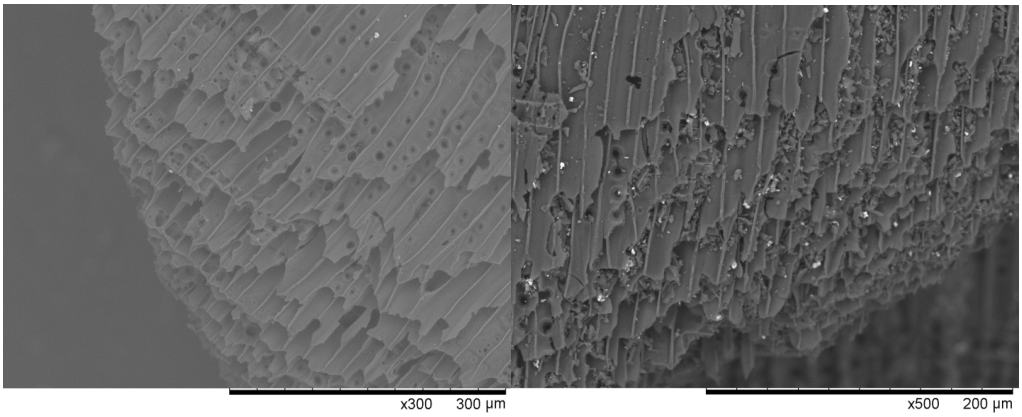

Figure 2.6: *SEM images of Viking char fresh (left) and spent after cracking tests at 800°C*

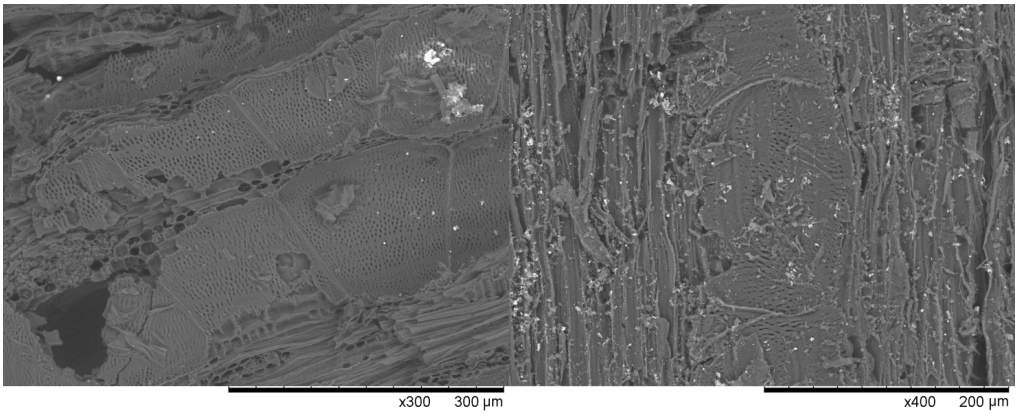

Figure 2.7: *SEM images of AC-CO_2 fresh (left) and spent after cracking tests at 800°C (right)*

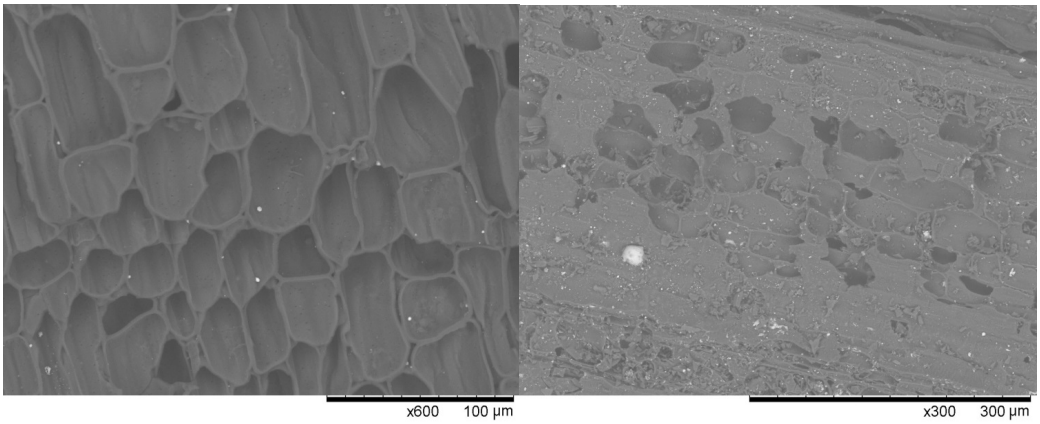

Figure 2.8: *SEM images of AC-H_2O fresh (left) and spent after cracking tests at 800°C (right)*

The only evident difference that could be observed between the fresh and the spent samples was the presence of fractures and micro-particles on the surface. Such difference could be observed in the Viking char, AC-CO_2 and AC-H_2O. Nestler et al. [40], also used SEM on fresh wood char and spent char, used for the cracking of naphthalene at 850 °C, for 5 hours. They reported similar morphological modifications and ascribed the increased fracturing of the tracheids to the heterogenous cracking of naphthalene.

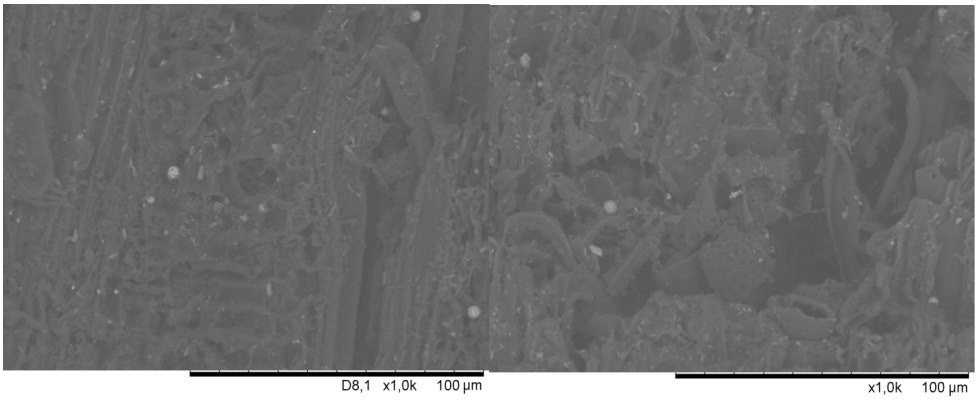

Figure 2.9: *SEM images of PC-N_2 fresh (left) and spent after cracking tests at 800°C (right)*

SEM images of PC-N_2 showed a more disordered surface, with a less defined structure in comparison with the other char samples. To the naked eye, the color of the PC-N_2 spent at 800°C appeared different from the fresh one; however SEM did not reveal any significant difference in the microscopic structure of the two samples. Two examples of PC-N2 SEM images are shown in Figure 2.9. This particular char stood out as different form the other materials tested, in agreement with the rest of the characterization results that are described in Paper II.

References

[1] Li C, Suzuki K. Tar property , analysis , reforming mechanism and model for biomass gasification — An overview. Renew Sustain Energy Rev 2009:594–604. doi:10.1016/j.rser.2008.01.009.

[2] Asadullah M. Biomass gasification gas cleaning for downstream applications: A comparative critical review. Renew Sustain Energy Rev 2014;40:118–32. doi:10.1016/j.rser.2014.07.132.

[3] Abu El-Rub Z, Bramer EA, Brem G. Experimental comparison of biomass chars with other catalysts for tar reduction. Fuel 2008;87:2243–52. doi:10.1016/j.fuel.2008.01.004.

[4] Hosokai S, Kumabe K, Ohshita M, Norinaga K, Li C, Hayashi J-I. Mechanism of decomposition of aromatics over charcoal and necessary condition for maintaining its activity. Fuel 2008;87:2914–22. doi:10.1016/j.fuel.2008.04.019.

[5] Fuentes-Cano D, Gómez-Barea A, Nilsson S, Ollero P. Decomposition kinetics of model tar compounds over chars with different internal structure to model hot tar removal in biomass gasification. Chem Eng J 2013;228:1223–33. doi:10.1016/j.cej.2013.03.130.

[6] Klinghoffer N, Castaldi MJ, Nzihou A. Catalyst Properties and Catalytic Performance of Char from Biomass Gasification. I&Ec 2012:13113–22. doi:10.1021/ie3014082.

[7] Griffiths DML, Mainhood JSR. The cracking of tar vapour and aromatic compounds on activated carbon. Fuel 1967:167–76.

[8] Boroson ML, Howard JB, Longwell JP, Peters W a. Heterogeneous cracking of wood pyrolysis tars over fresh wood char surfaces. Energy & Fuels 1989;3:735–40. doi:10.1021/ef00018a014.

[9] Brandt P, Larsen E, Henriksen U. High tar reduction in a two-stage gasifier. Energy & Fuels 2000;14:816–9. doi:10.1021/ef990182m.

[10] Al-Rahbi AS, Onwudili JA, Williams PT. Thermal decomposition and gasification of biomass pyrolysis gases using a hot bed of waste derived pyrolysis char. Bioresour Technol 2016;204:71–9. doi:10.1016/j.biortech.2015.12.016.

[11] Krerkkaiwan S, Mueangta S, Thammarat P, Jaisat L, Kuchonthara P. Catalytic Biomass-Derived Tar Decomposition Using Char from the Co-pyrolysis of Coal and Giant Leucaena Wood Biomass. Energy & Fuels 2015;29:3119–26. doi:10.1021/ef502792x.

[12] Park J, Lee Y, Ryu C. Reduction of primary tar vapor from biomass by hot char particles in fixed bed gasification. Biomass and Bioenergy 2016;90:114–21. doi:10.1016/j.biombioe.2016.04.001.

[13] Frazier RS, Jin E, Kumar A. Life cycle assessment of biochar versus metal catalysts used in syngas cleaning. Energies 2015;8:621–44. doi:10.3390/en8010621.

[14] Benedetti V, Patuzzi F, Baratieri M. Gasification char as a potential substitute of activated carbon in adsorption applications. Energy Procedia 2016;00.

[15] Benedetti V, Patuzzi F, Baratieri M. Characterization of char from biomass gasification and its similarities with activated carbon in adsorption applications. Appl Energy 2018;227:92–9. doi:10.1016/j.apenergy.2017.08.076.

[16] Galhetas M, Mestre AS, Pinto ML, Gulyurtlu I, Lopes H, Carvalho AP. Chars from gasification of coal and pine activated with K2CO3: Acetaminophen and caffeine adsorption from aqueous solutions. J Colloid Interface Sci 2014;433:94–103. doi:10.1016/j.jcis.2014.06.043.

[17] Ducousso M, Weiss-Hortala E, Nzihou A, Castaldi MJ. Reactivity enhancement of gasification biochars for catalytic applications. Fuel 2015;159:491–9. doi:10.1016/j.fuel.2015.06.100.

[18] García-García A, Gregório A, Franco C, Pinto F, Boavida D, Gulyurtlu I. Unconverted chars obtained during biomass gasification on a pilot-scale gasifier as a source of activated carbon production. Bioresour Technol 2003;88:27–32.

[19] Kilpimaa S, Runtti H, Kangas T, Lassi U, Kuokkanen T. Physical activation of carbon residue from biomass gasification: Novel sorbent for the removal of phosphates and nitrates from aqueous solution. J Ind Eng Chem 2015;21:1354–64. doi:10.1016/j.jiec.2014.06.006.

[20] Klinghoffer N. Utilization of char from biomass gasification in catalytic applications. PhD thesis, Columbia University, USA 2013.

[21] Hervy M, Berhanu S, Weiss-Hortala E, Chesnaud A, Gérente C, Villot A, et al. Multi-scale characterisation of chars mineral species for tar cracking. Fuel 2017;189:88–97. doi:10.1016/j.fuel.2016.10.089.

[22] Patuzzi F, Prando D, Vakalis S, Rizzo AM, Chiaramonti D, Tirler W, et al. Small-scale biomass gasification CHP systems: Comparative performance assessment and monitoring experiences in South Tyrol (Italy). Energy 2016;112:285–93. doi:10.1016/j.energy.2016.06.077.

[23] Hansen V, Müller-Stöver D, Ahrenfeldt J, Holm JK, Henriksen UB, Hauggaard-Nielsen H. Gasification biochar as a valuable by-product for carbon sequestration and soil amendment. Biomass and Bioenergy 2015;72:300–8. doi:http://dx.doi.org/10.1016/j.biombioe.2014.10.013.

[24] Mastral A, García T, Murrillo R, Callén MS, Lopez JM, Navarro M V, et al. Study of the Adsorption of Polyaromatic Hydrocarbon Binary Mixtures on Carbon Materials by Gas-Phase Fluorescence Detection. Energy & Fuels 2003:669–76.

[25] García T, Murillo R, Cazorla-Amorós D, Mastral AM, Linares-Solano A. Role of the activated carbon surface chemistry in the adsorption of phenanthrene. Carbon N Y 2004;42:1683–9. doi:10.1016/j.carbon.2004.02.029.

[26] Hu X, Hanaoka T, Sakanishi K, Shinagawa T, Matsui S, Tada M, et al. Removal of Tar Model Compounds Produced from Biomass Gasification Using Activated Carbons. J Japan Inst Energy 2007;86:707–7011. doi:10.1093/bioinformatics/btu635.

[27] Sun Q, Yu S, Wang F, Wang J. Decomposition and gasification of pyrolysis volatiles from pine wood through a bed of hot char. Fuel 2011;90:1041–8. doi:10.1016/j.fuel.2010.12.015.

[28] Dabai F, Paterson N, Millan M, Fennell P, Kandiyoti R. Tar formation and destruction in a fixed-bed reactor simulating downdraft gasification: Equipment development and characterization of tar-cracking products. Energy & Fuels 2010;24:4560–70. doi:10.1021/ef100681u.

[29] Matsuhara T, Hosokai S, Norinaga K, Matsuoka K, Li CZ, Hayashi JI. In-situ reforming of tar from the rapid pyrolysis of a brown coal over char. Energy & Fuels 2010;24:76–83. doi:10.1021/ef9005109.

[30] Phuphuakrat T, Namioka T, Yoshikawa K. Tar removal from biomass pyrolysis gas in two-step function of decomposition and adsorption. Appl Energy 2010;87:2203–11. doi:10.1016/j.apenergy.2009.12.002.

[31] Sueyasu T, Oike T, Mori A, Kudo S, Norinaga K, Hayashi JI. Simultaneous steam reforming of tar and steam gasification of char from the pyrolysis of potassium-loaded woody biomass. Energy & Fuels 2012;26:199–208. doi:10.1021/ef201166a.

[32] Hosokai S, Norinaga K, Kimura T, Nakano M, Li C-Z, Hayashi J. Reforming of Volatiles from the Biomass Pyrolysis over Charcoal in a Sequence of Coke Deposition and Steam Gasification of Coke. Energy & Fuels 2011;25:5387–93. doi:10.1021/ef2003766.

[33] Cudahy JJ, Helsel RW. Removal of products of incomplete combustion with carbon. Waste Manag 2000;20:339–45. doi:10.1016/S0956-053X(99)00335-9.

[34] Mastral AM, García T, Murillo R, Callén MS, López JM, Navarro M V. PAH Mixture Removal from Hot Gas by Porous Carbons . From Model Compounds to Real Conditions. Ind Eng Chem Res 2003:5280–6.

[35] Karatza D, Musmarra D. Fly Ash Capture of Mercuric Chloride Vapors from Exhaust Combustion Gas. Environ Sci Technol 1998;32:3999–4004.

[36] Jess A. Mechanisms and kinetics of thermal reactions of aromatic hydrocarbons from pyrolysis of solid fuels. Fuel 1996;75:1441–8. doi:10.1016/0016-2361(96)00136-6.

[37] Egsgaard H, Ahrenfeldt J, Ambus P, Schaumburg K, Henriksen UB. Gas cleaning with hot char beds studied by stable isotopes. J Anal Appl Pyrolysis 2014;107:174–82. doi:10.1016/j.jaap.2014.02.019.

[38] Mani S, Kastner JR, Juneja A. Catalytic decomposition of toluene using a biomass derived catalyst. Fuel Process Technol 2013;114:118–25. doi:10.1016/j.fuproc.2013.03.015.

[39] Song Y, Zhao Y, Hu X, Zhang L, Sun S, Li CZ. Destruction of tar during volatile-char interactions at low temperature. Fuel Process Technol 2018;171:215–22. doi:10.1016/j.fuproc.2017.11.023.

[40] Nestler F, Burhenne L, Amtenbrink MJ, Aicher T. Catalytic decomposition of biomass tars: The impact of wood char surface characteristics on the catalytic performance for naphthalene removal. Fuel Process Technol 2016;145:31–41. doi:10.1016/j.fuproc.2016.01.020.

[41] Fuentes-Cano D, Parrillo F, Ruoppolo G, Gómez-Barea A, Arena U. The influence of the char internal structure and composition on heterogeneous conversion of naphthalene. Fuel Process Technol 2018;172:125–32. doi:10.1016/j.fuproc.2017.12.015.

[42] Korus A, Samson A, Szle A, Katelbach-woz A. Pyrolytic toluene conversion to benzene and coke over activated carbon in a fixed-bed reactor. Fuel 2017;207:283–92. doi:10.1016/j.fuel.2017.06.088.

[43] Nitsch X, Commandré J-M, Valette J, Volle G, Martin E. Conversion of Phenol-Based Tars over Biomass Char under H2 and H2O Atmospheres. Energy & Fuels 2014:28 (2014) 6936-6940. doi:10.1021/ef500980g.

[44] Zhang Y, Luo Y, Wu W, Zhao S, Long Y. Heterogeneous Cracking Reaction of Tar over Biomass Char, Using Naphthalene as Model Biomass Tar. Energy & Fuels 2014;28:3129–37. doi:10.1021/ef4024349.

[45] Krerkkaiwan S, Tsutsumi A, Kuchonthara P. Biomass derived tar decomposition over coal char bed. ScienceAsia 2013;39:511. doi:10.2306/scienceasia1513-1874.2013.39.511.

[46] Di Gregorio F, Parrillo F, Salzano E, Cammarota F, Arena U. Removal of naphthalene by activated carbons from hot gas. Chem Eng J 2016;291:244–53. doi:10.1016/j.cej.2016.01.081.

[47] Quantachrome Instruments - DFT Models n.d. http://www.quantachrome.com/technical/dft.html (accessed June 6, 2018).

[48] Ahrenfeldt J, Henriksen U, Jensen TK, Gøbel B, Wiese L, Kather A, et al. Validation of a continuous combined heat and power (CHP) operation of a two-stage biomass gasifier. Energy & Fuels 2006;20:2672–80. doi:10.1021/ef0503616.

[49] Thommes M, Kaneko K, Neimark A V, Olivier JP, Rodriguez-reinoso F, Rouquerol J, et al. Physisorption of gases , with special reference to the evaluation of surface area and pore size distribution (IUPAC Technical Report). Pure Appl Chem 2015. doi:10.1515/pac-2014-1117.

[50] Sing KSW, Everett DH, Haul RAW, Moscou L, Pierotti RA, Rouqueról J, et al. REPORTING PHYSISORPTION DATA FOR GAS / SOLID SYSTEMS with Special Reference to the Determination of Surface Area and Porosity 1985;57:603–19.

[51] Coughlin RW, Ezra FS. Role of Surface Acidity in the Adsorption of Organic Pollutants on the Surface of Carbon. Environ Sci Technol 1968;2:291–7. doi:10.1021/es60016a002.

[52] Rodríguez-Reinoso F. The role of carbon materials in heterogeneous catalysis. Carbon N Y 1998;36:159–75. doi:10.1016/S0008-6223(97)00173-5.

[53] Bansal RC, Donnet J-B, Stoeckli F. Active Carbon. New York and Basel: Marcel Dekker, Inc.; 1988.

[54] Klinghoffer NB, Castaldi MJ, Nzihou A. Influence of char composition and inorganics on catalytic activity of char from biomass gasification. Fuel 2015;157:37–47. doi:10.1016/j.fuel.2015.04.036.

[55] Lillo-Ródenas M, Cazorla-Amorós D, Linares-Solano A. Behaviour of activated carbons with different pore size distributions and surface oxygen groups for benzene and toluene adsorption at low concentrations. Carbon N Y 2005;43:1758–67. doi:10.1016/j.carbon.2005.02.023.

[56] Chiang Y, Chiang P, Huang C. Effects of pore structure and temperature on VOC adsorption on activated carbon. Carbon N Y 2001;39:523–34.

[57] Tomków K, Siemieniewska T, Czechowski F, Jankowska A. Formation of porous structures in activated brown-coal chars using O2, CO2 and H2O as activating agents. Fuel 1977;56:121–4.

[58] Mastral AM, García T, Murillo R, Callen MS, Lopez JM, Navarro M V. Development of efficient adsorbent materials for PAH cleaning from AFBC hot gas. Energy & Fuels 2004;18:202–8. doi:10.1021/ef030058+.

[59] Moldoveanu SC. Techniques and Instrumentation in Analytical Chemistry - Pyrolysis of Organic Molecules. vol. 28. Elsevier Science Ltd; 2009.

[60] Moliner R, Suelves I, Lázaro MJ, Moreno O. Thermocatalytic decomposition of methane over activated carbons: Influence of textural properties and surface chemistry. Int J Hydrogen Energy 2005;30:293–300. doi:10.1016/j.ijhydene.2004.03.035.

[61] Wu W, Luo Y, Su Y, Zhang Y, Zhao S, Wang Y. Nascent Biomass Tar Evolution Properties under Homogeneous/Heterogeneous Decomposition Conditions in a Two-Stage Reactor. Energy & Fuels 2011;25:5394–406. doi:10.1021/ef2007276.

Chapter 3

Producer gas upgrading

As explained in Chapter 1, the double stage gasifier developed at DTU represents a good example of char utilization for elimination of tar. The TwoStage gasification process is schematized in Figure 3. 1. Wood chips are fed to the inlet of the auger reactor. The feedstock is pyrolyzed while moving towards the second stage along the screw. After the first pyrolysis stage in the auger, volatiles are partially combusted by air injection in the throat zone. The char produced in the pyrolysis stage falls towards the grate, forming a fixed bed that acts as a hot catalytic substrate for reforming of tar. Partial oxidation leads the temperature to increase up to 1100°C. The high temperature induces extensive gasification of carbon contained in the char, achieving a very high burn-off. Indeed, the carbon conversion efficiency within the process is close to 99%. Periodically, the char is removed from the bottom of the bed by moving the grate. Residual char is transported to a designated container where it is stockpiled. During normal operation of the Viking demonstration plant at DTU, Risø Campus, wood chips are fed with a rate of 15 Kg/h. The residual char is generated with a rate of 150 to 200 g/h. Further details of the process can be found in Brandt et al. [1] and Ahrenfeldt et al. [2].

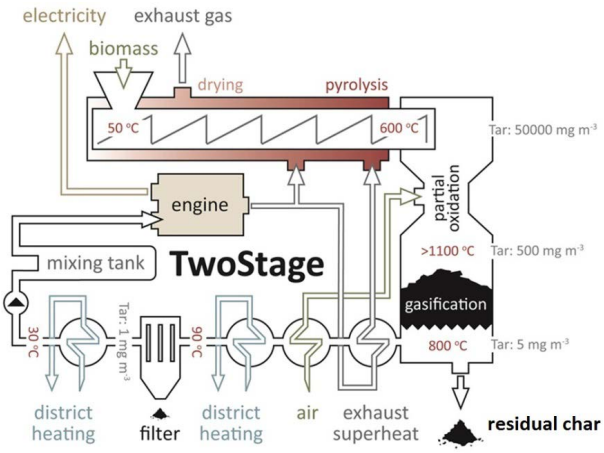

Figure 3.1: *Diagram of the TwoStage – Viking gasifier. Adapted from [3]*

3.1 Design and construction of the gas upgrading unit

The gas upgrading test unit was developed with the aim to emulate the second stage – the gasification reactor- of the Viking gasifier. With this in mind, a smaller reactor was designed with the objective to use for the cleaning and upgrading of the producer gas generated by the Low Temperature-Circulating Fluidized Bed (LT-CFB) gasifier. The unit was conceived to be connected to the LT-CFB main outlet pipe through a slip-stream connection. Gas sampling and analysis on the raw gas and downstream of the test unit would be used to monitor the quality of the producer gas before and after the treatment. The aim was to obtain a similar upgrading effect on the LT-CFB producer gas as the one occurring in the TwoStage process. For this reason it was deemed necessary to maintain the same volumetric ratio between the inlet gas flow, the partial oxidation volume and the volume of the char bed. Because of the unavoidable heat losses that would occur during operation of the test unit, it was decided to enclose the reactor in an electric furnace to maintain the bed of char at high temperature. The dimensions of the oven posed limitations on the dimensioning of the reactor, which had to be about 0.5 m tall and 0.015 m wide to fit into the furnace. Considering the thickness of the steel and a 10 cm layer of insulation in the top part of the reactor, the dimensions of the internal volume of the test reactor were fixed at 0.4 m in height and 0.125 m internal diameter (i.d.). Therefore, the volume available inside the test reactor was calculated to be approximately 22 times smaller than the volume inside the gasification reactor of the Viking. Hence, the volumetric flow of LT-CFB producer gas to be fed to the reactor was defined using the same scaling ratio. As the producer gas flow of the Viking is about 40 Nm^3/h, a slip-stream of about 1.8 Nm^3/h was to be fed to the test unit. In this way, the residence time of the gas inside the test reactor was close to the residence time of the gas in the Viking reactor (between 2.5 and 3 s). Table 3.1 compares the dimensions of the Viking reactor and the test reactor.

Table 3.1: *Overview and comparison of dimensions in the second stage of the Viking gasifier and the reactor for the gas upgrading unit.*

	Unit	Viking Reactor	Test reactor	Ratio Viking/test reactor
Internal diameter	[m]	0.350	0.125	2.8
Reactor height	[m]	1.25	0.4	3.1
Reactor volume	[m^3]	0.108	$4.9*10^{-3}$	22
Height/i.d. ratio	-	3.6	3.2	-
Freeboard/charbed volume ratio	-	~ 1	~ 1	-
Gas flow	[Nm^3/h]	40	1.82	22
Gas flow (800°C)	[m^3/h]	146.5	6.7	22
Superficial velocity (800°C)	[m/s]	0.428	0.15	2.8
Residence time (800°C)	[s]	2.92	2.7	1.1

Figure 3.3 shows the three-dimensional shapes of the gasification reactor in the Viking gasifier and the cylindrical reactor designed for the gas upgrading unit. The air inlet in the Viking gasifier is tangential, and it generates a swirling effect that has been found to be beneficial for the gas mixing and for partial oxidation reactions [4]. Therefore, the air inlet in the test unit was also given a tangential direction. The air inlet was placed close to the producer gas inlet on the top of the reactor. The air and the producer gas inlets had an internal diameter of 6 and 21 mm, respectively.

The gas could leave the reactor from the bottom, below the grate. The outlet pipe was equipped with sampling ports for gas analysis: one was connected to an online gas analyzer, one to the Petersen Column, and the third was equipped with a silicon septum for Solid Phase Adsorption (SPA) sampling. The reactor was equipped with 6 thermocouples distributed along the height to monitor the temperature distribution. Figure 3.4 shows the final drawing of the test reactor.

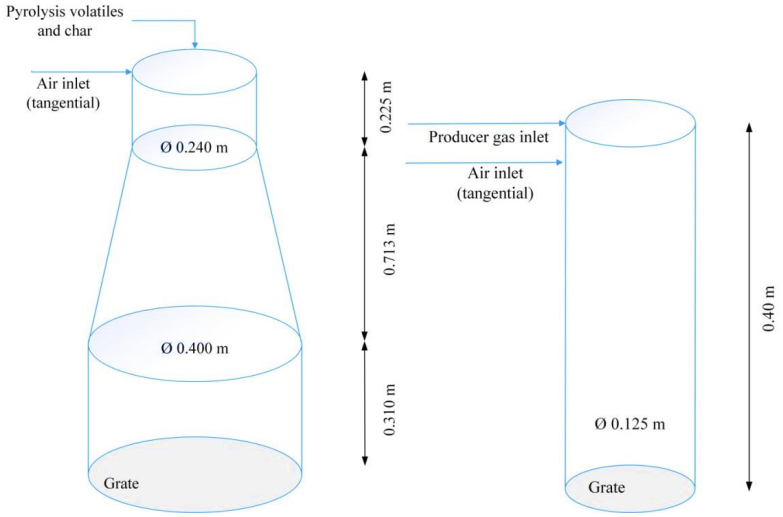

Figure 3.3: *Scheme of the Viking gasification reactor (left) and the test reactor (right)*

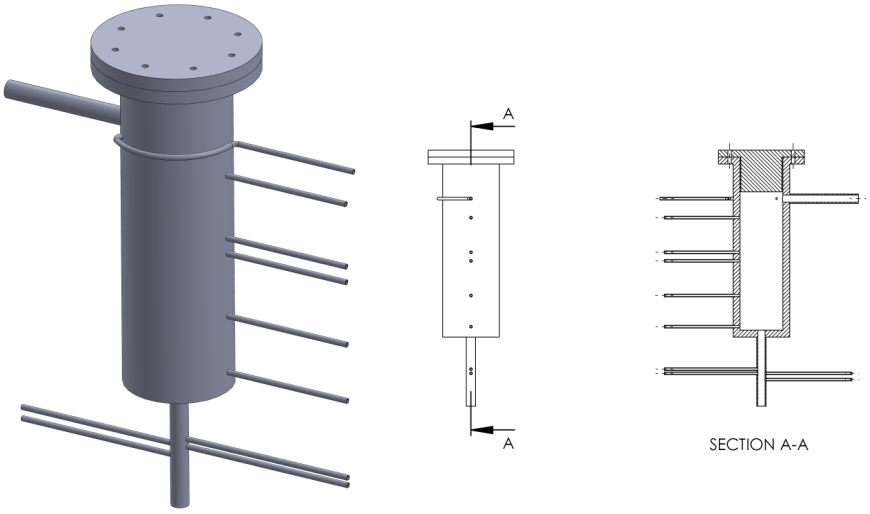

Figure 3.4: *Final drawing of test reactor*

The reactor was built using heat-resistant steel MA 253. The reactor was connected to the main outlet pipe of the LT-CFB gasifier trough a slip-stream pipe of about 90 cm. The slip stream pipe was made of stainless steel 316L and was equipped with a high temperature valve to open and close the flow of producer gas through the gas upgrading unit. On the side of the slip-stream pipe, an additional inlet was constructed to allow a flow of nitrogen to sweep the reactor during the heating-up and cooling down phases. The cylindrical electric furnace was mounted around the reactor. The air inlet was connected to the compressed air circuit through a calibrated rotameter. In order to ensure the flow through the gas upgrading unit, a gas pump was connected at the outlet of the system. To protect the pump, the gas was cooled down and the condensate was collected in a flask upstream of the pump. A drawing of the whole gas upgrading setup is shown in Paper III. Figure 3.5 and 6 show the reactor for the gas upgrading unit, before and after being connected to the main outlet pipe of the LT-CFB gasifier.

Figure 3.5: *The reactor before being connected to the LT-CFB gasifier*

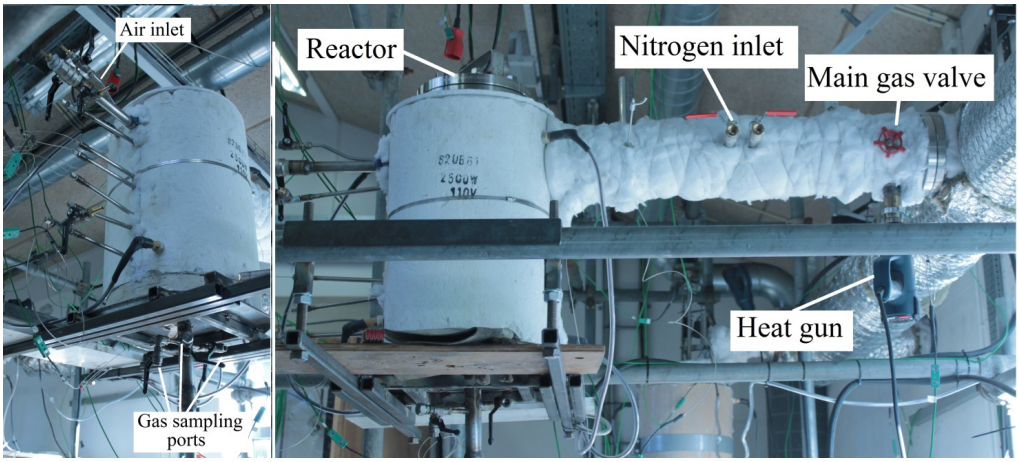

Figure 3.6: *Views of the reactor enclosed in the electric furnace and connected with the main outlet pipe of the LT-CFB gasifier at DTU, Risø Campus.*

Figure 3.7: *Sieved Viking char (<3.15 mm), prior to being used as bed material in the test reactor*

References

[1] Brandt P, Larsen E, Henriksen U. High tar reduction in a two-stage gasifier. Energy & Fuels 2000;14:816–9. doi:10.1021/ef990182m.

[2] Ahrenfeldt J, Henriksen U, Jensen TK, Gøbel B, Wiese L, Kather A, et al. Validation of a continuous combined heat and power (CHP) operation of a two-stage biomass gasifier. Energy & Fuels 2006;20:2672–80. doi:10.1021/ef0503616.

[3] Egsgaard H, Ahrenfeldt J, Ambus P, Schaumburg K, Henriksen UB. Gas cleaning with hot char beds studied by stable isotopes. J Anal Appl Pyrolysis 2014;107:174–82. doi:10.1016/j.jaap.2014.02.019.

[4] Gerun L, Paraschiv M, Vijeu R, Bellettre J, Tazerout M, Gøbel B, et al. Numerical investigation of the partial oxidation in a two-stage downdraft gasifier. Fuel 2008;87:1383–93. doi:10.1016/j.fuel.2007.07.009.

Application of residual char from biomass gasification in a producer gas upgrading system

Giulia Ravenni*, Zsuzsa Sárossy, Jesper Ahrenfeldt, Ulrik Birk Henriksen
Technical University of Denmark (DTU), Department of Chemical and Biochemical Engineering, Frederiksborgvej 399, 4000 Roskilde, Denmark
*Corresponding author: Giulia Ravenni Phone: +45 93 51 15 92 E-mail: grav@kt.dtu.dk

Manuscript submitted to Elsevier journal "Fuel".

Abstract

A gas upgrading unit was designed, built and tested for the treatment of producer gas from the LT-CFB gasifier at DTU, Risø Campus. Producer gas was generated from straw gasification and was rich in primary tar. Residual char from wood gasification was used to assist the cracking and reforming of tar, also in combination with partial oxidation by air injection. The unit was maintained at 800°C via electric heating. The effect of temperature (thermal cracking) was evaluated with an empty reactor. The effect of residual char was tested by adding a 200 mm tall char bed inside the reactor. The influence of partial oxidation was assessed combining the presence of char with air injection at excess air ratios (λ) values of 0.2 and 0.5. In presence of char, tar was extensively reduced and reforming reactions enriched the product gas with H_2 and CO. However, a steadily increasing deactivation was observed. The addition of air had the effect to decelerate deactivation. When the highest λ was tested, the activity was maintained during a 5 hours test. Even under the harshest reaction conditions, the consumption of the bed was limited. Recovered spent chars were characterized in terms of composition and surface structure to evaluate structural changes. The experiments demonstrated the effectivity and the durability of the char-based cleaning system. The experience gained during the tests was used to formulate recommendations for further implementation and upscaling of the char-based gas upgrading unit.

Keywords: gasification, biomass, tar removal, char, gas upgrading

1. Introduction

The quality of producer gas generated by gasification of biomass is very often compromised by the presence of contaminants, especially tar. This issue prevents the use of producer gas as a fossil-free substitute for natural or synthesis gas. If this problem is overcome, biomass producer gas could be directly used as a fuel for alternative engines and turbines or for the catalytic synthesis of biofuels and bio-chemicals.

Producer gas quality can vary significantly depending on the gasification technology, and it is a particularly critical issue for the Low Temperature-Circulating Fluidized Bed (LT-CFB) gasifier. This gasification platform was designed to convert ash-rich fuels such as straw: the highest temperature reached within the process is about 750°C, thus avoiding any risk of melting and agglomeration. The LT-CFB concept is schematized in Figure 1 and a detailed description of the process can be found elsewhere [1–3].

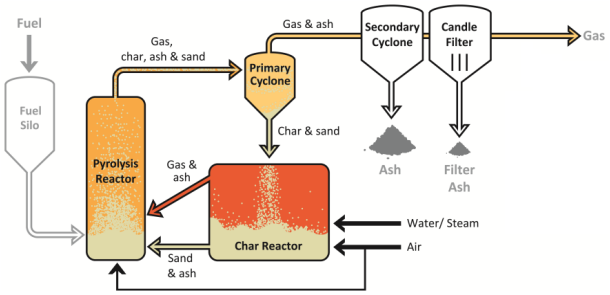

Figure 1: *Schematic of LT-CFB process*
(Adapted from Thomsen et al. [3], Copyright 2017, with permission from Elsevier)

The drawback of the LT-CFB process design is that the producer gas is rich in tars (about 25 g/Nm^3), including abundant primary tar species from the pyrolysis stage. In addition to a heavy tar load, the gas phase is low in H_2 and CO, and has quite low heating value. The upgrade of the LT-CFB producer gas would be particularly beneficial to valorize low-quality feedstock such as marginal biomass and residues. In order to improve the producer gas quality and facilitate its use for catalytic synthesis, it is necessary to reform tar into stable gas species. In this way, the energy contained in the tar fraction would not be lost, but transferred to the permanent gas phase.

High levels of tar conversion are achieved with different process designs as in downdraft gasifiers. For example, the TwoStage demonstration plant at DTU, Risø Campus - the Viking gasifier - generates a virtually tar-free gas [4,5]. The Viking is a double-stage wood gasifier, where reduction takes place in a fixed-bed downdraft reactor. Pyrolysis volatiles undergo partial oxidation in the throat zone where temperature is above 1100°C, before passing through a fixed bed of char at about 800°C. The beneficial effect of partial oxidation on the quality of producer gas has been studied and explained [6], whereas the role of the char bed has not yet been completely understood. The hypothesis is that primary tar compounds are first converted into Polycyclic Aromatic Hydrocarbons (PAH) species by partial oxidation and afterwards the char bed efficiently removes multi-ring molecules [4]. Indeed, according to the work of Egsgaard et al. [7], char is able to bind aromatic compounds at temperatures above 600°C, with increasing efficiency with the number of rings in the molecule. This hypothesis is supported by the fact that several authors reported a catalytic effect of carbonaceous materials with different origins for tar cracking and reforming [8–14]. Often, a higher reactivity is observed towards polyaromatic hydrocarbons [15–18]. Moreover, the effectivity of char towards tar decomposition has been found to improve when partial oxidation is combined with the passage through a hot char bed [16,18–20].

The interaction between aromatic species and the surface of char has been observed by various authors [21–23], who agree on the general reaction pathway. Aromatic species undergo cracking reactions on the active sites of the char surface. In presence of water or CO_2, the deposited carbon (coke) is reformed into CO and H_2, while under inert conditions, coke deposits deactivate the surface of char.

Several studies have shown that char has an improved catalytic activity in comparison with pure ashes [24–27]. This is due to the fact that the carbonaceous matrix acts as a support for the inorganic species and has inherent catalytic properties given by defects and random ordering in the graphene-like aromatic sheets [28–31]. Therefore, the catalytic properties of char derive from the synergy between inorganics present at the surface (such as Ca, K or Mg) and carbon itself.

Gasification is in many ways comparable with an activation treatment, therefore it can improve the surface features and catalytic properties of char [32,33]. Gasification-derived char is usually considered as a waste material, and its valorization would increase the overall feasibility of the gasification process and would be especially beneficial for small-scale gasifiers [34]. The solid residue generated by the

Viking gasifier (hereby called "Viking char") features an extensive specific surface area and large porosity; therefore it is a particularly promising substrate for gas treatment applications.

The use of char and char beds to improve the producer gas quality has been implemented in the design of some gasification plants. Zeng et al. [35] applied a similar process as in the Viking gasifier to coal gasification. Also in this case, the combination of a pyrolysis reactor with a downdraft fixed bed gasifier produced an extensive reforming of tar. Choi et al.[36] developed a three-stage gasifier featuring a fixed bed reactor filled with activated carbon to remove tar generated during gasification of dried sewage sludge. Zhang et al. [31,37] implemented and tested a hot gas cleaning system based on biomass char in a gasification system fed with mallee wood. Palla Assima et al. [27] used pellets of residual char and ash from a commercial gasification plant for reforming of pure tar extracted from primary syngas. All of these studies concluded that char is a promising material to support the reforming of tar into stable gases. However, the examples of carbon-based gas upgrading integrated into gasification systems are still limited and further research and optimization is needed for full-scale application.

In this work, residual char from the Viking gasifier (Viking char) has been used in a gas treatment unit for the upgrading of producer gas generated by the 100kW_{th} LT-CFB gasifier operated at DTU, Risø Campus. In order to prove the effectivity of residual gasification char as a substrate for the treatment of producer gas, an upgrading unit was designed, built and tested. An air inlet at the top of the reactor was used to investigate the role of partial oxidation in combination with the passage of the gas through the hot char bed. Online and offline gas and tar analysis were used to evaluate the quality of the gas before and after the upgrading step. In addition, characterization tests were performed on the Viking char before and after using it for gas treatment, to estimate the structural modifications caused by the experiments. The char consumption and the stability of the gas quality achieved at the outlet of the system were evaluated in order to define the feasibility of this gas treatment solution and envisage the possibility for upscaling.

2. Materials and methods

2.1 Test reactor and bed material

In order to test the effect of a hot bed of gasification residual char, a test reactor was designed, taking the gasification reactor of the Viking gasifier as a model. The dimensions were scaled down, but the

volume ratio between the partial oxidation zone and the char bed was maintained. The cylindrical test reactor was 400 mm tall, with an internal diameter of 125 mm and was made of heat-resistant steel (MA 253). At the bottom, a grate was placed to support the char bed. The top part of the reactor was equipped with an inlet for air and one for producer gas. The air flow was controlled by a rotameter. The test reactor was placed inside an electric furnace and was maintained at a temperature of 800°C during the tests. This temperature was indicated as the minimum temperature needed to achieve extensive conversion of tar species over the surface of chars [38,39]. The temperature profile inside the reactor was continuously monitored through thermocouples placed at different heights. Producer gas was extracted from the main outlet of the 100kW$_{th}$ LT-CFB gasifier via a 900 mm long slip-stream pipe connected to the reactor. The extraction port was placed downstream of a high-capacity ceramic filter for particulate. To avoid tar condensation in the connecting pipe, the walls were maintained at a temperature above 250°C by means of a heat gun and thermal insulation. To ensure and control the flow of producer gas through the system, a gas pump was connected downstream of the reactor. To prevent condensation of tar and water inside the pump, the gas was first passed in a water-cooled pipe and the condensate was collected in a flask. The total amount of gas flowing through the system was measured by a gas meter placed just before the outlet. The experimental setup is schematized in Figure 2.

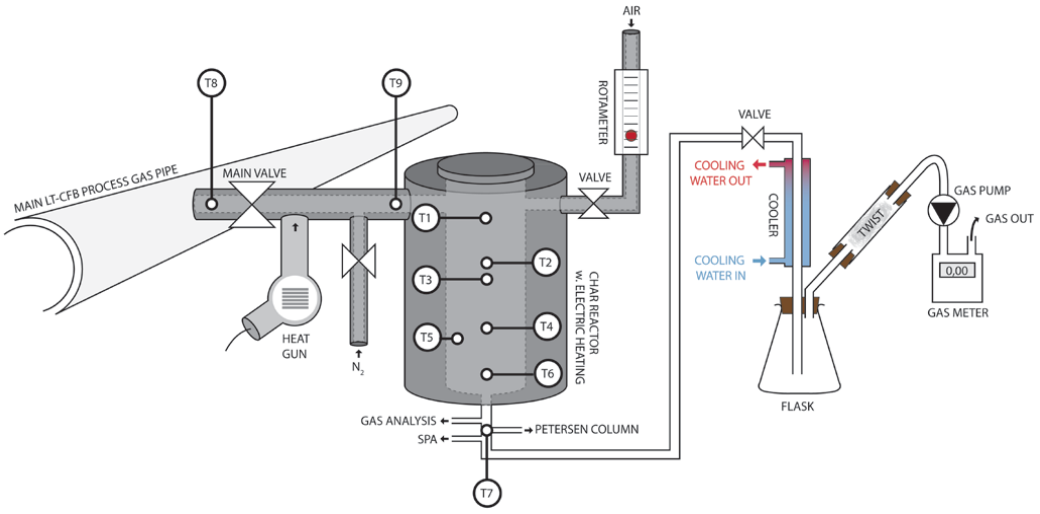

Figure 2: *Diagram of the test reactor and sampling system*

The residual gasification char used in the experiments as bed material was collected from the ash container of the Viking gasifier and sieved with a 3.15 mm sieve (Retsch, Germany) to remove small particles and powder. No further treatment was made to the char before using it in the reactor.

2.2 Setup operation

Before the start of the tests the reactor was cleaned from residual powder or particles. In the runs where the effect of the char bed was to be tested, the reactor was loaded with a fresh bed of Viking char, 200 mm tall (up to the level between T2 and T3 in Figure 2). The reactor was then sealed with bolts and a graphite gasket.

Before the start of each test, the reactor was flushed with N_2 for 30 minutes (about 5 l/min), to remove any oxygen. The reactor was then heated up to 800°C. Once the temperatures measured inside the reactor were stable, the N_2 flow was interrupted and producer gas flow was initiated by opening the main valve and starting the gas pump downstream. The temperature of producer gas flowing in the main gas pipe was about 600°C. However, the temperature of the gas flow measured at the inlet of the reactor (T9 in Figure 2) was only 300°C, due to heat losses in the slip-stream line.

In all experiments, the downstream gas pump was operated with a constant flow of 30 ± 1 l/min. As a consequence, the amount of extracted producer gas varied in the tests when an air flow was added. Production of gases inside the reactor as a result of reforming reactions also affected the flow through the reactor. Mass balance calculations were solved to obtain the actual flow of producer gas at the inlet of the reactor and to calculate the excess air ratio (λ) for each test. As the gas flow was not identical in every test, the gas residence time in the reactor varied in the range 2.5 - 2.9 s. The residence time was calculated considering the gas superficial velocity inside the reactor. The pressure drop through the char bed was estimated with a differential manometer connected below and above the bed and resulted to vary between 50 and 100 Pa in all experiments.

Experiments were designed to evaluate thermal cracking at 800°C in an empty reactor (TC test) and thermal reforming in presence of the char bed (TR test), at the same temperature. In addition, two tests were run with partial oxidation, with different air flows injected in the zone above the char bed (tests PO1 and PO2). Table 1 summarizes the experimental conditions. The electric furnace set-point was maintained at 820°C in all tests. This was necessary to guarantee a char bed temperature (T4) of 800°C.

Table 1: *Overview of experimental conditions.*

		TC	TR	PO1	PO2
Test duration	[min]	60	122	110	302
Initial weight of bed material	[g]	-	267	248	247
T2 (bed top)	[°C]	834	795	830	855
T4 (bed center)	[°C]	820	798	805	804
Air flow	[Nm^3/min]	-	-	$4.8*10^{-3}$	$9.5*10^{-3}$
Gas residence time	[s]	2.5	2.9	2.7	2.7

At the end of each test, the producer gas flow to the reactor was stopped and the electric furnace was turned off. The reactor was left to cool down, while a flow of N_2 was maintained through the char bed. The reactor was then opened and the spent char bed was recovered.

2.3 Gas sampling and analysis

The LT-CFB raw producer gas was sampled directly from the outlet pipe of the gasifier. Sampling ports were placed about 2 meters upstream of the extraction port connected to the reactor. After the passage through the unit, gas was sampled using the sampling ports below the reactor (depicted in Figure 2).

Two different methods were used for tar analysis. Solid Phase Adsorption (SPA) LC-NH_2 tubes (Supelco, USA) were used to extract gas samples of 100 ml. During each test, both SPA samples were taken at regular intervals of about 20 minutes on the producer gas and on the gas flow at the outlet of the gas upgrading unit. SPA samples were utilized to evaluate the composition of the tar mixture, by means of stable isotope dilution and GC-MS analysis. SPA samples were desorbed overnight, submerged in about 10 ml of analytical-grade acetone (purity 99.8%, Merck, Germany). At this stage, a known amount of standard mix was also added, containing the following deuterated compounds: phenol d6, naphthalene d8, acenaphthene d10, fluorene d10, anthracene d10, phenanthrene d10, pyrene d10 (Cambridge Isotope Laboratories, USA). After desorption, the liquid phase was concentrated to 1 ml and analyzed using an Agilent 7890B gas chromatograph interfaced to an Agilent 5977B Mass Selective Detector (Agilent, Denmark). Samples (1 µl) were injected in split mode (1:20). The source and rod temperatures were 230 °C and 150 °C, respectively. The products were separated using two HP-5ms ultra inert columns (15 m, 0.25 mm, 0.25 µm coating) (Agilent, Denmark). The carrier gas was He at a flow rate of 1.2 ml/min.

Separation of products was achieved using a temperature program from 70 to 250 °C at 10 °C/min. The applied ionization energy was 70 eV. Full mass spectra were recorded every 0.3 s (mass range m/z 40–450). Products were identified using the NIST search engine version 2.0 f. (Agilent, Denmark).

Samples obtained by using a Petersen column filled with acetone (250 ml) were used to estimate the total gravimetric tar in the producer gas and after the reactor. Gas was bubbled through the solvent for about 30 minutes; the total amount of sampled gas was measured by a gas meter at the outlet of the sampling system. The acetone sample was collected by emptying and rinsing the column. Sub-samples of 25 ml were concentrated by rotary evaporation (Rotavapor, Buchi, Switzerland) until the solvent was completely removed. The samples were placed in an oven overnight, to remove moisture. The residue was considered as gravimetric tar. The analysis was run in duplicates on each sample. One to three Petersen column samples were collected after the reactor during each test. At least one sample was taken during each test from the main gasifier outlet pipe, to assess the tar content in the untreated producer gas. The water content of producer gas was measured with a condenser similar to the one used at the outlet of the system shown in Figure 2. The method is described in detail elsewhere [3,40].

The gas composition (N_2, H_2, CO, CO_2, CH_4) was monitored with an online gas analyzer equipped with a thermal conductivity analyzer, an infrared analyzer (ABB, Denmark), and an oxygen analyzer (M&D products, Germany). The gas analyzer was connected with the outlet of the gas upgrading unit for the duration of the tests, and was connected to the gasifier outlet for the rest of the time.

Gas sampling bags (multi-layer foil, Restek, Denmark) were also used for additional sampling and offline analysis with a multi-column gas chromatograph (Trace 1300 GC, Thermo Scientific, USA) equipped with a Thermal Conductivity Detector (TCD) for detection of light gases and a Flame Ionization Detector (FID) for detection of C1-C6 hydrocarbons. The gas composition obtained from gas bags was used to estimate the specific higher heating value (HHV) of the raw gas and of the gaseous products after the reactor. The combination of these sampling and analysis techniques was used to monitor the quality of producer gas and evaluate the tar removal and reforming effect of the reactor under different conditions.

2.4 Calculation of mass and elements balances

Mass balances calculations were performed to determine the amount of producer gas flowing into the reactor from the slip-stream connecting pipe. The reactor containing the char bed was taken as the control volume. The balances were solved with the data available for each test. The inlet flow to the reactor was considered as the sum of three separate phases. The mass flow of stable gas species ($\dot{m}_{gas}$) included O_2, N_2, CO, CO_2, CH_4, H_2 and C1-C6 hydrocarbons. The mass flows of tar and water ($\dot{m}_{tar}$, $\dot{m}_{H2O}$) were considered based on their measured concentrations (in g/Nm³). The air flow ($\dot{m}_{air}$) was accounted for the tests with partial oxidation. The change in the bed weight during each test, divided by the test duration was considered as $\dot{m}_{char}$. The mass balance equation was written as in equation (1)

$$\dot{m}_{gas,in} + \dot{m}_{tar,in} + \dot{m}_{H2O,in} + \dot{m}_{air} + \dot{m}_{char} = \dot{m}_{gas,out} + \dot{m}_{tar,out} + \dot{m}_{H2O,out} \quad (1)$$

The mass flows were obtained from the volumetric flows measured during the experiments, multiplied by the density. Gas density values at ambient pressure (1 bar) and temperature (20°C) were approximated by considering the ideal gas law, as in equation (2). The molar weight of the gas (M_{gas}) was calculated by a weighted average based on the gas composition.

$$\rho_{gas}\left(\frac{Kg}{m^3}\right) = \frac{p(kPa) * M_{gas}\left(\frac{Kg}{kmol}\right)}{R\left(\frac{kJ}{kmol*K}\right) * T(K)} \quad (2)$$

Once the mass balance was solved for each test, the molar flows of single elements (O, C, H and N) could be calculated for the inlet and outlet flows. For this purpose, tar was considered as pure phenol (C_6H_5OH) at the inlet and as pure naphthalene ($C_{10}H_8$) at the outlet, as these were the most abundant species detected at the two locations. The initial water content of the bed material (10 wt%) has been considered lost during the heating up phase when accounting for the mass change in the bed. The rest of the char was considered as pure carbon.

The water content of the gas could not be measured at the same time at the inlet and at the outlet of the reactor. For TC and TR tests, water was measured at the inlet, whereas for tests PO1 and PO2 it was measured at the outlet of the reactor. The missing values were assessed based on the H balance.

$$\lambda = \frac{\dot{m}_{air}}{\dot{m}_{air,stoichiometric}} \quad (3)$$

For the tests with air injection, the mass balance results were used to calculate the stoichiometric molar flow of air and assess the excess air ratio (λ), defined in equation (3).

2.5 Char characterization

Residual char from the Viking gasifier was characterized prior to be used as bed material in the test reactor. The water content was assessed by drying the samples at 105 °C for 24 hours. The elemental composition (CHN) was evaluated by an Elemental Analyzer EuroEA (Eurovector, Italy). The specific surface area was quantified by Brunauer-Emmett-Teller (BET) analysis through N_2 adsorption at 77 K (Nova 2200, Quantachrome Instruments, USA). Prior to these measurements, char samples were grinded and degassed for 6 hours at 150°C. The pore volume distribution was evaluated through the Quenched Solid Density Functional Theory (QSDFT) using the calculation model for slit and cylindrical pores on the adsorption branch: this method is recommended for chemically and physically activated carbons [41]. The densities of char powders, used as inputs for the BET and DFT calculations, were measured with a helium pycnometer (Quantachrome Instruments, USA). After the experiments, the residual bed was collected and weighed. Spent char samples for elemental analysis and surface characterization were collected randomly from the bed material after the experiments. Only after the PO2 test, which had the longest duration, two char samples were extracted from the char bed: one from the very top of the bed and one from the bottom, close to the grate.

3. Results

3.1 LT-CFB producer gas quality assessment

The quality of the producer gas generated by the LT-CFB gasifier was evaluated by measuring the gas composition, the tar content and the composition of the tar mixture. Table 2 shows the results of the analysis on the untreated producer gas. Results are an average of the measurements performed on the raw producer gas in the days when gas upgrading tests were run.

Table 2: *Results of LT-CFB producer gas analysis.*
**Heating value calculated based on the concentrations of permanent gas species*

	Gravimetric tar	Water content	O_2	H_2	CO	CO_2	CH_4	N_2	Σ C1-C6	HV*
	g/Nm³	g/Nm³	Vol%	Vol%	Vol%	Vol%	Vol%	Vol%	Vol%	MJ/Nm³
Average	23.6	250	0.94	4.80	11.7	18.4	3.43	58.2	1.90	5.2
±	3	30	0.11	0.36	0.75	0.84	0.09	0.50	0.08	0.2

The gas analysis confirmed the low H_2 and CO content in the gas, together with the high tar load. The SPA samples retained only a small fraction of total tar. However, the GC-MS analysis of these samples was used to evaluate the species present in the tar mixture. Among the quantified compounds, phenol was by far the most abundant. The chromatographic analysis showed also the presence of other similar compounds such as ethyl- and methyl- phenol. This was not unexpected for the LT-CFB as pyrolysis volatiles, rich in primary tar species, are carried away in the producer gas.

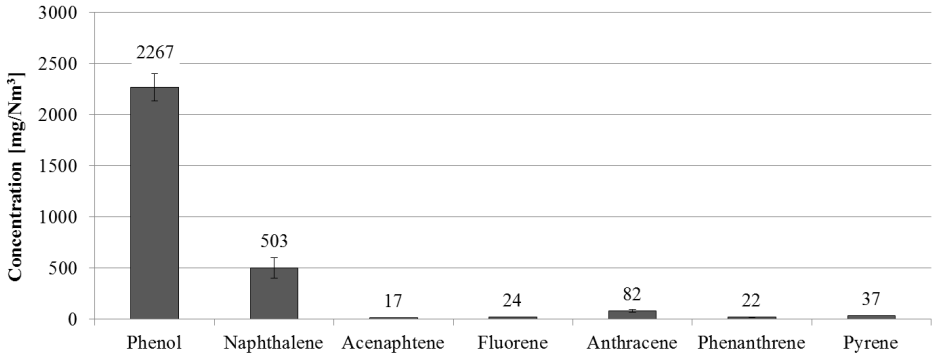

Figure 3: *Concentration of tar species in the LT-CFB producer gas. Samples extracted with SPA method.*

3.2 Effect of gas upgrading unit on the product composition

Figure 4 shows the molar yields of gravimetric tar and permanent gases calculated as in equation (4), where mol_{out} and mol_{in} stand for the molar flows [mol/min] at the outlet and inlet of the gas upgrading unit.

$$Molar\ yield\ [\%] = \frac{mol_{out} - mol_{in}}{mol_{in}} * 100 \qquad (4)$$

Note that, when calculating the molar yield of stable gases, the amount of air added for partial combustion has been subtracted from the products. Tar was extensively reduced in presence of the char bed. At the same time, permanent gases were produced; in particular H_2 and CO. Figure 5 shows the molar yields of the single gas species. An overview of the results from the analysis on the gas after the reactor is given in Table 3 for the different conditions.

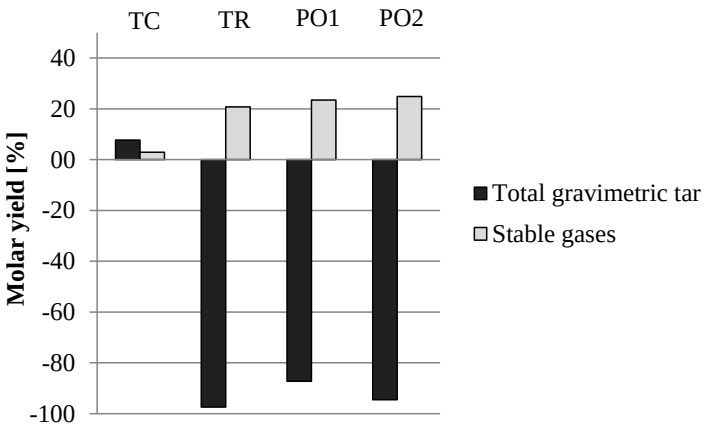

Figure 4: *Average molar yields of stable gases (O_2, N_2, H_2, CO, CO_2, H_2, C1-C6 hydrocarbons) and tar*

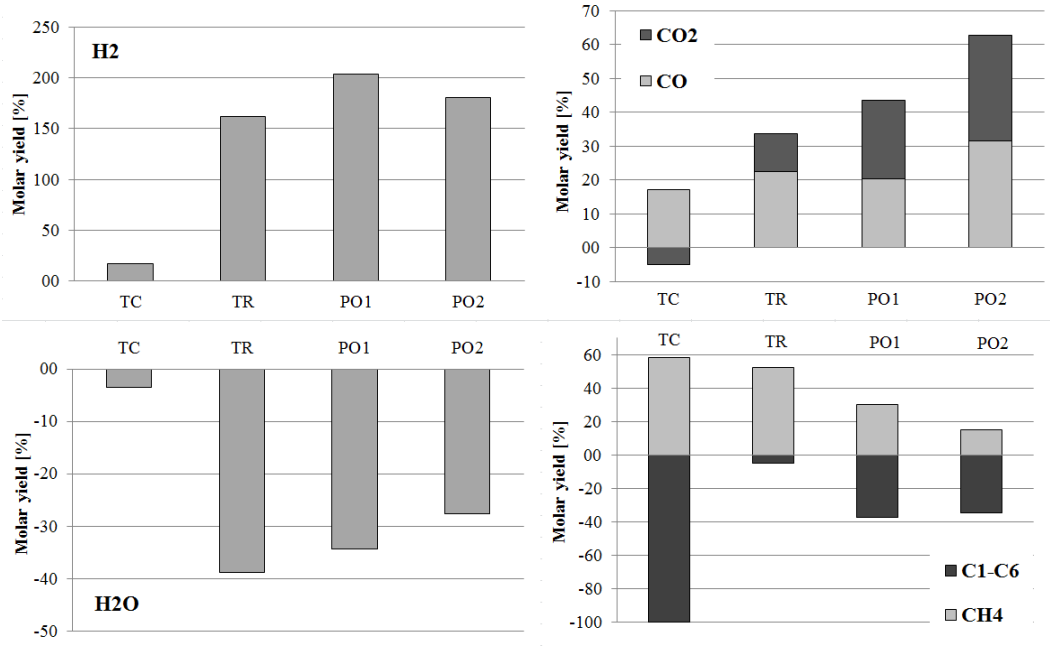

Figure 5: *Yields of gaseous species and water, in the tests TC, TR, PO1 and PO2.*

Table 3: *Overview of average gas compositions after the passage through the gas upgrading unit, in different test conditions. n.m. = not measured.*
**Heating value was calculated on the base of the permanent gases composition*

	Gravimetric tar	**O_2**	**H_2**	**CO**	**CO_2**	**CH_4**	**N_2**	**Σ C1-C6**	**HV***
	g/Nm³	Vol%	Vol%	Vol%	Vol%	Vol%	Vol%	Vol%	MJ/Nm³
TC	21.4 ± 2	0.1	5.4	14.8	17.9	5.7	56	n.m.	4.9
TR	0.6 ± 0.2	1.0	12.2	13.8	18.7	5.1	48.6	2	6.6
PO1	1.9 ± 0.3	0.9	13.4	10.7	16.9	3.5	53.8	0.6	4.9
PO2	0.6 ± 0.3	0.9	12	10.3	16.1	2.4	57.6	0.3	4.0

3.2.1 Thermal Cracking mode (TC)

During TC test, the reactor was heated by the electric furnace. The maximum temperature measured in the flow inside the reactor was 834°C. Despite the high temperature, under these conditions the tar content was not reduced. On the contrary, a slightly positive yield of total gravimetric tar was observed, and was ascribed to condensation of light species into heavier ones or soot particles. The composition of tar samples analyzed by GC-MS revealed a higher concentration of PAH species, as a consequence of gas-phase condensation reactions of light tar [15,42]. Figure 6 shows the tar mixture composition of the untreated producer gas (as in Figure 3) compared with the one measured after TC test. The concentrations of naphthalene and anthracene showed the largest increase.

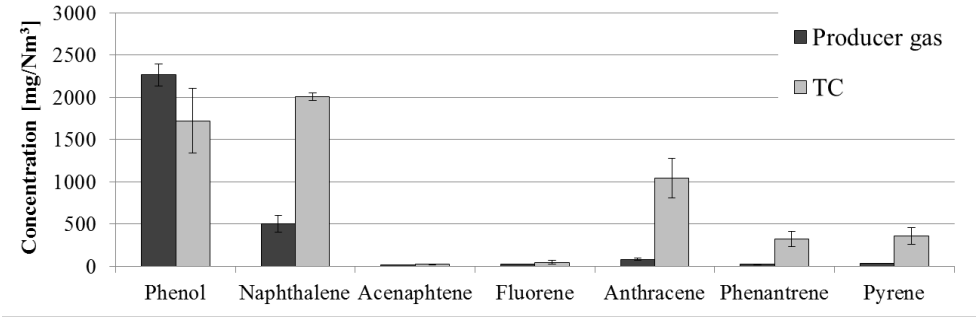

Figure 6: *Comparison of tar composition measured for the untreated producer gas and for the gas after the reactor in TC test.*

Even though the C1-C6 hydrocarbons were not measured in the gas after the reactor in this test, the molar flow of CO in the exit gas suggests that they were completely converted. The consumption of H_2O and CO_2, together with the production of CO and H_2, suggest that C1-C6 hydrocarbons were reformed following the endothermic reactions (5) and (6).

$C + CO_2 \rightarrow 2CO$ (dry reforming) (5)

$C + H_2O \rightarrow CO + H_2$ (steam reforming) (6)

CH_4 was also formed, most probably as a result of H_2 reaction with methyl radicals, which are produced during the pyrolysis of methylated tar species (e.g. toluene, methyl-naphthalene etc) [39,43]. As a result of these reactions, the molar flow of permanent gas species in increased by 3% with respect to the inlet flow and the gas composition is different from the one at the inlet.

3.2.2 Thermal Reforming (TR)

During this test, the same settings were adopted as for the TC test, but Viking char was loaded inside the reactor. The presence of the char bed had a dramatic effect on the gas quality in comparison with the previous test. During the first hour of experiment, tar species were cracked and reduced to 0.6 ± 0.2 g/Nm³ at the outlet, achieving a 98% reduction. However, this effect was not completely stable throughout the test, but was found to decline, as shown by the GC-MS analysis of SPA samples (Figure 7a).

The decreasing tar removal efficiency with time was caused by deactivation of the char surface. Deactivation was probably a consequence of structural changes caused by carbon deposition and gasification reactions, as discussed in section 3.4. The GC-MS analysis revealed that naphthalene was the main component in the residual tar after the reactor. This was not unexpected, as naphthalene is considered as the most refractory of the tar species and is often found to endure the passage through char beds [4,5,16]. During the first part of the experiment, naphthalene concentration was similar to that of the raw producer gas (close to 500 mg/Nm³). On the contrary, during the second half of the experiment, the naphthalene concentration increased to reach 1400 mg/Nm³. A similar trend was observed for anthracene, which increased up to 600 mg/Nm³, as compared to about 80 mg/Nm³ in the untreated producer gas. It can be therefore inferred that naphthalene, anthracene and possibly other

multi-rings aromatics were produced by the decomposition of tar on the surface of char. Their production seemed to be enhanced by the deactivation of the char surface. This is in agreement with observations by Wu et al. [16], who also detected naphthalene and anthracene enduring cracking and reforming over char, and ascribed their presence to ongoing polymerization reactions. Korus et al. [39] have studied the heterogeneous pyrolysis of toluene over active carbon, and have observed an increased production of benzene when the carbon surface was deactivated and covered in coke. Benzene is likely to react with radicals to form larger PAHs, as a consequence of phenyl radicals interacting with the formed aromatic rings [44]. The increased production of aromatic molecules in the second half of this test seems to confirm these observations. The decreased number of active sites on the surface of char in the final part of the test is confirmed by the increased concentration of phenol at the outlet of the reactor. It can be inferred that if the char surface can offer sufficient active sites for coke deposition, than the aromatic molecules can polymerize into solid carbon deposits. If the surface lacks active sites, poly-aromatic molecules endure in the gas phase. The deactivation of the char surface was also attested by a steady decrease in the H_2 production with time. A similar decrease was also observed in the concentration of CO, confirming that the main pathway for H_2 production was steam reforming.

Under TR conditions, the content of hydrocarbons was reduced, but they were not removed completely. The char bed favored the decomposition of tar species while inhibiting the reforming of C1-C6 hydrocarbons. It is also possible that hydrocarbons were formed by the decomposition of tar molecules as observed by Park et al. [11] in similar conditions.

Because of the presence of steam in the producer gas, the solid carbon produced by cracking of tar was partly gasified. Nevertheless, the total carbon content of the bed increased in the course of the test, indicating a net carbon accumulation. The consumption of H_2O, together with CO and H_2 formation suggest that both steam reforming (6) and water-gas shift reactions (7) took place.

$$CO + H_2O \leftrightarrow CO_2 + H_2 \text{ (water-gas shift)} \quad (7)$$

Dry reforming did not seem to occur, as the CO_2 content increased. A lower CH_4 yield was observed in comparison with TC mode. CH_4 molecules were probably also involved in reforming reactions: decomposition of methane has been found to be enhanced by the presence of active carbon [45,46] and gasification-derived char [47]. The molar flow of permanent gas species at the outlet increased by 22%

with respect to the inlet flow and the gas composition at the outlet of the reactor was enriched in H_2 and CO. On average, the gaseous products after the reactor had a heating value of 6.6 MJ/Nm³.

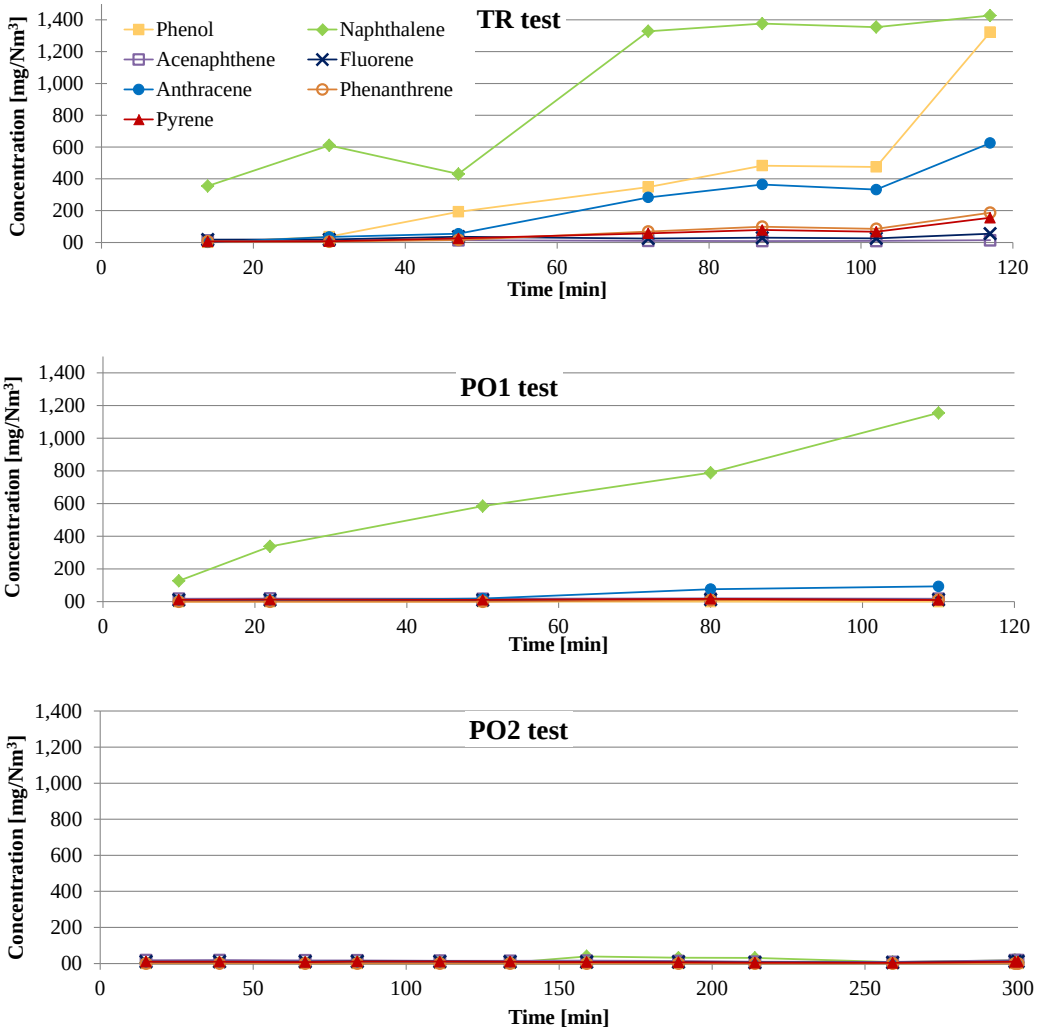

Figure 7: *Evolution of tar composition after the reactor in obtained from analysis of SPA samples in TR (a), PO1 (b) and PO2 (c) conditions.*

3.2.3 Partial oxidation -1 (P01)

As in the previous test, the char bed was maintained at a temperature of 800°C by the electric heating. An air flow of 4.7 l/min (25 °C) was injected in the freeboard space for partial oxidation. As a consequence, part of the inlet flow was combusted forming CO and CO_2. Because the of the relatively low temperature of the inlet flows, the partial combustion only led to a mild temperature increase in the reactor and in the top part of the char bed. The highest temperature measured in this zone was 830°C.

The presence of the char bed, combined with mild oxidation conditions resulted in an extensive reduction of hydrocarbons. Moreover, the gravimetric tar measured at the outlet was reduced to 1.9 ± 0.3 g/Nm^3.

The performance of the gas treatment unit was found to decrease during the test, even though the deactivation was less abrupt than in the previous TR test without air addition. The declining effect on tar conversion is visible in Figure 7b. Phenol was absent in the outlet stream, as a result of oxidative conditions. On the other hand, the concentration of naphthalene in the outlet flow was found to increase during the test. At the end of the experiment it had reached 1200 g/Nm^3. As in the previous experiment, an increase was also observed in the concentration of anthracene. The increased yields of multi-ring aromatics can be explained as for the TR mode. Yet, the trends were less severe in this case, due to the effect of partial combustion. Indeed, because of the increased temperature, reforming reactions occurred at a higher rate, thus limiting the amount of carbon deposited on the surface. As a result, in comparison with the TR test, the surface structure was degraded more gradually and the activity of the char bed was maintained for a longer time. Further details about the causes of deactivation are given in section 2.5. The reduced activity of the char surface was again confirmed by a decreasing H_2 production with time. The concentrations of CO and H_2 were highest at the start of the test and they decreased gradually but steadily.

As for the previous test, steam reforming and water-gas shift reactions consumed water and produced CO and H_2. As a result, the molar flow of permanent gas species increased by 24 % with respect to the inlet flow. The heating value of the stable gas phase was virtually unchanged in comparison with the untreated producer gas. This was the result of two opposed effects: the production of CO_2 and CO due to combustion, and the increased conversion of water to H_2 supported by the higher temperature.

3.2.4 Partial oxidation - 2 (P02)

In this test, an air flow of 9.5 l/min (at 25˚C) was injected for partial oxidation. The increased combustion produced a higher concentration of CO and CO_2 in the outlet flow. As in PO1, a considerable fraction of the energy generated by combustion was consumed to heat up the inlet flows. The highest temperature measured in the freeboard zone was 855˚C. These conditions led to an effective reduction of tar species: gravimetric tar at the outlet of the reactor was reduced to 0.6 ± 0.3 g/Nm^3.

During this test, the performance of the gas treatment unit showed no sign of decline. In order to verify the durability of the effect on the quality of the producer gas, the experiment was protracted for 300 min. Despite the longer duration, the tar concentration and the composition of the gas phase at the outlet were stable throughout the test. The results of tar analysis with SPA method are shown in Figure 7c for the whole duration of the experiment.

Intensified oxidative conditions increased the rate of reforming reactions, which involved also a fraction of the char bed. As a result, a net carbon loss was observed in the bed after 300 minutes. The reforming reactions involving carbon at the surface of char particles were effective in maintaining the activity of the char bed.

In comparison with PO1, consumption of water and production of H_2 were lower. At the same time, an increased concentration of CO at the outlet suggests that this change is the result of a variation in the equilibrium of the water-gas shift reaction (equation 7). Due to the fact that this reaction is moderately exothermic, high temperature can hinder the production of CO_2 and H_2. Indeed, at a temperature of 850˚C and higher, the equilibrium of the reaction is shifted to the reagents [48]. The molar flow of the permanent gas species increased by 25 % with respect to the inlet flow. The change in the gas composition at the outlet of the reactor resulted in a decrease of heating value of the gas phase in comparison with the inlet, as shown in Table 3. However, the loss of chemical energy via oxidation was partially balanced by the H_2 and CO production.

The results obtained under the tested conditions indicate that a temperature of at least 850˚C is required to maintain an extensive and durable effect on the gas quality. In these experiments, such temperature has been achieved by combusting a fraction of the inlet flow. It is important to keep in mind that, in an optimized gas upgrading unit, the inlet flows (producer gas and air) would be at a

higher temperature. Indeed, heat losses from the producer gas can be easily limited by extracting the gas closer to the filter, thus avoiding the long path in the lines to the gas upgrading unit. Moreover, air supplied for partial oxidation could be pre-heated. In this way, a bed temperature of 850°C or above could be achieved with a lower air flow than in PO2.

3.3 Results of mass and element balances

The solution of mass balances for each test gave the molar flow of stable gas species at the inlet of the reactor and allowed the calculation of the excess air ratio (λ), where partial oxidation was used. An overview of the results is given in Table 4.

Table 4: *Overview of inlet conditions for the different tests. Values in bold are results of calculations.*

Inlet	Stable gas species mol/min	Tar mol/min	Water mol/min	Air mol/min	Air, stoichiometric mol/min	λ -
TC	**1.3**	$6.5*10^{-3}$	0.46	-		
TR	**0.97**	$6.5*10^{-3}$	0.37	-		
PO1	**0.86**	$4.3*10^{-3}$	**0.29**	0.19	**0.40**	**0.2**
PO2	**0.66**	$3.1*10^{-3}$	**0.25**	0.39	**0.72**	**0.5**

The balances of hydrogen and nitrogen were closed with a maximum error of 3%. In the balances performed for TR, PO1 and PO2 tests, a surplus of carbon and a deficit of oxygen were found at the outlet. The carbon surplus corresponded in weight with the oxygen deficit. A hypothesis to explain this result is that oxygen was locally bound in the hot char bed. Wang et al.[49] observed an increased oxygen content in char that was subject to steam activation. Song at al. [50] reported a similar effect on char that was exposed to pyrolysis volatiles. It is also possible that oxygen reacted with ash-forming elements forming clusters of solid oxides ($CaCO_3$, K_2O, SiO_2). Indeed, a few of such clusters were found in the spent bed material, but they were difficult to quantify. Another hypothesis is that the carbon flow at the inlet was somehow underestimated. Sampling of tar with the Petersen column has been found to slightly underestimate the total tar content [40]. Furthermore, additional carbon could have been transported in residual dust or soot particles. Indeed, in a previous campaign with the LT-CFB gasifier, the particle loading had been quantified after the high-capacity ceramic filter and found to range from 0.5 to 1.5 g/Nm³ [51].

3.4 Characterization of fresh and spent char samples

After each test, the spent bed material was collected and weighed to quantify the mass change. Fresh Viking char and spent char samples were characterized in terms of elemental composition, surface area and pore distribution in order to investigate the deactivation mechanism. Results are collected in Table 5. Even though the carbon concentration increased in the three spent samples, the substantial increase in the bed weight indicates that a net carbon accumulation occurred only in the TR test. In the PO1 test, the carbon content and bed weight did not change significantly, suggesting that the carbon deposited at the surface of char was also gasified away. On the other hand, the significant weight loss measured in the bed after test PO2 suggests a net loss of carbon.

Table 5: *Initial and final weight of bed material and elemental composition on fresh and spent chars.*

	Dry bed weight		Elemental analysis		
	Before test	**After test**	**C**	**H**	**N**
	g	g	wt%	wt%	wt%
Fresh	-	-	87.6	0.63	0.10
TR	240	262	94.5	0.22	0.61
PO1	223	220	93.5	0.70	0.23
PO2	222	152	90.4	0.68	0.31

These considerations are well in agreement with the observed deactivation trends. The operating conditions of test PO2 induced a gasification rate that was higher than the rate of carbon deposition. Under these circumstances, char underwent a net loss of carbon, and its activity was maintained for a longer period of time, as predicted by Hosokai et al. [21]. On the other hand, carbon accumulation can explain the deactivation tendency observed in both test TR and PO1, when the gasification rate was not high enough to balance the carbon deposition.

BET and DFT analysis showed major modifications at the surface of chars after the experiments. As expected, the highest reduction in surface area and pore volume was measured after TR and PO1 test. Results were similar also for the sample obtained from the top of the char bed after PO2 test. On the contrary, the sample collected from the bottom of the bed after PO2 was found to still have a very large surface area, DFT analysis of spent chars also showed significant changes in the pore size range from 2

to 15 nm (small mesopores). Table 6 shows how the loss of pore volume affects both micropores and small mesopores. Figure 8 reports the surface area distribution of fresh and spent chars. A significant reduction of the surface area in the small mesopores range can be observed for the spent char samples, with the exception of PO2 – bed bottom. In this case, the surface area in this range has increased in comparison with the fresh char. It appears as some of the micropore volume was lost in favor of mesopore volume. Such increase was probably induced by gasification reactions, that were driven by the higher temperature measured for test PO2. The fact that the surface of char at the bottom of the bed was still similar to the fresh material also shows that deactivation proceeds from the top layer to the bottom layer. Furthermore, this also explains the high activity of this particular char bed, even after 5 hours of operation: some layers in the bed were still active towards tar decomposition.

Table 6: *Overview of BET and DFT analysis results for fresh and spent char samples. Variation percentage is referred to the fresh char*

	Surface area	Variation	Total pore volume	Variation	Micropores (0-2 nm)	Variation	Small Mesopores (2-15 nm)	Variation
	m^2/g	%	cm^3/g	%	cm^3/g	%	cm^3/g	%
Fresh	1253		0.79		0.37		0.35	
TR	281	-77.5	0.18	-77.8	0.08	-77.0	0.07	-79.1
PO1	315	-74.8	0.24	-70.3	0.09	-75.8	0.11	-69.7
PO2 top	306	-75.6	0.28	-64.1	0.07	-80.7	0.15	-57.7
PO2 bottom	915	-27.0	0.70	-11.9	0.23	-37.3	0.36	+2.9

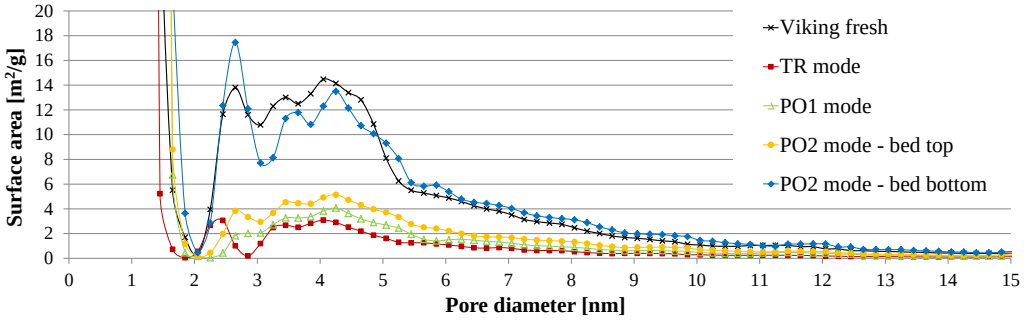

Figure 8: *Comparison of surface area distributions, obtained with QSDFT analysis on fresh and spent char*

Micropores are known to contain active sites for carbon deposition. However, these results show that the surface degradation, as effect of heterogeneous cracking reactions not only affects the micropores, but also the small mesopores.

Overall, these results corroborate the hypothesis that deposition of elemental carbon generates a decrease in the surface area and pore volume at the surface of char, while reforming reactions remove solid carbon increasing the size of pores. It is interesting to notice that even when a limited amount of carbon is left at the surface and not gasified (as in PO1), the surface structure of char suffers extensive deterioration, and porosity is reduced. This evidence suggests that deactivation can be delayed by applying operating conditions that favor the gasification of deposited carbon. Nevertheless, on the long run, char would still deactivate as a consequence of the degradation of the surface structure.

3.5 Feasibility of full-scale implementation of carbon-based gas cleaning

The discussed results indicated that, in order to achieve a durable gas quality avoiding deactivation, it is necessary to consume some of the char bed by gasification reactions. In PO1 mode, virtually no carbon was depleted from the bed, even if the surface structure affected and therefore the surface suffered deactivation. In PO2 mode, higher λ and reactor temperature caused a gradual bed consumption: about 10 g of carbon were lost from the bed per Nm^3 of producer gas which passed through the reactor.
In total, the 100 kW_{th} LT-CFB gasifier produces about 45 Nm^3/h of producer gas; therefore about 450 g/h of char would be needed to continuously treat the gas. On the other hand, the 75 kW_{th} TwoStage gasifier operates with a dry biomass feed rate of 15 kg/h, producing about 3.75 kg/h of pyrolysis char. If it were to produce 500 g/h of residual char, it should operate with a carbon burn-off of about 86 wt%. The Viking char that was used in these experiments was generated with a 99 wt% burn-off; however it is likely that its performance as a gas cleaning substrate would not be significantly damaged by a lower burn-off. This was verified by the fact that spent char from the bottom of the bed in the PO2 test had a degraded surface but was still active for gas upgrading, with the same performance as fresh char.

4. Conclusions

In this work, a gas upgrading unit was designed, built and tested for the treatment of producer gas from the LT-CFB gasifier at DTU, Risø Campus. Producer gas was generated from straw gasification and was

rich in primary tar. The unit was designed to emulate the tar reforming taking place inside the second stage of the TwoStage gasifier; featuring a bed of char and a freeboard zone with an air inlet for partial oxidation. The char used in the tests was derived from wood chips and was the solid residue of the TwoStage demonstration plant – the Viking gasifier. Gas treatment was performed with a fixed bed of char, also combined with air injection for partial combustion. The results showed a considerable effect of the char bed on the gas quality. Even without air addition, the presence of Viking char inside the reactor favored the decomposition of tar species inducing a 98% reduction in the tar concentration. However, the presence of the char bed alone without air injection resulted in a significant deactivation of the char surface, during a 2 hours test. Temperature played an important role in the reforming of tar into stable gases. In the tests with air injection, oxidation reactions depleted some of the chemical energy of the gas, but the higher temperature increased the rate of reforming reactions. In this way, the activity of the char bed was maintained for a longer time. In particular, in the test with the highest air flow (PO2), the bed temperature was raised to 855°C. Under these conditions, the rate of reforming reactions was high enough to maintain the activity of the char bed for a period of 5 hours. After this time, the experiment was interrupted but the gas upgrading was still stable and running. Pre- and post-experimental characterization of the char surface revealed that spent chars had lost a significant fraction of their surface area and pore volume. The only exception was represented by char samples collected at the bottom of the bed after test PO2. In this case, the surface area was similar to that of fresh char, while the volume contained in the mesopores had increased. These findings clarified the reason why the char bed was still active after a 5 hours test. These results indicated that reforming reactions are able to extend the activity of the char bed, but even when virtually no carbon is deposited on the surface of the char, the pore size distribution is modified and the surface structure is degraded. This suggests that, even under optimized conditions, the char will eventually deactivate. Nevertheless, the longest experiments performed with PO2 conditions demonstrated that a fixed bed of gasification residual char is able to upgrade producer gas by reducing more than 97% of tar and increasing the H_2 and CO content of the gas phase. This effect was stable for a period of 300 minutes, with a char consumption of 10 g of char per Nm^3 of producer gas. Considering the residual char generation rate of the Viking gasifier, its repurposing as a gas treatment substrate would be feasible. However, future work should also be addressed to the testing of the LT-CFB´s own residual char as substrate for gas upgrading. The results indicate that it is possible to use the solid residue of gasification for efficient and reliable upgrading of biomass producer gas.

References

[1] Ahrenfeldt J, Thomsen TP, Henriksen U, Clausen LR. Biomass gasification cogeneration - A review of state of the art technology and near future perspectives. Appl Therm Eng 2013;50:1407–17. doi:10.1016/j.applthermaleng.2011.12.040.

[2] Thomsen TP, Hauggaard-Nielsen H, Gøbel B, Stoholm P, Ahrenfeldt J, Henriksen UB, et al. Low temperature circulating fluidized bed gasification and co-gasification of municipal sewage sludge . Part 2 : Evaluation of ash materials as phosphorus fertilizer. Waste Manag 2017;66:145–54. doi:10.1016/j.wasman.2017.04.043.

[3] Thomsen TP, Sárossy Z, Gøbel B, Stoholm P, Ahrenfeldt J, Jappe F, et al. Low temperature circulating fluidized bed gasification and co-gasification of municipal sewage sludge . Part 1 : Process performance and gas product characterization. Waste Manag 2017;66:123–33. doi:10.1016/j.wasman.2017.04.028.

[4] Brandt P, Larsen E, Henriksen U. High tar reduction in a two-stage gasifier. Energy & Fuels 2000;14:816–9. doi:10.1021/ef990182m.

[5] Ahrenfeldt J, Henriksen U, Jensen TK, Gøbel B, Wiese L, Kather A, et al. Validation of a continuous combined heat and power (CHP) operation of a two-stage biomass gasifier. Energy & Fuels 2006;20:2672–80. doi:10.1021/ef0503616.

[6] Ahrenfeldt J, Egsgaard H, Stelte W, Thomsen T, Henriksen UB. The influence of partial oxidation mechanisms on tar destruction in TwoStage biomass gasification. Fuel 2013;112:662–80. doi:10.1016/j.fuel.2012.09.048.

[7] Egsgaard H, Ahrenfeldt J, Ambus P, Schaumburg K, Henriksen UB. Gas cleaning with hot char beds studied by stable isotopes. J Anal Appl Pyrolysis 2014;107:174–82. doi:10.1016/j.jaap.2014.02.019.

[8] Griffiths DML, Mainhood JSR. The cracking of tar vapour and aromatic compounds on activated carbon. Fuel 1967:167–76.

[9] Boroson ML, Howard JB, Longwell JP, Peters WA. Heterogeneous cracking of wood pyrolysis tars over fresh wood char surfaces. Energy & Fuels 1989;3:735–40. doi:10.1021/ef00018a014.

[10] Al-Rahbi AS, Onwudili JA, Williams PT. Thermal decomposition and gasification of biomass pyrolysis gases using a hot bed of waste derived pyrolysis char. Bioresour Technol 2016;204:71–9. doi:10.1016/j.biortech.2015.12.016.

[11] Park J, Lee Y, Ryu C. Reduction of primary tar vapor from biomass by hot char particles in fixed bed gasification. Biomass and Bioenergy 2016;90:114–21. doi:10.1016/j.biombioe.2016.04.001.

[12] Sun Q, Yu S, Wang F, Wang J. Decomposition and gasification of pyrolysis volatiles from pine wood through a bed of hot char. Fuel 2011;90:1041–8. doi:10.1016/j.fuel.2010.12.015.

[13] Dabai F, Paterson N, Millan M, Fennell P, Kandiyoti R. Tar formation and destruction in a fixed-bed reactor simulating downdraft gasification: Equipment development and characterization of tar-cracking products. Energy & Fuels 2010;24:4560–70. doi:10.1021/ef100681u.

[14] Phuphuakrat T, Namioka T, Yoshikawa K. Tar removal from biomass pyrolysis gas in two-step function of decomposition and adsorption. Appl Energy 2010;87:2203–11. doi:10.1016/j.apenergy.2009.12.002.

[15] Matsuhara T, Hosokai S, Norinaga K, Matsuoka K, Li CZ, Hayashi JI. In-situ reforming of tar from the rapid pyrolysis of a brown coal over char. Energy & Fuels 2010;24:76–83. doi:10.1021/ef9005109.

[16] Wu W, Luo Y, Su Y, Zhang Y, Zhao S, Wang Y. Nascent Biomass Tar Evolution Properties under Homogeneous/Heterogeneous Decomposition Conditions in a Two-Stage Reactor. Energy & Fuels 2011;25:5394–406. doi:10.1021/ef2007276.

[17] Krerkkaiwan S, Tsutsumi A, Kuchonthara P. Biomass derived tar decomposition over coal char bed. ScienceAsia 2013;39:511. doi:10.2306/scienceasia1513-1874.2013.39.511.

[18] Sueyasu T, Oike T, Mori A, Kudo S, Norinaga K, Hayashi JI. Simultaneous steam reforming of tar and steam gasification of char from the pyrolysis of potassium-loaded woody biomass. Energy & Fuels 2012;26:199–208. doi:10.1021/ef201166a.

[19] Zhao S, Luo Y, Zhang Y, Long Y. Experimental investigation of the synergy effect of partial oxidation and bio-char on biomass tar reduction. J Anal Appl Pyrolysis 2015;112:262–9. doi:10.1016/j.jaap.2015.01.016.

[20] Hosokai S, Norinaga K, Kimura T, Nakano M, Li C-Z, Hayashi J. Reforming of Volatiles from the Biomass Pyrolysis over Charcoal in a Sequence of Coke Deposition and Steam Gasification of Coke. Energy & Fuels 2011;25:5387–93. doi:10.1021/ef2003766.

[21] Hosokai S, Kumabe K, Ohshita M, Norinaga K, Li C, Hayashi J-I. Mechanism of decomposition of aromatics over charcoal and necessary condition for maintaining its activity. Fuel 2008;87:2914–22. doi:10.1016/j.fuel.2008.04.019.

[22] Fuentes-Cano D, Gómez-Barea A, Nilsson S, Ollero P. Decomposition kinetics of model tar compounds over chars with different internal structure to model hot tar removal in biomass gasification. Chem Eng J 2013;228:1223–33. doi:10.1016/j.cej.2013.03.130.

[23] Nitsch X, Commandré J-M, Valette J, Volle G, Martin E. Conversion of Phenol-Based Tars over Biomass Char under H2 and H2O Atmospheres. Energy & Fuels 2014:28 (2014) 6936-6940. doi:10.1021/ef500980g.

[24] Abu El-Rub Z, Bramer EA, Brem G. Experimental comparison of biomass chars with other catalysts for tar reduction. Fuel 2008;87:2243–52. doi:10.1016/j.fuel.2008.01.004.

[25] Klinghoffer NB, Castaldi MJ, Nzihou A. Influence of char composition and inorganics on catalytic activity of char from biomass gasification. Fuel 2015;157:37–47. doi:10.1016/j.fuel.2015.04.036.

[26] Huang Q, Lu P, Hu B, Chi Y, Yan J. Cracking of model tar species from the gasification of municipal solid waste using commercial and waste derived catalysts. Energy & Fuels 2016:acs.energyfuels.6b00711. doi:10.1021/acs.energyfuels.6b00711.

[27] Palla Assima G, Marie-Rose S, Lavoie JM. Role of fixed carbon and metal oxides in char during the catalytic conversion of tar from RDF gasification. Fuel 2018;218:406–16. doi:10.1016/j.fuel.2017.12.039.

[28] Rodríguez-Reinoso F. The role of carbon materials in heterogeneous catalysis. Carbon N Y 1998;36:159–75. doi:10.1016/S0008-6223(97)00173-5.

[29] Hervy M, Berhanu S, Weiss-Hortala E, Chesnaud A, Gérente C, Villot A, et al. Multi-scale characterisation of chars mineral species for tar cracking. Fuel 2017;189:88–97. doi:10.1016/j.fuel.2016.10.089.

[30] Min Z, Yimsiri P, Asadullah M, Zhang S, Li C-Z. Catalytic reforming of tar during gasification. Part II. Char as a catalyst or as a catalyst support for tar reforming. Fuel 2011;90:2545–52. doi:10.1016/j.fuel.2011.03.027.

[31] Zhang S, Asadullah M, Dong L, Tay HL, Li CZ. An advanced biomass gasification technology with integrated catalytic hot gas cleaning. Part II: Tar reforming using char as a catalyst or as a catalyst support. Fuel 2013;112:645–53. doi:10.1016/j.fuel.2013.03.015.

[32] Benedetti V, Patuzzi F, Baratieri M. Characterization of char from biomass gasification and its similarities with activated carbon in adsorption applications. Appl Energy 2018;227:92–9. doi:10.1016/j.apenergy.2017.08.076.

[33] Zhang LX, Matsuhara T, Kudo S, Hayashi JI, Norinaga K. Rapid pyrolysis of brown coal in a drop-tube reactor with co-feeding of char as a promoter of in situ tar reforming. Fuel 2013;112:681–6. doi:10.1016/j.fuel.2011.12.030.

[34] Patuzzi F, Prando D, Vakalis S, Rizzo AM, Chiaramonti D, Tirler W, et al. Small-scale biomass gasification CHP systems: Comparative performance assessment and monitoring experiences in South Tyrol (Italy). Energy 2016;112:285–93. doi:10.1016/j.energy.2016.06.077.

[35] Zeng X, Wang F, Li H, Wang Y, Dong L, Yu J, et al. Pilot verification of a low-tar two-stage coal gasification process with a fluidized bed pyrolyzer and fixed bed gasifier. Appl Energy 2014;115:9–16. doi:10.1016/j.apenergy.2013.10.052.

[36] Choi YK, Mun TY, Cho MH, Kim JS. Gasification of dried sewage sludge in a newly developed three-stage gasifier: Effect of each reactor temperature on the producer gas composition and impurity removal. Energy 2016;114:121–8. doi:10.1016/j.energy.2016.07.166.

[37] Zhang S, Song Y, Song YC, Yi Q, Dong L, Li TT, et al. An advanced biomass gasification technology with integrated catalytic hot gas cleaning. Part III: Effects of inorganic species in char on the reforming of tars from wood and agricultural wastes. Fuel 2016;183:177–84. doi:10.1016/j.fuel.2016.06.078.

[38] Zhang Y, Luo Y, Wu W, Zhao S, Long Y. Heterogeneous Cracking Reaction of Tar over Biomass Char, Using Naphthalene as Model Biomass Tar. Energy & Fuels 2014;28:3129–37. doi:10.1021/ef4024349.

[39] Korus A, Samson A, Szle A, Katelbach-woz A. Pyrolytic toluene conversion to benzene and coke over activated carbon in a fixed-bed reactor. Fuel 2017;207:283–92. doi:10.1016/j.fuel.2017.06.088.

[40] IEA Bioenergy - Task 33. Gas analysis in gasification of biomass and waste - Guideline report. 2018.

[41] Quantachrome Instruments - DFT Models n.d. http://www.quantachrome.com/technical/dft.html (accessed June 6, 2018).

[42] Moldoveanu SC. Techniques and Instrumentation in Analytical Chemistry - Pyrolysis of Organic Molecules. vol. 28. Elsevier Science Ltd; 2009.

[43] Jess A. Mechanisms and kinetics of thermal reactions of aromatic hydrocarbons from pyrolysis of solid fuels. Fuel 1996;75:1441–8. doi:10.1016/0016-2361(96)00136-6.

[44] Shukla B, Susa A, Miyoshi A, Koshi M. In Situ direct sampling mass spectrometric study on formation of polycyclic aromatic hydrocarbons in toluene pyrolysis. J Phys Chem A 2007;111:8308–24. doi:10.1021/jp071813d.

[45] Muradov N, Smith F, T-Raissi A. Catalytic activity of carbons for methane decomposition reaction. Catal Today 2005;102–103:225–33. doi:10.1016/j.cattod.2005.02.018.

[46] Moliner R, Suelves I, Lázaro MJ, Moreno O. Thermocatalytic decomposition of methane over activated carbons: Influence of textural properties and surface chemistry. Int J Hydrogen Energy 2005;30:293–300. doi:10.1016/j.ijhydene.2004.03.035.

[47] Klinghoffer N, Castaldi MJ, Nzihou A. Catalyst Properties and Catalytic Performance of Char from Biomass Gasification. I&Ec 2012:13113–22. doi:10.1021/ie3014082.

[48] Schuster F. Handbuch - Brenngase und ihre Eigenschaften. Vieweg. Braunschweig: 1978.

[49] Wang YG, Chen XJ, Yang SS, He X, Chen ZD, Zhang S. Effect of steam concentration on char reactivity and structure in the presence/absence of oxygen using Shengli brown coal. Fuel Process Technol 2015;135:174–9. doi:10.1016/j.fuproc.2015.01.016.

[50] Song Y, Zhao Y, Hu X, Zhang L, Sun S, Li CZ. Destruction of tar during volatile-char interactions at low temperature. Fuel Process Technol 2018;171:215–22. doi:10.1016/j.fuproc.2017.11.023.

[51] Narayan V, Jensen PA, Henriksen UB, Egsgaard H, Nielsen RG, Glarborg P. Behavior of Alkali Metals and Ash in a Low-Temperature Circulating Fluidized Bed (LTCFB) Gasifier. Energy & Fuels 2016;30:1050–61. doi:10.1021/acs.energyfuels.5b02464.

3.2 Details of mass and energy balances for the operation of the gas upgrading unit

Mass and enthalpy balances were solved for the gas-upgrading unit. As explained in Paper III, the mass balances were used to quantify the flow of gas that was extracted from the gasifier. On the base of the resulting mass and molar flows, enthalpy balances were drawn to quantify the enthalpy flows in and out of the system. The following section presents in detail the assumptions, calculations and results of the mass and energy balances. Calculations were performed separately for each day of the unit operation, by using the data available for the specific day. The operating conditions of each test are reported in detail in Paper III. In short, the effect of thermal cracking was quantified in an empty reactor (TC test) and thermal reforming was evaluated in presence of a char bed (TR test). In addition, two tests were run with partial oxidation, (tests PO1 and PO2), with different air flows. Table 3.2 summarizes the experimental conditions. Here and in the following, all the volumetric flows are referred to standard conditions (20°C, 1 bar). The units (l, min, g, mol, J) were chosen for numerical convenience in the calculations.

Table 3.2: *Summary of operating conditions*

		TC	TR	PO1	PO2
Test duration	[min]	60	122	110	302
Char bed (start)	[g]	-	267	248	247
Air flow	[l/min]	-	-	4.8	9.5

For an easier understanding of the following equations, Table 3.3 collects a list of the available data and the measuring techniques through which it was obtained. Gas analysis methods are described in detail in [1].

Table 3.3: *Overview of the available data and measurements methods for the different days*
**this method could not be applied simultaneously at inlet and outlet. Missing values were obtained by closing the hydrogen balance*

Quantity	Unit	Measurement method
$\dot{V}_{gas,out}$ (20°C, 1 bar)	[l/min]	Gas meter at outlet
Gas phase composition (O_2, N_2, CO, CO_2, CH_4, H_2, C1-C6 gases)	[Vol%]	Offline GC-MS analysis (gas sample collected in gas bags)
Tar, in and out	[g/l]	Gravimetric tar measurement with Petersen column
H_2O, in and out	[g/l]	Condensation method* (described in Appendix I)
$\dot{V}_{air}$ (20°C, 1 bar)	[l/min]	Calibrated rotameter

3.2.1 Mass balances

The balance was solved for each test by considering the producer gas as three separate phases: dry gas phase, water and tar. The terms considered in the inlet and outlet streams are visualized in Figure 3.8.

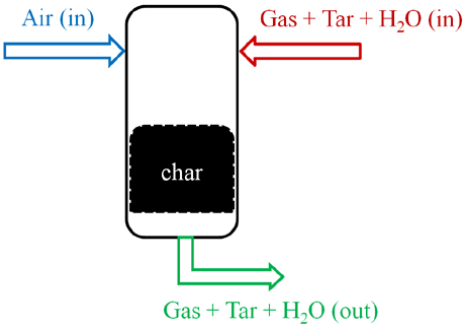

Figure 3.8: *Inlet and outlet streams for the gas upgrading unit*

During the unit operation, the volumetric flows of air and dry gas at the outlet were measured at ambient temperature and pressure (20°C, 1 bar). On these premises, the mass flows at the inlet and outlet of the system were written as in (1) and (2).

$$\dot{m}_{in} = \dot{m}_{gas,\,in} + \dot{m}_{tar,\,in} + \dot{m}_{H2O,\,in} + \dot{m}_{air} \quad (1)$$

$$\dot{m}_{out} = \dot{m}_{gas,out} + \dot{m}_{tar,\,out} + \dot{m}_{H2O,\,out} \quad (2)$$

The mass balance for the reactor can be written as in equation (3), where Δm_{char} is the change in the bed weight before and after the test [g], and Δt_{exp} is the test duration [min].

$$\dot{m}_{out} = \dot{m}_{in} + \frac{\Delta m_{char}}{\Delta t_{exp}} \quad (3)$$

If $\dot{m}_{in}$ and $\dot{m}_{out}$ are written as in (1) and (2), then the only unknown term is $\dot{m}_{gas,in}$. The other terms were calculated based on the available data, as presented in equations (4-7)

$$\dot{m}_{out} = \dot{V}_{gas,\,out}\left[\frac{l}{min}\right] * \rho_{gas,\,out}\left[\frac{g}{l}\right] + tar_{out}\left[\frac{g}{l}\right] * \dot{V}_{gas,\,out}\left[\frac{l}{min}\right] + H_2O_{out}\left[\frac{g}{l}\right] * \dot{V}_{gas,\,out}\left[\frac{l}{min}\right] \quad (4)$$

$$\dot{m}_{tar,in} = \dot{V}_{gas,\,in}\left[\frac{l}{min}\right] * tar_{in}\left[\frac{g}{l}\right] \quad (5)$$

$$\dot{m}_{H2O,in} = \dot{V}_{gas,\,in}\left[\frac{l}{min}\right] * H_2O_{in}\left[\frac{g}{l}\right] \quad (6)$$

$$\dot{m}_{air} = \dot{V}_{air}\left[\frac{l}{min}\right] * \rho_{air}\left[\frac{g}{l}\right] \quad (7)$$

The molar weight of the gas (M_{gas}) was calculated by a weighted average based on the gas composition. The density of the gaseous phase was approximated as in equation (8) by considering it as ideal gases at ambient pressure (1 bar) and room temperature (20°C).

$$\rho_{gas}\left[\frac{g}{l}\right] = \frac{p[kPa] * M_{gas}\left[\frac{g}{mol}\right]}{R\left[\frac{J}{mol*K}\right] * T[K]} \quad (8)$$

$\dot{m}_{gas,\,in}$ was calculated as in equation (9).

$$\dot{m}_{gas,\,in} = \frac{\dot{m}_{out} - \dot{m}_{air} - \dot{m}_{char}}{tar_{in} + H_2O_{in}} \quad (9)$$

Because the density of the inlet gas was also known based on the gas composition, the volumetric flow ($\dot{V}_{gas,\,in}$) could be then calculated as in equation (10).

$$\dot{V}_{gas,\,in} = \frac{\dot{m}_{gas,in}}{\rho_{gas,\,in}} \quad (10)$$

The values of inlet flows resulting from these calculations were validated with the nitrogen balance of the system. It was assumed that nitrogen entering the system with the producer gas and air injection was not involved in reactions and was completely recovered in the product gas during the unit operation. It is also assumed that the nitrogen content of tar was negligible. On these premises, the nitrogen balance was formulated as in equation (11) and $\dot{V}_{gas,\,in}$ was calculated from equation (12)

$$N_{2,\,gas\,in} + N_{2,\,air} = N_{2,\,gas\,out} \quad (11)$$

$$N_{2,gas\,in}[Vol\%] * \dot{V}_{gas,\,in} + N_{2,\,air}[Vol\%] * \dot{V}_{air} = N_{2,\,gas\,out}[Vol\%] * \dot{V}_{gas,out} \quad (12)$$

The values of $\dot{V}_{gas,\,in}$ obtained with both calculation methods are shown in the first two columns of Table 3. The good agreement between the values supports that the assumptions were valid in both cases. Results obtained from the mass balances (second column in Table 3.4) were considered for further calculations. Details of the gas flows at the inlet and outlet of the unit are summarized in Table 3.4.

Table 3.4: *Overview on the gaseous flows at inlet and outlet of the unit. Values for the inlet were obtained by solving mass balances. Volumetric flows and densities are referred to 20°C and 1 bar.*

	Inlet						Outlet				
	$\dot{V}_{gas}$ (N_2) l/min	$\dot{V}_{gas}$ l/min	ρ_{gas} Kg/m³	$\dot{m}_{gas}$ g/min	M_{gas} g/mol	$\dot{n}_{gas}$ mol/min	$\dot{V}_{gas}$ l/min	ρ_{gas} Kg/m³	$\dot{m}_{gas}$ g/min	M_{gas} g/mol	$\dot{n}_{gas}$ mol/min
TC	30.5	31.3	1.22	38.3	29.4	1.30	32.1	1.20	38.5	28.8	1.34
TR	23.8	23.3	1.24	29.0	29.9	0.970	28.2	1.14	32.1	27.4	1.17
PO1	21.3	20.5	1.23	25.1	29.5	0.853	30.1	1.12	33.6	26.9	1.25
PO2	16.1	15.9	1.22	19.4	29.3	0.663	29.4	1.13	33.3	27.2	1.22

The gas pump downstream of the system was manually regulated through a throttling valve on the suction side. The volumetric flow was monitored regularly with the gas meter and a stop watch. The manual regulation explains the fluctuations in the flow at the outlet of the system for the different tests. Larger variations are found in the volumetric flows at the inlet. Indeed, by keeping the total outlet flow rather constant, the flow of extracted producer gas changed depending on the amount of air injected and on the amount of gas generated by reforming of tar and char.

3.2.2 Gas species and elements balance

Once the mass and molar flows were known for both outlet and inlet streams, a balance could be drawn of the single gas species and for the single elements.

To calculate the flows of single elements the following assumptions were made:

- C1-C6 hydrocarbons were considered as pure ethylene (C_2H_4). This was the most abundant species detected by GC-MS analysis of gas samples
- Air composition was considered as 21% O_2 and 79% N_2
- Tar was considered as pure phenol at the inlet (C_6H_5OH) and pure naphthalene at the outlet (C_6H_8). These two species were the most abundant detected in the tar mixtures sampled at the inlet and outlet of the unit (see Paper III).
- $\dot{m}_{char}$ was considered as a flow of pure carbon

The molar flows for the single components in the gas phase are shown in Table 4. Molar flows were calculated on the base of the concentrations, which were measured as indicated in Table 1. However, some of said concentrations could not be measured during the tests. This is the case for the concentration of hydrocarbons at the outlet in the TC test. It was approximated to zero, by closing the

carbon balance. In a similar way, missing data on the water content of the gas phase were calculated by closing the hydrogen balance. The values that were obtained in this way are in bold character in Table 3.5. The molar flows of the single elements are presented in Table 3.6, together with the total mass flows at inlet and outlet.

Table 3.5: *Molar flows of gas species at inlet and outlet of the system. The values are based on the volumetric composition and on the results of mass balances.*
Values in bold could not be measured and are calculated by closing of elements balances.

		O_2 mol/min	H_2 mol/min	CO mol/min	CO_2 mol/min	CH_4 mol/min	N_2 mol/min	C_2H_4 mol/min	Tar mol/min	H_2O mol/min
TC	Inlet	0.002	0.062	0.169	0.253	0.048	0.768	0.026	0.006	0.434
	Outlet	0.001	0.072	0.198	0.240	0.076	0.749	**0.000**	0.007	**0.420**
TR	Inlet	0.008	0.042	0.123	0.190	0.034	0.558	0.022	0.0065	0.373
	Outlet	0.012	0.143	0.162	0.219	0.059	0.569	0.021	0.0002	**0.227**
PO1	Inlet	0.009	0.041	0.099	0.153	0.030	0.497	0.017	0.004	**0.294**
	Outlet	0.012	0.168	0.134	0.211	0.044	0.673	0.008	0.0006	0.167
PO2	Inlet	0.006	0.035	0.072	0.117	0.022	0.389	0.012	0.003	**0.247**
	Outlet	0.011	0.147	0.126	0.196	0.029	0.705	0.003	0.0002	0.145

Table 3.6: *Molar flows of single elements at inlet and outlet of the system. The values are based on the on the results of mass balances*

	Inlet					Outlet				
	O mol/min	**C** mol/min	**H** mol/min	**N** mol/min	**Total** g/min	**O** mol/min	**C** mol/min	**H** mol/min	**N** mol/min	**Total** g/min
TC	1.12	0.57	1.33	1.54	47.5	1.10	0.57	1.33	1.50	46.7
TR	0.90	0.44	1.10	1.12	36.2	0.85	0.48	1.06	1.14	36.4
PO1	0.81	0.34	0.89	1.31	36.3	0.75	0.41	0.88	1.35	36.6
PO2	0.74	0.26	0.72	1.4	35.5	0.69	0.36	0.72	1.4	35.7

3.2.3 Stoichiometric air and excess air ratio (λ) calculation

The stoichiometric air flow relative to the producer gas flow (including its tar content) was calculated on the basis of the mass balances results. The reaction of complete combustion was written as in equation (13), considering the fuel as constituted exclusively by carbon, hydrogen and oxygen.

$$C_aH_bO_c + e\left(O_2 + \frac{79}{21}N_2\right) = aCO_2 + \frac{b}{2}H_2O + e\frac{79}{21}N_2 \qquad (13)$$

Where *a*, *b*, *c* indicate the molar flows of C, H and O, respectively while *e* indicates the molar flow of oxygen required for complete combustion of the fuel. Stoichiometric oxygen was obtained as in (14), derived from equation (13)

$$e = a + \frac{b}{2} - \frac{c}{2} \tag{14}$$

Based on the stoichiometric air flow, the excess air ratio (λ) was calculated as the ratio between $\dot{m}_{air}$ and $\dot{m}_{air,stoichiometric}$. Results are shown in Table 3.7, for the test when air injection was used.

Table 3.7: *Overview of flows of combustibles at the inlet, injected air flows, stoichiometric air and λ.*

Inlet	$\dot{m}_{gas}$ g/min	$\dot{m}_{tar}$ g/min	$\dot{m}_{air}$ g/min	$\dot{m}_{air,stoichiometric}$ g/min	λ -
PO1	25.1	0.45	5.7	28.2	0.20
PO2	19.4	0.32	11.5	21.1	0.53

3.2.4 Enthalpy balances

Based on the results of mass balances, enthalpy balances were drawn. The inlet and outlet conditions are visualized in Figure 3.9. The temperature of the flow at the inlet of the reactor was measured with a thermocouple and was 300˚C± 5˚C under stable flow conditions, for all tests. It is to be noticed that the temperature of the producer gas generated by the LT-CFB is about 600˚C; however heat losses along the slip stream pipe caused the reduction to 300˚C at the inlet of the reactor.

The temperature of the outlet flow was measured with a thermocouple placed below the grate supporting the char bed. In all experiments the temperature was 790 ± 5˚C. Injected air was not pre-heated, and its temperature was approximately 20˚C.

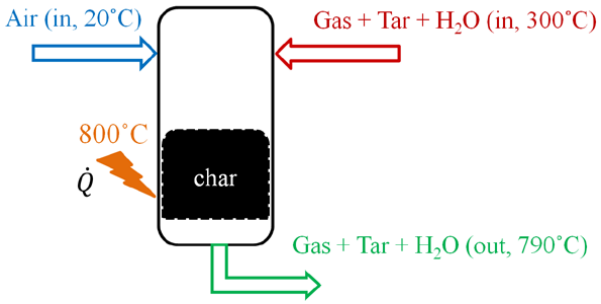

Figure 3.9: *Inlet and outlet flow boundary conditions used for the enthalpy balances*

The overall energy balance was written as in equation (15).

$$\frac{dU}{dT} = \dot{Q} + H_{gas,out} - H_{gas,in} \tag{15}$$

Where $\frac{dU}{dT}$ is the variation of internal energy within the system boundaries and $H_{gas,\,in}$ and $H_{gas,out}$ are the absolute enthalpy values in the inlet and outlet flows. The heat provided by the electric heating ($\dot{Q}$) has not been measured during the experiments, therefore it is the unknown term in this equation. The other terms have been calculated as in equations (16) to (18). Here, the specific enthalpies of the components (h) are expressed in $\left[\frac{J}{mol}\right]$, while the molar flows (n) are in $\left[\frac{mol}{min}\right]$.

$$H_{gas,in}\left[\frac{J}{min}\right] = \sum_i h^i_{gas,in} * n^i_{gas,in} + h_{tar,in} * n_{tar,in} + h_{H2O,in} * n_{H2O,in} + h_{air,in} * n_{air,in} \tag{16}$$

$$H_{gas,out}\left[\frac{J}{min}\right] = \sum_i h^i_{gas,out} * n^i_{gas,out} + h_{tar,out} * n_{tar,out} + h_{H2O,out} * n_{H2O,out} \tag{17}$$

$$\frac{dU}{dT}\left[\frac{J}{min}\right] = h_{char}\left[\frac{J}{mol}\right] * n_{char}\left[\frac{mol}{min}\right] \tag{18}$$

The variation of internal energy in the system was written using the specific enthalpy of char, and the molar flow of char, calculated as for the mass balances. Because char is a solid its internal energy and enthalpy are equivalent, therefore the assumption $h_{char} = u_{char}$ is valid.

The enthalpy of the gas phase was calculated by summing the enthalpies of the single gas species: O_2, H_2, CO, CO_2 and CH_4. Using the same approximation as the mass balances, the sum of light hydrocarbons in the gas phase was considered pure ethylene. In the same way, tar at the inlet was considered as pure phenol and tar at the outlet pure naphthalene. The specific enthalpy of each

component was calculated by summing up the enthalpy of formation in standard conditions (20°C, 1 bar), h_f^0, and the sensible enthalpy change related with the temperature difference between the standard and the actual conditions. An example of the calculations for the inlet stream is reported in equations (19) to (22).

$$h_{gas(i)573K}\left[\frac{J}{mol}\right] = h_{f,i}^0(298K) + \int_{298}^{573} c_p(i)dT \quad (19)$$

$$h_{tar,573K}\left[\frac{J}{mol}\right] = h_f^0(phenol, 298K) + c_{p,\,phenol} * \Delta T_{298K}^{573K} \quad (20)$$

$$h_{air,298K}\left[\frac{J}{mol}\right] = h_f^0(air, 298K) \quad (21)$$

$$h_{char,1073K}\left[\frac{J}{mol}\right] = h_f^0(char,\ 298K) + c_{p,\,char} * \Delta T_{298K}^{1073K} \quad (22)$$

The values for the standard enthalpy of formations and enthalpy variations were found tabulated in "An Introduction to Combustion", by S.R.Turns [2]. Thermodynamic data for phenol and naphthalene were obtained online [3,4]. The specific heat capacity of naphthalene and ethylene were obtained through Engineering Equation Solver (EES) software. The heat capacity of char was approximated as an average of the values proposed for wood char by Fredlund (1998) and Koufopanos (1989) [5]. The standard enthalpy of formation for char has been considered zero, as for pure carbon. Air at 20°C was considered as constituted by pure oxygen and nitrogen. Being this the reference state, its contribution to the enthalpy balance was zero. Results from enthalpy calculations are reported in detail in Table 3.9 to 3.12. Table 3.8 summarizes, for the four tests, the values of total enthalpy (ΔH) and of enthalpy of formation with reference to standard conditions (ΔH_f^o). Enthalpy calculations showed that, in all tests, the total enthalpy (H) was higher at the outlet than at the inlet. This difference can be attributed to the heat supplied by the electric furnace. A large fraction of the energy supplied to the system increased the sensible enthalpy ($\Delta H_{sensible}$) at the outlet. Such increase was quantitatively comparable for all tests, and corresponded to the energy needed for the heating of the inlet flows.

Table 3.8: *Absolute and standard enthalpy for the different tests.*

	H (inlet) J/s	H (outlet) J/s	ΔH J/s	H_f^o(inlet) J/s	H_f^o(outlet) J/s	ΔH_f^o J/s	$\Delta H_{sensible}$ J/s
TC	-3501	-2895	606	-3775	-3723	52	554
TR	-2807	-2051	756	-3019	-2705	313	443
PO1	-2233	-1719	515	-2411	-2355	56	459
PO2	-1787	-1536	252	-1928	-2137	-210	461

As mentioned earlier, the producer gas reached the reactor at a temperature of about 300°C, while air was injected at room temperature. In TC, PO1 and particularly in TR conditions, the enthalpy of formation of the products also increased as a consequence of reactions occurring within the control volume. Such increase was mainly due to the progress of steam reforming reactions. In the experiments with air addition, as a consequence of oxidation reactions, the content of CO_2 and CO increased at the outlet, thus decreasing the standard enthalpy of formation of the product gas. In the PO2 test, with the highest air flow, the net balance ΔH_f^o was negative. However, the loss represented only about 11% of the original value. This was possible due to the fact that the reforming reactions counterbalanced oxidation reactions and contained the net loss. Partial combustion supported the endothermic reforming reactions by providing heat.

As described in Paper III, PO2 test conditions (λ = 0.5) showed the best and longest stability of the gas upgrading effect. This was mainly due to the temperature in the center of the reactor, which was the highest in all the tests (855°C). Temperature is a very important parameter for the operation of the unit, as it governs the reforming reactions and the water-gas shift equilibrium. If the inlet gas was at a higher temperature and air was preheated, a lower air flow to partial oxidation would have been necessary to achieve the same temperature conditions (i.e. λ = 0.2, as in PO1 test). In view of future implementations and upscaling of the gas upgrading unit, it is crucial to limit the heat losses upstream of the char bed. The addition of an oxidizing agent is beneficial for maintaining a high temperature in the zone above the char bed, and to favor the conversion of tar compounds into heavier multi-rings aromatics [6]. However, a lower λ value is helpful in preserving the chemical energy of the gas, and its heating value.

Table 3.9: *Overview of enthalpy calculations results for TC test (no char bed, no air injection)*

TC		Char	Tar	H_2O	O_2	H_2	CO	CO_2	CH_4	N_2	C_2H_4	Total
Gas composition	[Vol%]	-	-	-	0.12	4.77	13	19.41	3.71	58.99	2	
Inlet flow	[mol/min]	-	0.0065	0.4344	0.002	0.062	0.169	0.253	0.048	0.768	0.026	
h_o^f	[J/mol]	-	-165000	-241845	0	0	-110541	-393546	-74831	0	52283	
$h_{sensible,300°C}$	[J/mol]	-	39875	9561	8402	8016	8142	11658		8099	15867.5	
h_{total}	[J/mol]	-	-125125	-232284	8402	8016	-102399	-381888	-63127	8099	68150.5	
H	[J/s]	-	-13.56	-1681.7	0.2	8.3	-288.8	-1608.0	-50.8	103.6	29.6	-3501
H_o^f	[J/s]	-	-17.88	-1750.9	0.00	0.00	-311.7	-1657.1	-60.2	0.00	22.7	-3775
Gas composition	[Vol%]	-	-	-	0.1	5.4	14.8	17.9	5.7	56		
Outlet flow	[mol/min]	-	0.0070	0.4196	0.001	0.072	0.198	0.240	0.076	0.750	0.000	
h_o^f	[J/mol]	-	15573	-241845	0	0	-110541	-393546	-74831	0	52283	
$h_{sensible,790°C}$	[J/mol]	-	213435	28638	24933	22579	23807	36881		23548	64719	
h_{total}	[J/mol]	-	229008	-213207	24933	22579	-86734	-356665	-32095	23548	117002	
H	[J/s]	-	26.7176	-1491.0	0.6	27.2	-286.7	-1425.8	-40.9	294.5	0.0	-2895
H_o^f	[J/s]	-	1.81685	-1691.33	0.00	0.00	-365.37	-1573.27	-95.26	0.00	0.00	-3723
ΔH (outlet -inlet)	[J/s]	-	40.27	190.67	0.34	18.94	2.09	182.14	9.95	190.87	-29.57	**606**
ΔH_o^f (outlet -inlet)	[J/s]	-	19.69	59.61	0.00	0.00	-53.64	83.78	-35.04	0.00	-22.68	**52**

Table 3.10: *Overview of enthalpy calculations results for TR test (char bed, no air injection)*

TR		**Char**	**Tar**	**H_2O**	**O_2**	**H_2**	**CO**	**CO_2**	**CH_4**	**N_2**	**C_2H_4**	**Total**
Gas composition	[Vol%]	-	-	-	0.85	4.36	12.72	19.6	3.5			
Inlet flow	[mol/min]	-0.011	0.0065	0.373	0.008	0.042	0.123	0.190	0.034	0.0065	0.373	
h_o^f	[J/mol]	0	-165000	-241845	0	0	-110541	-393546	-74831	-165000	-241845	
$h_{sensible,300°C}$	[J/mol]	1716	39875	9561	8402	8016	8142	11658		39875	9561	
h_{total}	[J/mol]	1716	-125125	-232284	8402	8016	-102399	-381888	-63127	-125125	-232284	
H	[J/s]	-0.32	-13.48	-1444.0	1.2	5.7	-210.6	-1210.1	-35.7	-13.48	-1444.0	-2807
H_o^f	[J/s]	0.00	-17.77	-1503.5	0.00	0.00	-227.3	-1247.1	-42.3	-17.77	-1503.5	-3019
Gas composition	[Vol%]	-	-	-	1.02	12.2	13.8	18.7	5.05			
Outlet flow	[mol/min]	-	0.0002	0.227	0.012	0.143	0.162	0.219	0.059	0.0002	0.227	
h_o^f	[J/mol]	-	15573	-241845	0	0	-110541	-393546	-74831	15573	-241845	
$h_{sensible,790°C}$	[J/mol]	-	213435	28638	24933	22579	23807	36881		213435	28638	
h_{total}	[J/mol]	-	229008	-213207	24933	22579	-86734	-356665	-32095	229008	-213207	
H	[J/s]	-	0.62	-806.6	5.0	53.8	-233.7	-1302.2	-31.6	0.62	-806.6	-2051
H_o^f	[J/s]	-	0.04	-914.98	0.00	0.00	-297.85	-1436.91	-73.78	0.04	-914.98	-2705
ΔH (outlet -inlet)	[J/s]	0.32	14.10	637.40	3.81	48.13	-23.12	-92.11	4.07	14.10	637.40	**756**
ΔH_o^f (outlet -inlet)	[J/s]	0.00	17.82	588.49	0.00	0.00	-70.52	-189.83	-31.44	17.82	588.49	**313**

Table 3.11: *Overview of enthalpy calculations results for PO1 test (char bed and air injection)*

PO1		**Char**	**Tar**	**H_2O**	**O_2**	**H_2**	**CO**	**CO_2**	**CH_4**	**N_2**	**C_2H_4**	**Total**
Gas composition	[Vol%]	-	-	-	1.1	4.8	11.6	17.9	3.48	58.3	2.01	
Inlet flow	[mol/min]	0.0019	0.004	0.296	0.009	0.041	0.099	0.153	0.030	0.497	0.017	
h_o^f	[J/mol]	0	-165000	-241845	0	0	-110541	-393546	-74831	0	52283	
$h_{sensible,300°C}$	[J/mol]	1705	39875	9561	8402	8016	8142	11658		8099	15867.5	
h_{total}	[J/mol]	1705	-125125	-232284	8402	8016	-102399	-381888	-63127	8099	68150.5	
H	[J/s]	0.05	-8.99	-1145.9	1.3	5.5	-168.9	-971.9	-31.2	67.1	19.5	-2233
H_o^f	[J/s]	0.00	-11.85	-1193.1	0.00	0.00	-182.3	-1001.5	-37.0	0.00	14.9	-2411
Gas composition	[Vol%]	-	-	-	0.92	13.4	10.7	16.9	3.54	53.8	0.6	
Outlet flow	[mol/min]	-	0.0006	0.167	0.012	0.168	0.134	0.211	0.044	0.673	0.008	
h_o^f	[J/mol]	-	15573	-241845	0	0	-110541	-393546	-74831	0	52283	
$h_{sensible,790°C}$	[J/mol]	-	213435	28638	24933	22579	23807	36881		23548	64719	
h_{total}	[J/mol]	-	229008	-213207	24933	22579	-86734	-356665	-32095	23548	117002	
H	[J/s]	-	2.10	-593.4	4.8	63.1	-193.5	-1256.8	-23.7	264.1	14.6	-1719
H_o^f	[J/s]	-	0.14	-673.1	0.00	0.00	-246.6	-1386.7	-55.23	0.00	6.54	-2355
ΔH (outlet -inlet)	[J/s]	-0.05	11.09	552.5	3.47	57.61	-24.6	-284.9	7.54	197.0	-4.84	**515**
ΔH_o^f (outlet -inlet)	[J/s]	0.00	12.00	520.0	0.00	0.00	-64.3	-385.2	-18.21	0.00	-8.40	**56**

Table 3.12: *Overview of enthalpy calculations results for PO2 test (char bed and air injection)*

PO2		**Char**	**Tar**	**H_2O**	**O_2**	**H_2**	**CO**	**CO_2**	**CH_4**	**N_2**	**C_2H_4**	**Total**
Gas composition	[Vol%]	-	-	-	0.87	5.24	10.9	17.7	3.31	58.7	1.87	
Inlet flow	[mol/min]	0.0144	0.003	0.248	0.006	0.035	0.072	0.117	0.022	0.389	0.012	
h_o^f	[J/mol]	0	-165000	-241845	0	0	-110541	-393546	-74831	0	52283	
$h_{sensible,300°C}$	[J/mol]	1705	39875	9561	8402	8016	8142	11658		8099	15867.5	
h_{total}	[J/mol]	1705	-125125	-232284	8402	8016	-102399	-381888	-63127	8099	68150.5	
H	[J/s]	0.41	-6.46	-959.8	0.8	4.6	-123.4	-747.2	-23.1	52.6	14.1	-1787
H_o^f	[J/s]	0.00	-8.53	-999.3	0.00	0.00	-133.2	-770.0	-27.4	0.00	10.8	-1928
Gas composition	[Vol%]	-	-	-	*0.92*	*12*	*10.3*	*16.05*	*2.4*	*57.6*	*0.28*	
Outlet flow	[mol/min]	-	0.0002	0.145	0.011	0.147	0.126	0.196	0.029	0.704	0.003	
h_o^f	[J/mol]	-	15573	-241845	0	0	-110541	-393546	-74831	0	52283	
$h_{sensible,790°C}$	[J/mol]	-	213435	28638	24933	22579	23807	36881		23548	64719	
h_{total}	[J/mol]	-	229008	-213207	24933	22579	-86734	-356665	-32095	23548	117002	
H	[J/s]	-	0.649	-514.8	4.7	55.2	-182.1	-1166.8	-15.7	276.5	6.7	-1536
H_o^f	[J/s]	-	0.044	-583.96	0.00	0.00	-232.1	-1287.50	-36.61	0.00	2.98	-2137
ΔH (outlet -inlet)	[J/s]	-0.4	7.1	445.0	3.9	50.6	-58.7	-419.7	7.4	223.9	-7.4	**252**
ΔH_o^f (outlet -inlet)	[J/s]	0.00	8.57	415.31	0.00	0.00	-98.89	-517.52	-9.23	0.00	-7.82	**-210**

References

[1] IEA Bioenergy - Task 33. Gas analysis in gasification of biomass and waste - Guideline report. 2018.

[2] Turns SR. An Introduction to Combustion - Concepts and Applications. McGraw-Hill International Editions; 1996.

[3] US Department of Commerce. Phenol - NIST Chemistry WebBook. Natl Inst Stand Technol n.d. https://webbook.nist.gov/cgi/cbook.cgi?ID=C108952&Mask=2 (accessed November 6, 2018).

[4] DDBST GmbH. Dortmund DataBank n.d. http://www.ddbst.com/en/EED/PCP/HFO_C123.php (accessed November 6, 2018).

[5] Hankalin V, Ahonen T, Raiko R. Finnish-Swedish Flame Days. Therm Prop a Pyrolysing Wood Part 2009:1–16.

[6] Ahrenfeldt J, Egsgaard H, Stelte W, Thomsen T, Henriksen UB. The influence of partial oxidation mechanisms on tar destruction in TwoStage biomass gasification. Fuel 2013;112:662–80. doi:10.1016/j.fuel.2012.09.048.

Chapter 4

Char characterization

The TwoStage gasification process has been described in detail in Chapter 3. Residual char was produced during operation of the TwoStage "Viking" demonstration plant at DTU, Risø Campus. Char was collected from the Viking ash container and analyzed with various techniques. The aim was to investigate its properties and potential as a bed material for producer gas treatment. This chapter presents results of analyses performed on char samples from the Viking gasifier, which were not included in the previous chapters. The analyzed char samples include the Viking char itself, char samples collected from the reactors of the Viking gasifier, at different locations, and char samples that had been used in gas upgrading tests.

The properties of carbonaceous materials mainly depend on the feedstock that is carbonized and on the production process [1]. For example, the properties of char can be affected by temperature, pressure, oxygen levels and duration of the thermal treatment [2]. With the aim to investigate the carbonization process within the TwoStage gasification process, samples were also collected at different positions inside the Viking gasifier. Internal samples from the pyrolysis and gasification reactors were analyzed and compared with the residual char. Compositional analysis was also performed on the feed material, spruce wood chips.

The residual Viking char has been characterized as well in detail, with various techniques, before and after being used in the gas upgrading reactor for producer gas treatment. Paper III reports results of the elemental analysis and the N_2 adsorption at 77 K of these samples. This section includes further results obtained through additional analytical methods that have been applied to spent char samples. The characterization on fresh and spent chars was performed on one hand to investigate the modifications of the char surface caused by the contact with tar-rich producer gas. On the other hand, these analyses were used for a preliminary evaluation of the biochar properties of spent samples, in view of a possible use on agricultural soil. This option would be beneficial for the overall carbon balance of the gasification system, as the biochar incorporation in soils is considered a method for carbon sequestration [3]. The use of Viking char for soil amendment has been previously investigated [4]. An incubation study of 22

months with a temperate loam soil revealed that this char has a good carbon sequestration potential, due in particular to its stability and resistance to microbial degradation [5]. With this in mind, the results of the surface characterization were considered also in terms of biochar quality, and a specific test was performed to quantify the contamination of Polycyclic Aromatic Hydrocarbon (PAH) species.

4.1 Samples description and analytical methods

Wood chips (spruce) and residual char have been collected at the Viking gasifier demonstration plant at DTU, Risø Campus (Figure 4.1). The wood chips used as feedstock are stored in a dedicated container near the plant. When the gasifier is in operation, the char in the gasification reactor is collected below the grate and is extracted by mean of a cochlea. The screw leads the residual char to a dedicated container where it is stockpiled. Figure 4.1 shows the Viking gasifier with the screw conveyor leading the char to the external container.

Figure 4.1: *The 75 kW_{th} Viking gasifier at Risø Campus*

Internal char samples were extracted at different positions inside the Viking gasifier, when the gasifier was not in operation and completely cooled down. Samples from the pyrolysis auger were collected by slowly moving the screw, while char was unloaded in the second reactor. The total length of the screw

was about 3.36 m, and a total of 5 samples were extracted from this stage (Pyrolysis 1-5). During the Viking gasifier operation, the residence time of solids in the pyrolysis stage is about 30 minutes.
Recovery of char samples from the bed in the gasification reactor was possible with a vacuum cleaner, which was thoroughly cleaned after the extraction of each sample. In this way, four samples were collected from different layers of the char bed. Layer I was recovered from the top of the bed, while layers II, III, IV were closer to the grate. It is to be noticed that the collected char samples were left in reactors after the gasifier was shut down, during the natural cooling phase. Therefore they experienced a prolonged residence time in comparison with the solids moving through the reactors during normal operation. The estimated position of the samples inside the gasifier is shown in Figure 4.2.

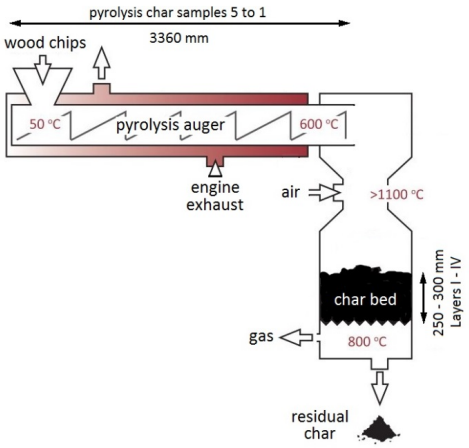

Sample	Distance from wood chips inlet [m]
Pyrolysis 5	0.7
Pyrolysis 4	1.4
Pyrolysis 3	2.2
Pyrolysis 2	2.7
Pyrolysis 1	3.2

Figure 4.2: *Simplified diagram of the reactors in the Viking gasifier, with indication of the estimated positions of the char samples inside the auger*

Spent char samples were collected after the LT-CFB producer gas upgrading tests. Three spent char samples were collected after the tests of Thermal Reforming (TR), Partial Oxidation 1 (PO_1) and Partial oxidation 2 (PO_2). Notice that the duration of tests TR and PO_1 was about 2 hours, while test PO_2 lasted for 5 hours. The experimental conditions are described in detail in Paper III. Table 4.2 reports a summary of the characterization techniques used on the different samples.

4.1.1 Scanning Electron Microscopy (SEM)

SEM images were taken with a TM 3000 microscope (Hitachi, Japan). Samples were prepared by placing char particles on sample holders, covered with double-faced carbon adhesive tape. Because of the high

carbon content of the samples, they were considered as conductive enough not to be covered with a metal layer prior to the analysis. The accelerating voltage applied during the observations was 15 kV.

Table 4.1: *Overview of the applied characterization techniques*

	Spruce wood chips	Residual Viking char	Internal char samples	Spent char samples
SEM imaging		✓		✓
Proximate composition	✓	✓		
Elemental composition	✓	✓		✓
N_2 adsorption at 77 K		✓	✓	✓
ICP -OES		✓		
PAH contamination		✓		✓
TGA		✓		✓
XRD		✓		✓

4.1.2 Composition

Prior to any analysis, chars were reduced to powder in a ball mill. The moisture content was evaluated by drying the samples for 90 minutes in an oven at 106°C. The content of volatiles was evaluated by using a muffle furnace, following CEN/TS 15148. The ash fraction was determined in two ways, following DIN EN 14775 and DIN 51719, which prescribe incineration at 550°C and 815°C respectively. In both cases, the fixed carbon content was calculated by difference.

The elemental composition (CHNS) was measured with a VarioEL III (Elementar Analysensystem GmbH, Germany). The trace elements present in the chars were detected by Inductively Coupled Plasma-Optical Emission Spectrometry (ICP-OES) (Varian 720 ES).

4.1.3 Particle size distribution

The Viking char has an abundant powdery fraction that makes it difficult to handle it. The material collected from the container at the Viking gasifier has been sieved and divided in three fractions:

particles smaller than 0.5 mm, larger than 1 mm and intermediate. To do this, Viking char was sieved using a 0.5 and a 1 mm sieve mounted on a shaker (Retsch, Germany).

4.1.4 Surface characterization

The specific surface area of these samples was quantified by Brunauer-Emmett-Teller (BET) analysis through N_2 adsorption at 77 K (Nova 2200, Quantachrome Instruments, USA). Char samples were prepared by pulverization in a ball mill and drying to remove moisture. Before each measurement, char samples were degassed at 150°C for 6 hours. The pore volume distribution was evaluated through Quenched Solid Density Functional Theory (QSDFT) using the calculation model for slit and cylindrical pores on the adsorption branch: this method is recommended for chemically and physically activated carbons [6]. The densities of char powders, used as inputs for the BET and DFT calculations, were measured with a helium pycnometer (Quantachrome Instruments, USA).

4.1.5 PAH contamination assessment

The content of PAH species in the char was assessed by Soxhlet extraction with toluene following DIN EN 15527. The method is recommended by the European Biochar Certificate (EBC) [7]. Analysis was performed by Eurofins Umwelt Laboratories, Freiberg, Germany. The analysis identified 16 PAH compounds, following the recommendation of the United States Environmental Protection Agency (EPA) [8]. The limit of detection was 0.1 mg/Kg for each compound.

4.1.6 Thermogravimetric analysis (TGA) and X- Ray Diffraction (XRD)

Thermal degradation of fresh and spent char samples was tested in a Netzsch TG 209 F3 Tarsus thermogravimetric analyzer (NETZSCH-Gerätebau GmbH, Selb, Germany). Samples were analyzed in two different atmospheres, in N_2 and in synthetic air and all analyses were performed with a flow rate of 20 ml/min. The samples (approximately 10 mg) were heated from 36 to 900° followed by an isothermal step at 900°C for one hour.

For XRD, phase characterization of the samples was carried out using a diffractometer (Bruker AXS D8 Discover) in a Bragg–Brentano θ–2θ configuration, with a Cu Kα source (1.5418 A), over a θ–2θ angular range of 10°– 60°.

4.2 Characterization of Viking residual char

4.2.1 SEM imaging of char particles

SEM images of the Viking residual char showed that the TwoStage thermal treatment leaves the original wood structure largely unaltered. A few examples of SEM images are shown in Figure 4.3 (a,b,c). The typical structure of softwood, as described by Parham and Gray [9] can be easily distinguished. Longitudinal wood cells, or tracheids, are visible in radial and transversal sections (Figure 4.3a and 4.3b). Ray cells, which grow orthogonally to the tracheids, are visible in Figure 4.3c. Pits on the cellular walls are also clearly noticeable: in wood they provide lateral communication among longitudinal cells.

While observing Viking char samples, mineral species could be easily detected because of their lighter color, which stood out against the darker carbon-rich phase. White particles of inorganic material can be seen, especially in the tracheid walls and on the border of pits (Figure 4.3a and 4.3c). Figure 4.4 shows a variety of spherical and irregular particles of inorganic material: some of them were not deposited on char particles but constituted the loose powder fraction of char. In the char particles originating from wood bark, shown in Figure 4.5, crystals in form of parallelepipeds are clearly visible embedded in a disordered structure, without directional fibers. Similar particles have been identified as crystalline phases of calcium carbonate, derived from the thermal degradation of calcium oxalate [10]. The presence of minerals in different phases is a consequence of the high-temperature TwoStage process, which can cause the degradation and agglomeration of inorganic elements present in wood. Indeed, during pyrolysis and gasification, a major fraction of the inorganic elements are retained and concentrated in the solid product [11,12].

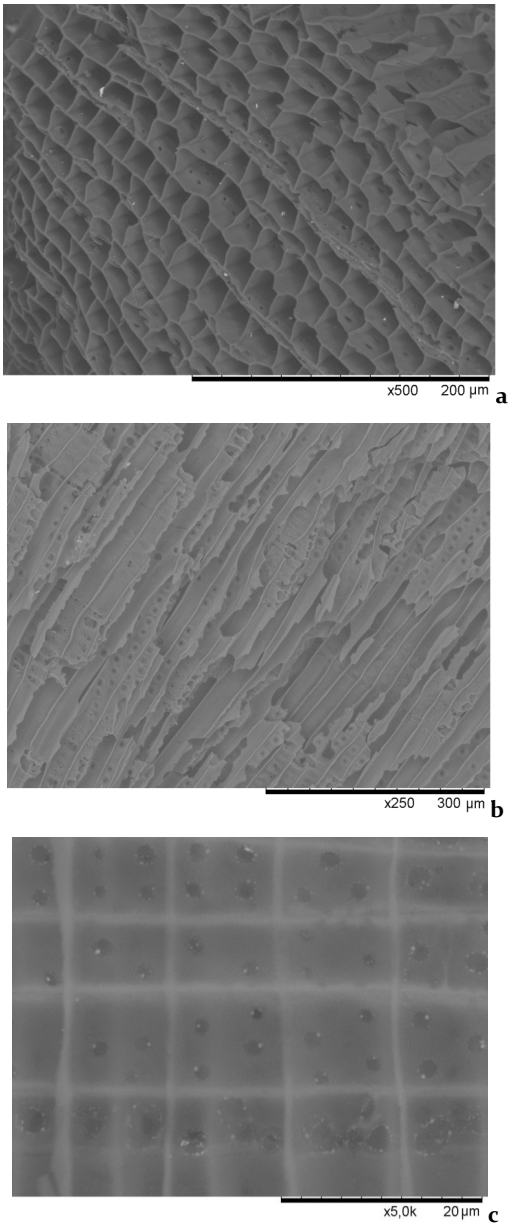

Figure 4.3: *Softwood cellular structure visible in biochar particles in transversal (a) and radial (b,c) directions. Ray cells are visible in (c).*

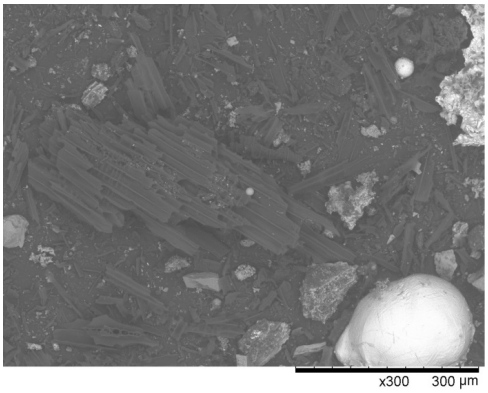

Figure 4.4: *Char and mineral particles found in Viking residual char*

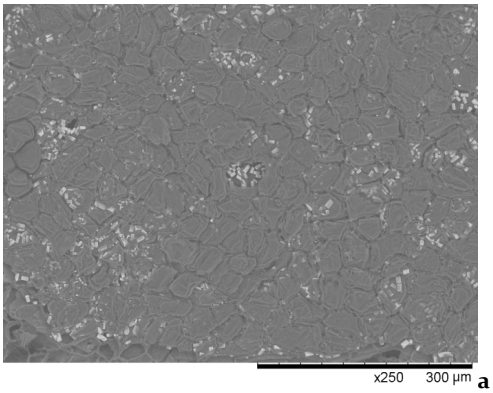

Figure 4.5: SEM images of char particles derived from wood bark, with calcium-containing crystals

The composition of the inorganic fraction of Viking char was determined by ICP-OES analysis, described later in this chapter. However, the SEM observations were useful to visualize the microscopic structure of char, revealing a very open and porous surface, with a heterogeneous distribution of minerals in various phases. Both these features are positive in view of a possible use of this material for catalytic processes.

4.2.2 Particle size distribution and surface area measurements

The particle size distribution presented in Figure 4.6 shows that about 60% of the particles in the Viking char could not pass through the 1 mm sieve. This is a positive feature in view of using this char as a fixed bed material, because a large amount of fine particles could cause an excessive pressure drop through the bed. However, a certain amount of particles smaller than 0.5 mm are present in the char.

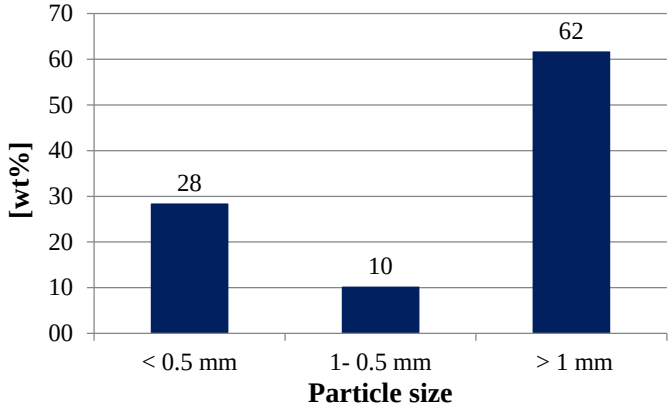

Figure 4.6: *Particle size classes obtained with 1 mm and 0.5 mm sieves*

Figure 4.7 compares the isotherms obtained with N_2 adsorption and desorption at 77 K on samples from different size fractions. The fraction of char with particles larger than 1 mm had a significantly higher specific surface area (1126 m^2/g) in comparison with the powder fraction smaller than 0.5 mm (495 m^2/g). The lower specific surface area is probably a consequence of the fact that the powder fraction also contains loose mineral species alongside char particles. However, the BET measurement on the full Viking char sample (not sieved) revealed a surface area of 1030 m^2/g. Note that the measurement was repeated on the batch of Viking char that was used in the laboratory tests as bed material, and the

surface area resulted to be even higher (1253 m^2/g). In comparison with chars derived from other gasification technologies, this char has a particularly large specific surface area, probably as a consequence of the gradual carbonization process divided into stages [13].

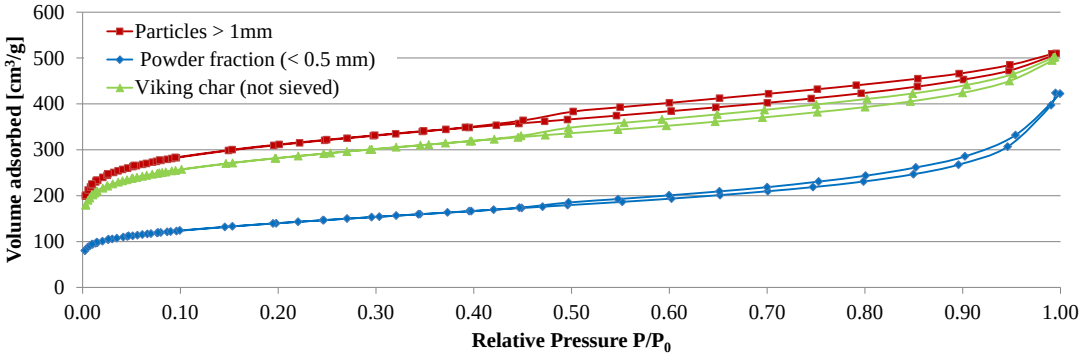

Figure 4.7: *Adsorption and desorption isotherms (obtained with N_2 adsorption at 77 K) for different size fractions of Viking char.*

4.3 Comparison of composition results obtained from spruce wood chips and Viking char

Results from the proximate analysis are showed in Figure 4.8. The difference in the content of volatiles between the wood and char sample is an obvious consequence of the carbonization process. The ash content derived by incineration at 550°C was higher than the one obtained at 815°C, and the difference is especially visible on the char samples. The discrepancy is caused by the fact that at the higher temperature some of the inorganics contained in the ash fraction can also be volatilized. The ash content obtained by incineration at 550°C was considered more reliable. Considering the change in the composition, it can be estimated that the burn-off of the char was about 95%.

Table 4.2 reports the results of the elemental analysis on the Viking char and the wood samples. The elemental composition of the residual char is reported in Paper II, but it is also shown here for the sake of comparison with the composition of the gasifier feed.

Table 4.3 shows the complete results obtained through ICP-OES analysis on the Viking char. Some of the results are already reported in Paper II, but here the full set of detected elements is reported. The most abundant elements were Ca, K and Mg, but traces of other metallic species such as Fe, Mn and Al were also detected.

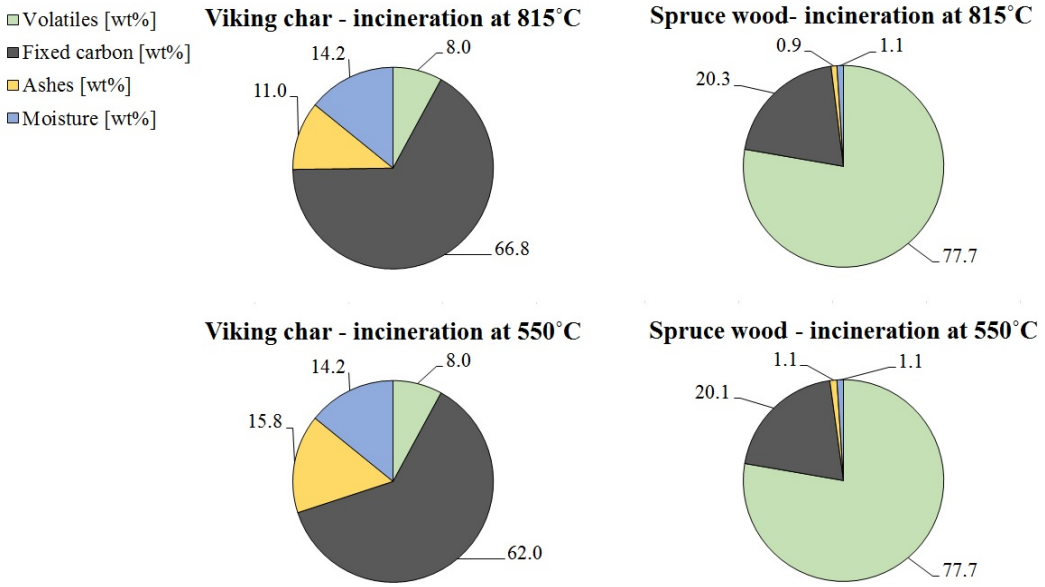

Figure 4.8: *Overview of proximate composition of spruce wood chips (Viking feed) and Viking char*

Table 4.2: *Elemental composition results obtained from spruce wood chips (Viking feed) and Viking char*

	C	H	N	S
Spruce wood [wt%]	53.8	4.9	0.1	0.06
Viking char [wt%]	87.6	0.6	0.1	0.04

Table 4.3: *ICP OES results obtained from Viking char. Cd and Pb were below the detection limit.*

	[wt%]		[wt%]		[wt%]
Al	0.024	**Fe**	0.089	**Ni**	7E-04
Ba	0.026	**K**	2.070	**P**	0.124
Ca	2.092	**Li**	4E-05	**Pb**	-
Cd	-	**Mg**	0.205	**S**	0.081
Cr	0.002	**Mn**	0.047	**V**	7E-05

4.4 Structural evolution of char within the TwoStage process

Figure 4.9 shows the isotherm curves obtained with N_2 adsorption and desorption at 77 K. The graph in Figure 4.10 shows the evolution of the BET surface area and DFT pore volume, following the progress of pyrolysis and gasification inside the Viking gasifier. It is interesting to notice that even the char sample extracted near the inlet of the pyrolysis stage (Pyrolysis 5) has a relatively high surface area (200 m^2/g).

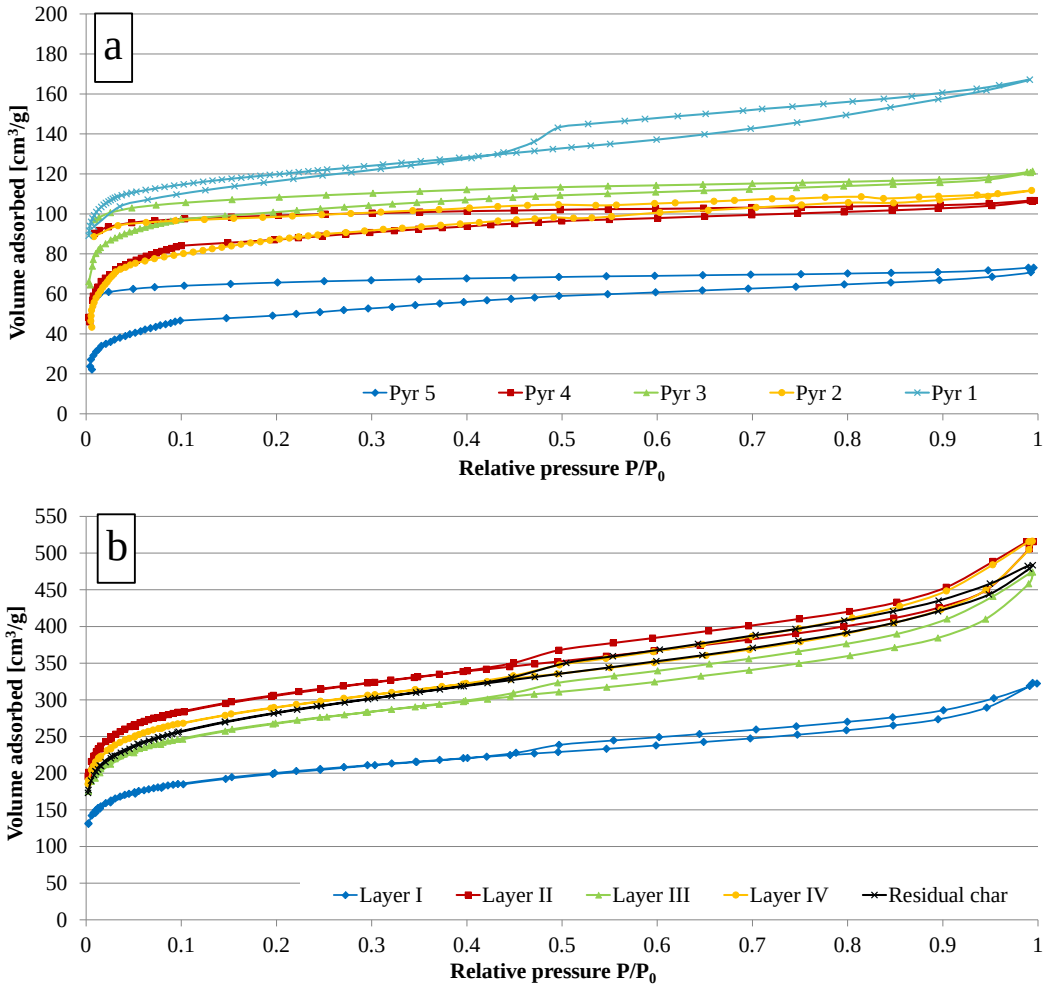

Figure 4.9: *Plot of the isotherms obtained from N_2 adsorption and desorption (77 K). Samples from pyrolysis stage (a) and from the char bed (b).*

The progression of pyrolysis induces an increase in the surface area and in the pore volume, but the increase becomes much steeper for samples at the end of the pyrolysis stage (Pyrolysis 2 and 1) and the samples from the top of char bed. The steep increase is due to the severity of the reaction conditions in this area of the gasifier, where the temperature exceeds 1100°C.

Samples taken from the char bed maintain a very high surface area, due to the gasification reactions taking place within the bed. The simultaneous deposition of carbon from tar cracking and the extensive steam reforming reactions supported by the high temperature in the bed (close to 800°C) are able to maintain the porosity of the material all the way down the grate. The evolution of the surface structure of wood char inside this gasifier is very much similar to an activation process.

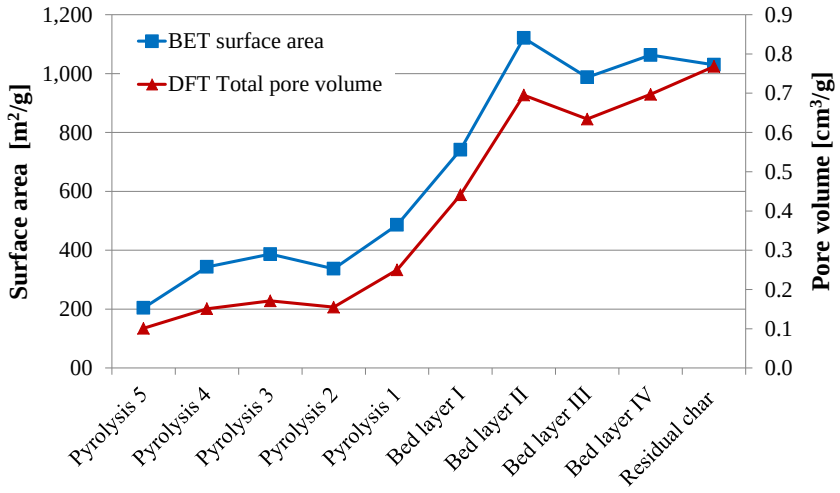

Figure 4.10: *Evolution of BET surface area and DFT pore volume following the progression of TwoStage gasification in the Viking gasifier*

The "activation" of char can be visualized in detail by looking at the evolution of the volume contained in the micropores and in small mesopores. The evolution of the pore volume divided by the pore size is showed in Figure 4.11a and 4.11b.

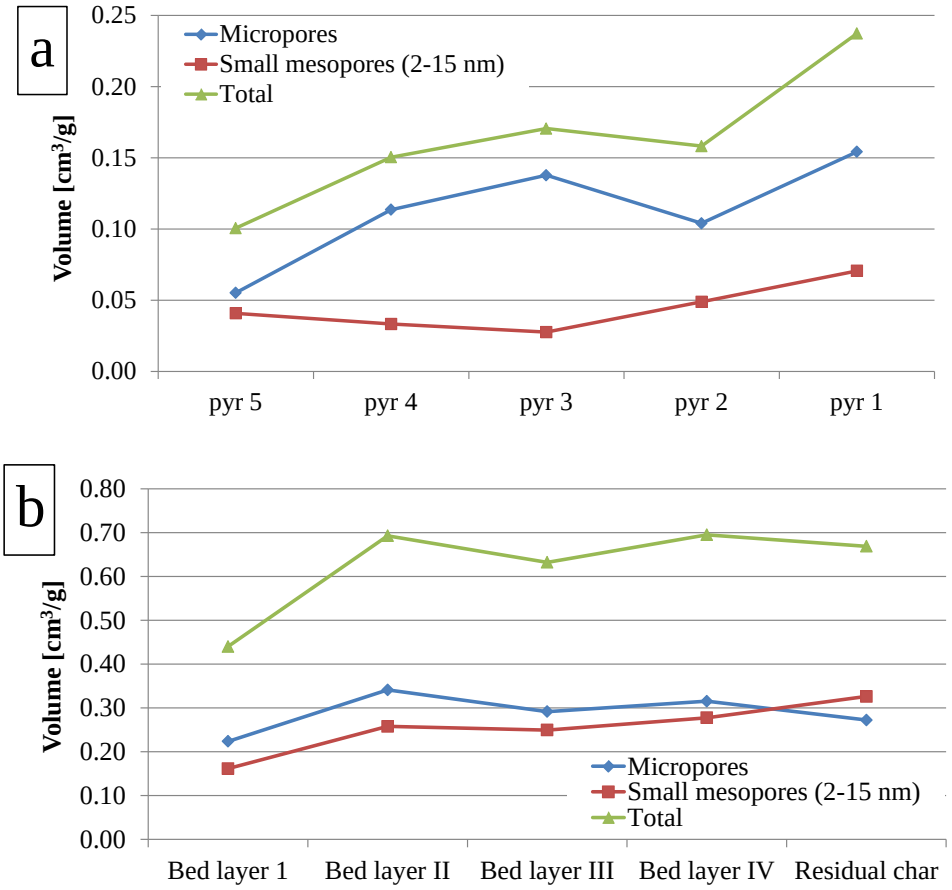

Figure 4.11: *Evolution of pore volume in samples from the pyrolysis stage (a) and from the char bed (b)*

Again, the most dramatic increase in both the micropore and small mesopores volume happens in the hottest zone of the gasifier. This effect is not only due to the temperature itself, but also to the presence of steam which is generated in the drying stage and carried along in the gas flow. In the char bed, further reforming reactions at the surface of char cause the collapsing of micropores into larger pores. The affect is visible also in the surface area distribution showed in Figure 4.12a and 4.12b.

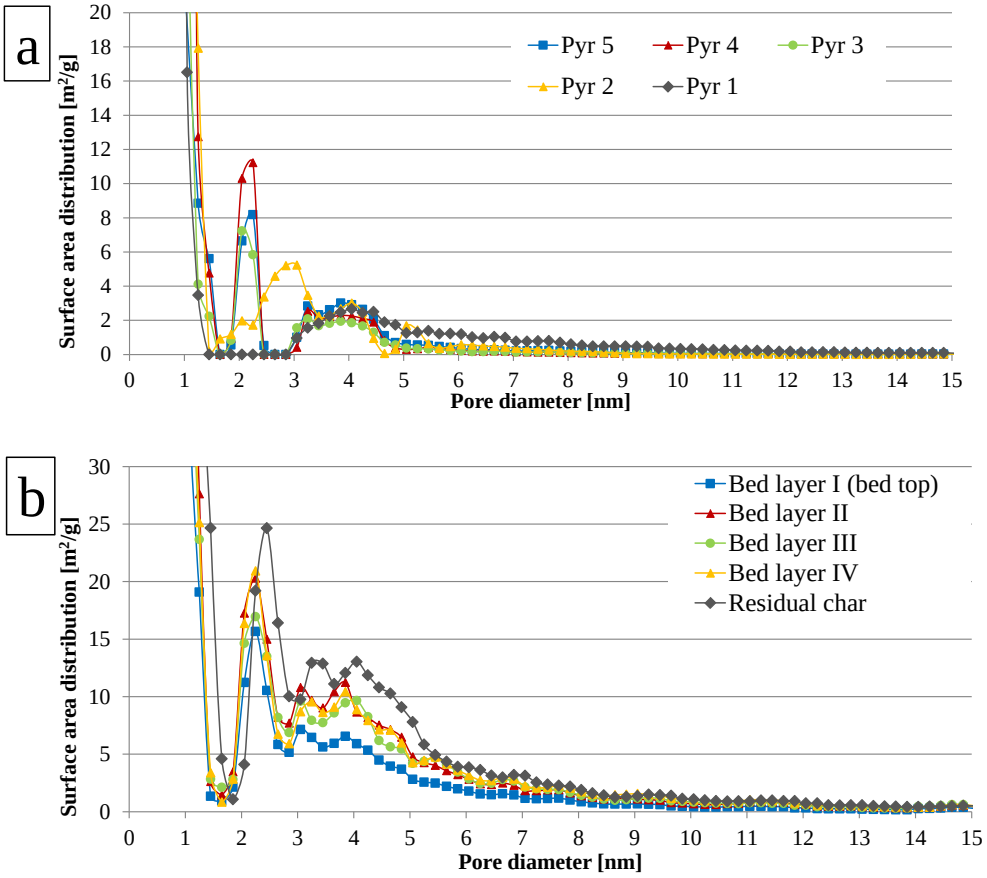

Figure 4.12: *Surface area distribution in the small mesopores range (2 to 15 nm) for (a) pyrolysis stage samples and (b) char bed samples.*

Progressing into the pyrolysis stage, micropores are formed, while pores with a diameter around 2 nm are gradually eliminated. In the gasification stage, the surface area in the range of small mesopores is gradually increased while the char is moved down towards the grate. This final part of the "activation" is responsible for the wide pore size distribution that is measured on the residual Viking char.

4.5 Additional analyses of Viking char samples used for gas upgrading tests

A sieved fraction (>3.15 mm) of Viking char was used in gas upgrading tests on real producer gas. After each test, the spent bed material was collected from the reactor and analyzed. The operating conditions are summarized in Table 4.4.

Table 4.4: *Overview of experimental conditions for the gas upgrading tests*

	Test duration [min]	**Air excess ratio (λ)**	**Max bed temperature** [°C]	**Bed weight loss** [wt%]
Thermal Reforming (TR)	122	0	795	9
Partial oxidation 1 (PO1)	110	0.2	830	-2
Partial oxidation 2 PO2)	302	0.5	855	-32

The results of the elemental analysis and surface characterization (N_2 adsorption at 77 K) of these samples are reported and discussed in Paper III. Additional TGA and XRD analysis confirmed the structural changes caused by the reforming of tar taking place at the surface of char.

The XRD pattern for the fresh char and the spent samples are plotted in Figure 4.13. The patterns clearly shows that the surface of samples includes mainly an amorphous carbon phase (reflection 002 and 001), identified by the broad peaks approximately at 24.4° and 43.5°. Fresh char showed the broadest peaks, while the three spent samples exhibited sharper peaks. The difference in the peak shape suggests that the carbon in the spent samples has a more ordered phase in comparison with the fresh sample. The change in the crystalline structure could be caused by the deposition of solid carbon on the surface of char during the gas upgrading tests. The diffraction pattern also shows minor peaks related with various calcium oxides; in particular lime (CaCO), calcite ($CaCO_3$) and portlandite ($Ca(OH)_2$). This was not unexpected, considering the large amount of Ca detected by ICP-OES. The diffraction pattern generated by the Viking char samples were similar to those found on residual gasification char in Benedetti et al. [14]. These peaks are more evident in spent samples. This effect could be an effect of the migration of alkali and other inorganic species towards the surface of char. This phenomenon has been reported when char is subject to gasification at high temperature (800-1000°C)[15].

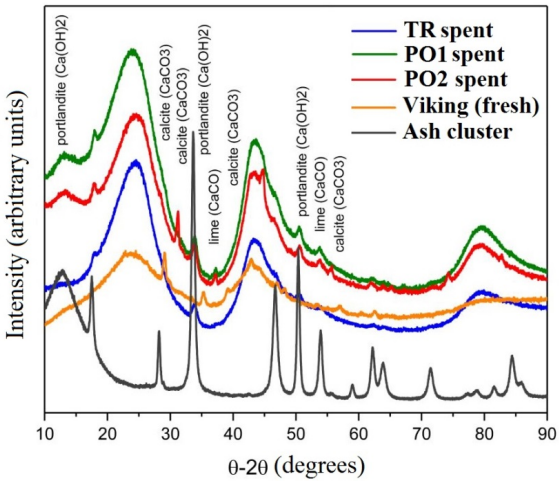

Figure 4.13: *XRD patterns from fresh and spent char samples*

The presence of clusters of unidentified origin in the spent char beds has been mentioned in Paper III. XRD analysis was also performed on one of the white clusters collected after the PO1 test. Similar agglomerates where also found after test PO2. The XRD pattern showed that the cluster contained more crystalline phases of the same Ca-containing compounds also detected in the char samples. It can be inferred that the cluster resulted from agglomeration of ash forming elements, and Ca in particular. These results support the hypothesis that oxygen reacted with inorganic species to form solid oxides during the gas upgrading tests.

The TGA analysis of fresh and spent samples in air and nitrogen revealed a different behavior of the spent samples in comparison with fresh char. Figure 4. 14 shows the mass loss curves in air atmosphere, while Table 4.5 collects the initial mass loss temperatures and the ash residue at the end of the test.

Table 4.5: *Results from TGA analysis in synthetic air atmosphere*

TGA, air	Mass loss onset temperature [°C]	Ash residue [wt%]
Viking fresh	526.5	4.4
TR	605	3.5
PO1	587	3.3
PO2	564	5.0

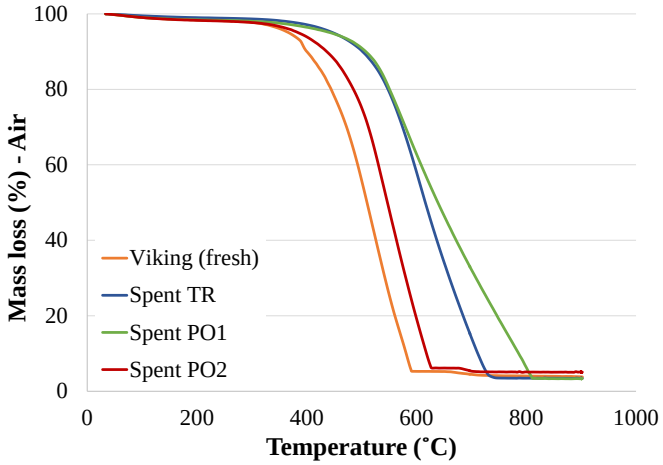

Figure 4.14: *Mass loss curves in synthetic air atmosphere*

Thermal degradation followed a similar trend for all samples. A small loss was observed a around 100°C due to moisture evaporation, followed by a greater mass loss (approx. 80-90 %) around 600°C, when CO_2 leaves the system. The mass loss curves in N_2 atmosphere are shown in Figure 4.15.

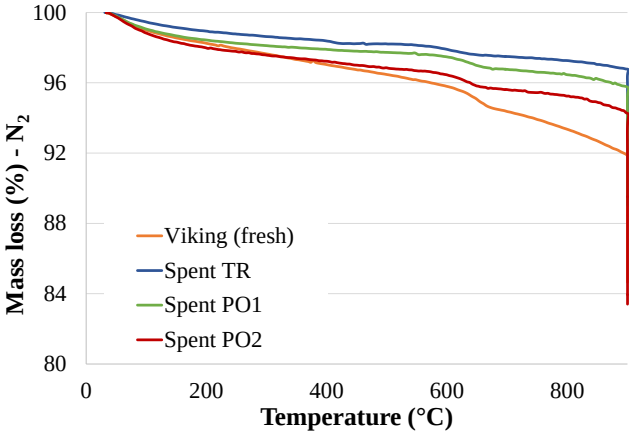

Figure 4.15: *Mass loss curves in nitrogen atmosphere*

Under these conditions, the maximum weight loss temperatures for the Viking fresh char, spent chars TR, PO1 and PO2 were 651°C, 604°C, 645°C and 640°C, respectively. The total mass loss was highest of the fresh Viking char (15.3%) whereas the lowest mass loss was seen in the TR spent char (6.4%).

Overall, spent samples exhibited a higher resilience to mass degradation in both N_2 and air atmosphere. The higher thermal stability of spent samples is in agreement with the increased crystalline order of the spent chars detected with XRD. Indeed, more ordered carbon such as graphitized carbon is less reactive in comparison with disordered, amorphous carbon [2] .

Fresh and spent char samples were also analyzed to quantify the contamination of PAH species. The results of the toluene extractions showed that the content of PAH species in the fresh char can vary between 2 and 11 mg/Kg. The variance might be due to local temperature differences inside the gasifier. However, values are well below the limits for soil applications. The PAH contamination limits recommended by the European Biochar Guidelines (EBC) [7] are 12 mg/Kg for basic quality grade biochar and 4 mg/Kg for premium grade.

Higher PAH levels are usually detected in chars derived from gasification processes [2,16]. The low level of contamination in the Viking char is a result of the efficient decomposition of aromatics in the partial oxidation zone and in the char bed. In addition, the solids are separated from the producer gas at a high temperature (750˚C), well above the condensation temperature of PAH species: in this way the risk of condensation on the char surface is minimized [4].

The results obtained from the spent samples show an even lower level of PAH contamination in comparison with the original char. In particular, no PAH species were extracted from the char sample collected after the PO2 test, which was the one performed with the longest duration (5 hours). An overview of the results, as received from the Eurofins laboratories, is given in Table 4.6.

The decrease in PAH release via toluene extraction can also be ascribed to the enhanced crystalline order of the char surface, which has the effect to increase the stability of the aromatic structures present on the surface of the char. However, it is important to mention that the method development for a safe determination of PAH contamination is still underway. Different methods from toluene extraction have been suggested [17]. Biological experiments, such as germination tests should be performed for a more reliable prediction of possible toxic effects.

Table 4.6: *Summary of results from Soxhlet extraction with toluene (as reported by Eurofins laboratories)*

	Viking fresh [mg/Kg]	**Viking fresh [mg/Kg]**	**Spent TR [mg/Kg]**	**Spent PO1 [mg/Kg]**	**Spent PO2 [mg/Kg]**
Naphthalene	8.2	0.6	1	0.5	< 0.1
Acenaphthylene	1.2	0.1	< 0.1	0.1	< 0.1
Acenaphthene	< 0.1	< 0.1	< 0.1	0.2	< 0.1
Fluorene	< 0.1	< 0.1	< 0.1	< 0.1	< 0.1
Phenanthrene	0.9	0.6	0.3	0.8	< 0.1
Anthracene	0.1	< 0.1	< 0.1	0.2	< 0.1
Fluoranthene	0.2	0.2	< 0.1	0.2	< 0.1
Pyrene	0.2	0.1	< 0.1	0.2	< 0.1
Benz(a)anthracene	< 0.1	< 0.1	< 0.1	0.1	< 0.1
Chrysene	< 0.1	< 0.1	< 0.1	0.2	< 0.1
Benzo(b)fluoranthene	< 0.1	< 0.1	< 0.1	< 0.1	< 0.1
Benzo(k)fluoranthene	< 0.1	< 0.1	< 0.1	< 0.1	< 0.1
Benzo(a)pyrene	< 0.1	< 0.1	< 0.1	< 0.1	< 0.1
Indeno(1,2,3-cd)pyrene	< 0.1	< 0.1	< 0.1	< 0.1	< 0.1
Dibenz(a,h)anthracene	< 0.1	< 0.1	< 0.1	< 0.1	< 0.1
Benzo(g,h,i)perylene	< 0.1	< 0.1	< 0.1	< 0.1	< 0.1
Total 16 EPA-PAH excl. LOQ	**10.8**	**1.6**	**1.3**	**2.5**	**(n. c.)**

4.6 Conclusions

The characterization of Viking char attested the promising properties of this material in view of its use as a catalyst or as an adsorbent. SEM imaging showed that the structural morphology of softwood was largely maintained in the char, while the inorganic ash fraction was distributed in different phases. The surface area measurements confirmed the very large specific surface area and pore volume of this material, in agreement with previous measurements [4].

The characterization of samples extracted at different locations inside the Viking gasifier shed light into the carbonization process taking place in the pyrolysis and gasification stages. The well-developed

porosity of the residual material is obtained thanks to a gradual pyrolysis, which alone generates char with a surface area close to 500 m^2/g. The high temperature, downdraft gasification finalizes the "activation" of the solids by increasing the micro- and mesopores volume of char and achieving a surface area over 1000 m^2/g.

Both the elemental analysis results, TGA, XRD and the PAH contamination assessment gave promising results in view of a possible end-life application of Viking char as biochar, even after being used for high temperature gas treatment of producer gas. Indeed, the carbon content of spent char samples was increased, due to solid carbon deposition during the decomposition of tar. Moreover, the carbon deposited on the surface appears to have a more ordered structure. The increasingly ordered structure explains the decreasing reactivity towards thermal degradation both in N_2 and air atmosphere. This is a positive feature in view of increasing the carbon stability and recalcitrance to respiration in soils. Indeed, the form of the carbon and its crystallinity is considered as a key factor determining the quality of biochar[18]. In particular, pyrolytic carbon and soot which are formed upon decomposition of tar on the surface of chars, are considered as a very stable carbon form [19].

It can be argued that the spent chars offer a much lower specific surface area in comparison with the fresh one. However, the measured values of spent chars are close to 300 m^2/g, still well above 100 m^2/g, which is the minimum recommended value for a good biochar performance in soil [2].

Finally, the decrease in PAH contamination on spent char samples suggests that they might be even safer for soil application than the original char. Overall, these results suggest the possibility to use similar high-temperature processes (for example reforming of pyrolysis oil) for improving the quality of biochar for soil application. A similar concept was proposed by Huang et al. [20]. Further tests and extended characterization of spent chars should be performed in order to verify this hypothesis.

Acknowledgements

The XRD analysis reported in this chapter were obtained in collaboration with Simone Sanna (DTU Energy). Thermogravimetric analysis of char samples was performed by Zsuzsa Sárossy (DTU, Chemical Engineering). BET and ICP-OES measurements were run at the Institute for Energy Technology at TU Berlin, with the help of Mrs. Susanne Hoffmann.

References

[1] Zhao L, Cao X, Mašek O, Zimmerman A. Heterogeneity of biochar properties as a function of feedstock sources and production temperatures. J Hazard Mater 2013;256–257:1–9. doi:10.1016/j.jhazmat.2013.04.015.

[2] Schimmelpfennig S, Glaser B. One Step Forward toward Characterization: Some Important Material Properties to Distinguish Biochars. J Environ Qual 2012;32. doi:10.2134/jeq2011.0146.

[3] Lehmann J, Gaunt J, Rondon M. Bio-char sequestration in terrestrial ecosystems - A review. Mitig Adapt Strateg Glob Chang 2006;11:403–27. doi:10.1007/s11027-005-9006-5.

[4] Hansen V, Müller-Stöver D, Ahrenfeldt J, Holm JK, Henriksen UB, Hauggaard-Nielsen H. Gasification biochar as a valuable by-product for carbon sequestration and soil amendment. Biomass and Bioenergy 2015;72:300–8. doi:http://dx.doi.org/10.1016/j.biombioe.2014.10.013.

[5] Hansen V, Müller-Stöver D, Munkholm LJ, Peltre C, Hauggaard-Nielsen H, Jensen LS. The effect of straw and wood gasification biochar on carbon sequestration, selected soil fertility indicators and functional groups in soil: An incubation study. Geoderma 2016;269:99–107. doi:10.1016/j.geoderma.2016.01.033.

[6] Quantachrome Instruments - DFT Models n.d. http://www.quantachrome.com/technical/dft.html (accessed June 6, 2018).

[7] European Biochar Foundation (EBC), Arbaz S. Guidelines for a Sustainable Production of Biochar. Eur Biochar Found 2016. doi:10.13140/RG.2.1.4658.7043.

[8] EPA U. Substance Details - Polycyclic organic matter - 16-PAH n.d. https://iaspub.epa.gov/sor_internet/registry/substreg/substance/details.do?displayPopup=&id=6012.

[9] Parham RA, Gray RL. Formation and structure of Wood. In: Rowell R, editor. Chem. Solid Wood, Washington, DC: American Chemical Society; 1984, p. 3–56. doi:10.1021/cr9502357.

[10] Rees F, Watteau F, Mathieu S, Turpault M-P, Le Brech Y, Qiu R, et al. Metal Immobilization on Wood-Derived Biochars: Distribution and Reactivity of Carbonate Phases. J Environ Qual 2017;46:845. doi:10.2134/jeq2017.04.0152.

[11] Narayan V, Jensen PA, Henriksen UB, Egsgaard H, Nielsen RG, Glarborg P. Behavior of Alkali Metals and Ash in a Low-Temperature Circulating Fluidized Bed (LTCFB) Gasifier. Energy & Fuels 2016;30:1050–61. doi:10.1021/acs.energyfuels.5b02464.

[12] Wiinikka H, Johansson AC, Sandström L, Öhrman OGW. Fate of inorganic elements during fast pyrolysis of biomass in a cyclone reactor. Fuel 2017;203:537–47. doi:10.1016/j.fuel.2017.04.129.

[13] Benedetti V, Patuzzi F, Baratieri M. Gasification char as a potential substitute of activated carbon in adsorption applications. Energy Procedia 2016;00.

[14] Benedetti V, Patuzzi F, Baratieri M. Characterization of char from biomass gasification and its similarities with activated carbon in adsorption applications. Appl Energy 2017:1–8. doi:10.1016/j.apenergy.2017.08.076.

[15] Klinghoffer N, Castaldi MJ, Nzihou A. Catalyst Properties and Catalytic Performance of Char from Biomass Gasification. I&Ec 2012:13113–22. doi:10.1021/ie3014082.

[16] Basso D, Patuzzi F, Valentinuzzi F, Mimmo T, Tonon G, Baratieri M. Bioenergy and other high-value products to enhance soil fertility and mitigate climate change: the wood-up project on woody biomass gasification in south-tyrol, Copenhagen: Proceedings of 26th European Biomass Conference; 2018.

[17] Fabbri D, Rombolà AG, Torri C, Spokas KA. Determination of polycyclic aromatic hydrocarbons in biochar and biochar amended soil. J Anal Appl Pyrolysis 2013;103:60–7. doi:10.1016/j.jaap.2012.10.003.

[18] Brewer CE, Schmidt-Rohr K, Satrio JA, Brown RC. Characterization of Biochar from Fast Pyrolysis and Gasification Systems. Environ Prog Sustain Energy 2009;28:386–96. doi:DOI 10.1002/ep.

[19] Elmquist M, Cornelissen G, Kukulska Z, Gustafsson Ö. Distinct oxidative stabilities of char versus soot black carbon: Implications for quantification and environmental recalcitrance. Global Biogeochem Cycles 2006;20:1–11. doi:10.1029/2005GB002629.

[20] Huang Y, Kudo S, Masek O, Norinaga K, Hayashi JI. Simultaneous maximization of the char yield and volatility of oil from biomass pyrolysis. Energy & Fuels 2013;27:247–54. doi:10.1021/ef301366x.

Conclusion

This work was aimed at understanding and optimizing the use of char for the upgrading of producer gas. The objective was to investigate the interaction between the surface of char and tar species, in order to design and operate a char-based gas cleaning unit for the upgrading of the tar-rich gas generated in the LT-CFB gasifier.

The first part of the work was dedicated to reviewing the existing literature concerning the performance of carbonaceous materials for tar removal and conversion. The literature study showed that the use of char and active carbon for the treatment of producer gas is the focus of various active research groups. Several studies described the pattern of interaction between tar species and carbonaceous solids at high temperatures. The cracking of aromatics is supported by the contact with the surface of chars. Here, solid carbon is deposited as coke and H_2 gas is produced. In absence of a reforming agent which can participate in gasification reactions, coke deposition gradually deactivates the char surface. Despite the fact that the mechanism is qualitatively well described, it is difficult to quantitatively define and generalize the performance of carbonaceous surfaces. Indeed, the efficiency of char for tar cracking and reforming can differ significantly depending on several factors, as revealed by the literature study focused on actual pyrolysis and gasification derived tar. First and foremost, the characteristics of char vary on a broad spectrum, depending on the parent material and on the carbonization and activation conditions. Secondly, the extent of the achievable tar decomposition and its durability over time depends largely on the reaction conditions such as temperature and atmosphere composition.

In many cases, the use of carbonized solids for gas treatment is referred to as “adsorption” or “catalysis” without a univocal and clear rationale. With the aim to observe and distinguish the different modes of interaction between chars and aromatics, the experiments in the laboratory were planned to cover a broad temperature range, 250 to 800°C. The results, showed that the adsorption of aromatics on chars was efficient only at relatively low temperature (250°C). On the other hand, cracking of aromatics with production of hydrogen was observed starting from 600°C and became quantitatively significant at 800°C. Residual char from the Viking gasifier was compared with other wood-derived chars and commercial active carbon. In parallel with the adsorption and cracking tests, compositional and surface characterizations were performed on the tested materials. The results were useful to understand the

relationship between the properties of chars and their performance in the removal or conversion of aromatics. The performance of Viking char was comparable or superior to that of the other materials. In particular, the large specific surface area and the broad pore size distribution were found to be beneficial to achieve and maintain a high level of conversion of aromatic molecules over time. In general, results showed that the surface structure of chars plays an important role in their deactivation pathway when used as a support for cracking of aromatic molecules.

Following the laboratory-scale experiments, Viking residual char was applied to the treatment of actual producer gas generated by the 100 kW_{th} LT-CFB gasifier operated at DTU, Risø Campus. For this purpose, a char-based gas upgrading unit was designed and built. Char from the Viking gasifier was used as bed material inside the unit, which was also equipped with an air inlet for the partial oxidation of tar above the char bed. Online gas analysis and offline tar quantification were used to monitor the quality of the gas before and after the char-based treatment. During the tests, the unit was maintained at 800°C by electric heating, while a constant flow of tar-rich producer gas was passed through the unit. The effect of temperature was evaluated through a thermal cracking test, with an empty reactor and no air injection. In the following tests, the reactor was loaded with a char bed of about 300 g. Its performance was evaluated at three different air excess ratios: $\lambda = 0$, $\lambda = 0.2$ and $\lambda = 0.5$.

The presence of the char bed inside the reactor had a significant effect on the composition of the gas phase and on the tar content. In all the tests when the reactor was loaded with char, the H_2 content at the outlet more than doubled in comparison with the producer gas original composition. The extent of tar removal was close to 100%. The highest tar conversion (98%) was achieved in the test with $\lambda = 0$. However, in these conditions surface deactivation of char was observed. This caused the tar concentration to increase over time in the product gas at the outlet of the unit, in particular naphthalene and anthracene. At the same time, the H_2 concentration was declining.

The injection of air facilitated the decomposition of tar and prevented the deactivation of the char bed. With $\lambda = 0.2$, deactivation progressed at a lower rate. When the air flow was increased to attain $\lambda = 0.5$, deactivation was not observed. The unit was operated continuously for a 5 hours long experiment, after which the gas upgrading unit was still delivering a constant H_2 production and extensive tar conversion (97%). These operating conditions delivered the best results in terms of stability of the gas quality. The reforming of tar generated H_2 and CO and improved the quality of the product gas. Steam reforming

reactions were favored by partial oxidation, mostly as a result of an increased temperature inside the reactor. Char itself participated in reforming reactions, but was consumed at a slow rate: after the tests most of the bed material could be recovered, even after 5 hours of operation.

The mass and energy balance calculations performed for all experiments showed that the temperature in the partial oxidation zone and in the char bed was affected significantly by the heat losses upstream of the unit. The temperature of the producer gas at the inlet of the reactor was as low as 300°C, and air was not pre-heated before injection. The relatively low temperature of the inlet flows limited the temperature increase induced by partial oxidation. These considerations suggested that the unit could be improved my limiting the heat losses. In this way, optimal efficiency in gas upgrading could be achieved by using an excess air ratio lower than 0.5.

The recovered, spent chars were characterized with various techniques and compared with the original Viking char. The aim of the analyses was to verify the modifications induced by the contact with the hot gas and to investigate the causes of deactivation. In this sense, the decreased surface area and porosity confirmed the same deactivation mechanism that was described in literature and observed in the laboratory experiments.

Furthermore, the spent materials were preliminarily evaluated in view of a potential application on soils as biochar. This was done to explore the possibility to use the Viking char, even after its application to hot gas cleaning, as biochar with a potential carbon-sequestration effect. This end-life utilization was deemed positive for the overall carbon balance of the system, possibly making it negative. The results obtained from spent char samples were encouraging. In comparison with the original material, spent char samples were found to have an increased content of carbon, an increased stability to thermal degradation and even a lower toxic contamination by PAH species, well within the limits for premium-grade biochar. This interesting outcome suggested an alternative application for the gas upgrading unit: a similar high temperature treatment could be developed with the purpose to upgrade low-quality biochar.

The results confirmed and improved the knowledge of the surface features of wood char produced in the Viking gasifier. Analyses were also conducted on the feed material (spruce wood chips) and on char samples extracted at different locations inside the gasifier. The results allowed the visualization of the structural evolution of the solids in the stages of the process.

In conclusion, promising results were obtained when applying residual gasification char to tar conversion and producer gas upgrading. The experiments with the gas-upgrading demonstration unit were useful to indicate possible improvements in view of an upscaling of the gas treatment system.

While the overall outcome of this study was undoubtedly positive, further work could be done to gain deeper insights. Future experiments with the gas upgrading unit should test different operating conditions. For example, in order to limit the N_2 content of the product gas, air could be substituted with CO_2-diluted oxygen. The unit could also be used to evaluate the performance of other residual chars, such as the one generated by the LT-CFB or other gasification platforms. Furthermore, additional gas analysis techniques should be applied to verify the effect of the gas upgrading unit on contaminants such as sulfur compounds (H_2S, SO_2), ammonia (NH_3) and chlorine compounds (CH_3Cl, HCl).

The carbon sequestration potential of char should be considered as a mean of reducing the net carbon emissions of the system. Additional evaluation of biochar characteristics of residual gasification char should be performed, possibly including biological analyses such as germination and microbial tests. Furthermore, alternative uses of residual chars for the production of carbon-based materials could be explored.

Finally, the properties of residual gasification chars should be further investigated also in relation to other gasification technologies. The char generated in the Viking demonstration plant was the main focus of this study. The remarkable structural and chemical features of this specific material led to promising results in the tested application for conversion of tar, and other possible applications can be envisioned as well. This work gives evidence that, through sensible process design and technical wisdom, gasification plants can generate a high-quality solid residue with several options for being commercialized and valorized.

Appendix I

Gas analysis methods: sampling, quantification and analysis

The following description reviews the sampling and analytical methods that have been applied for the quantification and analysis of tar and for the measurement of the water content in producer gas. These methods have also been described as part of the guideline report "Gas analysis in gasification of biomass and waste", compiled by International Energy Agency (IEA) -Task 33 and published in 2018 [1]. In addition, two video tutorials have been produced and are available online [2,3].

The first two sections describe the tar quantification and analysis through Solid Phase Adsorption (SPA) and Petersen column sampling. In the frame of this work, these methods have been used in the preliminary experimental activity with tar model compounds (described in the second chapter, section 2.1), as well as during the experimental campaigns at the 100 kW_{th} LT-CFB gasifier described in the third chapter of the thesis. Details are also given about of the analysis with Gas Chromatography coupled with Mass Spectrometry (GC-MS) and the quantification of compounds with deuterated standards. The description of the condensation method for total tar and water content assessment has been adapted from the MSc thesis by Claus Dalsgaard Jensen [4], who also operated the sampling device and kindly supplied the results of his measurements.

A.1 Solid Phase Adsorption (SPA)

The solid Phase Adsorption (SPA) method for tar analysis was first proposed by Brage et al. [5]. This method is generally considered as a convenient way to quantify tar and evaluate its composition. The producer gas generated by the 100 kW_{th} LT-CFB gasifier is characterized by a high tar load and SPA was not reliable to quantify the total tar concentration. Condensation methods were rather adopted for this purpose. However, SPA measurements were used to evaluate the composition of the tar mixture, in particular to detect and quantify heavy tar components in the gas, such as Polycyclic Aromatic Hydrocarbon (PAH) species. The SPA measurement includes three phases: sampling, processing of samples and GC-MS analysis.

A.1.1 Sampling

Gas samples were extracted manually, with a 100 ml syringe (PIC, Italy) assembled to a 15 cm long needle (Percutaneous Entry Thinwall needle SDN-18-15.0, Cook Medical, USA). The SPA cartridge (Supelclean LC-NH2 SPE tubes, 1 ml, Supelco/Sigma Aldrich, Germany) was connected to the syringe by means of silicon tube, as shown in Figure A.2. To facilitate the assembling with the syringe, the SPA tubes were cut, as shown in Figure A.1.

Figure A.1: LC-NH2 *tubes*

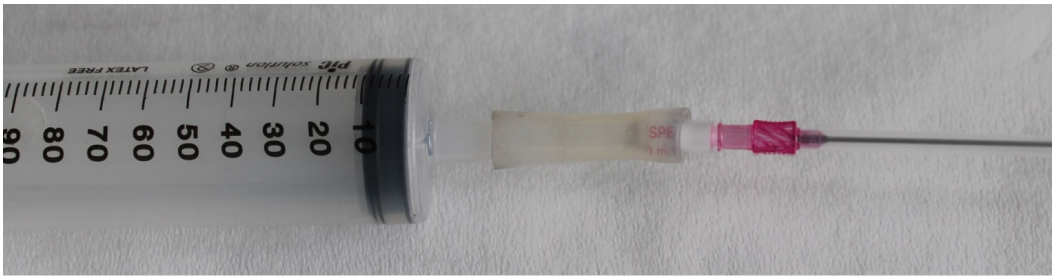

Figure A.2: *Assembled SPA sampling syringe*

The gas sample was extracted through a port mounted on the gas pipe. The port was equipped with a valve and a silicon septum, as shown in Figure A.3. The needle could be inserted in the septum, until its tip was positioned as close as possible to the center of the gas flow. The syringe was then gradually filled

with 100 ml of gas, by manually pulling the syringe piston. Once sampling was finished, the port was closed, and the SPA tube was stored in an air-tight bag. Samples were stored in the refrigerator until further processing.

Figure A.3: *Example of gas port with silicon septum for SPA sampling*

A.1.2 Sample processing

Prior to analysis, it was necessary to desorb the SPA sample into a solution, which could be injected into the GC-MS instrument. The cartridge was first removed from the plastic tube and was transferred into a glass vial of 25 ml. The sample was then covered with about 10 ml of clean, analytical grade acetone (purity 99.8%, Merck, Germany). At this stage, deuterated species were added to the sample in known amounts (i.e. 1 ml of standard solution), as internal standards for quantification. The standard solutions had been previously prepared in 100 ml volumetric glass flasks. About 20 mg of deuterated compound (eg. phenol d6, naphthalene d8) were added to the flask, and the exact weight was noted down. The flask was then filled to 100 ml with pure acetone. After the addition of standards, the vial containing the SPA sample was manually shaken before being stored overnight in the refrigerator. The following day, the liquid sample was transferred to a pear-shaped flask and evaporated completely with a rotary evaporator (Rotavap, Buchi, Switzerland). The sample was then re-dissolved in 1 ml of acetone and transferred to a 2 ml brown vial, suitable for the GC-MS auto-sampler.

A.1.3 Analysis

The samples were analyzed by GC-MS using an Agilent 7890B gas chromatograph interfaced to an Agilent 5977B Mass Selective Detector (Agilent, Denmark). Samples (1 µl) were injected in split mode (1:20). The source and rod temperatures were 230 °C and 150 °C, respectively. The products were separated using two HP-5ms ultra inert columns (15 m, 0.25 mm, 0.25 µm coating) (Agilent, Denmark). The carrier gas was He at a flow rate of 1.2 ml/min. Separation of products was achieved using a temperature program from 70 to 250 °C at 10 °C/min. The applied ionization energy was 70 eV. Full mass spectra were recorded every 0.3 s (mass range m/z 40–450). Products were identified using NIST search engine version 2.0 f. (Agilent, Denmark).

The quantification of the single compounds was performed by integrating the chromatogram peaks relative to the compound and to its labelled isotope. The ratio between the resulting peak areas was used to quantify the abundance of the original molecule, knowing the exact amount of label added to the sample.

A.2 Petersen column

The Petersen column for sampling of tar is considered as an alternative to the use of 6 impinger bottles, according to the tar protocol [6]. In this work, the Petersen column method has been used to quantify the total gravimetric tar. As for SPA, the measurement included three phases: sampling, sample processing and analysis.

A.2.1 Sampling

The Petersen column assembly is shown in Figure A.4. The column was connected to a cooling system for the jacket refrigeration of the two stages. A gas pump was connected downstream of the pump, to draw the gas through the washing stages. In addition, a gas meter was connected at the outlet of the system, to measure the volumetric flow of gas through the column during sampling (See Figure A.4).

Figure A.4: *Petersen column setup arranged for sampling at the 100kWth LT-CFB gasifier*

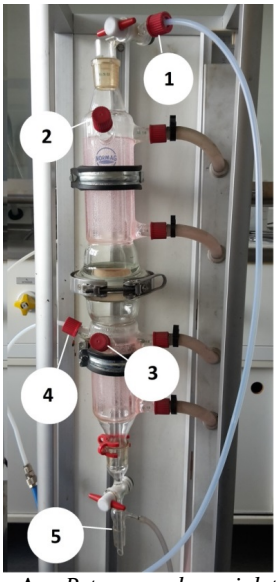

Figure A.5: *Petersen column inlets and outlets*

Before operation, the column was refrigerated. 150 ml of acetone were added to the upper stage, and 100 ml to the lower stage (through openings (2) and (3) in Figure A. 5). The pump was connected to the column outlet (1). The flow through the column was initiated by starting the gas pump. The gas entered through the column inlet (4). The sampling duration was measured with a stop-watch. After about 30 minutes passed, the gas flow was interrupted. The sample was then recovered from the solvent drain (5), and collected in an Erlemeyer flask. Both stages and the sampling line were rinsed and the rinsing solvent was recovered with the rest of the sample. The sample was transferred to a brown glass bottle, stored in the refrigerator.

A.2.2 Sample processing for gravimetric tar determination

The liquid sample obtained with the Petersen column was first transferred to graduated cylinders to measure the total volume. Pear-shaped glass bottles, suitable for rotary evaporation, were carefully washed and dried. Empty, dry flasks were then weighed on an analytical scale. Two sub-samples of 25 ml were then transferred to pear shaped flasks for rotary evaporation. The solvent was completely evaporated and the flasks were then dried overnight in an oven at a temperature of about 70 °C. The residues left in the flasks after evaporation and drying were considered as gravimetric tar. Figure A.6 shows two flasks with Petersen colum tar samples from the LT-CFB gasifier.

Figure A.6: *Pear-shaped bottles after evaporation and drying of Petersen column sub-samples.*

A.2.3 Sample processing for tar composition analysis

Petersen column samples were also analyzed with GC-MS. A sub-sample was transferred to a 20 ml volumetric flask, together with a known amount of internal standard mix (i.e. 1 ml). About 2 ml of the solution was then transferred into a GC-MS vial. Volumetric flasks containing the sub-samples are showed in Figure A.7.

Figure A.7: *Tar samples obtained by sampling with Petersen column from gas with different tar concentration.*

A.2.4 Analysis

The GC-MS analysis was conducted with the same column and method as described for the SPA samples.

A.2.5 Tar analysis results comparison: GC-MS analysis on SPA and Petersen column samples

During the experimental campaign on the 100kWth LT-CFB gasifier in November 2017, both SPA and Petersen column were used to sample producer gas. Figure A. 8 shows the overlaid chromatograms obtained from a SPA and a Petersen column sample, taken at the same time during the gasifier operation. Note that the tallest peaks result from the internal standard addition in both samples.

The quantification results obtained from the two sampling techniques are very well in agreement for the quantified compounds. The main difference was observed for compounds with lower retention times such as furfurals and phenols. This class of compounds is better detectable in Petersen column samples, whereas SPA samples offer a better quantification of larger aromatics.

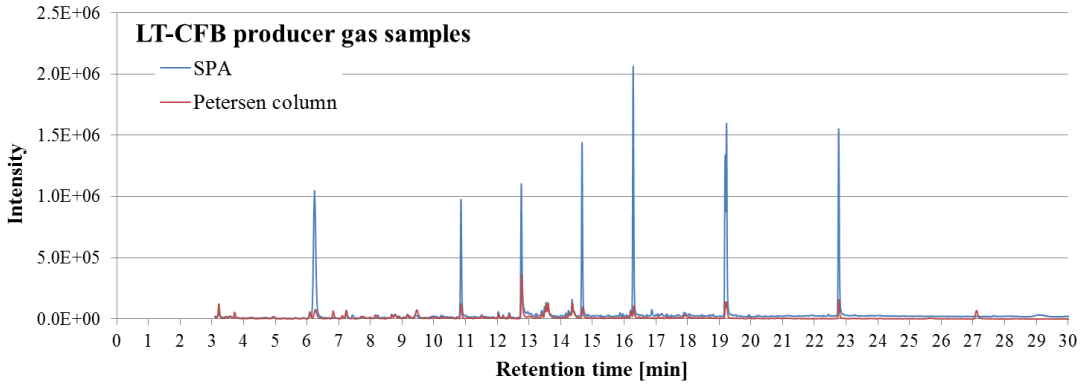

Figure A.8: *Chromatograms obtained from SPA and Petersen column samples*

A.3 Total tar and water content measurement with total tar condenser

The total tar content in the product gas can also be determined by condensation at room temperature. This technique is particularly suitable for measuring the tar content of tar-rich producer gas, and it can also be used to measure the water content in the gas. The condensation apparatus is schematized in Figure A.9.

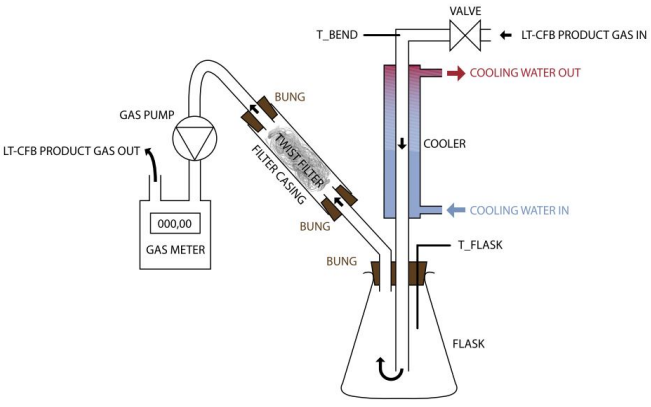

Figure A.9: *Diagram of the tar and water condensation setup [4,7]*

A.3.1 Sampling

The clean and dry setup for condensation was connected to a gas outlet on the main gas stream. As for the Petersen column, a gas pump was connected downstream to draw the gas through the system. The extracted gas was cooled by mean of a counter current water condenser. The total volume of sampled gas was measured through a gas meter at the outlet. Sampling was performed for 1 to 3 hours. Figure A.10 shows the setup arrangement during gas sampling.

Figure A.10: *Tar and water condensation setup*

A.3.2 Sample processing

The total condensate was determined by measuring the weight difference of the entire setup before and after sampling. The total condensate could be easily divided into a light and a heavy fraction. The light fraction was mainly made up by water, plus a relatively small amount of water-soluble tar. GC-MS analysis of this fraction showed the presence of phenol, cresol and xylenol and high amounts of methanol, acetone and acetic acid. The heavy fraction was thicker and darker and was mainly made up of insoluble organic compounds. The water content of both fractions was determined by Karl Fischer titration.

A.3.3 Total tar determination using Petersen column and total tar condenser – a comparison

During the gas sampling campaign carried out at the 100kWth LT-CFB gasifier at Risø Campus in November 2017, the total tar condenser has been used to sample producer gas in parallel with the Petersen column. Table A.1 reports the total or gravimetric tar measured on the same day with the two techniques.

Table A.1: *Comparison of total tar in producer gas obtained on the same day with Petersen column and total tar condenser.*

Sampling day	Petersen column [g/Nm^3]	Total tar condenser [g/Nm^3]	Water content wt% of tar
09-11-17	20.2	22.0	7.39
27-11-17	25.0	31.6	9.44
28-11-17	29.1	34.2	11.9

The results show the same trends, but the condensation unit gives higher values for the total tar in the producer gas. The total tar condenser provided a more reliable quantification of total tar concentration in the LT-CFB producer gas. However, the Petersen column is easier to connect to any given gas outlet, while the condensation unit requires more space and a specially designed producer gas outlet to function properly.

References

[1] IEA Bioenergy - Task 33. Gas analysis in gasification of biomass and waste - Guideline report. 2018.

[2] IEA Bioenergy Task 33. Gas analysis special report. Video blog 4, DTU SPA sampling n.d. https://www.youtube.com/watch?v=QV8gG-BoEKs (accessed November 17, 2018).

[3] IEA Bioenergy Task 33. Gas analysis special report. Video blog 5, DTU Petersen sampling n.d. https://www.youtube.com/watch?v=TVkVb5A2YOo (accessed November 17, 2018).

[4] Dalsgaard Jensen C. Characterization of product gas from gasification of straw in an LT-CFB gasifier for the catalytic conversion of tar to bio-oil. Technical University of Denmark, 2018.

[5] Brage C, Yu Q, Chen G, Sjöström K. Use of amino phase adsorbent for biomass tar sampling and separation. Fuel 1997;76:137–42. doi:10.1016/S0016-2361(96)00199-8.

[6] Good J, Ventress L, Knoef H, Group BT, Zielke U, Hansen PL, et al. Sampling and analysis of tar and particles in biomass producer gases - Technical Report. 2005.

[7] Thomsen TP, Sárossy Z, Gøbel B, Stoholm P, Ahrenfeldt J, Jappe F, et al. Low temperature circulating fluidized bed gasification and co-gasification of municipal sewage sludge . Part 1 : Process performance and gas product characterization. Waste Manag 2017;66:123–33. doi:10.1016/j.wasman.2017.04.028.

Appendix II

Collection of conference proceedings

- Ravenni G. Henriksen U.B., Ahrenfeldt J., Sárossy Z. "*Tar Removal from Biomass Producer Gas by Using Biochar*". Oral presentation. Proceedings 25th European Biomass Conference (EUBCE) 2017, Stockholm, Sweden
- Ravenni G., Sárossy Z., Ahrenfeldt J., Henriksen, U.B. "*Residual char from gasification integrated in a tar removal system*". Oral presentation. Proceedings of 26th European Biomass Conference (EUBCE) 2018, Copenhagen, Denmark
- Ravenni G., Elhami H.O., Neubauer Y., Ahrenfeldt J., Henriksen U.B. "*Comparison of wood chars from gasification and pyrolysis for adsorption and conversion of tar model compounds*". Oral presentation. Proceedings of the International conference in Engineering for Waste and Biomass valorization (WasteEng) 2018, Prague, Czech Republic

TAR REMOVAL FROM BIOMASS PRODUCER GAS BY USING BIOCHAR

Ravenni G., Henriksen U.B., Ahrenfeldt J., Sárossy Z.

grav@kt.dtu.dk, +4593511592

Technical University of Denmark (DTU), Department of Chemical and Biochemical Engineering
Frederiksborgvej 399, 4000 Roskilde, Denmark

ABSTRACT: The biomass-derived char (biochar) produced in the gasifier as a residue, is a potential solution for removing tars from producer gas. This work investigates the interaction between tar compounds and biochar. Residual biochar from a TwoStage gasifier was tested as bed material in a laboratory setup. Phenol and naphthalene were chosen as model tars, and entrained in a nitrogen flow. The gaseous stream was sampled before and after the biochar bed to evaluate the extent of conversion. The biochar bed (30g) was tested at 250˚C, 500˚C and 600˚C, with for 3 consecutive hours. The compounds concentration in the gas phase was quantified by stable isotope dilution analysis, using Gas Chromatography-Mass Spectrometry (GC-MS). Results showed a significant effect of biochar on the removal of phenol, at all temperatures. Naphthalene was removed less efficiently at higher temperature, and this trend was even more visible with a smaller char bed (17g). The characterization of the residual biochar from the TwoStage gasifier showed high carbon content and a specific surface area comparable with active carbon. Scanning Electron Microscopy revealed that the wood structure is largely maintained in the biochar particles, and the main inorganic components are calcium, potassium and silicon in form of oxides.
Keywords: gasification, gas cleaning, tar removal, biochar

1 INTRODUCTION

Removing tars from biomass derived producer gas is considered a major obstacle to the downstream processing of producer gas. An effective and economically viable solution is needed to pave the way for biofuel synthesis and several other applications. A potential solution for gas cleaning is the use of biomass-derived char (biochar), which is a by-product of gasification itself. Biochar usually has a lower surface area and adsorption capacity in comparison with activated carbons but shares some of their features. This is particularly true if the char undergoes a certain degree of gasification, which is analogous to an activation process. Biochar has a porous structure, it has a high specific surface area and it is generally rich in micropores. The biochar surface has oxygen-containing functional groups (acidic and basic) that can exert a great influence on the adsorption capacity[1], [2]. Moreover, the surface often contains minor elements such as Alkali and Alkaline Earth Metals (AAEM) that are able to catalyze reactions. For these reasons, gasification derived biochar offers a good adsorption capacity, together with a potential catalytic effect on tar cracking, and hence could be successfully applied to gas cleaning. In recent years, the application of non-activated carbonaceous material to gas treatment has been suggested and studied by several authors [3]–[7]. Biochar is continuously generated by the process. If used for removing tars, the problem of deactivation can be avoided by continuously recycling it into the system along with fresh feedstock.

The use of a char bed for gas conditioning has been implemented in the TwoStage gasification concept, developed at Technical University of Denmark (DTU) over several decades. In this process, pyrolysis and gasification are carried out in two separate reactors: after the pyrolysis step, the volatiles are partially combusted before contacting with the char bed where gasification takes place. A flow diagram of the TwoStage system is showed in Fig. 1. Further details about this gasification system can be found in [8]. The combination of partial oxidation and passage through the char bed generates a nearly tar-free gas. The “Viking” gasifier at DTU, Risø is a TwoStage gasification plant (80 kW_{th}) which has been operated for more than 3000 hours. During operation of the Viking gasifier, only 0.002-0.1 mg/Nm^3 of naphthalene could be detected in the gas[8]. Producer gas from the “Viking” gasifier has been applied to successfully to both gas engine operation and fuel cell stacks[9].

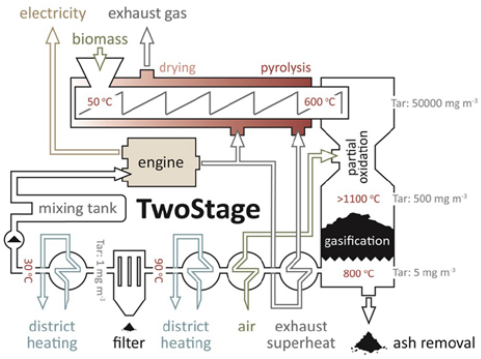

Figure 1: Schematic of the TwoStage gasification process

This work aims at understanding the role of the char bed in gas cleaning. The interaction between tar model compounds and the surface of biochar has been investigated in the experimental work here presented, focusing on phenol and naphthalene as representatives of different tar classes. At the same time, the residual char from the TwoStage gasifier has been characterized with different analytical methods to determine its characteristics and identify the reason of its efficacy in removal of tars.

2 MATERIALS AND METHODS

The laboratory setup for testing char bed interaction with tar model compounds is schematically presented in Fig. 2. A steady nitrogen flow of 1 l/min controlled by a high precision mass flow controller (MFC, Bronkhost) was passed through a tube coated with melted crystals of the compound (phenol or naphthalene): because of their relatively high vapor pressure, a significant amount of the compounds could be added to the flow. The gas enriched with model compound entered the oven where it was first preheated, then passed in a stainless steel (316L) reactor containing the biochar bed. The reactor had an internal diameter of 5.5cm and total height of 30cm. The char bed was supported by a stainless steel grate. A preheating pipe (0.25cm internal diameter, 220cm length) was coiled around the reactor body. The biochar used for all tests was recovered from the ash container of the TwoStage "Viking" gasifier at DTU, Risø Campus, which had been fed with spruce wood chips. The material was used for the tests without any further treatment. The concentration of the model compounds in the gas flow was measured before and after the passage through the bed by sampling with Solid Phase Adsorption (SPA) technique. SPA tubes were LC-NH_2 SPE tubes (Supelco, USA). Each sample was taken manually with a 100ml syringe. The gas quantity sampled varied among 100ml, 200ml and 300ml. In addition, the outlet gas flow was washed with acetone through a Petersen Column, to verify the results from the SPA measurements. The Column was filled with acetone in two washing stages, and its jacket was refrigerated for the whole duration of sampling. A single experiment was carried out for 60 minutes: during this time, 6 SPAs samples (3 at inlet and 3 at outlet) were collected after 20, 40 and 50 minutes from the start of the experiment. For the washing in the Petersen Column, 250ml of acetone was used and recovered for analysis after each experiment. The thermal decomposition of the model compounds was evaluated in 1 hour experiments with the empty reactor at 250˚C, 500˚C and 600˚C. When the reactor was filled with char, the same bed was tested in 3 consecutive experiments, maintaining a constant temperature (250˚C, 500˚C and 600˚C). Before the start of each experiment the setup was heated up until the temperature measure by thermocouples T2 and T3 was constant. Thermocouple 2 was placed about 1 cm below the surface of the char bed, while Thermocouple 3 measured the temperature beneath the grate holding the char bed.

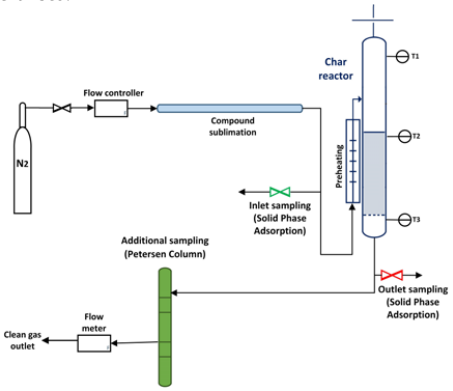

Figure 2: Laboratory setup with sampling system

The concentration of the model compounds in the gas flow was quantified by stable isotope dilution analysis, using labelled compounds (phenol d5, naphthalene d8) as tracers for the Gas Chromatography-Mass Spectrometry (GC-MS) analysis.
SPA cartridges were processed on the same day. The cartridges were covered with acetone and a known volume of standard solution containing labelled compounds. The samples were left desorbing overnight. Afterwards, the samples were concentrated to a volume of 1 ml and were analyzed with GC-MS. A known volume was taken out of the collected acetone samples from the Petersen Column and the appropriate labelled compound was added before GC-MS analysis. All samples were analyzed using a Hewlett Packard HP 6890 gas chromatograph interfaced to a HP5973 Mass Selective Detector (Agilent, Denmark). Samples (1µl) were injected in the split mode (1:20) using an HP 7683 autosampler (Agilent, Denmark). The source and rod temperatures were 230 ˚C and 150 ˚C, respectively. The products were separated using a 0.32mm i.d.x 30m WCOT-fused silica column coated with VF 23 ms with a thickness of 0.25 µm (Analytical, Denmark). The carrier gas was Helium with a flow rate of 1.2 ml/min. Separation of products was achieved using a temperature program from 70 to 250˚C at 10˚C / min.
The composition of the TwoStage residual biochar was evaluated through elemental analysis (VarioEL III, Elementar Analysensysteme GmbH, Germany) and proximate analysis. The specific surface area of the char was determined by the Brunauer-Emmett-Teller (BET) method by nitrogen gas sorption at 77 K (Nova 2200, Quantachrome instruments, USA). The surface of the char particles was analyzed by Scanning Electron Microscopy coupled with Energy Dispersive X-Ray Spectroscopy (SEM-EDS)(TM 3000, Hitachi, Japan). The particle size distribution of the residual char from the TwoStage gasifier was determined by manual sieving, using 1mm and 0.5mm sieves (Retsch, Germany).

3 RESULTS AND DISCUSSION

3.1 Char testing laboratory setup

The experimental conditions for all the tests run with the setup are reported in Table I.

Table I. Experimental conditions tested with the char bed setup

Model compound	Temperature (˚C)	Char bed (g)	Residence time (s)
Phenol	250	-	
Inlet	250	30	10.4
concentration:	500	-	
572 ± 110	500	30	7
mg/Nm^3	600	-	
	600	30	6.2
Naphthalene	250	-	
Inlet	250	30	10.4
concentration	600	-	
234 ± 37	600	30	6.2
mg/Nm^3	600	17	2.7

For both model tar compounds, the conversion X after the reactor was calculated as

$$X(\%) = ((C_{in} - C_{out})/C_{in})*100$$

where C_{in} is the concentration at the inlet and C_{out} is the concentration measured at the outlet of the reactor. Both measurements were taken with SPA. The Petersen Column measurements were used to validate the value of concentration obtained by SPA sampling. Overall, they were in good agreement with the average of the concentration values measured with SPA at the outlet of the reactor.

All the tests run using phenol as a model compound showed a positive effect of the char bed in cleaning the gas stream. The phenol conversion at 250˚C, 500˚C and 600˚C are showed in Fig. 3.

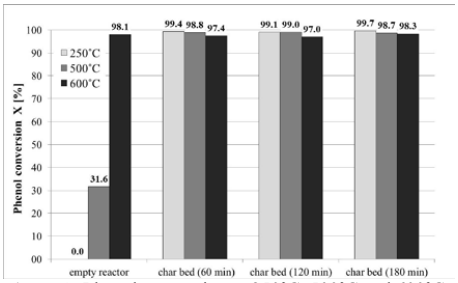

Figure 3: Phenol conversion at 250˚C, 500˚C and 600˚C

At 250˚C, the effect of the char bed is especially significant. The passage through the empty reactor left all the phenol unconverted, while in presence of biochar, virtually no phenol could be detected at the outlet. Similar results were found at 500˚C and 600˚C. However, at these higher temperatures, a certain degree of phenol decomposition was already observed with an empty reactor. The effect was particularly strong at 600˚C. The conversion of phenol in the empty reactor experiments was probably due to a catalytic effect of the material of the reactor (Stainless steel 316L). The effect of the char bed on the phenol in this temperature range is probably due to simple adsorption on the char surface, as the temperature is too low for chemisorption. For chemical bonding reactions to take place, higher temperatures are needed[10].

Results from the experiments carried out with naphthalene are showed in Fig. 4. No significant decomposition was observed after the passage through the empty reactor.

At 250˚C, the effect of the char bed was marked, as in presence of biochar no naphthalene was collected at the outlet. At 600˚C, with a residence time of 6.2s, the naphthalene conversion was not complete. It decreased from 95.4% to 86.6% during the three consecutive hours of experiment. When the residence time was reduced to 2.7s by using a smaller amount of char in the reactor, the effect was even more visible: in this case the conversion of naphthalene decreased from 92.8% to 81.6%. The diminished effect of the char bed on the removal of naphthalene validates the hypothesis that it is an adsorption process happening at the char surface: the higher temperature hinders adsorption, and at the same time it is not high enough for binding to take place between the compounds and the surface. Indeed, Egsgaard et al. [10], observed irreversible binding of aromatics to the char surface starting at 650˚C and becoming quantitatively significant only at 800˚C. Further experiments will investigate the char-tar interaction at higher temperatures.

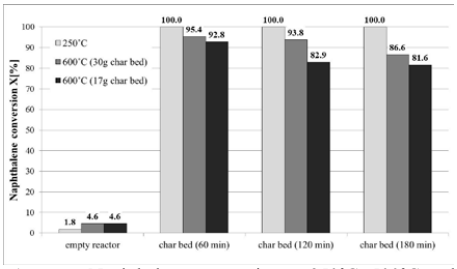

Figure 4: Naphthalene conversion at 250˚C, 500˚C and 600˚C

3.2 Characterization of Viking gasifier residual char

In order to understand the causes of the high effectiveness of the TwoStage gasifier in tar removal, the properties of the residual char have been investigated. The proximate composition and the elemental analysis results (C, H, N, S) are reported in Table II.

Table II. Proximate and elemental analysis results from residual TwoStage gasifier char

Proximate composition		
Volatiles (db%)	6.8	CEN/TS 15148
Fixed carbon (db%)	79.6	
Ashes (db%)	13.6	DIN EN 14775
Elemental composition		
C (wt%)	78.0	
H (wt%)	0.07	
N (wt%)	0.82	
S (wt%)	0.15	
Σ PAH (mg/Kg^{-1})	0.69	[11]

The chemical analysis showed a high carbon content in the in the gasification residues. The same material had been analyzed for Polycyclic Aromatic Hydrocarbons (PAHs) in a previous publication ([11]) and the total content of 9 different species (Acenaphthene, Fluorene, Phenanthrene, Fluoranthene, Pyrene, Benzo(bjk)fluoranthene, Benzo(a)pyrene, Indeno(1,2,3-cd)pyrene and Benzo(ghi)perylene) was found to be 0.69 mg/Kg^{-1}. The low content of PAHs is due to the separation of the solid residue from the producer gas at high temperature (750˚C) within the TwoStage process: no significant PAHs condensation is possible at such temperature, which is well above the PAHs dew point. The low PAHs content is also indicating that the aromatic molecules formed in the partial oxidation zone are decomposed in the char bed[11].

The biochar was divided in 3 particle size fractions by manual sieving, using 1mm and 0.5mm sieves (Retsch, Germany). The specific surface area measurements were performed on the original sample (non-sieved), on the particles larger than 1mm and on the powder fraction (> 0.5mm). Results are reported in Table III. Larger

particles have a larger surface area and pore volume in comparison with the powder fraction, which is richer in ash particles. The BET specific surface area of the residual biochar from the Viking gasifier (1030 m^2/g) is very high in comparison with other chars used in gas cleaning investigations ([4], [12], [13]) and is comparable with commercial activated carbons. Activated carbons have a surface area in the range of 500 to 2000 m^2/g, whereas their pore volume varies from 0.20 to 0.60 cm^3/g[14].

Table III. Results from BET measurements on different fractions of the TwoStage residual char

	Particles > 1mm	Particles < 0.5 mm	Non-sieved sample
Weight fraction of total sample (%)	62	28	100
BET specific surface area (m^2/g)	1126	495	1030
Total pore volume (cm^3/g)	0.78	0.61	0.75

SEM analysis of the char particles showed that the structure of the wood cells was maintained extensively. Pits and perforations on the cell walls are clearly recognizable and contribute to the very high specific surface area of this material.

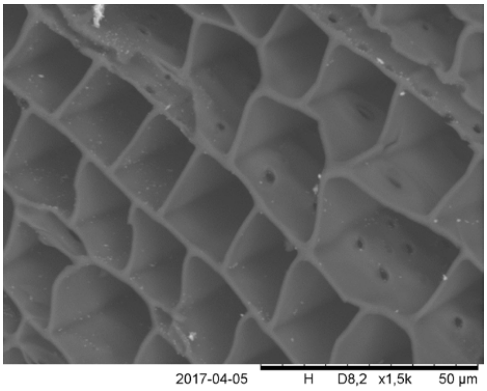

Figure 5: SEM image of Viking gasifier residual char

The Energy Dispersive Spectrometry (EDS) analysis confirmed the high carbon content in the biochar samples. Inorganics appear to be well dispersed, especially on the internal surfaces of the tracheary elements of the wood structure. The inorganics detected with SEM/EDS were calcium, potassium and silicon, present in form of oxides.

4 CONCLUSIONS

Understanding the nature of the tar-char interaction is necessary to implement the application of residual gasification biochar to cleaning of producer gas. This work is specifically aimed at investigating the mechanisms of tar decomposition on the biochar surface at different temperatures. An experimental setup was prepared for testing a biochar bed made of residual char from the Viking gasifier, which is a TwoStage process. Tests were carried out using phenol and naphthalene as model tars. Results from the laboratory setup suggest that the char bed is able to efficiently remove such aromatic molecules from a gaseous stream at 250˚C, 500˚C and 600˚C. However, the nature of the interaction between char and model tars is probably limited to physical adsorption at these temperatures. This is confirmed by the diminished effect on naphthalene at higher temperature (600˚C). The bed temperature is expected to influence the irreversibility of the tar-char interaction. The matter needs to be further investigated at temperatures up to 800˚C, with the objective to optimize tar removing and maximize tar conversion into stable gases (CO, CO_2, H_2). The characterization analysis showed that the residual char from the Viking gasifier is comparable to activated carbon in terms of specific surface area and pore volume. Further experimental work will be performed contacting the residual biochar with real producer gas with a high tar load. The results will be useful to develop a flexible, char-based gas cleaning solution, potentially applicable to different gasification processes.

6 REFERENCES

[1] M. Franz, H. a Arafat, and N. G. Pinto, “Effect of chemical surface heterogeneity on the adsorption mechanism of dissolved aromatics on activated carbon,” *Carbon N. Y.*, vol. 38, pp. 1807–1819, 2000.

[2] W.-J. Liu, F.-X. Zeng, H. Jiang, and X.-S. Zhang, “Preparation of high adsorption capacity bio-chars from waste biomass,” *Bioresour. Technol.*, vol. 102, no. 17, pp. 8247–8252, 2011.

[3] Z. Abu El-Rub, E. A. Bramer, and G. Brem, “Experimental comparison of biomass chars with other catalysts for tar reduction,” *Fuel*, vol. 87, no. 10–11, pp. 2243–2252, 2008.

[4] D. Fuentes-Cano, A. Gómez-Barea, S. Nilsson, and P. Ollero, “Decomposition kinetics of model tar compounds over chars with different internal structure to model hot tar removal in biomass gasification,” *Chem. Eng. J.*, vol. 228, pp. 1223–1233, 2013.

[5] S. Hosokai, K. Norinaga, T. Kimura, M. Nakano, C.-Z. Li, and J. Hayashi, “Reforming of Volatiles from the Biomass Pyrolysis over Charcoal in a Sequence of Coke Deposition and Steam Gasification of Coke,” *Energy & Fuels*, vol. 25, no. 11, pp. 5387–5393, 2011.

[6] X. Nitsch, J.-M. Commandré, J. Valette, G. Volle, and E. Martin, “Conversion of Phenol-Based Tars over Biomass Char under H 2 and H 2 O Atmospheres,” *Energy & Fuels*, p. 28 (2014) 6936-6940, 2014.

[7] S. Krerkkaiwan, A. Tsutsumi, and P. Kuchonthara, “Biomass derived tar decomposition over coal

char bed," *ScienceAsia*, vol. 39, no. 5, p. 511, 2013.
[8] J. Ahrenfeldt, U. Henriksen, T. K. Jensen, B. Gøbel, L. Wiese, A. Kather, and H. Egsgaard, "Validation of a continuous combined heat and power (CHP) operation of a two-stage biomass gasifier," *Energy and Fuels*, vol. 20, no. 6, pp. 2672–2680, 2006.
[9] R. Ø. Gadsbøll, J. Thomsen, C. Bang-Møller, J. Ahrenfeldt, and U. B. Henriksen, "Solid oxide fuel cells powered by biomass gasification for high efficiency power generation," *Energy*, vol. 131, pp. 198–206, 2017.
[10] H. Egsgaard, J. Ahrenfeldt, P. Ambus, K. Schaumburg, and U. B. Henriksen, "Gas cleaning with hot char beds studied by stable isotopes," *J. Anal. Appl. Pyrolysis*, vol. 107, pp. 174–182, 2014.
[11] V. Hansen, D. Müller-Stöver, J. Ahrenfeldt, J. K. Holm, U. B. Henriksen, and H. Hauggaard-Nielsen, "Gasification biochar as a valuable by-product for carbon sequestration and soil amendment," *Biomass and Bioenergy*, vol. 72, no. 0, pp. 300–308, 2015.
[12] S. Hosokai, K. Kumabe, M. Ohshita, K. Norinaga, C. Li, and J.-I. Hayashi, "Mechanism of decomposition of aromatics over charcoal and necessary condition for maintaining its activity," *Fuel*, vol. 87, no. 13–14, pp. 2914–2922, 2008.
[13] F. Nestler, L. Burhenne, M. J. Amtenbrink, and T. Aicher, "Catalytic decomposition of biomass tars: The impact of wood char surface characteristics on the catalytic performance for naphthalene removal," *Fuel Process. Technol.*, vol. 145, pp. 31–41, 2016.
[14] V. Benedetti, F. Patuzzi, and M. Baratieri, "Gasification char as a potential substitute of activated carbon in adsorption applications," *Energy Procedia*, vol. 0, 2016.

9 ACKNOWLEDGEMENTS

The authors thank Innovationsfonden for the financial support received as part of the project "SYNFUEL - Sustainable synthetic fuels from biomass gasification and electrolysis" (4106-00006B).
The authors would also like to thank Dr.-Eng. York Neubauer, Eng. Omid Henrik Elhami and Susanne Hoffman (TU Berlin, Institute for Energy Engineering) for their kind collaboration and Janet J. Bentzen (DTU, Energy Conversion Dpt.) for the help with SEM instrument.
Special thanks to Prof. Helge Egsgaard for the support with the analytical work.

RESIDUAL CHAR FROM GASIFICATION INTEGRATED IN A TAR REMOVAL SYSTEM

Ravenni G., Sárossy Z., Ahrenfeldt J., Henriksen U.B.

Technical University of Denmark (DTU), Department of Chemical and Biochemical Engineering
Frederiksborgvej 399, 4000 Roskilde, Denmark

grav@kt.dtu.dk, +4593511592

ABSTRACT: The Low Temperature-Circulating Fluidized Bed (LT-CFB) gasifier is a staged process, designed for conversion of straw and other ash-rich feedstock. The main drawback of this technology is the severe tar load in the producer gas, which limits the downstream applications to direct combustion. In this work, a reactor has been tested to clean and upgrade the LT-CFB producer gas by using residual gasification char. The char is a by-product of wood chips gasification in a 100kWth TwoStage gasifier (known as "Viking"). The test reactor was designed to investigate the effect of a char bed on the quality of producer gas, with and without addition of sub-stoichiometric air above the bed. The reactor was connected to the gas outlet of a 100kWth LT-CFB gasifier and maintained at 800˚C with electric heating. The quality of the gas has been evaluated in detail before and after the cleaning step, by monitoring changes in the gas composition and tar concentration. Results from Test A (with air injection) and Test B (without air injection) showed that the reactor is able to efficiently remove tars. The effect of partial oxidation improved the stability of the gas cleaning step. These preliminary tests demonstrated the effectivity of this solution to upgrade LT-CFB producer gas.
Keywords: gasification; straw; gas cleaning; tar removal; biochar; innovative concepts

1 INTRODUCTION

The thermochemical conversion of herbaceous biomass such as wheat straw is known to be problematic because of the high ash content in the feedstock. The Low Temperature-Circulating Fluidized Bed (LT-CFB) gasifier, schematized in Figure 1, is a staged process designed for the conversion of such fuels.

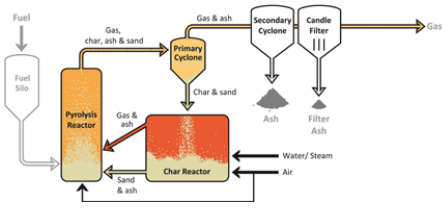

Figure 1: Diagram of LT-CFB gasifier [1]

The maximum temperature in the process is 750˚C, which makes this gasifier suitable to convert a variety of feedstocks with a high content of low-melting ashes: straw, biogas digestion residues, manure fibers and sewage sludge have been tested as feedstock [1]. However, the application of the LT-CFB producer gas is limited because of the severe tar load (up to 30 g/Nm^3), the high particulate content and the presence of S- and Cl- containing compounds. The gas quality is critical for integrating gasification into the energy system. The on-going Synfuel project [2] sets itself to use surplus electricity generated through wind or solar to produce H_2 by electrolysis and add it to producer gas. The synergy of high temperature electrolysis and gasification would make it possible to synthesize liquid fuels such as methanol.

A potential solution to improve the quality of producer gas for this application is to use gasification-derived char. Many gasification plants produce a solid residue which is rich in carbon and has surface properties that are comparable with activated carbon (AC) [3]. However, the solid residue produced by the LT-CFB gasifier is made of very fine particles, it is hard to handle and difficult to use in a separate reactor for gas treatment.

The char used in this study is produced in a TwoStage fixed bed gasifier (also known as "Viking" gasifier) from gasification of spruce wood chips. The same residual material has been previously tested in a laboratory-scale reactor [4] and has been chosen for this application not only because it has a particle size suitable for fixed bed operation (with particles up to 1-2 cm), but also because of its AC-like properties, with a Brunauer–Emmett-Teller (BET) specific surface area over 1000 m^2/g [5]. Moreover, it contains inorganics (mainly Ca, Si, K) which are well dispersed on the surface [3]. These characteristics suggest that this material could act as a catalyst to adsorb contaminants and reform tar into stable gases (H_2, CO, CH_4). The application of carbonaceous materials for removal of tars has been previously reported [6–8]. Particularly, the effectivity of this solution appears to be higher when coupled with partial oxidation of the producer gas prior to the passage to a fixed bed of char [9]. The present work reports results obtained by using an experimental reactor containing a hot bed of char, which was swept with producer gas during the operation of the 100kWth LT-CFB gasifier at DTU, Risø. The quality of the producer gas, before and after the passage through the reactor, was assessed in terms of tar content, gas composition and heating value. The durability of the char bed was evaluated with experiments of 120 minutes, to verify the sustainability of this gas treatment method.

2 MATERIAL AND METHODS

The residual gasification char used as bed material was collected from the ash container of the TwoStage, "Viking" gasifier and sieved with a 3.15 mm sieve (Retsch, Germany) to remove small particles and powder. The cylindrical test reactor was 500 mm tall, with an internal diameter of 125 mm, enough to contain a 200 mm char bed (about 300 g) and a freeboard space for partial oxidation reactions to take place above the bed. Producer gas and air inlets were placed at the top, while the gas outlet was placed at the bottom, below the grate

supporting the char bed. In all experiments, the reactor was maintained at 800˚C by an electric furnace. The temperature profile inside the reactor was monitored by thermocouples placed at different heights. A diagram of the reactor is shown in Figure 2.

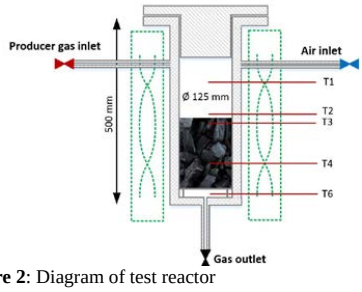

Figure 2: Diagram of test reactor

A slip stream was extracted from the gas outlet pipe during stable operation of the LT-CFB gasifier. The gas extraction port was placed downstream the cyclones and the ceramic filter (see Figure 1), so that the extracted gas was clean from particulate. Producer gas was fed to the reactor with a constant flow of 30 l/min. The residence time in the reactor was 2.5 s. Results from two separate experiments are presented in this work: Test A and B. During test A, a constant air flow of 9.5 l/min was fed through the dedicated inlet, whereas during test B no air was supplied.

Producer gas was sampled before and after the passage through the reactor, using LC-NH_2 Solid Phase Adsorption (SPA) tubes (Supelco, USA). The composition of the tar mixture was determined by stable isotope dilution analysis and Gas Chromatography coupled with Mass Spectrometry (GC-MS) (Agilent, Denmark). Samples obtained by mean of a Petersen column filled with acetone (250 ml) were used to estimate the gravimetric tar. Sub-samples of 25 ml were concentrated by rotary evaporation (Buchi, Switzerland) until the solvent was completely removed. The samples were then dried overnight at 100˚C. The residues were considered as gravimetric tar. The analysis was run in duplicates on each sample.

The gas composition (N_2, H_2, CO, CO_2, CH_4) was continuously measured with an online gas analyzer (FLSmidth, Denmark). Gas bags were also used for additional offline analysis with a multi-column gas chromatograph (ThermoScientific, USA) equipped with Flame Ionizing Detector (FID) and Thermal Conductivity Detector (TCD).

The combination of these techniques was used to monitor the quality of producer gas and evaluate the tar cracking and reforming effect of the char bed. After the experiments, the bed material was collected to determine the residual mass. In addition, Scanning Electron Microscopy (SEM) (TM 3000, Hitachi, Japan) was used on fresh and spent char samples, to evaluate changes in the surface structure.

3 RESULTS AND DISCUSSION

3.1 Producer gas analysis

The permanent gas composition of the particle-free producer gas is reported in Table I. The averaged values from online gas analysis were confirmed by offline measurements by GC-TCD. The offline analysis was also able to detect light hydrocarbons in the gas by FID. Light hydrocarbons made up about 2 Vol% of the gas. The heating value of the gas was calculated taking hydrocarbons into account and resulted 5.1 MJ/Nm^3.

Gravimetric tar resulted high as expected (27±4 g/Nm^3). The tar composition analysis showed that most of the tar mixture was made up by primary tar, namely phenols. This is due to the design of the LT-CFB gasifier, where pyrolysis volatiles are free to be carried away in the producer gas. Table II shows the average concentrations of the main tar compounds that were detected by GC-MS in the SPA samples.

Table I: Average producer gas composition

Gas composition	N_2	O_2	CO_2	CO	CH_4	H_2
Vol%	61.8	0.15	18.8	11.9	3.1	4.2
σ	0.7	0.1	1.0	0.6	0.2	0.5

Table II: Results of tar analysis on producer gas

Compound	Concentration (mg/Nm^3)
Phenol	930 ± 12
Naphthalene	130 ± 2.6
Acenaphthene	9 ± 5
Fluorene	20 ± 0.5
Anthracene	26 ± 1.3
Pyrene	9 ± 0.2

3.2 Results from test A – char bed with air injection

Test A was run with the reactor at 800˚C and air injection of 9.5 l/min above the char bed. The air flow was started right after the producer gas slip stream was opened, and the partial oxidation did not affect significantly the temperature inside the reactor. The gas composition was measured at the outlet throughout the experiment and the averaged values are reported in Table III.

Table III: Results of gas analysis after reactor - test A

Gas composition	N_2	O_2	CO_2	CO	CH_4	H_2
Vol%	54.8	0.11	14.4	13.3	2.7	14.8
σ	1.9	0.1	0.3	0.5	0.5	1

After passing through the test reactor, the H_2 content in the gas was more than tripled, increasing from 4.2 to 14.8 Vol%. The offline gas composition analysis with GC-TCD showed that no hydrocarbons survived the passage through the reactor. Nonetheless, thanks to the significant increase in the H_2 content, the calculated heating value of the gas after the reactor was 4.4 MJ/Nm^3. In addition, tar analysis by SPA and GC-MS in the outlet gas detected only naphthalene (24 mg/Nm^3) and traces of pyrene (0.3 mg/Nm^3). Both the gas and tar compositions were stable for the whole duration of the experiment.

Gravimetric tar, measured after 60 minutes from the start of the experiment, was reduced to 1.3 g/ Nm^3. After the test, the bed had lost about 15% of the original volume.

3.3 Results from test B – char bed without air injection

Test B was carried out as Test A, with the only difference that no air was injected in the test reactor. The effect on the producer gas quality was similar to Test A, but less stable: a constant decrease was observed in the H_2 concentration. Moreover, the CH_4 content was higher compared with raw producer gas and the value was stable for the duration of the experiment. The composition of the gas at the outlet of the reactor is reported in Table IV, after 30 and 120 minutes from the experiment start.

Table IV: Results of gas analysis after reactor - test B

Gas composition (Vol%)	N_2	O_2	CO_2	CO	CH_4	H_2
30 min	46.5	0.1	15.6	14.0	5.0	18.7
120 min	51.6	0.1	13.8	16.2	5.2	13.1

As in Test A, no hydrocarbons were detected in the gas by GC-TCD. However, because of the increased content of H_2 and CH_4, the calculated heating value of the outlet gas was 6.6 MJ/Nm^3.

Tar analysis showed clearly that the char bed was gradually deactivated during Test B. Naphthalene was detected already after 30 minutes, whereas at 60 minutes also phenols and larger PAHs started to appear in the gas after the reactor. Table V shows the tar composition after 30 and 120 minutes from the start of the experiment.

Table V: Results of tar analysis after reactor - test B

Compound	Concentration after 30 min (mg/Nm^3)	Concentration after 120 min (mg/Nm^3)
Phenol	0	535
Naphthalene	229	1136
Acenaphthene	22	55
Fluorene	0	86
Anthracene	16	327
Pyrene	0	35

Gravimetric tar, measured after 30 minutes from the start of the experiment, was reduced to 0.5 g/ Nm^3. No later measurement was made, but the value probably increased towards the end of the test.

After the test, the char bed volume had decreased by 5%.

3.4 SEM imaging of fresh and spent char samples

Scanning electron microscope was used to verify the changes in the structure of the char before and after the experiment. SEM imaging showed that the surface of spent char appears more fractured in comparison with fresh samples (Figure 3-5). This effect has been ascribed to cracking reaction taking place on the surface of char [10].

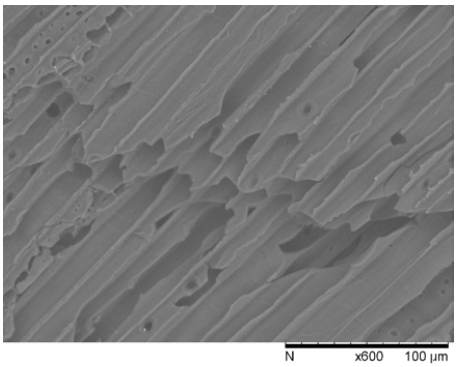

Figure 3: SEM images of fresh TwoStage char

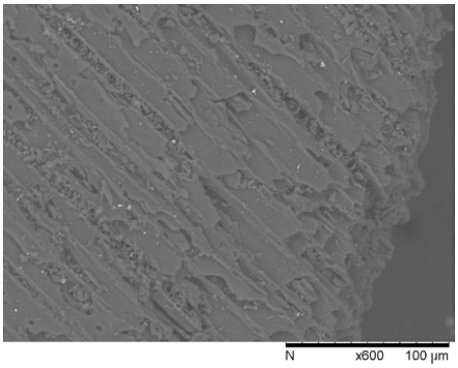

Figure 4: Spent char from Test A

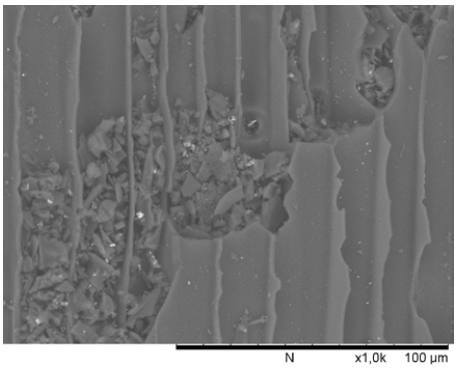

Figure 5: Spent char from Test B

4 CONCLUSIONS

The producer gas obtained from straw gasification with a LT-CFB gasifier was sampled and analyzed in terms of gas composition, gravimetric tar content and composition of the tar mixture. The same gas analysis was carried out on gas samples collected after the passage through a hot reactor (800˚C) containing a bed of char.

During Test A, when the char bed was combined with air injection, tar was almost completely removed from the gas. The H_2 content in the gas was more than tripled in comparison with the raw producer gas composition. The

effect of the reactor remained stable for the whole duration of the experiment (120 minutes).
During Test B, no air was injected in the test reactor over the char bed. In these conditions, the gas was enriched with H_2 and CH_4. However, the H_2 content in the gas after the reactor decreased steadily for the duration of the experiment. Also, tar species were detected in significant amounts already after 60 minutes from the experiment start, meaning that tar removal was not as efficient and steady as in Test A.
Both experiments affected significantly the producer gas quality. Test A demonstrated that air addition has advantages and drawbacks: it assists the conversion of tar, but it also decreases the heating value of the gas and it accelerates the consumption of the char bed. On the other hand, results from test B showed that the use of a char bed alone could not be sufficient to achieve acceptable gas purity. The synergy with partial oxidation appears to guarantee a more durable gas quality.
Further experimental work is required to optimize the amount of air to be injected for partial oxidation and to verify the stability of this gas treatment method over a longer time. In all probability, a supplementary gas filter should be used to remove the residual traces of contaminants prior to methanol synthesis. Nevertheless these results suggest that a char based cleaning system could be developed for effective large scale treatment of biomass producer gas.

6 REFERENCES

[1] Thomsen TP, Sárossy Z, Gøbel B, Stoholm P, Ahrenfeldt J, Jappe F, et al., Waste Manag 2017, 66:123–33.
[2] Innovation Fund Denmark. Synfuel project n.d. https://innovationsfonden.dk/en/node/391 (last access April 16th, 2018).
[3] Benedetti V, Patuzzi F, Baratieri M., Appl Energy, 2017:1–8.
[4] Ravenni G, Henriksen UB, Ahrenfeldt J, Sárossy Z. Proc. 25th EUBCE, Stockholm, 2017.
[5] Hansen V, Müller-Stöver D, Ahrenfeldt J, Holm JK, Henriksen UB, Hauggaard-Nielsen H., Biomass and Bioenergy 2015, 72:300–8.
[6] Abu El-Rub Z, Bramer EA, Brem G., Fuel 2008, 87:2243–52.
[7] Fuentes-Cano D, Gómez-Barea A, Nilsson S, Ollero P., Chem Eng J 2013, 228:1223–33.
[8] Hosokai S, Kumabe K, Ohshita M, Norinaga K, Li C, Hayashi J-I., Fuel 2008, 87:2914–22.
[9] Zhao S, Luo Y, Zhang Y, Long Y., J Anal Appl Pyrolysis 2015, 112:262–9.
[10] Nestler F, Burhenne L, Amtenbrink MJ, Aicher T., Fuel Process Technol 2016, 145:31–41.

5 ACKNOWLEDGEMENTS

The authors thank Innovationsfonden for the financial support received as part of the project “SYNFUEL - Sustainable synthetic fuels from biomass gasification and electrolysis” (4106-00006B)
The authors would also like to thank Susanne Hoffmann (Technical University of Berlin, Institute for Energy Engineering) for the help with char analysis, and DTU Energy Conversion for the support with electron microscopy.

COMPARISON OF WOOD CHARS FROM GASIFICATION AND PYROLYSIS FOR ADSORPTION AND CONVERSION OF TAR MODEL COMPOUNDS

G. RAVENNI[1], O.H. ELHAMI[2], Y. NEUBAUER[2], J. AHRENFELDT[1], U.B. HENRIKSEN[1]

[1]*Danmarks Tekniske Universitet, Department of Chemical and Biochemical Engineering, Frederiksborgvej 399, 2300 Roskilde, Denmark*
[2]*Technische Universität Berlin, Institute of Energy Engineering, EVUR, Fasanenstrasse 89, 10623 Berlin, Germany*

Keywords: char, activated carbon, gas cleaning, tar removal, tar model compounds

Abstract

The carbonaceous products of gasification or pyrolysis (chars) and active carbons (ACs) have been found suitable for adsorbing tar compounds and active as catalysts for tar conversion [1–4]; therefore they can be beneficial for the treatment of biomass producer gas. The aim of this work is to investigate the nature of the interaction between aromatic compounds (toluene and naphthalene) and chars with different surface structure. A dedicated setup was used to test a gasification-derived char, a commercial activated carbon, and a pyrolysis char (non-activated). A flow of N_2, mixed with vapors of toluene and naphthalene, was passed in a reactor housing a char bed and heated up to the desired temperature (250, 800˚C). The concentration of aromatics and the composition of the exit gas were continuously monitored. At 250˚C, a breakthrough behavior was observed, suggesting that physical adsorption was taking place. At 800˚C, H_2 and CH_4 were detected in the exit gas, indicating ongoing cracking reactions. Under these conditions, all chars showed signs of deactivation, but the pore structure of gasification char was beneficial in preserving the activity of this material. Characterization of spent chars showed carbon build-up on the surface of both gasification char and AC. In all tests, non-activated pyrolysis char was the least effective in reducing the concentration of aromatics, and no carbon deposited on its surface during the tests. Both gasification char and commercial AC appeared to be promising materials to be used as substrate for producer gas treatment and upgrading.

1- INTRODUCTION

Tar is a problematic contaminant found in biomass producer gas, because it can be very abundant and can easily condense and damage components. Tar is a mixture of organic compounds which very often have aromatic structures. The carbonaceous products of gasification or pyrolysis (chars) and active carbons (ACs) have been found effective in adsorbing tar compounds [1,2] and active as a catalyst for tar conversion [3–5]. Therefore they may be applied to gas treatment: particularly, the use of residual char from gasification would represent a favorable solution for downstream tar removal in biomass producer gas. Char is continuously produced in gasification plants. Spent char can be recycled within the system or find alternative end-life applications: for example, it could be a precursor for carbon materials or used as biochar for soil amendment, if the relevant thresholds for

noxious contaminants (e. g. heavy metals, polycyclic aromatic hydrocarbons, dioxins) are verified. Moreover, residual char is currently considered as waste, therefore its repurposing would represent an economic and environmental benefit [6]. The irreversibility of the interaction between aromatics and char surface is known to be influenced by temperature [7], but further research is needed in order to define the necessary char characteristics and the reaction conditions that can guarantee an efficient removal of tar by either physical adsorption or conversion (cracking). The aim of this work is to compare the performances of different chars in removing a mixture of toluene and naphthalene from a N_2 flow at different temperature (250 and 800˚C) and to identify the processes involved in the interaction between aromatic molecules and the surface of chars. Three materials were tested: a commercial activated carbon, a residual char from TwoStage gasification [8] of spruce wood chips and char obtained by pyrolysis of beech wood chips. These materials were compared to study the response of different carbonaceous surfaces to contacting aromatic compounds at different temperature levels.

2- MATERIALS AND METHODS

A laboratory setup was assembled at TU Berlin (Institute for Energy Engineering) to test the effects of three char beds on tar model compounds at different temperatures. A N_2 flow (4.7 l/min) was mixed with vapors of a toluene-naphthalene solution that was dosed with a syringe pump (Cetoni, Germany). Toluene and naphthalene were chosen as model representatives of different tar classes. The flow was passed in a heated stainless steel reactor of 500 mm in length with an internal diameter of 36 mm. Before each test, the reactor was filled with a 50 mm layer of alumina (Al_2O_3) beads (Sasol, Germany), used as a support for the tested bed materials. In all tests, the bed of char was 100 mm tall whereas the weight varied from 8 to 22 g, depending on the bulk density of chars. All chars were dried prior to the experiments. Concentrations of aromatics were monitored with a gas chromatograph equipped with flame ionization detector (GC-FID) (SRI Instruments, USA). The permanent gas composition (H_2, CO, CO_2, N_2, O_2, CH_4 and light hydrocarbons) was measured with a gas chromatograph with a thermal conductivity detector (microGC) (Inficon, Switzerland). Both instruments automatically sampled the gas flow in 3 and 5 minutes time intervals, respectively. The setup is schematized in Figure 1.

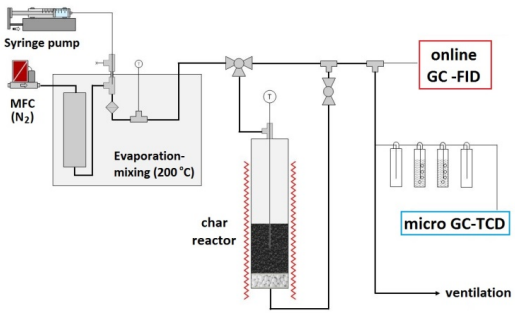

Figure 1: Experimental setup diagram

The concentrations of aromatics in the gas flow fed to the reactor were maintained at a constant value (C_0) during the experiments: 18280 ± 5% mg/Nm^3 for toluene and 1850 ± 5% mg/Nm^3 for naphthalene. Prior to each test, the toluene and naphthalene concentrations were measured in bypass mode until stable. Afterwards, the experiment was started by deviating the gas flow through

the reactor. The evolution of the instantaneous concentrations (C) of toluene and naphthalene was monitored alongside the gas composition, to detect possible decomposition products. All lines were heated to 200˚C to avoid any condensation prior to the GC measurements.
The effect of the char beds was evaluated at 250 and 800 ˚C, and blank experiments were run to quantify the effect of pure thermal decomposition and the effect of the alumina beads that were used as a support for the char beds. Three different chars were tested with the setup. Residual gasification char (Viking char) was collected at the TwoStage demonstration plant at DTU (known as the Viking gasifier) [8]. The commercial active carbon (W48) was a wood-derived, steam-activated AC and was kindly provided by Silcarbon Aktivkohle GmbH (Germany). The non-activated char (900NN) was produced at TU Berlin by pyrolysis of beech chips at 400˚C, followed by heat treatment at 900˚C under N_2 atmosphere to guarantee its thermal stability during high temperature experiments.
After the tests, spent chars were collected and weighed. The elemental composition (CHNS) of the fresh and spent materials was measured (VarioEL III, Elementar Analysensystem GmbH, Germany). In addition, the specific surface area was quantified by Brunauer-Emmett-Teller (BET) analysis through N_2 adsorption at 77K (Nova 2200, Quantachrome Instruments, USA).

3- RESULTS AND DISCUSSION

The characterization of chars by BET analysis prior to the experiments showed that the three materials had different surface properties. The residual gasification char (Viking) had the highest surface area and pore volume, while the pyrolysis char (900NN) showed a very limited surface area and pore volume. Table I compares the surface properties and elemental composition of the tested chars.

Char	BET surface area (m^2/g)	DFT pore volume (cm^3/g)	Density (Kg/m^3)	C (wt%)	H (wt%)	N (wt%)	S (wt%)
Viking	1235	0.78	88	87.6	0.63	0.10	0.04
W48 AC	553	0.24	221	88.9	0.19	0.33	0.09
900NN	35	0.02	198	93.1	0.26	0.92	0.37

Table I: Surface characteristics of the tested materials

The isotherms obtained by N_2 adsorption at 77K were compared with the ones described in the IUPAC Technical Report [9]. The shape of the isotherms (Figure 2) indicated that the Viking char is a micro-mesoporous carbon, also containing macropores (> 50nm in diameter). On the other hand, the other two chars appeared to have mainly narrow micropores (< ≈ 1nm).

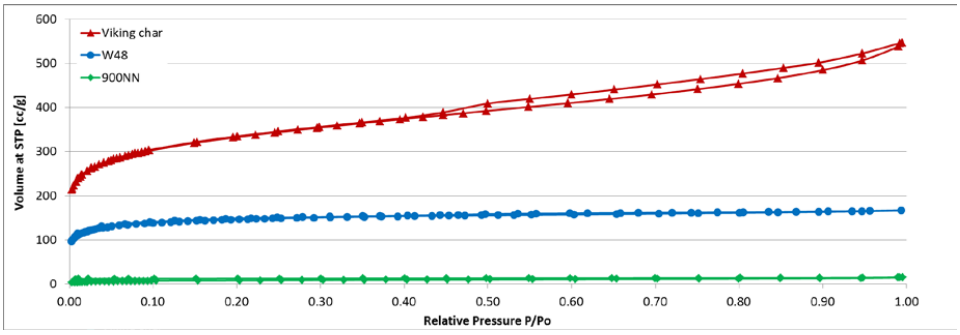

Figure 2: Isotherms obtained by nitrogen adsorption at 77K for the tested chars

Overall, during the experiments with the described setup, Viking char and the W48 AC gave similar or comparable results, whereas the 900NN pyrolysis char showed a markedly different behaviour. Figure 3 shows the evolution of the normalized concentration of naphthalene (C/C_0) at the outlet of the reactor, obtained by experiments at 250˚C.

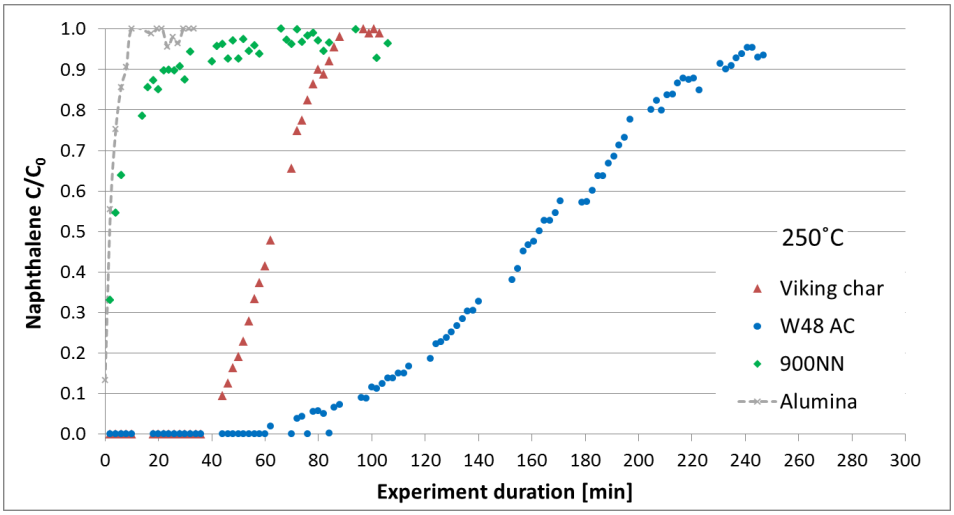

Figure 3: Naphthalene breakthrough curves obtained at 250˚C

Under these conditions, a preliminary test was performed by filling the reactor with alumina (130 g), to obtain the same bed height used in the char tests: the effect on the outlet concentration of naphthalene ceased after about 10 minutes from the start of the experiment.

During the tests at 250˚C, all three chars caused the naphthalene concentration to drop quickly when the gas flow was allowed through the reactor, and then to gradually increase again back to the original value (C_0). The typical shape of adsorption breakthrough curves could be identified, suggesting that the only way of interaction between the aromatics and the surface of char at this temperature was physical adsorption (physisorption). This was confirmed by the fact that only N_2 gas was detected by the microGC instrument at the outlet of the system.

The longest time to naphthalene breakthrough was measured during the experiment with W48 AC, but the effect was also due to the high density of this material. Indeed, the naphthalene adsorption capacity resulted to be comparable for W48 and Viking char: 60.5 mg/g_{char} and 61.2 mg/g_{char} respectively. In contrast, the adsorption capacity resulted dramatically lower for the 900NN pyrolysis char: 4.1 mg/g_{char} .

The high concentration of toluene caused the breakthrough to be almost instantaneous for all the materials; therefore it was not possible to calculate the adsorption capacity. Nevertheless, the relative differences between the chars were also confirmed in relation to toluene, with W48 AC showing the longest breakthrough time, followed by Viking char and 900NN.

When experiments were performed at higher temperature (800˚C), the concentration of naphthalene in the exit gas evolved differently and the typical breakthrough shape was not distinguishable anymore. The evolution of the relative concentrations is showed in Figure 4 for the three chars, together with the results obtained with the reactor filled exclusively with 30g Al_2O_3 (blank test). This amount of alumina was used in all tests as a support for the char beds.

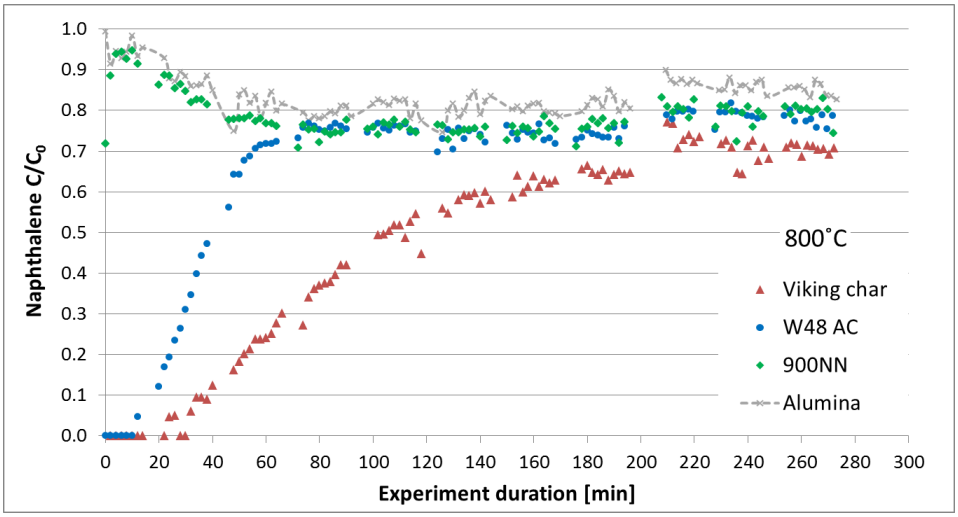

Figure 4: Naphthalene breakthrough curves obtained at 800˚C

It is evident that the effect of the 900NN char bed was negligible if compared with the blank test results. On the other hand, both Viking char and W48 AC assisted cracking reactions of naphthalene for an extended time. Under these conditions, H_2 and CH_4 were detected in the exit gas; both are identified as pyrolysis products of aromatic molecules, together with solid carbon (soot) and benzene [10]. Benzene was not detectable with the method used for the GC-FID. Both materials showed a decreased effect over time, as a consequence of surface deactivation. This was probably due to deposition of solid carbon over the porous surfaces of char: the phenomenon has been previously observed in similar experiments [5].

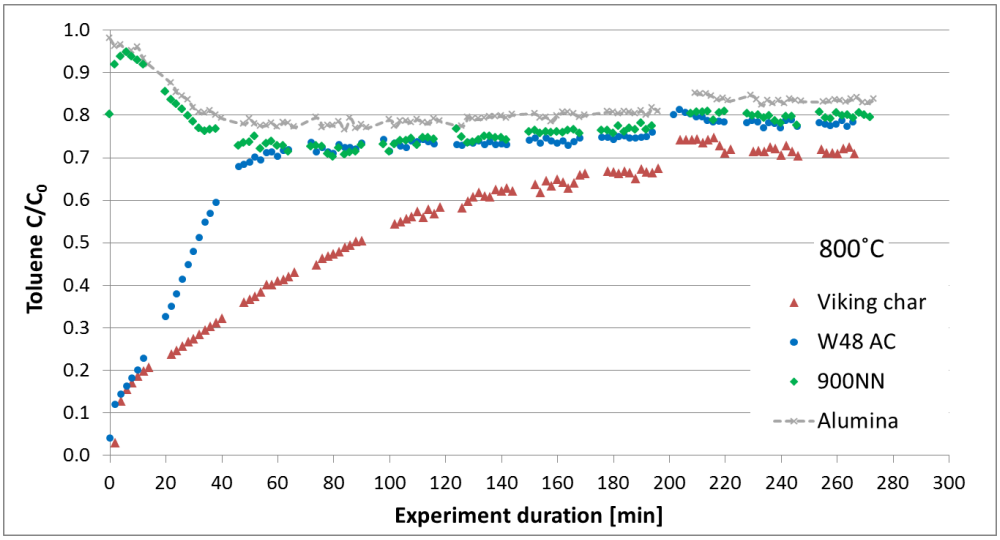

Figure 5: Toluene breakthrough curves obtained at 800˚C

A similar trend was observed for toluene (Figure 5) at 800˚C.

The gas composition at the outlet of the system measured by microGC confirmed that cracking reactions took place during the tests. H_2 was produced in the largest amount by Viking char and W48. The amount of H_2 generated by 900NN pyrolysis char was only slightly higher than the blank test with alumina. Figure 6 shows the evolution of H_2 in the exit gas.

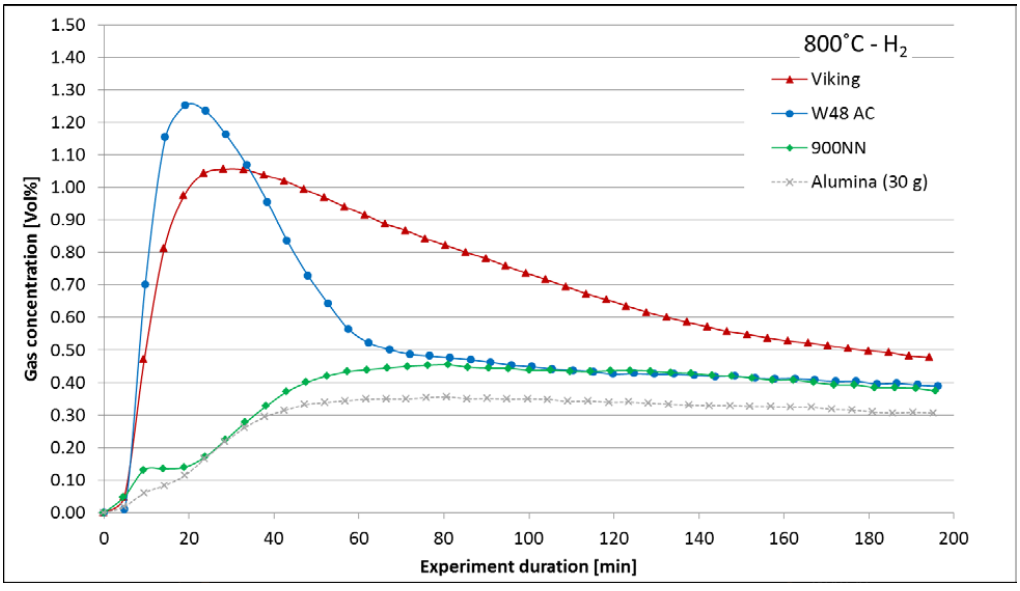

Figure 6: Concentration of H_2 detected in the exit gas during tests at 800˚C with three chars

The H_2 production was declining during all tests, confirming that the materials were undergoing deactivation. The shape of the H_2 curve relative to W48 AC shows a steep decline, while Viking char maintained a higher activity for a longer time. Such difference is likely to be due to the different pore size distribution of the two chars: according to the isotherms in Figure 2, W48 is rich in micropores, while Viking char also contains meso-and macropores. Micropores are easily blocked by carbon deposition, therefore the lack of larger pores led to a faster deactivation. The evolution of H_2 in the exit gas produced by the 900NN pyrolysis char followed closely the blank test results. The surface of this char appeared to have a negligible activity in comparison with the other tested materials.

Other than H_2, only CH_4 was detected in the exit gas, and only in small amounts. The CH_4 production from Viking and W48 curves peaked at 0.15 Vol% and 0.10 Vol% respectively, to then decline with a similar patter as for H_2. During 900NN char and alumina tests, hardly any CH_4 was detected at the outlet.

During the tests, the three chars were exposed for the same amount of time to the N_2 flow enriched with model compounds. After the tests, the spent chars were collected, weighed and analysed in terms of elemental composition and surface properties. Some of the results are collected in Table II. The weight of Viking char used as bed material increased from 9 to 14.6 g after the test. The gain was smaller for W48, which increased from 22.4 to 24.2 g, and it was even negative for 900NN char, which had an initial weight of 20.5 g and a final one of 19.8 g. For the three materials, the weight change corresponded quantitatively with the carbon content variation.

Char	BET surface area (m^2/g)	DFT pore volume (cm^3/g)	C (wt%)	H (wt%)	N (wt%)	S (wt%)
Viking	55	0.04	93.9	0.14	0.28	0.14
W48 AC	389	0.17	94.2	0.11	0.38	0.10
900NN	267	0.12	94.2	0.21	0.62	0.08

Table II: Analysis on spent chars from experiments at 800˚C

Viking char gained the most weight during the tests, and also its carbon content increased significantly. The same effect, less marked, was observed for W48. Again, 900N behaved differently, by losing some weight and some of its carbon content. Also its surface area increased significantly, in contrast with the other two chars. Results suggest that the naphthalene and toluene decomposed on the surface of Viking char and W48 active carbon following the mechanism described by [5] and confirmed by [3]. The carbon deposition appears to take place primarily on micropores, but also on larger pores, once the smaller ones are blocked and deactivated. Indeed, deposited carbon was particularly abundant on Viking char, which lost also most of the surface area during the experiment.

4- CONCLUSIONS

The experiments performed with the described setup on the three chars showed clearly the different ways of interaction between char and the tar model compounds at the two different temperatures (250 and 800˚C). Physical adsorption took place at 250˚C on all three tested materials: breakthrough curves could be identified in the evolution of the relative concentration at the outlet, while no gas was detected other than N_2. Pyrolysis char (900NN) showed a very low adsorption capacity. On the other hand, residual gasification char (Viking char) and the commercial AC (W48) showed much higher adsorption capacities and the two exhibited comparable performances.

At higher temperature (800˚C), the production of H_2 (and to some extent of CH_4) was clearly detectable in the exit gas. The evolution of the gaseous products showed that cracking of aromatics took place preferentially on the surface of Viking char and W48, while the surface of 900NN char was not significantly active. Both gasification char and AC showed signs of deactivation, but with different trends. Viking char suffered a slower deactivation, probably due to its pore structure with micropores as well as meso- and macropores. W48, solely rich in micropores, showed a steep deactivation. However, under real conditions, deactivation could be delayed through addition of a reforming agent to assist the reactions of deposited carbon. The characterization of spent chars revealed that Viking char and W48 gained weight and their carbon content increased. An opposite trend was observed for the 900NN char.

At 800˚C or higher temperatures, chars can assist cracking reactions of aromatics with H_2 production. However, the surface characteristics (specific surface area, pore volume and pore structure) are of importance in determining the performance of the carbonaceous materials: in these experiments, the surface of non-activated char did not perform nearly as well as the two chars with large BET area and developed porosity. In addition the pore size distribution appeared to influence the deactivation rate.

All in all, the results suggest that some chars could perform well if applied for gas cleaning and upgrading; in particular the residual gasification char tested in this work seems especially promising for this application. Finally, it is interesting to point out that the increased carbon content on the spent materials could hint to possible end-life applications with potential carbon sequestration benefits. Carbon-enriched chars could have interesting properties as soil enhancers (biochars) or as precursors for carbon based materials. Indeed, deposited carbon could have some degree of crystalline order [11]. Further experimental work in real conditions is needed to verify the effectivity of chars as materials for gas treatment and to optimize the reaction conditions to obtain an efficient and durable effect on the producer gas quality. In addition, further structural and chemical characterization should be carried out on spent chars to evaluate their suitability and safety for various end-life applications.

REFERENCES

[1] Mastral AM, García T, Callén MS, Navarro M V., Galbán J. Removal of naphthalene, phenanthrene, and pyrene by sorbents from hot gas. Environ Sci Technol 2001;35:2395–400. doi:10.1021/es000152u.

[2] Mastral A, García T, Murrillo R, Callén MS, Lopez JM, Navarro M V, et al. Study of the Adsorption of Polyaromatic Hydrocarbon Binary Mixtures on Carbon Materials by Gas-Phase Fluorescence Detection. Energy & Fuels 2003:669–76.

[3] Fuentes-Cano D, Gómez-Barea A, Nilsson S, Ollero P. Decomposition kinetics of model tar compounds over chars with different internal structure to model hot tar removal in biomass gasification. Chem Eng J 2013;228:1223–33. doi:10.1016/j.cej.2013.03.130.

[4] Klinghoffer N, Castaldi MJ, Nzihou A. Catalyst Properties and Catalytic Performance of Char from Biomass Gasification. I&Ec 2012:13113–22. doi:10.1021/ie3014082.

[5] Hosokai S, Kumabe K, Ohshita M, Norinaga K, Li C, Hayashi J-I. Mechanism of decomposition of aromatics over charcoal and necessary condition for maintaining its activity. Fuel 2008;87:2914–22. doi:10.1016/j.fuel.2008.04.019.

[6] Benedetti V, Patuzzi F, Baratieri M. Characterization of char from biomass gasification and its similarities with activated carbon in adsorption applications. Appl Energy 2017:1–8. doi:10.1016/j.apenergy.2017.08.076.

[7] Egsgaard H, Ahrenfeldt J, Ambus P, Schaumburg K, Henriksen UB. Gas cleaning with hot char beds studied by stable isotopes. J Anal Appl Pyrolysis 2014;107:174–82. doi:10.1016/j.jaap.2014.02.019.

[8] Ahrenfeldt J, Henriksen U, Jensen TK, Gøbel B, Wiese L, Kather A, et al. Validation of a continuous combined heat and power (CHP) operation of a two-stage biomass gasifier. Energy and Fuels 2006;20:2672–80. doi:10.1021/ef0503616.

[9] Thommes M, Kaneko K, Neimark A V, Olivier JP, Rodriguez-reinoso F, Rouquerol J, et al. Physisorption of gases , with special reference to the evaluation of surface area and pore size distribution (IUPAC Technical Report). Pure Appl Chem 2015. doi:10.1515/pac-2014-1117.

[10] Moldoveanu SC. Techniques and Instrumentation in Analytical Chemistry - Pyrolysis of Organic Molecules. vol. 28. Elsevier Science Ltd; 2009.

[11] Brown HR, Hesp WR, Taylor GH. Carbons obtained by thermal and catalytic cracking of coal tars. Carbon N Y 1966;4:193–9.

ACKNOWLEDGMENTS

The authors thank Innovationsfonden (Denmark) for the financial support received as part of the project “SYNFUEL - Sustainable synthetic fuels from biomass gasification and electrolysis” (4106-00006B), as well as the German Federal Ministry of Education and Research for the funding to the junior research group “NWG-TCKON” (FKZ: 03SF0442).
The authors would also like to thank Susanne Hoffmann (Technical University of Berlin, Institute for Energy Engineering) for the help with char analysis.

Department of Chemical and Biochemical Engineering - CHEC
Technical University of Denmark

Søltofts Plads, Building 229
2800 Kgs. Lyngby
Denmark
Phone: +45 45 25 28 00

www.kt.dtu.dk